UNIVERSITY OF LIVERPOOL

Rapid access to heterocycles using transition-metal catalysed C–H and C–C bond activation

Thesis submitted in accordance with the requirements of the University of Liverpool for the degree of Doctor in Philosophy by:

Manuel Barday

September 2018

« Je sers la science et c'est ma joie »

-Bazile Landouye-

Acknowledgement

Firstly, I would like to thank my supervisor Dr. Christophe Aïssa for the guidance and the constant help he has given me throughout the four years of this PhD. Moreover, I would like to thank him for reading this manuscript so many times.

Secondly, I wish to thank Dr. Gita Sedghi and Dr. James Gaynor who have always tried to arrange the demonstrating load to fit my schedule as best as possible.

This work would have not been possible without a great team to work with. Thank you to Kelvin, Steph, María and Tomas for a warm welcome in the group, and the help during my first years, still have a lot to learn. Thank you to Sarah and Fredeb who managed to deal with me for 1 and 3 years. Regardless of the difficult times that came with the PhD, I had a lot of fun, I hope you will finish well. Never forget Diggy diggy hole.

I would like to greatly thank Konstantin, Shane, Kathryn, Marta, Martin, Claudia and Robin who have helped me during the four years.

I wish to thank all the people that I have met, both in chemistry and outside, I had a great time in Liverpool.

Thank you to all the intern students for giving me so many stories to tell and for all the broken glassware.

Finally, I would like to thank my family and friends back in France for the support.

Copyright statement

The work presented in this thesis was done at the university of Liverpool, under the supervision of Dr. Christophe Aïssa between October 2014 and September 2018. Most of the first and second chapter has been published in peer-reviewed journals:

- M. Barday, K. Y. T. Ho, C. T. Halsall, C. Aïssa, *Org. Lett.*, **2016**, *18*, 1756.

- M. Barday, C. Janot, N. R. Halcovitch, J. Muir, C. Aïssa, *Angew. Chem. Int. Ed.*, **2017**, *56*, 13117.

I confirm that the work presented hereafter was conducted by me, unless explicitly stated.

Abstract

- ***Regioselective Synthesis of 3-Hydroxy-4,5-alkyl-substituted Pyridines Using 1,3-Enynes as Alkynes Surrogates.***

The regioselectivity of alkyne insertion in metal-catalysed cycloadditions is usually poor when the two alkyne substituents are alkyl groups, and mixtures of inseparable isomers are normally obtained.[1] In order to circumvent such a drawback, Fagnou's group used 1,3-enynes to control the regioselectivity of the insertion in Rh(III)-catalysed C–H functionalisation reactions applied to the synthesis of indoles.[2] In this work, we applied the same principle to the regioselective synthesis of pyridines by nickel-catalysed (4+2) cycloaddition with azetidinones. Thus, we showed that each of the regioisomers of 3-hydroxy-4,5-bisalkyl pyridines could be obtained by using 1,3-enynes, instead of simple alkynes, after classical functional group manipulations.[3] After further functionalisation this methodology enables an easy access to highly functionalised pyridinols that are important building blocks in medicinal chemistry research.

- ***Cross-coupling of α-Carbonyl Sulfoxonium Ylides with C–H Bonds.***

Since Corey's first report, sulfoxonium ylides have become important reagents in organic chemistry.[4] However, their potential to be used as carbene precursors in C–H functionalisation reactions remained unexplored, in stark contrast to diazo compounds. We have now established a Rh(III)-catalysed protocol that is applicable

[1] K. Y. T. Ho, C. Aïssa, *Chem. Eur. J.*, **2012**, *18*, 3486.
[2] D. R. Stuart, M. Bertrand-Laperle, K. M. N. Burgess, K. Fagnou, *J. Am. Chem. Soc.*, **2008**, *130*, 16474.
[3] M. Barday, K. Y. T. Ho, C. T. Halsall, C. Aïssa, *Org. Lett.*, **2016**, *16*, 8.
[4] E. J. Corey, M. Chaykovsky, *J. Am. Chem. Soc.*, **1965**, *87*, 1353.

to sp^2-hybridised C–H bonds and seven directing groups.[5] Moreover, we discovered that quinolines can be converted into benz[*c*]acridines in a hitherto unprecedented Ir-catalysed dehydrative cyclisation. Finally, deuterium labelling experiments suggest that the proto-demetalation is the rate determining step in the catalytic cycle.

[5] M. Barday, C. Janot, N. R. Halcovitch, J. Muir, C. Aïssa, *Angew. Chem. Int. Ed.*, **2017**, *56,* 13117.

Abbreviation

- Ad: Adamantyl
- APT: Attached proton test
- aq.: Aqueous
- Atm.: Atmosphere
- BHT: Butylated hydroxytoluene
- BINAP: 2,2′-Bis(diphenylphosphino)-1,1′-binaphthyl
- BINOL: 1,1′-Bi-2-naphthol
- Boc: *Tert*-butoxy carbonyl
- br.: Broad
- Calcd: Calculated
- cAMP: Cyclic adenosine monophosphate
- Cbz: Carboxybenzyl
- CI: Chemical ionization
- CMD: Concerted metallation/deprotonation
- CNT: Carbon nanotubes
- cod: 1,5-Cyclooctadiene
- coe: Cyclooctene
- conc.: Concentrated
- Conv.: Conversion
- cp*: 1,2,3,4,5-Pentamethylcyclopentadiene
- cp: Cyclopentadienyl
- CYP17: 17α-Hydroxylase-17,20-lyase
- CYP11B2: Aldosterone synthase
- d (*NMR*): Doublet
- dba: Dibenzylideneacetone
- 1,2-DCB: 1,2-Dichlorobenzene
- 1,2-DCE: 1,2-Dichloroethane
- DCM: Dichloromethane
- DBU: 1,8-Diazabicyclo[5.4.0]undec-7-ene
- DCC: *N,N*′-Dicyclohexylcarbodiimide
- DDQ: 2,3-Dichloro-5,6-dicyano-1,4-benzoquinone
- DFT: Density functional theory
- DG: Directing group
- DMF: Dimethylformamide

- DMSO: Dimethylsulfoxide
- dppb: 1,4-Bis(diphenylphosphino)butane
- dppp: 1,3-Bis(diphenylphosphino)propan-e
- *d.r.*: Diastereomeric ratio
- e: Even
- *e.e.*: Enantiomeric excess
- equiv.: Equivalent
- *e.r.*: Enantiomeric ratio
- ESI: Electrospray ionization
- FT-IR: Fourier-transform infrared spectroscopy
- HBQ: 10-hydrobenzo[h]quinoline
- HFIP: Hexafluoroisopropanol
- HMBC: Heteronuclear multiple-bond correlation
- HRMS: High-Resolution Mass Spectrometry
- IMes: 1,3-Dimesitylimidazol-2-ylidene
- IPr: 1,3-Bis(2,6-diisopropylphenyl)-1,3-dihydro-2*H*-imidazol-2-ylidene
- *J*: Coupling constant
- KIE: Kinetic Isotope Effect
- LDA: Lithium diisopropylamide
- LSD1: Lysine specific demethylase 1
- m *(IR)*: Medium
- m (*NMR*): Multiplet
- maj: Major
- *m*-CPBA: *Meta*-chloroperoxybenzoic acid
- MetAps: Methionine aminopeptidase
- min: Minor
- MOM: Methoxymethyl ether
- m.p.: Melting pot
- MS: Molecular sieve
- N/A: Non-applicable
- nbd: Norbornadiene
- NHC: *N*-heterocyclic carbene
- NMR: Nuclear Magnetic Resonance

- NOE: Nuclear Overhauser effect
- o: Odd
- o/n: overnight
- Pd/C: Palladium supported on charcoal
- PDE4: 4-Phosphodiesterase
- PE: Petroleum Ether
- Piv.: Pivalate
- ppm: Parts per million
- *p*-TSA: *P*-toluenesulfonic acid
- q (*NMR*): Quartet
- quant.: Quantitative
- quint. *(NMR)*: Quintet
- RCM: Ring-closing metathesis
- ROS: Reactive oxygen species
- RPE: Retinal pigment epithelium
- *r.r.*: Regioisomeric ratio
- r.t.: Room temperature
- s *(IR)*: Strong
- s (*NMR*): Singlet
- sat.: saturated
- SDP**:** 7,7′-Bis(diphenylphosphino)-2,2′,3,3′-tetrahydro-1,1′-spirobiindene
- sept. *(NMR)*: septuplet
- t (*NMR*): Triplet
- TCCA: Trichloroisocyanuric acid
- Tf: Triflate
- TFA: Trifluoroacetic acid
- TFE: trifluoroethanol
- THF: Tetrahydrofuran
- TMEDA: Tetramethylethylenediamine
- TMS: Trimethylsilyl
- TS: Transition-state
- Ts: Tosyl
- VEGF: Vascular endothelial growth factor
- vs *(IR)*: Very strong
- µW: Micro-wave
- w: Weak
- x% w/w: x% weight to weight

Experimental and analysis statement

Unless otherwise noted, all reactions were carried out in flame-dried glassware under a dry nitrogen atmosphere. THF was used after passage through Innovative Technology PureSolv MD system. HFIP was purchased from Fluorochem. Dry toluene and 1,4-dioxane were purchased from Acros.

Flash chromatography: Merck silica gel 60 (230-400 mesh). NMR: Spectra were recorded on a Bruker DRX 500 in $CDCl_3$; chemical shifts (δ) are given in ppm. The solvent signals were used as references and the chemical shifts converted to the TMS scale ($CDCl_3$: δ_C = 77.0 ppm; residual $CHCl_3$ in $CDCl_3$: δ_H = 7.26 ppm; residual H_2O in D_2O: 4.79 ppm); apparent splitting patterns are designated using the following abbreviations: s (singlet), d (doublet), t (triplet), q (quartet), quint. (quintuplet), sext (sextuplet), sept. (septuplet), m (multiplet), br (broad), and the appropriate combinations. In ^{13}C NMR, an APT sequence was used to separate methylene groups and quaternary carbons (e, even) from methine and methyl groups (o, odd). IR: PerkinElmer Spectrum 100 FT-IR spectrometer, wavenumbers in cm^{-1}. HRMS: determined at the University of Liverpool on micromass LCT mass spectrometer (ES^+) and Trio-1000 or Agilent QTOF 7200 mass spectrometers (CI). Melting points: Griffin melting point apparatus (not corrected). Elemental analyses: University of Liverpool. All commercially available compounds were used as received.

Table of content

Foreword

Transition-metal catalysed reactions have enabled an enormous step-forward in synthesis, especially in the building of complex frameworks. The activation of inert bonds such as C–H or C–C remains the preferred goal due to the high reward that it can bring.

In this thesis will be presented two complementary projects converging to the same goal, namely the synthesis of valuable heterocycles. The first chapter will be dedicated to the development of a nickel-catalysed C–C bond activation with conjugated 1,3-enyne to access the 3-pyridinol framework. While the second part will focus on the rhodium-catalysed C–H bond activation and cross-coupling with sulfoxonium ylides, which allowed the functionalisation of heterocycles and further transformation to benz[c]acridines.

Due to the gap between those two fields of organic chemistry, it was preferred to present the two projects in separate sections in order to enable a deeper introduction and a better emphasis of each topic.

Regioselective synthesis of 3-hydroxy-4,5-bis-alkyl pyridines using 1,3-enynes as alkyne surrogates

1 Introduction

3-pyridinols can be found in a variety of highly interesting biologically active natural compounds, with the most abundant being isoforms of vitamin B6 (Figure 1).[1, 2] Vitamin B6 is composed of six different interconvertible forms of 3-pyridinols. It has been reported as co-factors in a wide variety of reactions, including α/β/γ elimination/replacement, racemisation, transamination, and decarboxylation of amino-acids.[3, 4] Moreover, studies revealed that vitamin B6 could decrease the risks of cardiovascular diseases.[5] When linked to either cyclodextrins or dendrimers, these compounds were able to mimic the role of enzymes in the racemisation of chiral α-amino acids or decarboxylation of carboxylic acids.[6, 7]

Vitamin B6 :

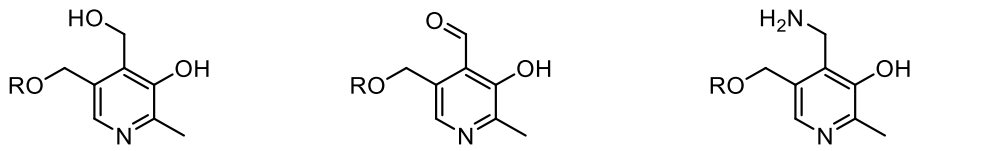

R = H : **Pyridoxine**
R = $P(O)(OH)_2$: **Pyridoxine Phosphate**

R = H: **Pyridoxal**
R = $P(O)(OH)_2$: **Pyridoxal Phosphate**

R = H: **Pyridoxamine**
R = $P(O)(OH)_2$: **Pyridoxamine Phosphate**

Figure 1 : Vitamin B6 forms

The worldwide production of pyridoxine, one of the main forms of vitamin B6, was estimated to be more than 2550 tonnes in 1993, showing how important this industry is in the current economy.[8] The main producers of pyridoxine are Roche (Switzerland), Takeda and Daiichi (Japan).

Due to the interesting biological properties exhibited by vitamin B6, several groups have reported the incorporation of a 3-pyridinol moiety in small molecules and have shown a wide range of biological properties.

2 Biological properties

2.1 Anti-oxidant properties

3-pyridinols are best known for their anti-oxidant properties. As compared to the phenolic counterpart, 3-pyridinols exhibit a greater air-stability due to the extra nitrogen atom embedded into the ring.[9]

They can be employed as radical scavengers, thus limiting the impact of Reactive Oxygen Species (ROS) within organisms.[10, 11] Substitution of the methyl group in pyridoxine by an alkyl-telluro group increased the potency of compound **1** as a chain breaking anti-oxidant (Figure 2). Those derivatives were able to inhibit the peroxidation of linoleic acid in *in vitro* trials better than α-Tocopherol **2**, a classical anti-oxidant.[12]

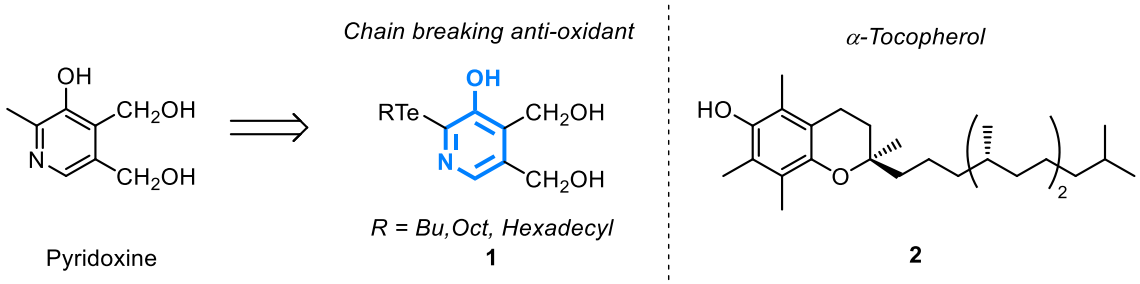

Figure 2: Chain breaking anti-oxidants

The same properties have been used to inhibit the 4-hydroxynonenal-induced cell death in adult retinal pigment epithelium (RPE), which is the major cause of irreversible vision loss.[13, 14] 4-hydroxynonenal is generated in the retinal pigment epithelium upon reaction with ROS, and is responsible for the degeneration of the RPE. The pyridinol **3** has proven potent in the inhibition of the production of 4-

hydroxinonenal, thus preventing the degeneration of RPE and the irreversible vision loss (Figure 3).[15]

ROS are also responsible for the decline of mitochondria in organisms, causing the development of degenerative diseases. Pyridinols **4a** and **4b** have been employed as radical scavengers and have shown great biological activity, along with metabolic stability.[16]

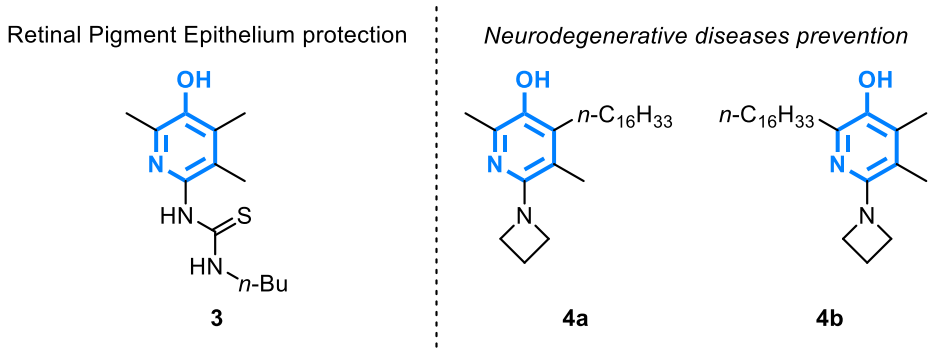

Figure 3: Structures of RPE and mitochondria protectors

2.2 Antiangiogenic activity

Angiogenesis is the biological process responsible for the creation of new blood vessels.[17] When out of control, this phenomenon is the cause of both the growth and spreading of tumoral cells. The angiogenesis in cancer cells is often triggered by a protein called vascular endothelial growth factor (VEGF).[18] Jeong and co-workers have shown that the angiogenesis can be controlled by targeting the production of VEGF. The same authors also reported three generations of 3-pyridinols, **5**, **6** and **7**, capable of inhibiting VEGF induced angiogenesis with the same efficiency as the licensed drug Sunitinib **8** (Figure 4).[19, 20, 21]

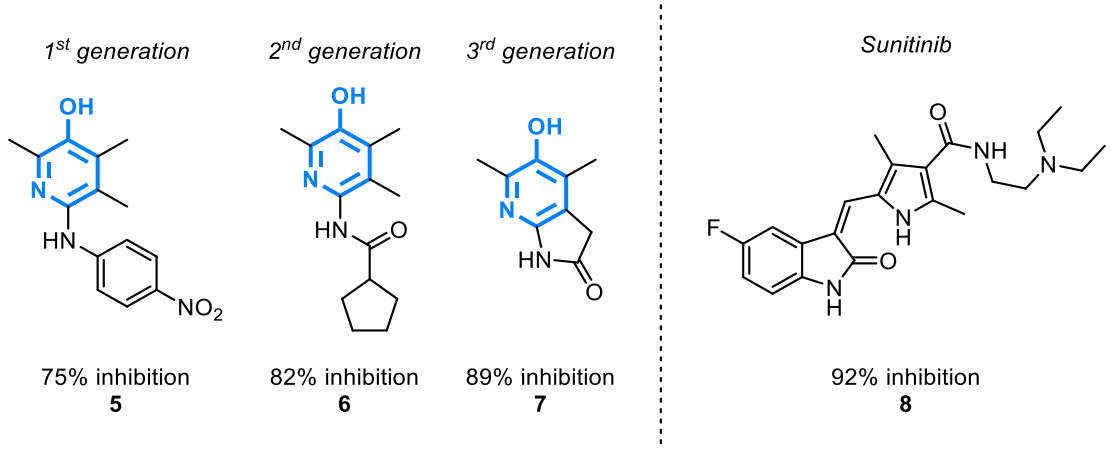

Figure 4: Structures of functionalised 3-pyridinols, Sunitinib and their inhibition levels of VEGF

2.3 Enzyme inhibitors

Methionine aminopeptidase (MetAps) is a cobalt-containing enzyme found in several bacterial pathogens which are responsible for severe diseases such as tuberculosis, urinary- and respiratory-tract infection, pneumonia or ulcers.[22] MetAps are key to the viability of the bacteria and are therefore a great target for the treatment of the associated diseases. Nan *et al.* have shown that the 3-pyridinol derivative **9** had good inhibition properties over MetAps (Figure 5).[23]

A similar approach was taken for the inhibition of CYP17 and CYP11B2.[24, 25] The former enzyme is responsible for the production of androgens leading to prostate cancer. Abiraterone has been shown to be a CYP17 inhibitor, however, this unfortunately led to an increase of cardiovascular risks due to the high concentration of aldosterone generated by the resulting increase of the enzyme CYP11B2. Hartmann and his group developed the 3-pyridinol **10** and showed that this small molecule could inhibit both enzymes, limiting the proliferation of prostate cancer and reducing the associated cardiovascular risks.[26]

Type 4 phosphodiesterase (PDE4) has been shown to be involved in asthma by hydrolysing cAMP.[27] Daxas **12**, a licensed drug produced by AstraZeneca, has proven to be efficient in the inhibition of this enzyme but side effects are often encountered. Sumiyoshi *et al.* have reported the use of compound **11** as a PDE4 inhibitor without undesired side effects.[28]

Finally, Song and co-worker have shown that the functionalised 3-pyridinol ether **13** had a great activity over LSD1, an enzyme responsible for the de-methylation of histones and the propagation of prostate and breast cancers.[29, 30]

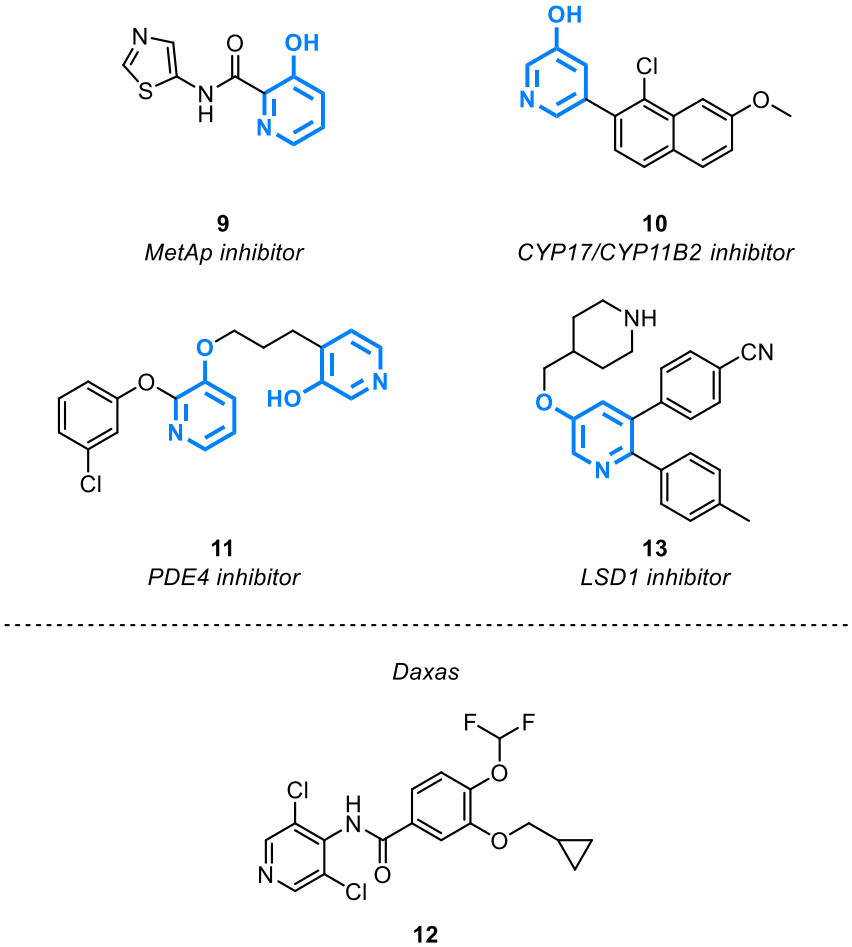

Figure 5: Structures of 3-pyridinols and their biological properties

3 Synthesis of 3-pyridinols

Although highly interesting in terms of its biological properties, methodologies for the synthesis of functionalised 3-pyridinols are limited in numbers. Below are presented the major works published to access the 3-pyridinol framework.

3.1 [4+2] Diels-Alder reaction

Harris *et al.* reported a pioneering work for the synthesis of 3-pyridinol through a Diels-Alder reaction involving the 1,3-oxazole **14** and the electron-poor alkene **15** (Figure 6).[31] An acid-promoted rearrangement of the cycloadduct **16** afforded the 3-pyridinol **17** in good yield. Unfortunately, only symmetrical alkenes were tolerated in this reaction, preventing the access to substituted pyridinols with multiple functional groups.

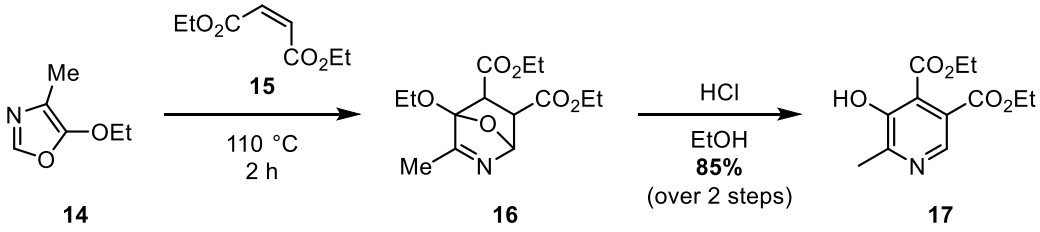

Figure 6 : Harris' Diels-Alder reaction

Importantly, this strategy led to the current synthesis used for the production of pyridoxine. The latest improved process was reported by Su and co-workers in which they obtained the pyridoxine in **56%** over six steps (Figure 7).[32] Firstly, the authors converted the alanine **18** to the alaninate **19** in excellent yield using oxalyl acid. This intermediate was transformed to the key-intermediate **20** in excellent yield upon cyclisation. Finally, the [4+2] Diels-Alder reaction with **21** followed by the acid-

promoted deprotection/re-aromatisation of the intermediate afforded the pyridoxine hydrochloride in excellent yield.

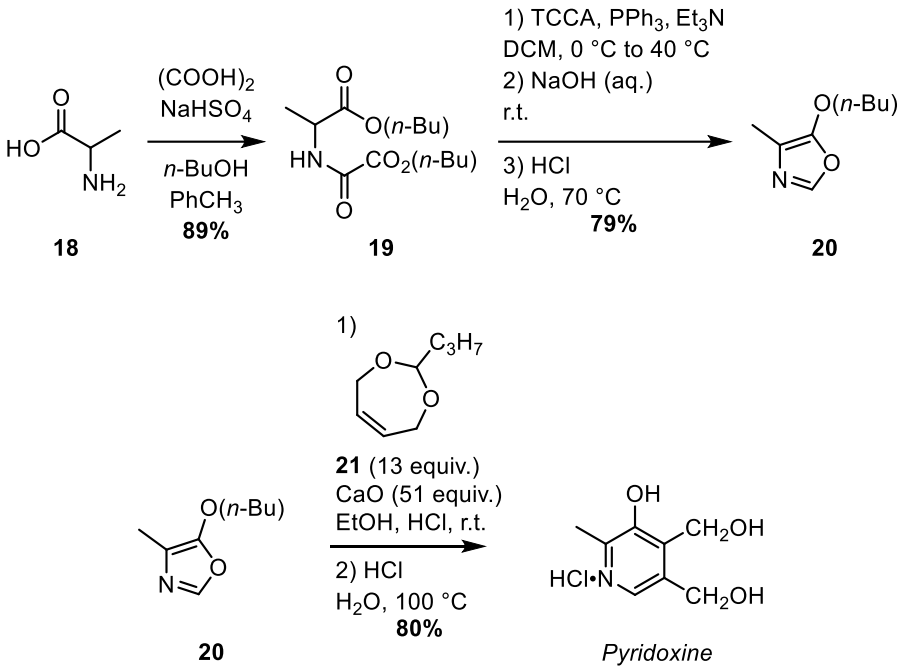

Figure 7: Synthesis of pyridoxine

Renard's group revisited this chemistry and synthesised highly-functionalised 3-pyridinols (Figure 8).[33,34,35,36] By starting from the fully functionalised oxazole **22**, the corresponding cycloadduct **23** was obtained in good yield. The reaction was either catalysed by neodymium triflate or microwave-assisted. Moreover, the authors showed that the reaction was not limited to bis-esteralkenes and the tri-substituted pyridinol **26** was obtained in low yield with acrylic acid **25**.

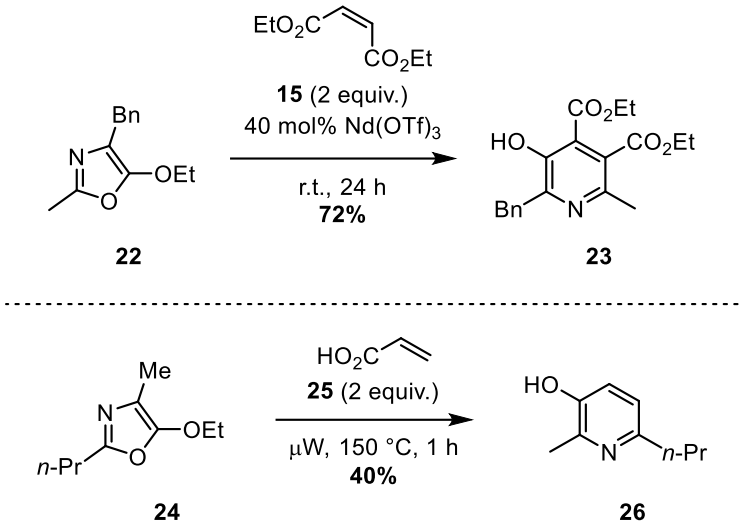

Figure 8: Renard's synthesis of functionalised 3-pyridinols

It is worth mentioning that in all cases only electron-poor alkenes were used, limiting the application of this methodology.

Finally, Arndt and co-workers reported a hetero-Diels-Alder reaction to synthesise 3-pyridinols. By using the highly functionalised diene **28**, they were able to obtain the tetra-substituted pyridinol **29** in good yield, in addition to the alternate regioisomer **30** (Figure 9).[37,38] This methodology was applied to the synthesis of **32** which is an important building block in the synthesis of the antibiotic nosiheptide **33**.

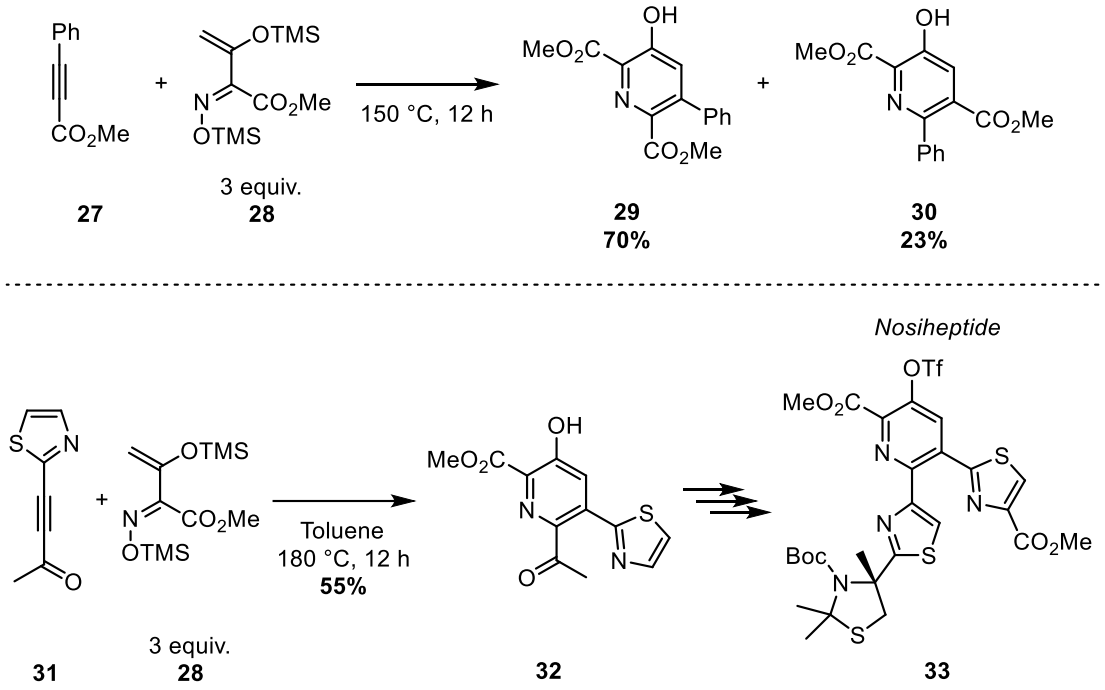

Figure 9: Arndt methodology to 3-pyridinols

3.2 Synthesis of 4,5-substituted 3-pyridinols

However, most functionalised 3-pyridinols with interesting biological activites were synthesised from the pyridoxine hydrochloride (Figure 10). Hecht and co-workers reported the transformation of the pyridoxine into the iodinate 3-pyridinol **34** in four steps with a moderate overall yield. The authors accessed the intermediate **36** in good yield through a Buchwald-Hartwig reaction with the azetidine **35**. The alkylation of **36** led to the two isomers **4a** and **4b** in moderate to low yield.

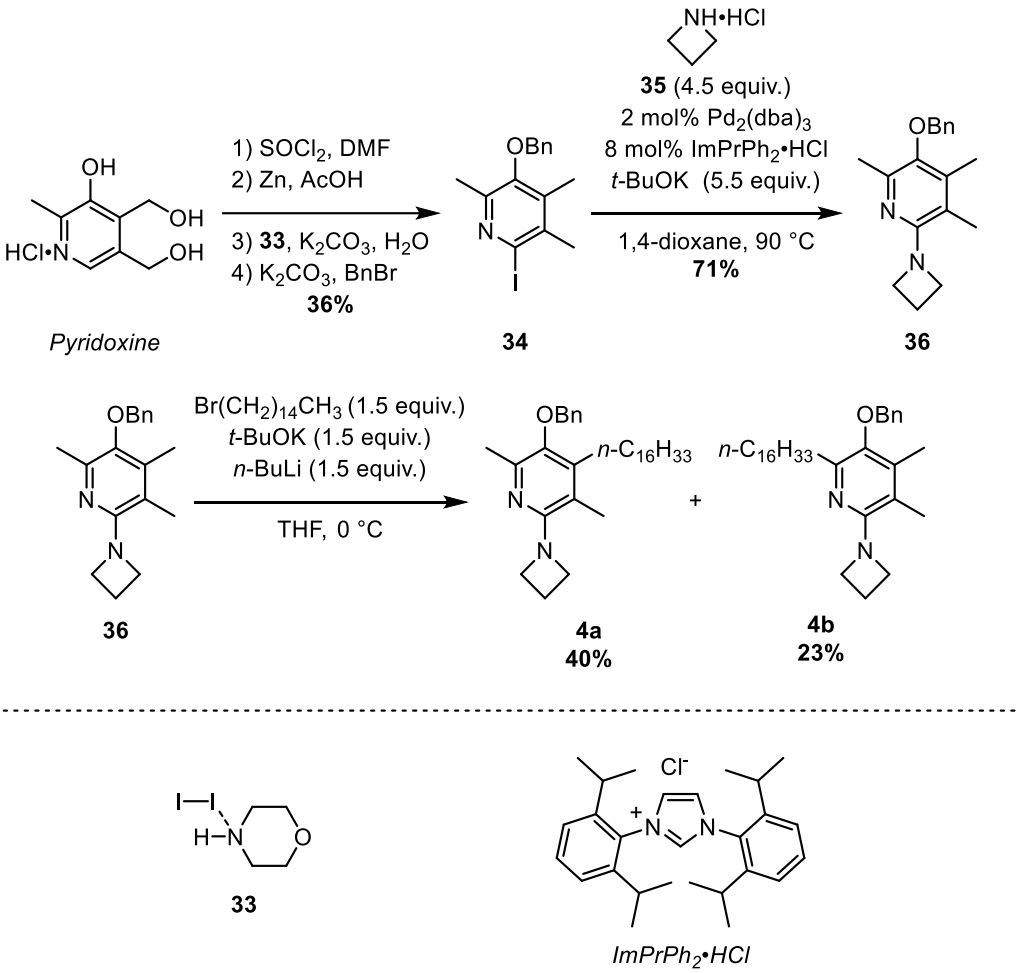

Figure 10: Synthesis of functionalised 3-pyridinol

3.3 Aldol condensation

Allevi's group developed an intramolecular aldol condensation to obtain 4,5-substituted 3-dihydropyridinones (Figure 11).[39] Starting from the diketone **37,** an aldol condensation followed by a crotonisation gave the 3-dihydropyridinone **38**, which could undergo re-aromatisation under basic conditions to form the pyridinium **39**. This method was also applied to the synthesis of pyridiniums bearing only alkyl chains, but with limited scope.

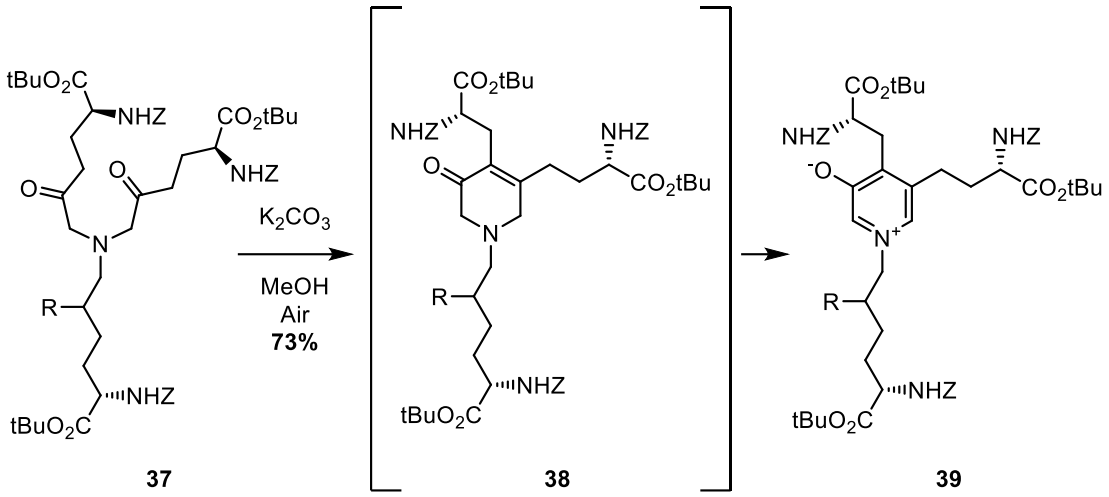

Figure 11: Allevi's route to pyridinium salts

3.4 Intramolecular electronic cyclisation

Fedorov *et al.* reported the rearrangement of a highly functionalised allene into the protected 3-pyridinol **43** (Figure 12).[40] A 1,5-hydrogen shift from the allene **40** led to the intermediate **41** which underwent a 6-π electron cyclisation to yield **42**. Elimination of methanol gave the protected pyridinol in excellent yield. However, harsh conditions were required to generate the desired pyridinol, preventing the general application of this method to structures bearing sensitive functional groups.

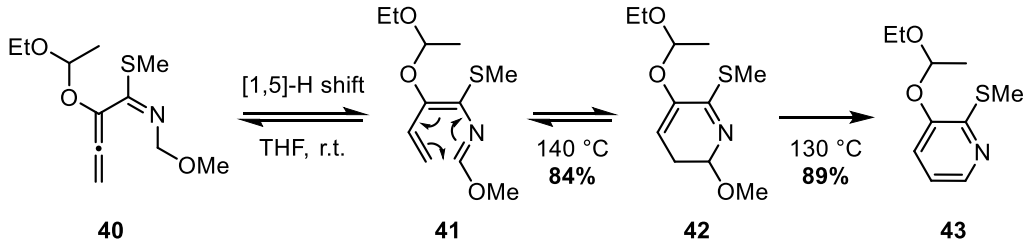

Figure 12: Fedorov's 1,5-hydrogen shift of allenes

3.5 Ring-closing metathesis

Recently, Yoshida and Donohoe independently reported similar methods to synthesise pyridinols (Figure 13).[41, 42] Both strategies relied on a ring-closing metathesis (RCM). Yoshida reported the direct cyclisation of the α-amino ketone **44** to afford the 3-dihydropyridinone **45**, which eventually was transformed into the pyridinol **46** upon re-aromatisation. To improve the yield of the RCM, Donohoe added an extra double bond to the substrate **47**, which was able to act as a relay during the cyclisation. Deprotection of the amine with DBU then led to the formation of **49** in good yield.

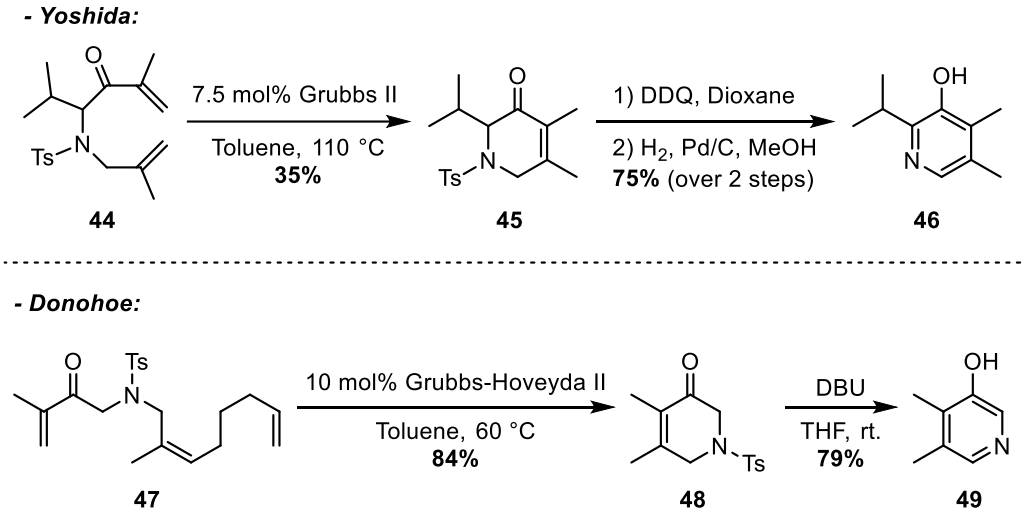

Figure 13 : Yoshida's and Donohoe's Ring Closing Metathesis

3.6 Palladium catalysed cyclisation

In 2011, Tong's group managed to synthesise pyridinol derivatives by applying an amino Heck reaction with oximes through a palladium (0) catalysis (Figure 14).[43] The cyclisation of **50** occurred to afford the six membered conjugated oxime **51**, which

was converted to **52** *via* an acid-promoted hydrolysis of the oxime group followed by a base-induced deprotection of the amine and concomitant re-aromatisation.

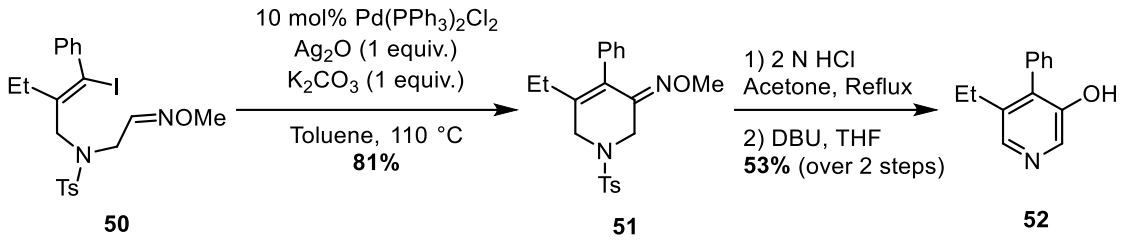

Figure 14 : Tong's Heck reaction

3.7 Nickel-catalysed (4+2) cycloaddition

The previous three examples highlight that catalytic cyclisation can be a powerful tool in the synthesis of highly substituted pyridinols. However, an extensive work is required to access the desired precursor of either mode of cyclisation, and this is particularly true for the synthesis of 3-pyridinols with varied substituents in positions 4 and 5.

In 2012, Aïssa's group addressed this issue by reporting a rapid synthesis of 3-pyridinols by the nickel catalysed (4+2) cycloaddition of alkynes with azetidinones (Figure 15).[44] They were able to isolate **56** in good overall yield in only three synthetic steps from the commercially available azetidinone **53**. The desired pyridinol **56** was obtained after the deprotection and oxidative re-aromatisation of **55**, in a one-pot sequence.

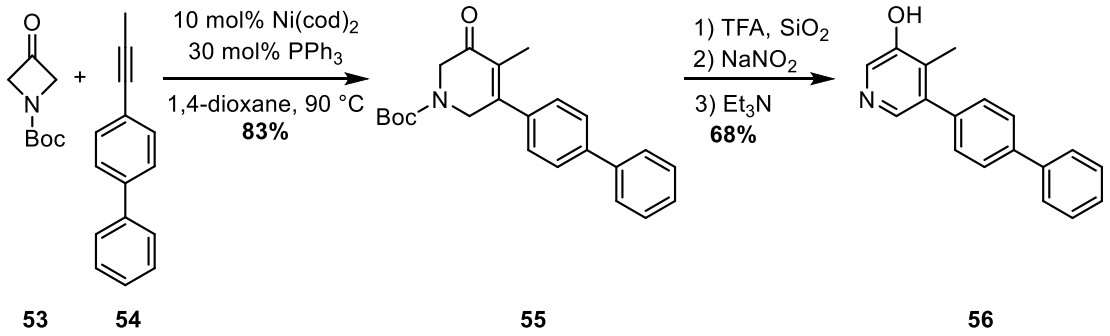

Figure 15 : Aïssa's route to functionalised 3-pyridinol

The substitution pattern on the final 3-pyridinol ring can be easily altered through this method by changing the alkyne, which appears more convenient than the synthesis of more complex precursors such as **44**, **47** or **50**.

The field of metal-catalysed C−C bond activation of four-membered rings, as exemplified in Figure 15, has been extensively studied and has proven useful for the rapid access to carbocycles and heterocycles *via* the insertion of unsaturated moieties. A brief review of this area is presented in the next section.

4 Metal-catalysed (4+2) cycloadditions

4.1 Cyclobutanones

4.1.1 Nickel-catalysed (4+2) cycloaddition

4.1.1.1 Alkynes

Murakami's group reported the first nickel-catalysed (4+2) cycloaddition of cyclobutanones with alkynes (Figure 16).[45] Various alkynes were tolerated with good to excellent yields when symmetrical substrates were used. The catalyst loading had to be increased to 20 mol% in order to obtain acceptable yields in the case of the

diethylcyclobutanone **59**. However, when using unsymmetrical alkynes, the authors reported a significant decrease in terms of yield along with the formation of two regioisomers. The problem arising from the lack of regioselectivity when dealing with unsymmetrical alkynes will be presented in depth later in this chapter. Nonetheless, this research group investigated the influence of both steric and electronic effects on the regioselectivity of the insertion. Steric hindrance was deemed to play an important role in the observed regioselectivity, as indicated by the preferential formation of 60. However, they did not see a significant electronic effect of either electron-withdrawing or -donating groups present on the benzene ring, as shown with **61** and **62**.

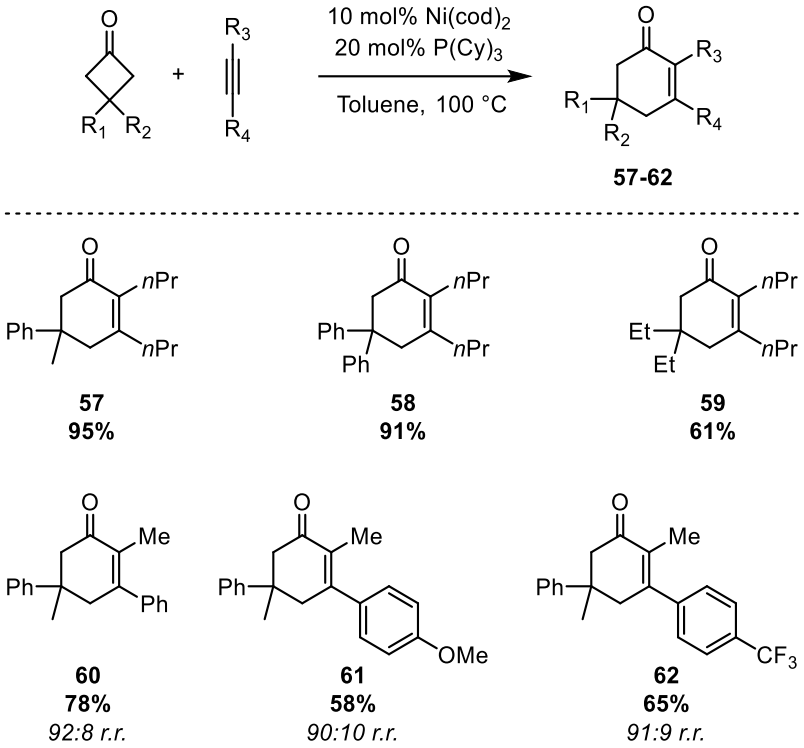

Figure 16 : Nickel-catalysed (4+2) cycloaddition of alkynes with bis-subsituted cyclobutanone

When the (4+2) cycloaddition was attempted on the substrate **63**, a mixture of the desired cycloadduct **65** and the linear ketone **66** was obtained (Figure 17).

However, changing the ligand from a phosphine to an *N*-heterocyclic carbene (NHC) led to the selective formation of the desired cycloadduct **65**.

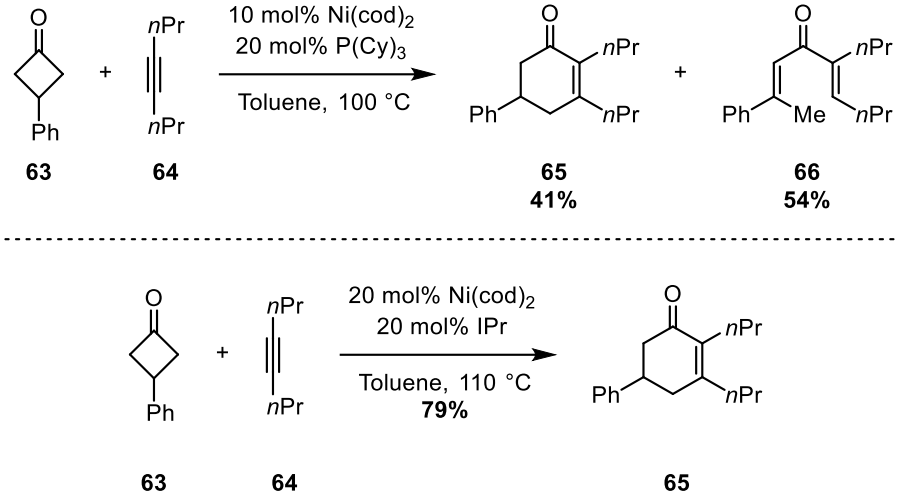

Figure 17: Nickel-catalysed (4+2) cycloaddition of alkynes with mono-subsituted cyclobutanone

The insertion of bisalkynes was also described by Murakami and his group. Thus, the bicyclic product **69** could be synthesised from the *gem*-disubstituted cyclobutanone **67** in excellent yield (Figure 18).[46]

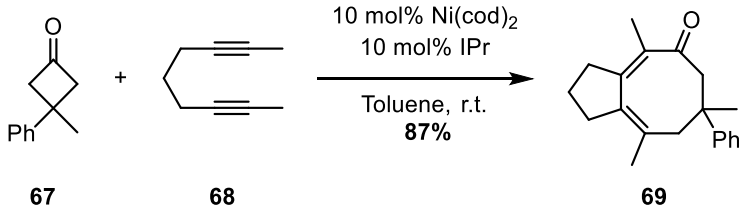

Figure 18: Nickel-catalysed (4+2+2) cycloaddition of diynes with di-subsituted cyclobutanone

4.1.1.2 Alkenes

Murakami's group has also reported the use of alkenes as cycloaddition partners. Although the intermolecular nickel catalysed (4+2) insertion of olefins in cyclobutanone failed regardless of the condition used, they were able to develop the intramolecular variant (Figure 19).[47] By mixing the functionalised cyclobutanone **70**

with the nickel catalyst in toluene, they could obtain the corresponding bicyclic ketone **71** in 90% yield.

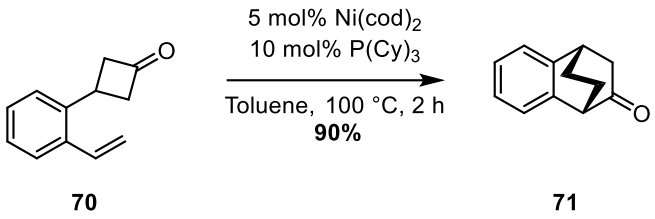

Figure 19: Intramolecular nickel-catalysed (4+2) cycloaddition of alkene with cyclobutanone

The authors expanded this reaction to the synthesis of enantio-enriched bicyclic ketones (Figure 20).[48] Using the phosphoramidite **73** as a ligand, the authors obtained the cycloadduct **74** in excellent yield and enantiomeric excess.

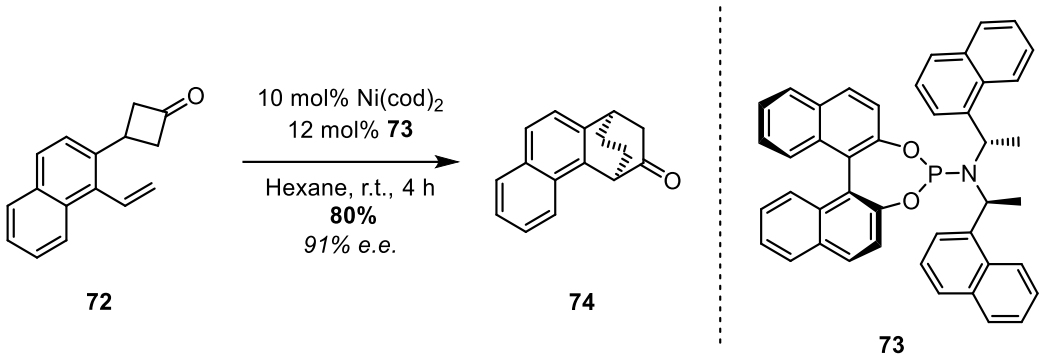

Figure 20: Asymmetric intramolecular nickel-catalysed (4+2) cycloaddition of alkene with cyclobutanone

4.1.2 Rhodium-catalysed (4+2) insertion

4.1.2.1 Alkenes

Prior to their work on the nickel catalysed cycloaddition of olefins with cyclobutanones, Murakami's group studied this reaction using a rhodium catalyst (Figure 21).[49] This cycloaddition was efficient with both electron-donating and electron-withdrawing substituents, although slightly faster with the latter.

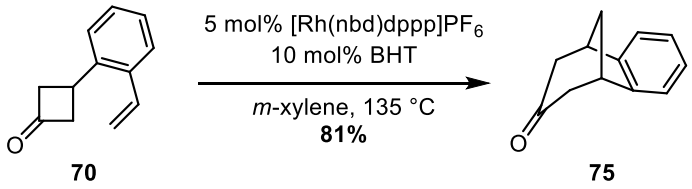

Figure 21 : Intramolecular rhodium-catalysed (4+2) cycloaddition of alkene with cyclobutanone

Interestingly, they showed that the outcome of the reaction was catalyst dependent. Two different mechanisms were invoked to explain the differences between the rhodium and nickel catalysis (Figure 22). The coordination of the nickel centre to the olefin and the carbonyl gives intermediate **A,** which is converted to **B** after an oxidative cyclisation. The bicyclo[2.2.2]octanone **71** is released upon β-carbon elimination to the intermediate **C**, followed by a reductive elimination of the nickel catalyst. With a rhodium catalyst, the direct oxidative C−C bond cleavage can occur to give **E** from the coordinated compex **D**. Intermediate **F** is obtained after insertion of the olefin into the pentarhodacycle. Reductive elimination re-generates the active catalyst and releases the bicyclo[3.2.1]octanone **75**.

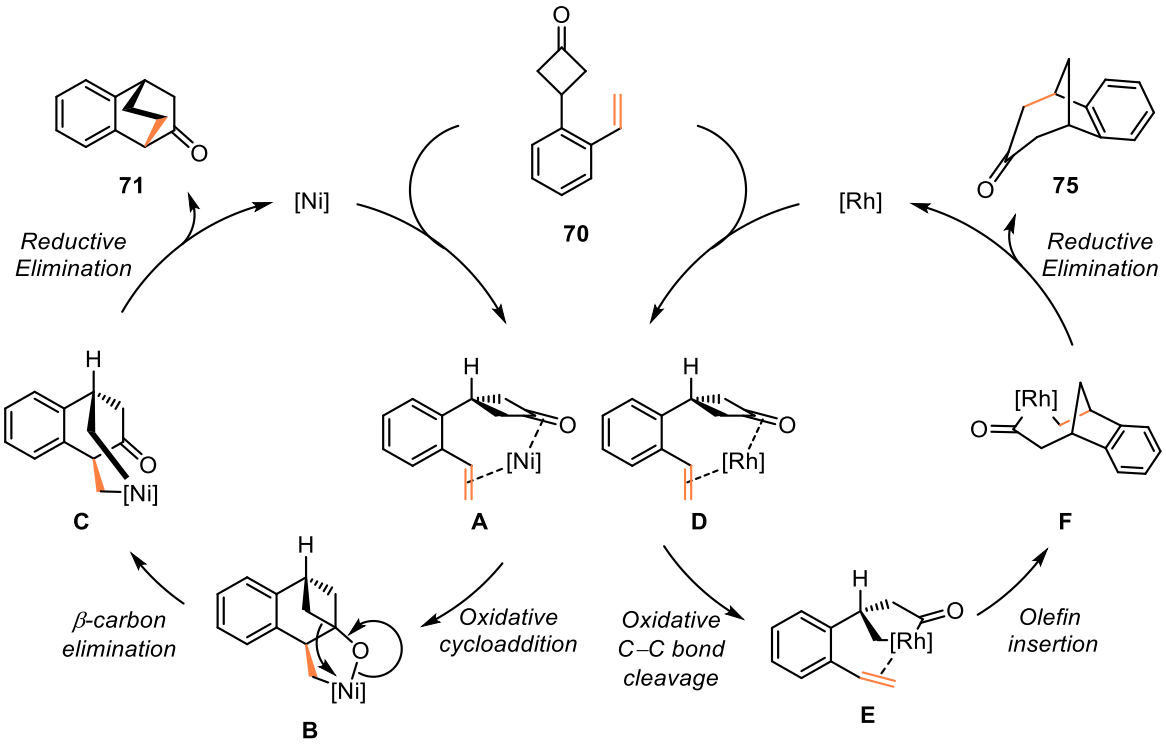

Figure 22: Mechanisms of the intramolecular nickel- and rhodium-catalysed (4+2) cycloaddition of alkenes with cyclobutanone

The authors could also access eight-membered rings in an efficient manner by changing the position of the aryl group bearing the olefin (Figure 23).[50] The two regioisomers **77** and **78** were produced during the process and were hydrogenated to give the bicyclic compounds **79** in almost quantitative yield.

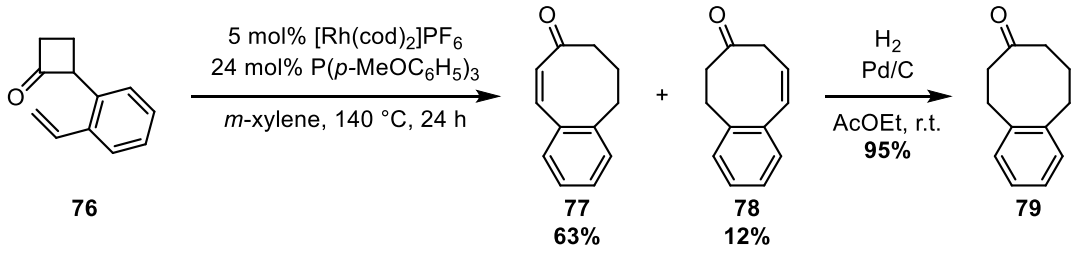

Figure 23: Intramolecular rhodium-catalysed (4+2) cycloaddition of alkene with 2-substituted cyclobutanone

In 2014, Cramer and co-workers reported the asymmetric version of this rhodium-catalysed alkene insertion (Figure 24).[51] Using the chiral bis-phosphine

ligand **81**, the authors were able to obtain the bicyclic ketone **82** in excellent yield and enantiomeric ratio. The enantiomeric differentiation occured during the oxidative addition of the rhodium catalyst into the cyclobutanone **80**.

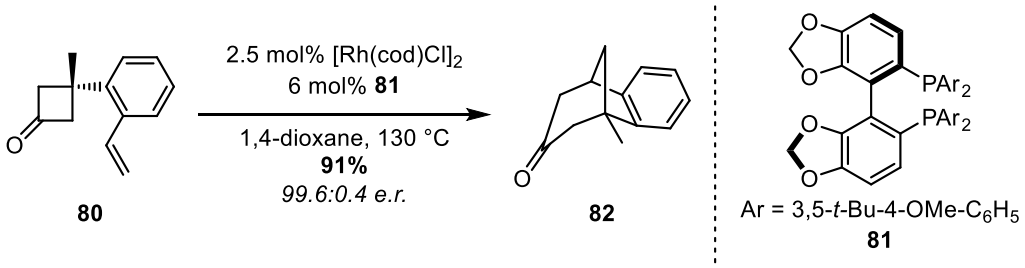

Figure 24: Asymmetric intramolecular rhodium-catalysed (4+2) cycloaddition of alkene with cyclobutanone

In 2000, Wender *et* al. reported that dienes could undergo an intramolecular (4+2+2) cycloaddition to yield bicyclic cyclooctaenes (Figure 25).[52] Remarkably, they were able to obtain most of their cycloadducts as single diastereoisomers. They reported that either the *N*-tosyl **83**, or the ether linker **85** were tolerated. Moreover, a methyl substituent on the olefin led to **84** in a decreased yield, but with no reduction of the observed diastereoselectivity.

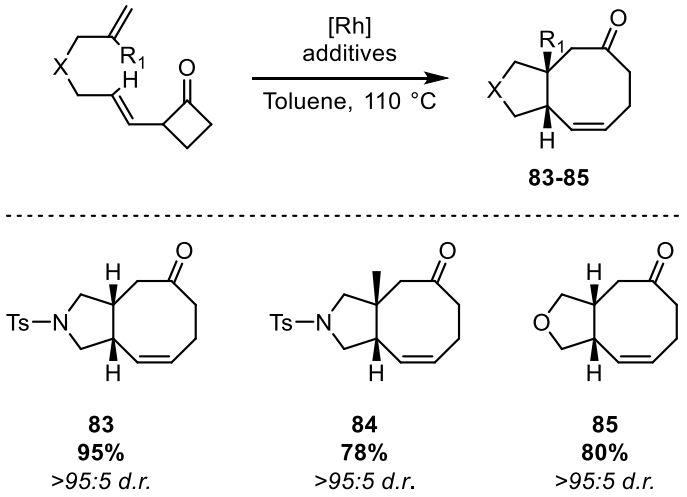

Figure 25 : Intramolecular rhodium-catalysed (4+2+2) cycloaddition of dienes with cyclobutanone

However, a common drawback of those rhodium-catalysed cycloaddition reactions is the competition between the (4+2) insertion and the decarbonylative pathway.[53] Dong and co-workers addressed this issue by developing a catalytic system involving the *in situ* conversion of the cyclobutanone **86** into an imine with the amino-pyridine additive **87**. The bridged bicyclic ketone **88** was isolated in excellent yield upon intramolecular cycloaddition of the olefin and hydrolysis of the transient imine (Figure 26).[54] Moreover, they showed that the reaction did not occur without the amino-pyridine additive, and instead a mixture of decarbonylated products was obtained. The asymmetric version of this reaction was reported to proceed in low yield with low enantiomeric excess.

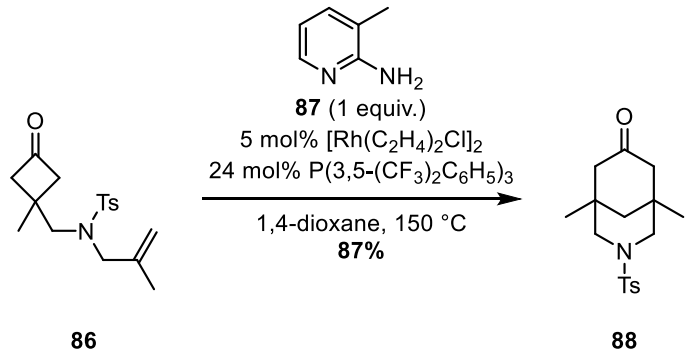

86 **88**

Figure 26: Intramolecular rhodium-catalysed (4+2) cycloaddition of alkene with activated cyclobutanone

Shortly after this report, the same authors took advantage of the decarbonylation pathway to produce eight-membered bicyclic compounds (Figure 27).[55] By changing to another rhodium pre-catalyst with XPhos, they could isolate the bridged eight-membered ring **89** in average yield. Interestingly, the cyclobutanone **70** gave only the decarbonylated cycloadduct **90**, as opposed to Murakami's and Cramer's reports.

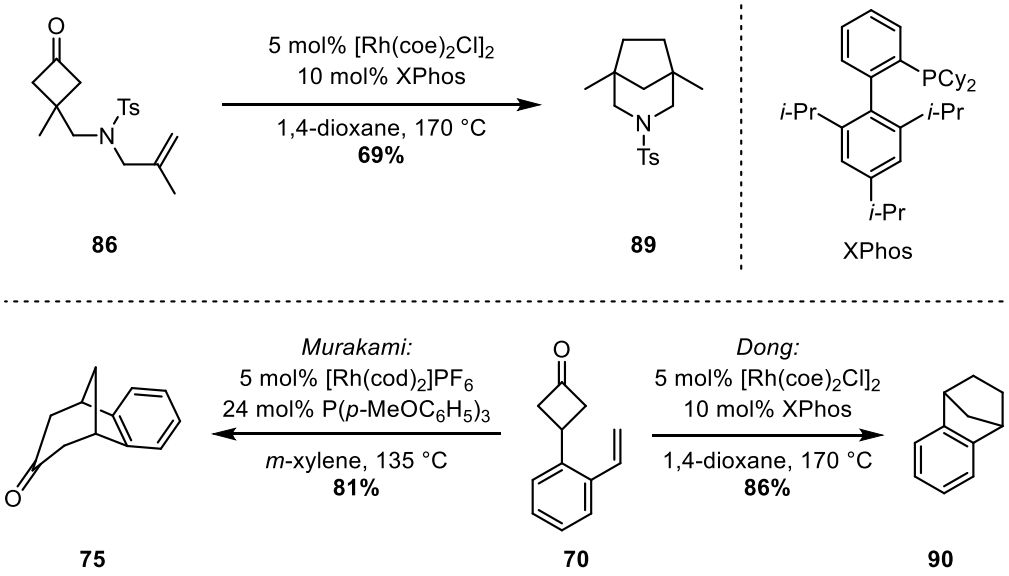

Figure 27: Intramolecular decarbonylative rhodium-catalysed (4+2) cycloaddition of alkene with cyclobutanone/comparison with previous work

4.1.2.2 Allenes

Whilst working on the rhodium-catalysed (4+2+2) cycloaddition of dienes, Wender and co-workers also applied this methodology to more challenging substrates such as allenes. For example, **92** could be obtained as the major diastereoisomer, in 91% yield from **91** (Figure 28).[52]

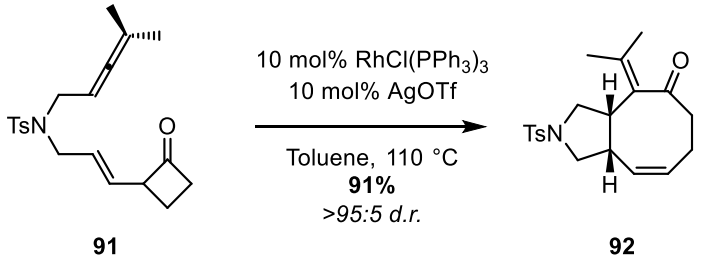

Figure 28 : Intramolecular rhodium-catalysed (4+2+2) cycloaddition of allene with cyclobutanone

In 2015, Dong's group reported that allenes could behave as a vinyl carbenoid and undergo a rhodium-catalysed (4+1) cycloaddition, as opposed to Wender's (4+2) cycloaddition (Figure 29).[56] By treating the tri-substituted allene **93**, the authors could

isolate the corresponding bridged bicyclo[3.2.1]nonanone **±94** in good yield. They also showed that the asymmetric version of this reaction could occur in excellent enantiomeric excess with the chiral phosphoramidite ligand **95**.

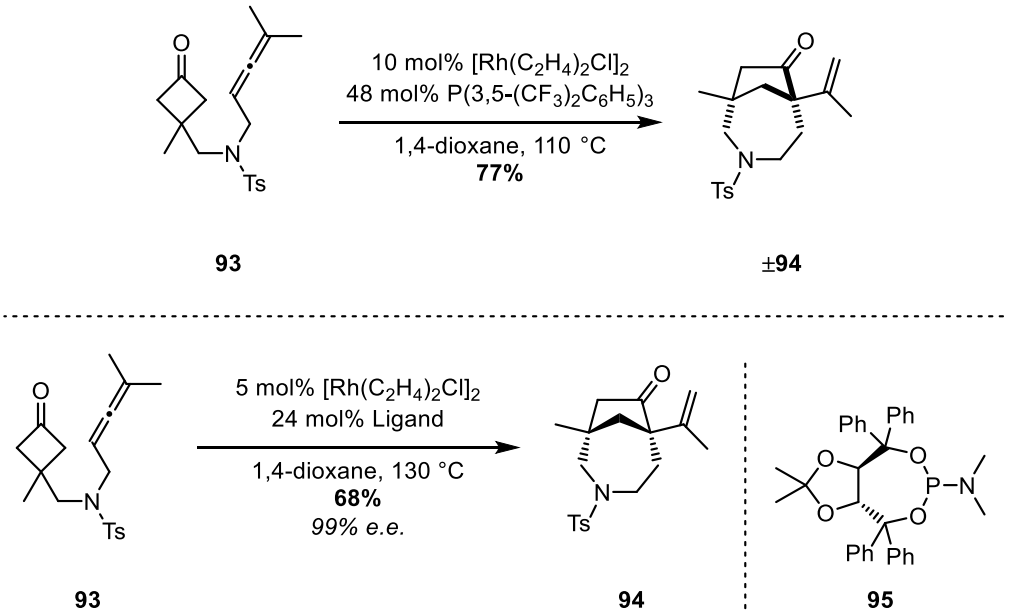

Figure 29: Intramolecular rhodium-catalysed (4+1) cycloaddition of allenes with cyclobutanone

4.1.3 Palladium-catalysed (4+4) cycloaddition

In 2014, Murakami and his group reported the use of a palladium catalyst for the cycloaddition of cyclobutanones bearing a silacyclobutane group (Figure 30).[57] Through C–C and C–Si bond cleavages, they could obtain the silabicyclo[5.2.1]decane **97** in excellent yield and diastereoselectivity. Moreover, the authors showed that the outcome of the reaction was ligand dependent as they could completely switch to the synthesis of the aldehyde **98** by using a less bulky phosphine.

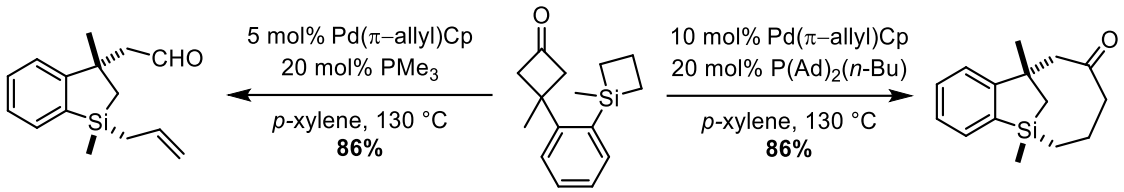

98 **96** **97**

Figure 30: Intramolecular palladium-catalysed (4+4) cycloaddition of silacyclobutane with cyclobutanone/ring opening of the cyclobutanone

4.2 Cyclobutenone

4.2.1 Nickel-catalysed (4+2) cycloaddition

As compared to cyclobutanones, the strain-energy of cyclobutenones is greatly increased because of the addition of an endocyclic double bond (31-34 kcal.mol^{-1} as compared to 26 kcal.mol^{-1} in cyclobutanones), explaining why most cycloaddition reactions must be executed at low temperature.[58]

Liebeskind *et al.* reported the (4+2) cycloaddition of alkynes with cyclobutenones to obtain functionalised phenols (Figure 31).[59] It is interesting that a phosphine ligand was not required to catalyse the reaction. Instead, it is believed that due to its nucleophilic character, a phosphine would inhibit the reaction by direct attack and opening of the cyclobutenone in an uncontrolled fashion.[60] Moreover, two additions of the nickel catalyst were required to drive the reaction to full conversion. Nonetheless, yields of the cycloaddition were ranging from 60% to 81%, without any selectivity when unsymmetrical alkynes were used, as illustrated with the product **100**.

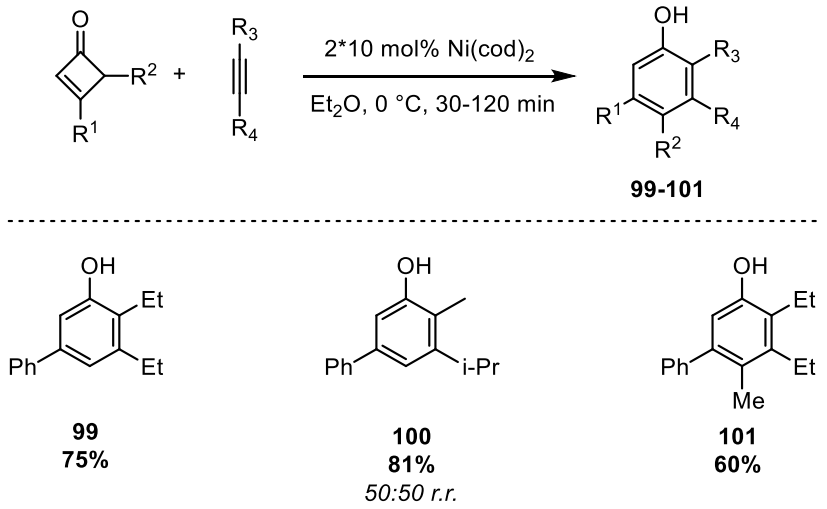

Figure 31: Nickel-catalysed (4+2) cycloaddition of alkynes with cyclobutenones

More recently, Harrity's group published two papers on the coupling of alkynes bearing with cyclobutenones (Figure 32).[61,62] Remarkably, they showed how, in a one pot reaction, nickel complexes could catalyse first the alkyne insertion followed by a Suzuki cross-coupling reaction to yield the biphenyl **105**.

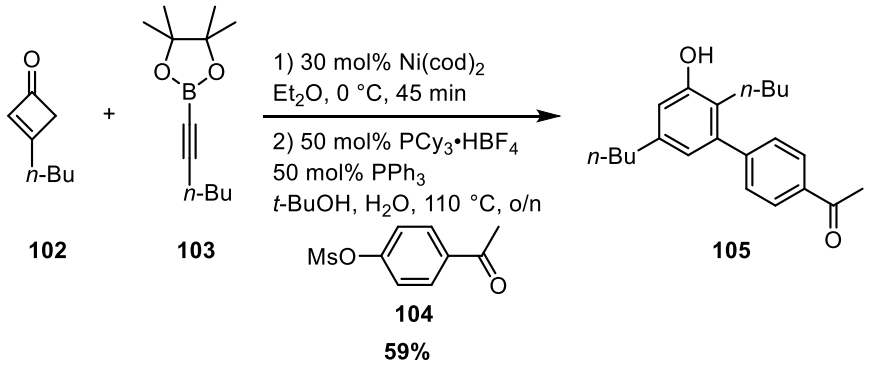

Figure 32: One-pot nickel-catalysed (4+2) cycloaddition of alkyne with cyclobutenone/Suzuki cross-coupling

4.2.2 Rhodium-catalysed (4+2) cycloaddition

Mitsudo's group showed that a rhodium complex could catalyse the cycloaddition of cyclobutenones and alkenes. At elevated temperature the authors

observed the insertion of 2-norbornene **107** into the cyclobutenone **106** (Figure 33).[63] Interestingly, the cyclohexenone **108** was obtained in excellent yield when the reaction was carried out under a carbon monoxide atmosphere. However, the cyclopentene derivative **109** was recovered as the sole product when the reaction was performed under an argon atmosphere. According to the authors, a reversible decarbonylation step can occur during the reaction, explaining why the cyclohexenone **108** was obtained when carbon monoxide was added to the reaction.

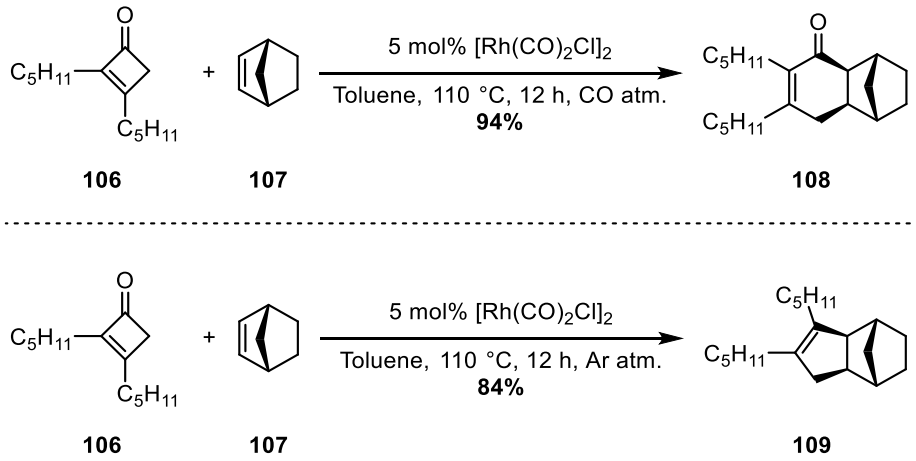

Figure 33: Rhodium-catalysed (4+2) cycloaddition/Decarbonylative rhodium-catalysed (4+2) cycloaddition of norbornene with cyclobutenone

In 2007, the same group reported the cycloaddition of both alkynes and electron-poor alkenes into cyclobutenone **110**, yielding the functionalised phenols **112** and **114** (Figure 34).[64] The authors did not observe the formation of a possible decarbonylated product, in contrast to the reaction of **106**.

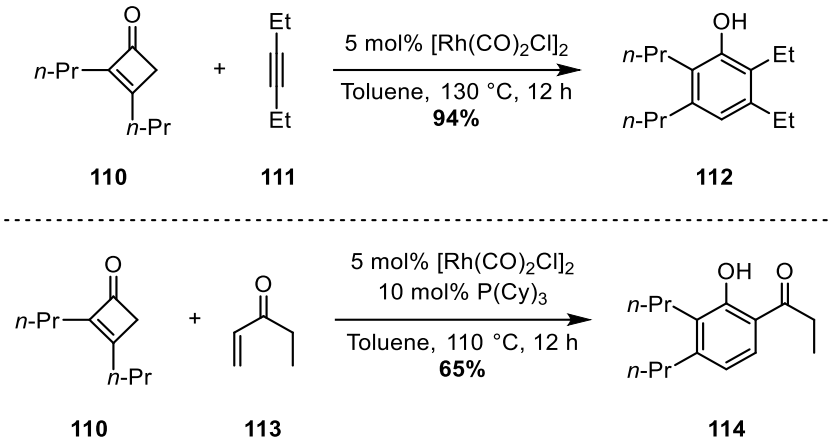

Figure 34: Rhodium-catalysed (4+2) cycloaddition of alkyne and alkene with cyclobutenone

4.2.3 Mechanistic insights

In 1990, Liebeskind *et al.* proposed that depending on the metal used, the cyclobutenone **115** could undergo ring-opening reaction *via* two pathways (Figure 35 and Figure 36).[65] With the cobalt complex **116**, they showed that the ring opens to generate the corresponding vinyl ketene complex **117**. The latter was further reacted with the alkyne **111** to yield the phenol **118**, which suggests that **117** is an intermediate in the cobalt-catalysed (4+2) cycloaddition of alkynes with cyclobutenones.

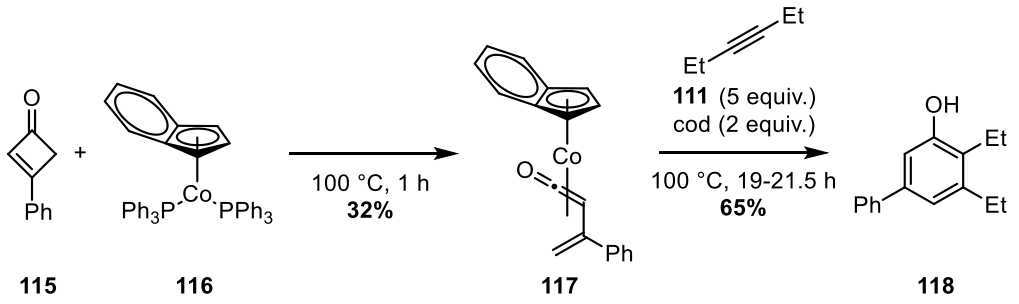

Figure 35: Cobalt-catalysed (4+2) cycloaddition of alkyne with cyclobutenone

However, another pathway was proposed proceeding *via* a direct oxidative addition of the metal inside the ring to form intermediate **A** (Figure 36). Insertion of

the alkyne would generate the heptametalacycle **B** which could give the desired product upon reductive elimination and re-aromatisation. In support of this rationale, the authors reported that the pentarhodacycle **120** was obtained when Wilkinson's catalyst **119** was reacted with the cyclobutenone **115**.[66]

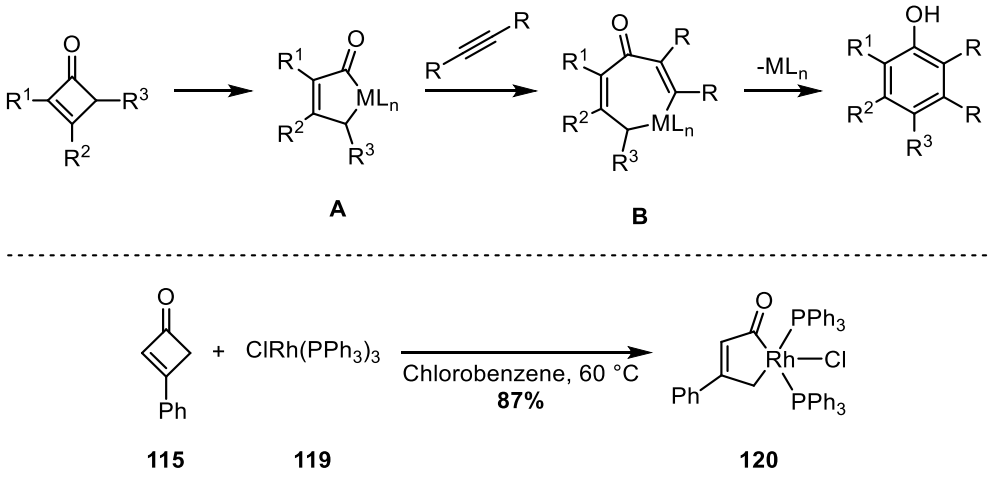

Figure 36: Alternative mechanism for the metal-catalysed (4+2) insertion of alkyne in cyclobutenone/isolation of a rhodium complex

These experiments suggest that both vinylketene complexes and metalla-cyclopentenones are possibly involved in the metal-catalysed cycloaddition of cyclobutenones.

The involvement of nickel complexes similar to **117** or **120** is likely, however, Liebeskind and Huffman were not able to isolate any intermediates. Harrity *et al.* isolated the ester **124** which arises from the attack of the phenol **123** onto the ketene-nickel intermediate **122** (Figure 37). Substituting the alkyne for phenol in the reaction gave the ester **125**, confirming that the vinyl ketene complex is more likely to be involved in the nickel catalysed (4+2) cycloaddition of cyclobutenones than a possible pentanickelacycle.

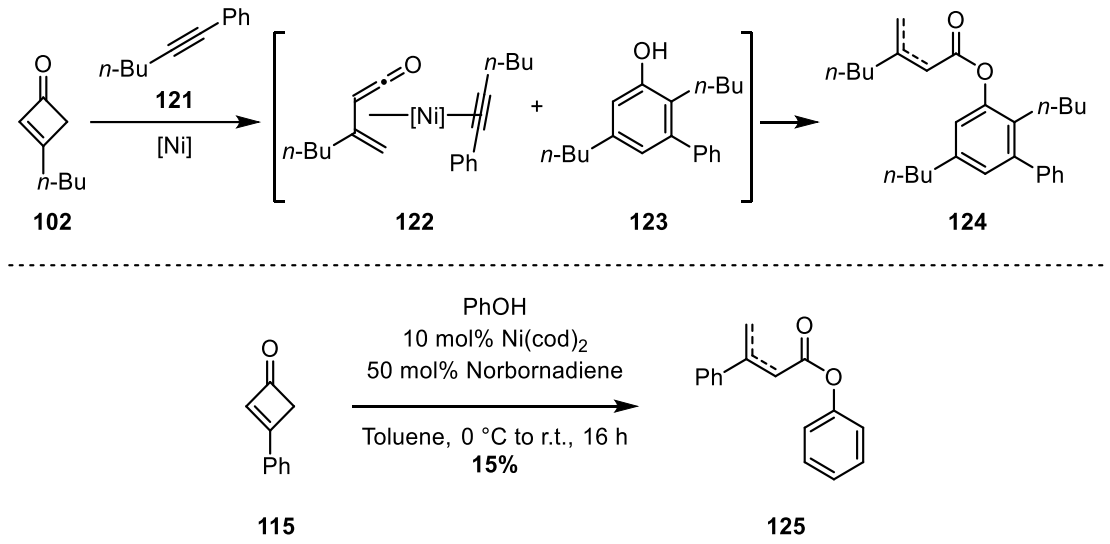

Figure 37: Isolation of intermediates in the nickel-catalysed (4+2) cycloaddition of alkynes with cyclobutenone

4.3 Benzocyclobutenone

4.3.1 Nickel-catalysed (4+2) cycloaddition

In contrast to cyclobutenones, benzocyclobutenones often require elevated temperatures to undergo ring-opening reactions.

Martin's group has shown that a nickel catalyst could trigger the ring opening reaction of benzocyclobutenones. The insertion of unsaturated substrates can occur in two positions, *ie.* proximal or distal (Figure 38). The reactivity of benzocyclobutenones typically involves the cleavage of the C^1–C^8 bond, as illustrated in the rearrangement of **126**.[67]

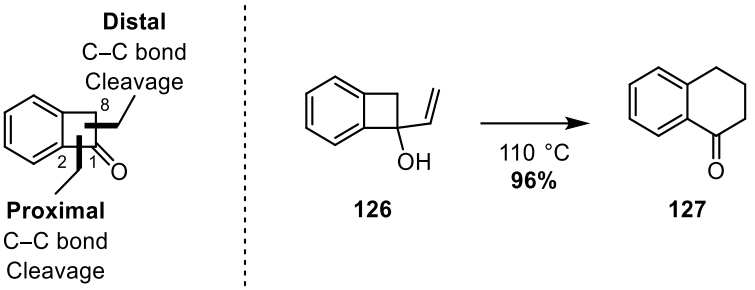

Figure 38: Distal C−C bond cleavage of benzocyclobutenone

However, Martin and co-workers reported that in the case of the α-substituted benzocyclobutenone **128**, the reaction proceeded through the unusual *proximal* C1−C2 bond cleavage (Figure 39).[68] The reactions of the diene **129** and alkyne **131** with the benzocyclobutenone **128** gave the corresponding benzocyclooctanone **130** and naphthol **132** respectively. Interestingly, when alkynes were used, the nickel/phosphine ratio had to be decreased to 1:1, in order to reach full conversion.

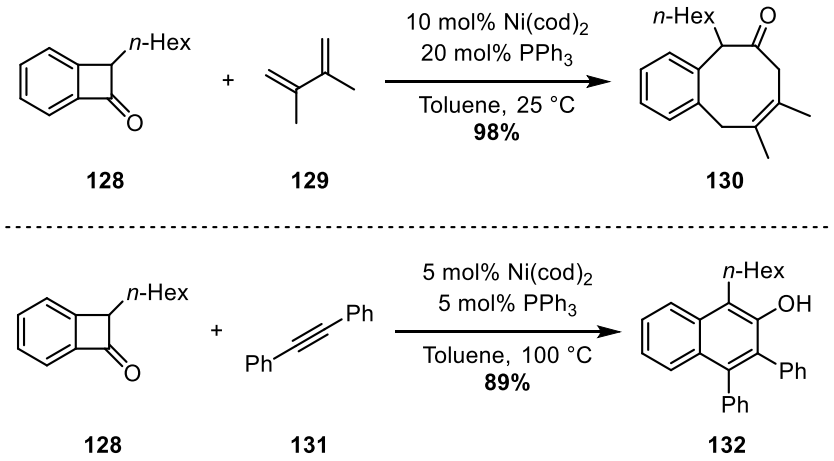

Figure 39: Nickel-catalysed (4+2) cycloaddition of diene and alkyne with benzocyclobutenone

4.3.2 Rhodium-catalysed (4+2) cycloaddition

Dong's group reported the rhodium-catalysed intramolecular insertion of alkene **133**, alkyne **135** and methyl oxime **137** in benzocyclobutenones (Figure 40).[69,

[70, 71] The asymmetric version of the alkene insertion has been reported by the same group.[72] Recently, they have used this approach to synthesise (–)-cycloclavine and the (–)-5-epi-cycloclavine derivative.[73]

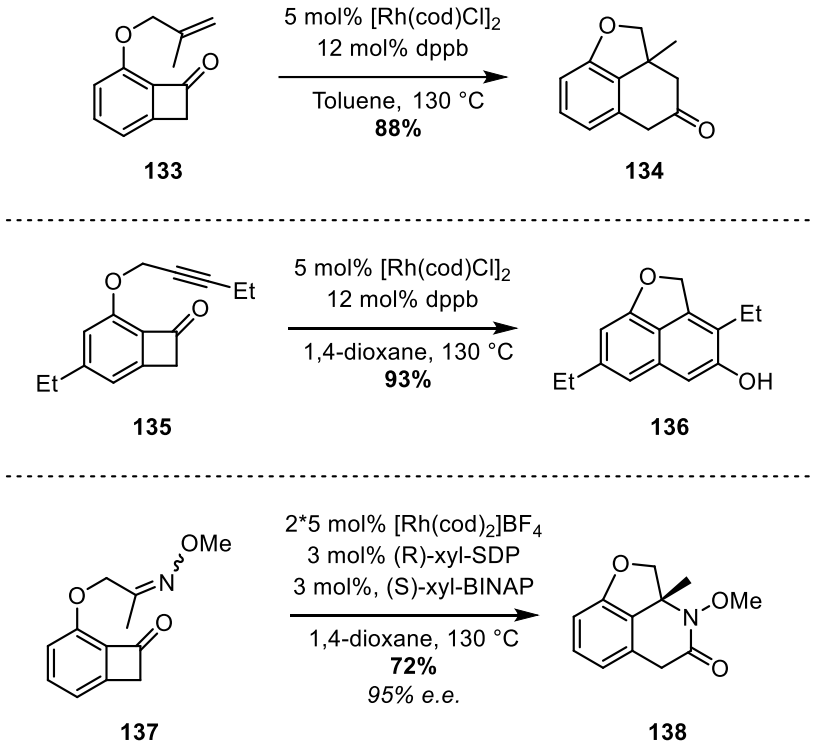

Figure 40: Intramolecular rhodium-catalysed (4+2) cycloaddition of alkene/alkyne/oxime with benzocyclobutenone

Moreover, Dong and co-workers have extended the reactivity of benzocyclobutenones to the intramolecular cobalt-catalysed (4+2) insertion of alkynes.[74]

4.4 Azetidinones & oxetanones

Investigations towards the reactivity of azetidinones and oxetanones in the presence of metal catalysts have also been reported. As seen previously, Aïssa's group reported an extensive study of the nickel-catalysed (4+2) cycloaddition of alkynes **139a-f** in the Boc-protected azetidinone **53**.[44] Symmetrical alkynes reacted almost

quantitatively (Table 1, entry **1**), while unsymmetrical alkynes led to a mixture of cycloadducts **140** and **141** (Table 1, entry **2-6**). Although highly regioselective, a trend connecting the steric hindrance of the alkyne and the corresponding ratio of products was observed. By decreasing the steric bulk of the alkyl group, a slight erosion of the regioselectivity was obtained (Table 1, entry **3** vs **4**). With a sterically biased alkyne, only one regioisomer was obtained, confirming that the steric hindrance is the main factor influencing the regioselectivity (Table 1, entry **6**). Moreover, electronic factors did not seem to guide the regioselectivity of the insertion, as both electron-donating and electron-withdrawing substituents on the aromatic ring led to the same regioisomeric ratio (Table 1, entry **3** vs **5**).

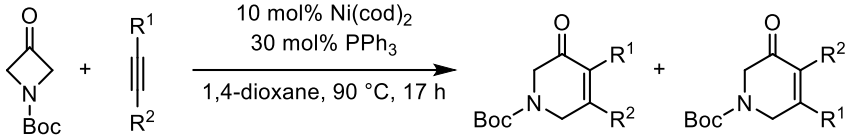

53 **139a-f** **140a-f** **141a-f**

Entry	R^1	R^2	Ratio (140/141)	Yield [%][a]
1	Ph	Ph	N/A	90
2	Me	Ph	87:13	92
3	*n*-Bu	*p*-$MeOC_6H_4$	89:11	89
4	*i*-Bu	*p*-$MeOC_6H_4$	84:16	91
5	*n*-Bu	*p*-$MeCOC_6H_4$	89:11	99
6	Me	*t*-Bu	100:0	87

a) Combined yield of **140** and **141**. *b)* Ratio determined by ^1H NMR of an inseparable mixture of **140** and **141**.

Table 1: Nickel-catalysed (4+2) cycloaddition of alkyne with Boc-protected azetidinone

In the same study, the authors reported the nickel-catalysed insertion of the alkyne **139e** into oxetanone **142** to obtain the pyranone **143** in high yield (Figure 41). However, a small decrease of regioselectivity was observed due to the lower steric impact of the oxygen during the regioselectivity-determining alkyne insertion, which will be presented in the next section.

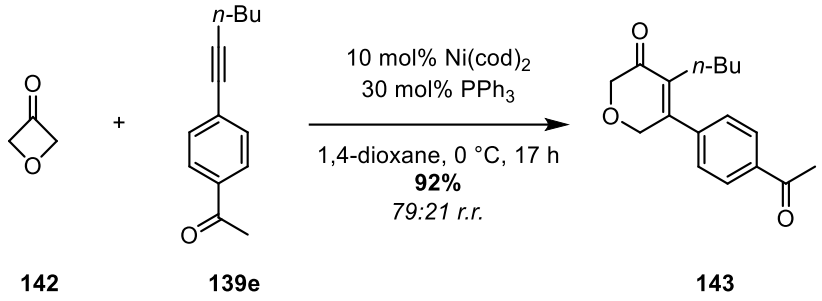

142 **139e** **143**

Figure 41: Nickel-catalysed (4+2) cycloaddition of alkyne with oxetanone

Shortly after this work was disclosed, two reports on the nickel-catalysed (4+2) cycloaddition of alkynes with azetidinone were published from Murakami's and Louie's group.[75, 76] Both groups showed that the catalyst loading could be decreased whilst maintaining good reactivity. The scope of substrates was extended to α-substituted azetidinones and to stannyl-substituted alkynes (Figure 42).

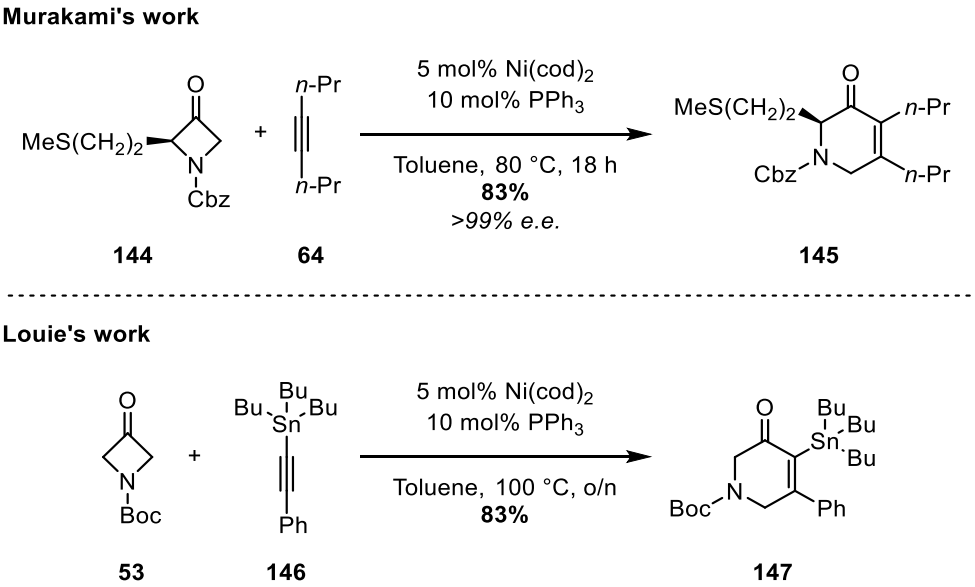

Figure 42: Nickel-catalysed (4+2) cycloaddition of alkyne with Boc-protected azetidinone reported by Louie and Murakami

Louie's group also showed that both the Boc-protected azetidinone **53** and the oxetanone **142** were suitable for the nickel-catalysed (4+2+2) cycloaddition of dienes and diynes with small rings (Figure 43).[77,78] Interestingly, they showed that the insertion of the diyne **148** could proceed at low temperature, whilst the diene **151** required an increase of both the amount of catalyst and the temperature. Nonetheless, they obtained the corresponding eight-membered rings in good yields.

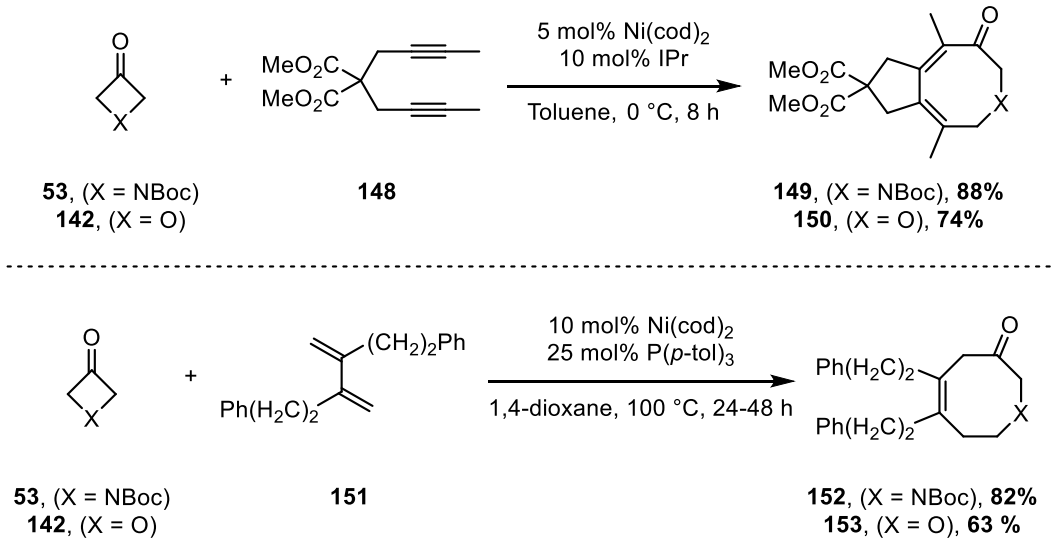

Figure 43: Nickel catalysed (4+2+2) cycloaddition of diyne and (4+4) cycloaddition of diene in oxetanone

4.5 Regioselectivity of the nickel-catalysed (4+2) cycloaddition of alkynes with four-membered rings

As shown previously, good levels of regioselectivity were achieved when alkynes bearing an aryl and alkyl substitutents were used in the reaction (See Table 1, entry **2-5**). Moreover, excellent selectivity was also achieved when the unsymmetrical alkyne **139f** was used, due to the significant steric differentiation between the two substituents of the alkyne. Similarly, the same outcome was obtained when the electronically biased alkyne **154** was mixed with the Boc-protected azetidinone **53** (Figure 44).

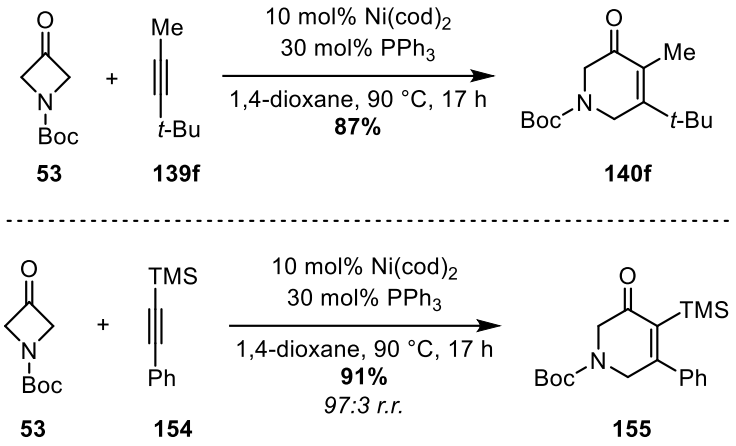

Figure 44: Regioselective nickel-catalysed (4+2) cycloaddition of biased alkynes with Boc-protected azetidinone

Two plausible mechanisms have been described for the nickel-catalysed (4+2) cycloaddition of alkynes in four membered rings (Figure 45). Both mechanisms rely on the complexation of the alkyne and the ring to the nickel center to generate the complex **A**. In 2005, Ogoshi and co-workers reported the formation and isolation of **157** which was converted to **158** in quantative yield, upon addition of trimethyl aluminium. [79,80] Thus, it was hypothesised that the mechanism leading to the six-membered ring could occur *via* the formation of the intermediate **B** through an oxidative cyclisation. A β-carbon elimination followed by reductive elimination would lead to the release of the active species along with the cycloadduct.

However, DFT calculations reported by Lin and co-workers suggested an alternative pathway. Although thought to be facile due to release of the ring strain, the authors have shown that the β-carbon elimination step is unlikely to proceed because of the high energy barrier (46.7 kcal.mol^{-1} and 56.5 kcal.mol^{-1} depending on the coordination model).[81] Instead, the oxidative addition of the nickel catalyst into the azetidinone ring through a C–C bond cleavage can afford complex **D**. The insertion of

the alkyne can occur in two positions, leading to either **C** or **E**. A final reductive elimination can regenerate the catalyst and liberate the cycloadduct.

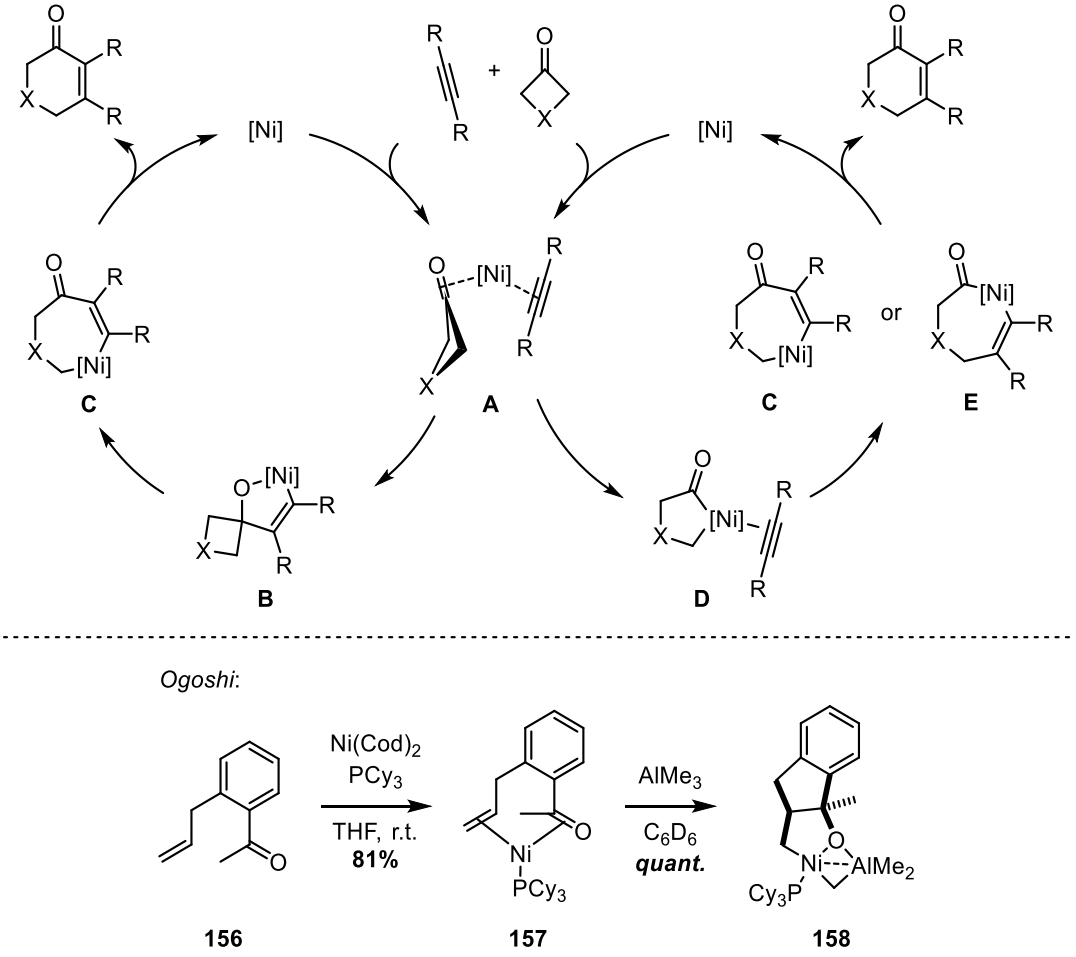

Figure 45: Plausible mechanisms for the nickel-catalysed (4+2) cycloaddition of alkyne with azetidinone

If considering the oxidative cyclisation pathway, an explanation for the observed regioselectivity was given based on the steric hindrance of the alkyne (Figure 46). After the coordination of the alkyne to the nickel catalyst, the two complexes **159** and **160** can be generated. The β-carbon elimination of these species would lead to **161** and **162**, whose reductive elimination would give the observed products. However, when comparing the stability of **159** versus **160**, it is easy to understand that a distabilising interaction between the large group of the alkyne and the azetidine ring

prevents the formation of **162**. Thus, the cycloadduct with the largest group in distal position in respect to the carbonyl group is thus favoured.

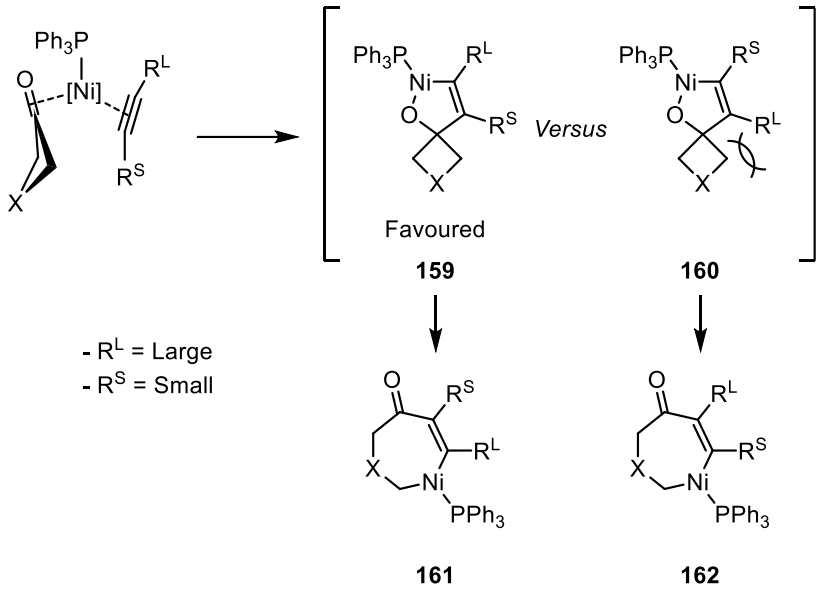

Figure 46 : Mechanism of the nickel catalysed (4+2) cycloaddition of alkynes with azetidinone

When considering the second mechanism Lin *et al.* proposed a different explanation. During the migratory insertion of an unsymmetrical alkyne bearing two alkyl groups, four different transition states can be considered (Figure 47). Calculations suggest that the migratory insertion of the alkyne into the Csp^3–Ni bond is disfavoured (**TS-1** and **TS-2**). Thus, the insertion must occur *via* the cleavage of the Csp^2–Ni bond with the largest group on the alkyne away from the carbonyl moiety in order to limit steric interactions (**TS-4**). This mechanism leads to the same regioselectivity that is observed experimentally and that was explained by the formation of the oxidative cyclisation intermediate **159**.

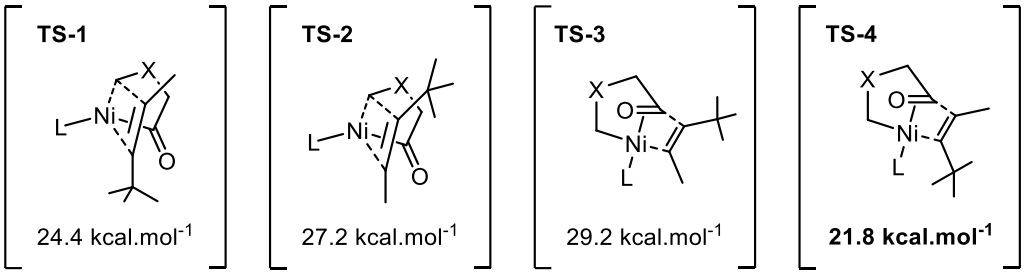

Figure 47: Four possible transition-states of the nickel-catalysed (4+2) cycloaddition of alkyne with azetidinone

Moreover, the calculation showed that the reactivity is completely reversed in the case of a silyl-substituted alkyne. Thus, the cleavage of the Csp^3–Ni becomes favoured and the alkyne acts as the electrophile. Due to the polarisation of the alkyne, a partial positive charge can be assumed on the methyl-substituted carbon, making the nucleophilic attack preferred on this site, and the transition-state **TS-1** favoured (Figure 48).

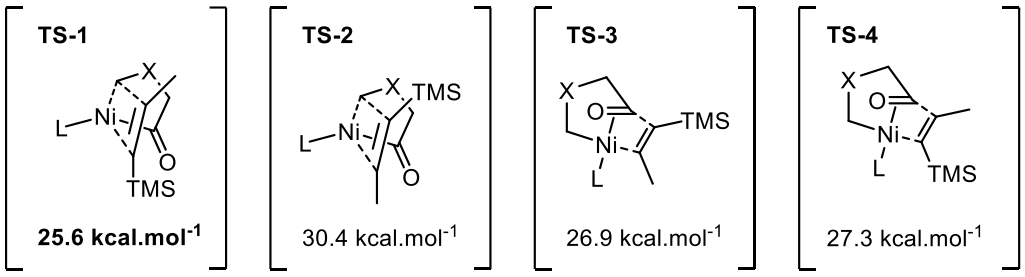

Figure 48: Four possible transition-states of the nickel-catalysed (4+2) cycloaddition of silylated-alkyne with azetidinone

Nonetheless, using the alkyne **163** with a decreased steric bias led to almost no selectivity and both products **164** and **165** were obtained as a 60:40 ratio (Figure 49). It is important to understand that this mixture of regioisomers could not be resolved by normal purification methods, making this (4+2) cycloaddition extremely limited in terms of possible applications.

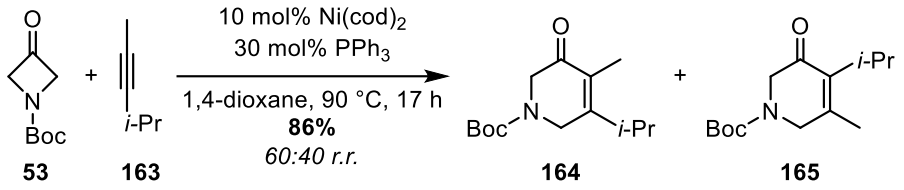

Figure 49: Non-regioselective nickel catalysed (4+2) cycloaddition of unsymmetrical alkynes

5 Aims and objectives

As seen previously in the introduction, efficient syntheses of functionalised pyridinols are scarce. Although elegant, the intramolecular cyclisations developed by Donohoe, Yoshida, Fedorov and Tong to access functionalised 3-pyridinols require an extensive synthesis of complex precursors prior to the key-step. However, methods relying on transition-metal catalysed cycloaddition have proven to be a possible alternative to overcome these issues. Aïssa, Louie and Murakami groups have shown that nickel catalysts could be used to access 3-dihydropyridinones from azetidinones and alkynes.[44, 75, 76] The transformation of those intermediates could give the desired 4,5-substituted 3-pyridinols upon re-aromatisation of the ring, enabling a rapid access to biologicaly interesting compounds such as **166** and **167** (Figure 50).

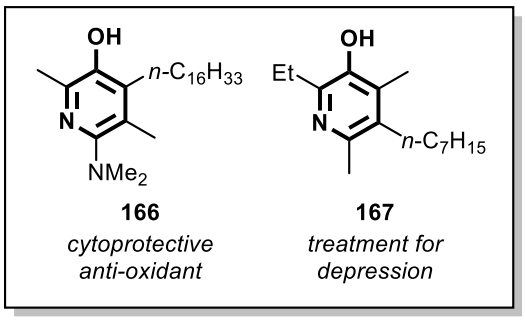

Figure 50: Possible target for the synthesis of 4,5-substituted 3-pyridinols

However, one remaining issue is the lack of regioselectivity regarding the cycloaddition of unsymmetrical alkynes substituted with alkyl groups. The aim of this project is to develop a new methodology enabling the access to 4,5-substituted 3-pyridinols *via* a regioselective nickel-catalysed (4+2) insertion of alkynes as the key-step of the synthesis.

6 Preliminary results and hypothesis

6.1 Effect of the ligand on the regioselectivity

The issue of regioselectivity is particularly relevant in the case of substituted alkynes without electronic or steric bias. Improvement of the regioselectivity was attempted by changing the ligand used for the (4+2) cycloaddition (Table 2). When subjecting the tosyl-protected azetidinone **168** and the non-biased alkyne **163** to the previously optimised conditions with triphenyl phosphine, the expected mixture of regioisomers **169**/**170** was obtained in good yield with a ratio of 54:46 (Table 2, entry **1**). When changing to a bulkier and more electron-rich phosphine, *i.e.* tricyclohexyl phosphine, the yield decreased and the selectivity switched in favour of **170** (Table 2, entry **2**). With another aromatic phosphine, the yield decreased as compared to the original attempt (Table 2, entry **3**). Using trimethyl phosphine did not improve the result (Table 2, entry **4**). Finally, using IMes·HCl led to the decomposition of the starting material due to the base used to generate the *N*-heterocarbene (NHC) (Table 2, entry **5**). Changing the solvent from THF to toluene and decreasing the NHC/base loading gave the same result, and decomposition of the azetidinone was observed (Table 2, entry **6**).

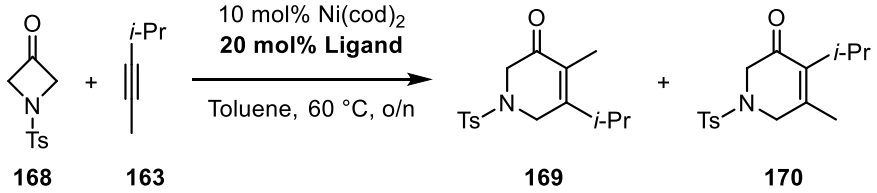

Entry	Ligand	Yield (%)[a]	Ratio (169/170)[b]
1	PPh_3	97	54:46
2	PCy_3	77	42:58
3	$P(Ph_2)t$-Bu	83	52:48
4	PMe_3	67	56:44
5[c]	IMes.HCl	Decomposition	N/A
6[d]	IMes.HCl	Decomposition	N/A

a) Combined yield. *b)* Determined by ^{1}H NMR using trimethoxybenzene as an internal standard. *c)* Using 10 mol% $Ni(cod)_2$, 20 mol% IMes, 20 mol% *t*-BuOK in THF. *d)* Using 12 mol% $Ni(cod)_2$, 10 mol% IMes, 10 mol% *t*-BuOK in toluene.

Table 2 : Optimisation of the regioselectivity of the nickel-catalysed (4+2) cycloaddition of alkyne with Tosyl-protected azetidinone

The low regioselectivity could not be resolved by changing the ligand and all attempts led to an unseparable mixture of products. A more comprehensive ligand screening would be required to gain further insight into the possible effects on the regioselectivity of the nickel catalysed reaction of unsymmetrical alkynes.

6.2 Conjugated 1,3-enynes as alkyne surrogates

In 2008, whilst working on a (3+2) cycloaddition of alkynes with α-unsaturated amides, Fagnou *et al.* reported the same issues of regioselectivity, when dealing with unsymmetrical bisalkylalkynes (Figure 51).[82] Using a rhodium catalyst, the authors obtained a mixture of **173** and **174** in 78% yield with a ratio of 1.8:1. Similarly to the

nickel-catalysed (4+2) cycloaddition, the compounds were inseparable through normal purification techniques and the mixture could not be resolved.

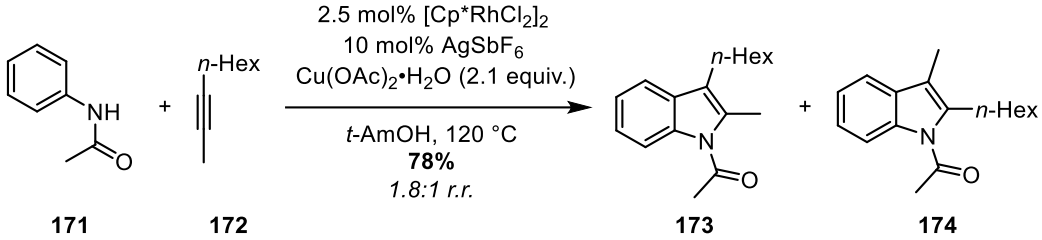

Figure 51 : Rhodium-catalysed (3+2) cycloaddition of alkynes with phenyl-acetamide

Nonetheless, in 2011 the authors reported the highly regioselective addition of conjugated 1,3-enynes that is controlled by electronic effects of the extra alkene (Figure 52).[83] To their delight, they were able to obtain one regioisomer over the other by changing the position of the double bond on the substrate. Hence, the 1,3-enyne **176** led to the formation of **177**, whereas the 1,3-enyne **179** gave **180**. It is noteworthy that, in all cases, only one isomer was observed with the double bond at the 2-position of the synthesised indole. Upon hydrogenation of the alkene, the complementary (3+2) regioisomers **178** and **181** were obtained in good yields. Thus, **176** and **179** were used as surrogates of the bis-alkylalkyne **182**, which would have led to a mixture of **178** and **181** if used in the rhodium catalysed (3+2) cycloaddition with **175**.

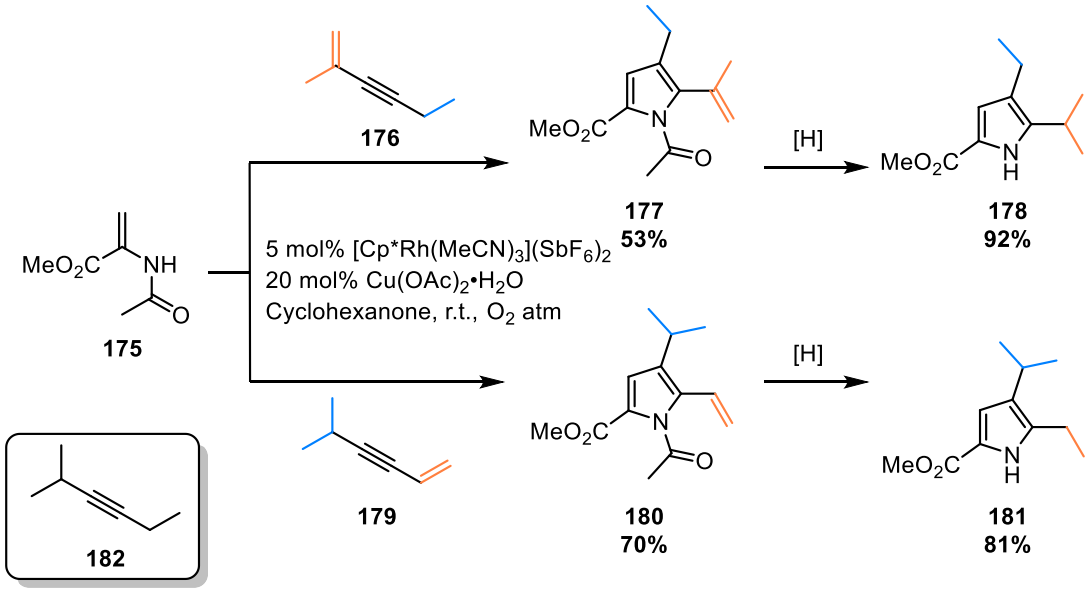

Figure 52 : Regioselective rhodium-catalysed (3+2) cyloaddition of conjugated 1,3-enynes with vinyl-acetamide

Jamison and Montgomery have also observed excellent regioselectivities in the nickel-catalysed reductive coupling of aldehydes with 1,3-enynes (Figure 53).[84, 85]

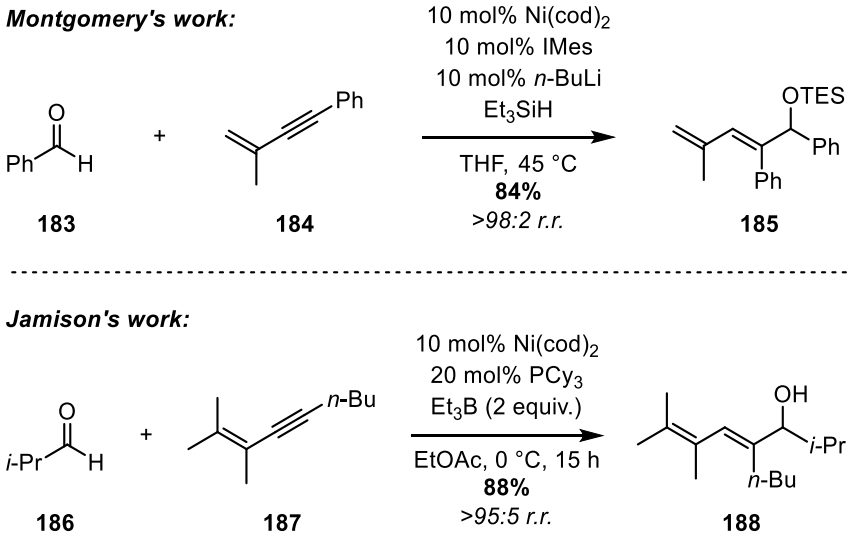

Figure 53: Nickel catalysed reductive coupling of 1,3-enynes with aldehydes

A computational study suggested that the complexation of the double bond to the metallic centre significantly decreases the energy barrier of the transition state,

making pathway **A** the most favoured (Figure 54).[86] When the alkene is not coordinated to the metal in pathway **B**, the calculated energy of the transition-state was almost 10 kcal.mol^{-1} higher, showing that this coordination is important both for the reactivity and the selectivity. Finally, pathway **C**, would lead to the formation of the minor regioisomer but was highly disfavoured with an energy barrier of 32.5 kcal.mol^{-1}.

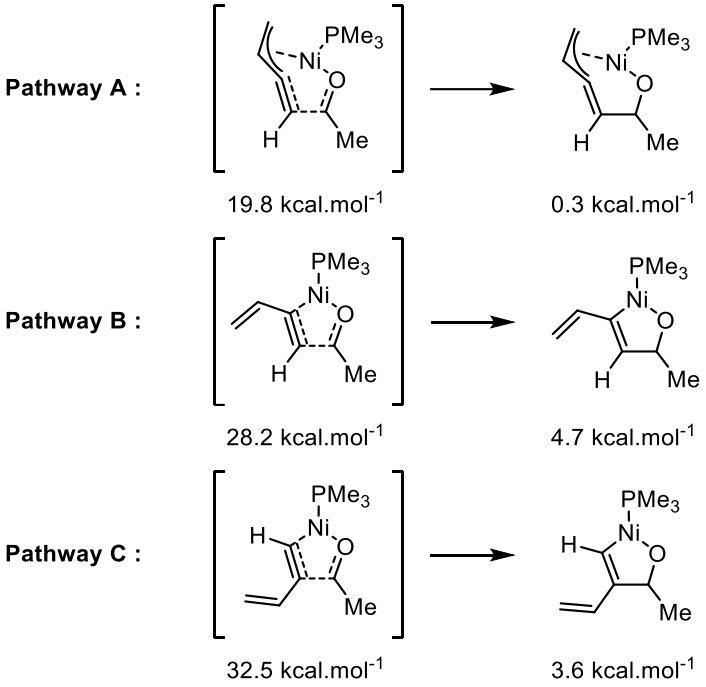

Figure 54 : Computational studies of a nickel catalysed coupling of aldehyde with conjugated 1,3-enynes

Therefore, when applying the same reasoning to the nickel catalysed (4+2) insertion of 1,3-enynes in azetidinones, the observed regioselectivity can be explained by the coordination of the olefin in the transition-state **TS-AB** in the regioselevity-determining step (Figure 55). The six-membered cycloadduct **D** is obtained with the alkene distal to the carbonyl group after β-carbon elimination to **C** and reductive elimination of the catalyst.

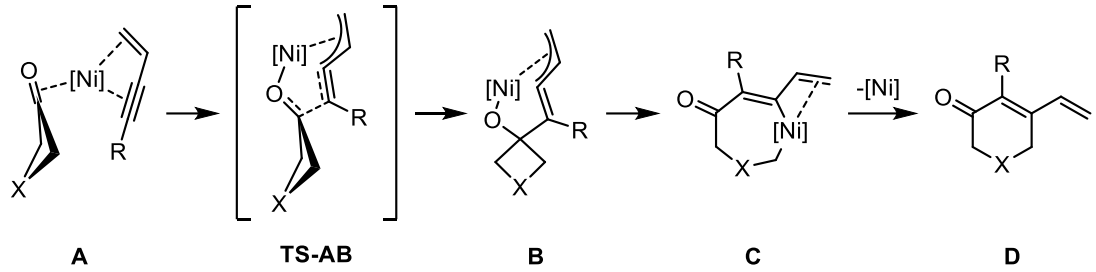

Figure 55 : Plausible mechanism of the nickel catalysed (4+2) cycloaddition of conjugated 1,3-enynes in azetidinone

However, if the reaction proceeds *via* the mechanism proposed by the computational study reported by Lin, then the regioselectivity could be explained by looking at the two transition states **TS-1** and **TS-2** (Figure 56).[81] In the case of the cycloaddition of unsymmetrical bis-alkylalkynes it has been shown that the Csp^2–Ni bond cleavage is favoured over Csp^3–Ni bond cleavage, thus only those two transition states are discussed here to explain the regioselectivity. If the coordination of the olefin to the metal is responsible of the regioselectivity of the reaction, then **TS-2** must be favoured over **TS-1**, leading to the same regioisomer observed experimentally.

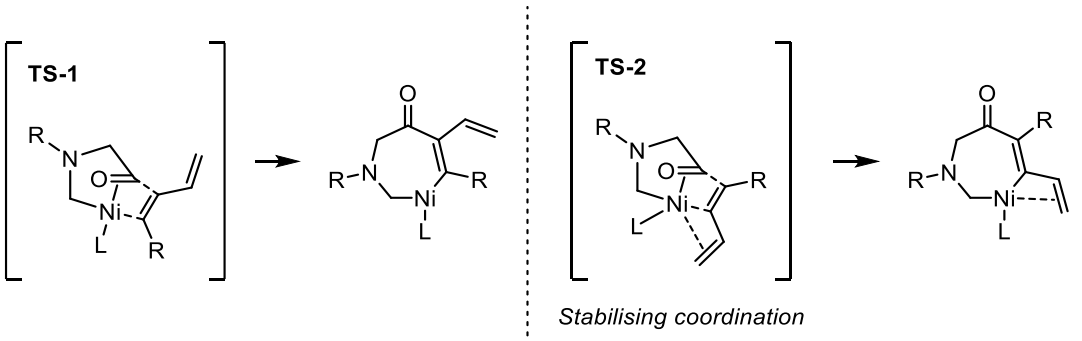

Figure 56: Two possible transition-states of the nickel-catalysed (4+2) cycloaddition of 1,3-enynes with azetidinone through the alternative mechanism

Thankfully, the conjugated 1,3-enyne **176** underwent the nickel-catalysed (4+2) cycloaddition with the Boc-protected azetidinone **53** to give a mixture of the regioisomers **189** and **190** (Figure 57).[44] Although the selectivity was not as good as

in the rhodium-catalysed (3+2) work described by Fagnou, Montgomery and Jamison, a simple column chromatography could resolve the mixture, making this method convenient to use.

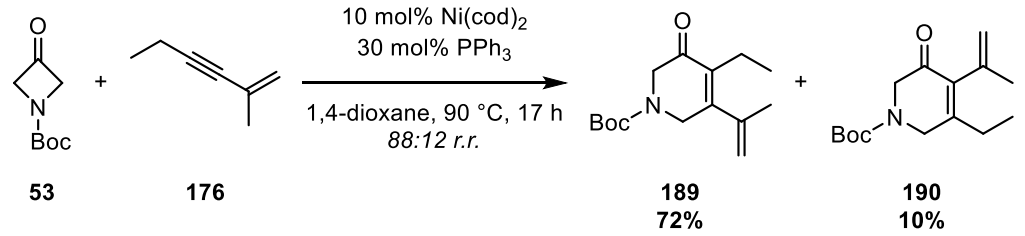

53 **176** **189** **72%** **190** **10%**

Figure 57 : Regioselective nickel catalysed (4+2) cycloaddition of conjugated 1,3-enynes with the boc-protected azetidinones

6.3 Hypothesis

It has been shown by the Aïssa group that Boc-protected azetidinone underwent the 2-steps sequence to 3-pyridinols, smoothly. However, the re-aromatisation of the ring was relatively demanding and required several manipulations to isolate the desired product. On the other hand, tosyl-protected azetidinones showed great results when used in the nickel-catalysed (4+2) insertion of alkynes and would allow an easier access to 3-pyridinols by elimination of the protecting group followed by immediate re-aromatisation.

The selectivity induced through electronic effects from the conjugated 1,3-enynes could allow an elegant and quick process towards the regioselective synthesis of 3-dihydropyridinones. Removal of the undesired double bond *via* hydrogenation followed by re-aromatisation of the ring would lead to the 4,5-substitued 3-pyridinol (Figure 58). By carefully selecting the 1,3-enyne used, a library of 3-pyridinols acting as pair of regioisomers could be accessed.

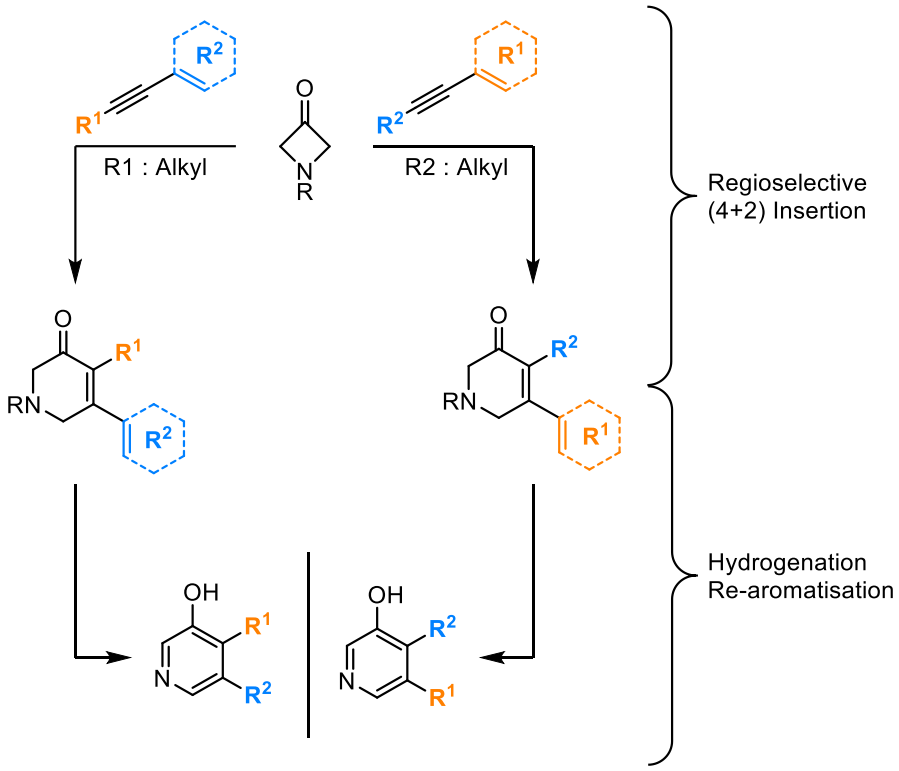

Figure 58: Regioselective synthesis of 3-hydroxy-4,5-alkyl-substituted pyridines using 1,3-enynes as alkynes surrogates

7 Nickel catalysed (4+2) cycloaddition of conjugated 1,3-enynes with azetidinones

7.1 1,3-Enynes synthesis

To judge the applicability of 1,3-enynes towards the (4+2) insertion in azetidinones, a panel of 1,3-enynes were carefully selected for their diversity with respect to the substitution pattern to assess the regioselectivity (Figure 59). Molecules **191a,c,e,g,i,k,m** will allow the study of the possible effects of the coordination of the alkene to the metal centre. Both highly hindered alkenes (**191a** and **191e**) and more accessible ones (**191c**, **191g** and **191k**) will be screened for the reaction. With

191b,d,**f**,**h**,**j,l**, the goal is to address the effects of the alkyl chain on the regioselectivity of the insertion. Different alkyl chains, with various substitution patterns, were selected in order to inverstigate as much as possible the impact of the steric hindrance on this side of the alkyne on the regioselectivity. Compounds **191i**, **191j** and **191m** will also provide information on the reaction selectivity when both steric and electronic factors are competing to direct the outcome of the insertion.

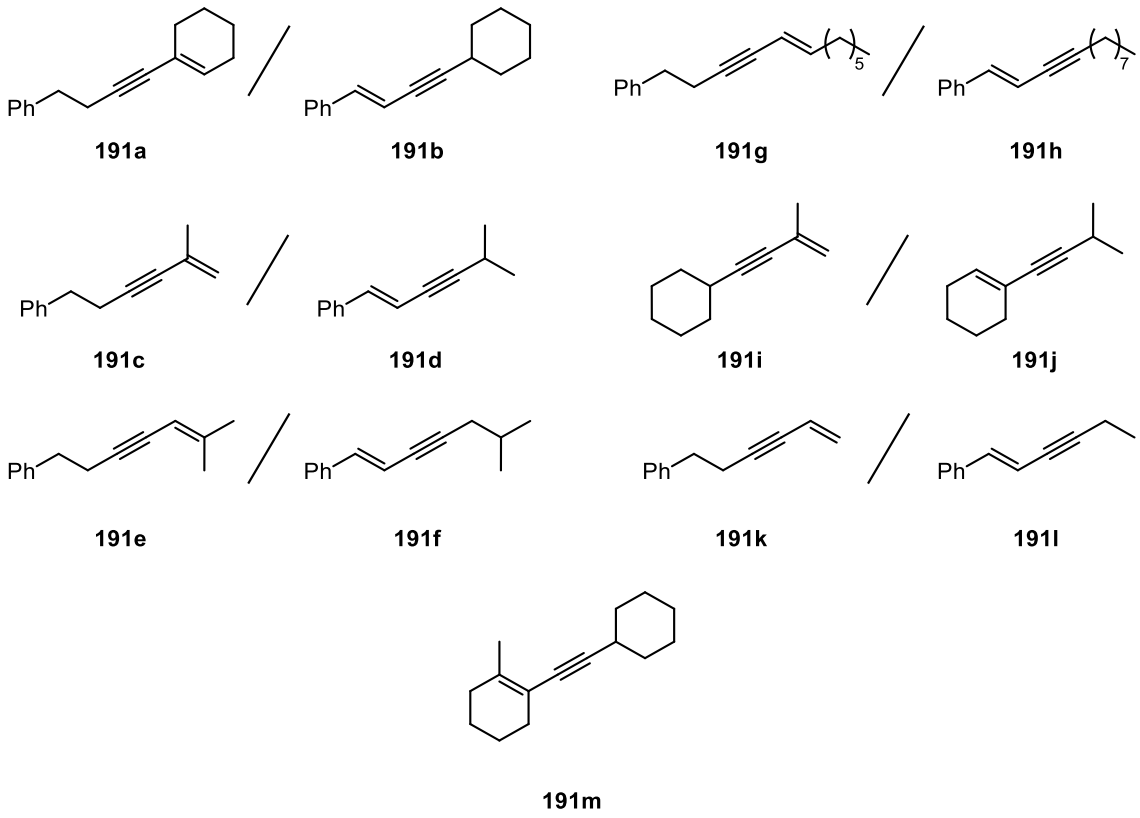

Figure 59 : Selected conjugated 1,3-enynes

All enynes but **191l** and **191m** were synthesised *via* a Sonogashira cross-coupling from a terminal alkyne and the corresponding alkenylbromide (Table 3). The use of classical conditions led, in most cases, to the desired 1,3-enyne in good to excellent yields. In the case of **191a** (Table 3, entry **1**), cyclohexenyl triflate had to be used instead of the corresponding bromide due to the high cost of the latter.

Interestingly, classical conditions did not allow the access to **191c**, **191e** nor **191g**, as no reaction occurred when subjected to the palladium catalyst (Table 3, entry **3**, **5** and **7**).

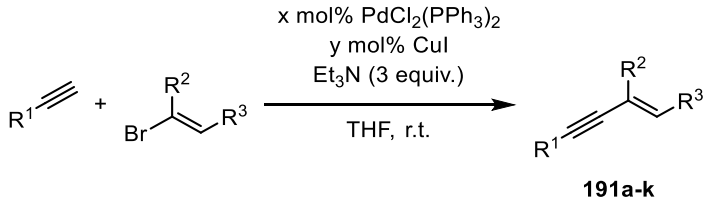

Entry	R^1	Alkene R^2	Alkene R^3	x (mol%)	y (mol%)	Product	Yield (%)
1	$Ph(CH_2)_2$	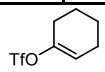		5	7	**191a**	51
2		H	Ph	5	7	**191b**	85
3	$Ph(CH_2)_2$	Me	H	5	7	**191c**	0
4	*i*Pr	H	Ph	5	7	**191d**	90
5	$Ph(CH_2)_2$			5	7	**191e**	0
6	*i*Bu	H	Ph	5	7	**191f**	Quant.
7	$Ph(CH_2)_2$	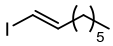		2	3	**191g**	0
8	$CH_3(CH_2)_7$	H	Ph	2	3	**191h**	85
9	Cy	H	Ph	5	7	**191i**	85
10	Cy	Me	H	2	3	**191j**	62
11	$Ph(CH_2)_2$	H	H	5	7	**191k**	97

Table 3: Synthesis of 1,3-enynes *via* Sonogashira cross-coupling

A palladium tetrakis(triphenylphosphine) catalyst was used for those entries instead of the palladium (II) pre-catalyst (Table 4). The addition of an external base was not required in this case as the solvent used was able to deprotonate the terminal

alkyne and generate the alkynyl copper derivative needed for the transmetallation step in the catalytic cycle. 1,3-enynes **191c**, **191e** and **191g** could thus be obtained in good yields.

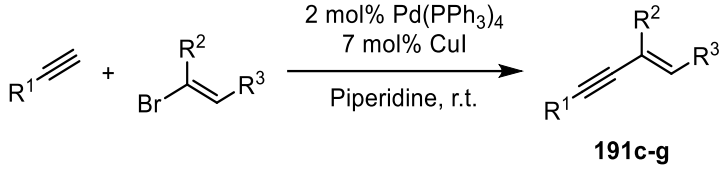

191c-g

Entry	R^1	Alkene		Product	Yield (%)
		R^2	R^3		
1	$Ph(CH_2)_2$	Me	H	**191c**	93
2	$Ph(CH_2)_2$			**191e**	83
3	$Ph(CH_2)_2$	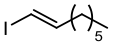		**191g**	60

Table 4: Alternative conditions for the Sonogashira cross-coupling

Following the general procedure to synthesise **191l** would involve using 1-butyne, a gas at room temperature. To avoid this obstacle, another route was developed involving the cross-coupling of styrene **192** with trimethylsilylacetylene **193**. Deprotection of **194** and alkylation with iodoethane would then give **191l** (Figure 60). The desired product was obtained in good yield over the three steps with traces of the *Z*-isomer that was formed from the small amount of *Z*-bromostyrene present in **192**.

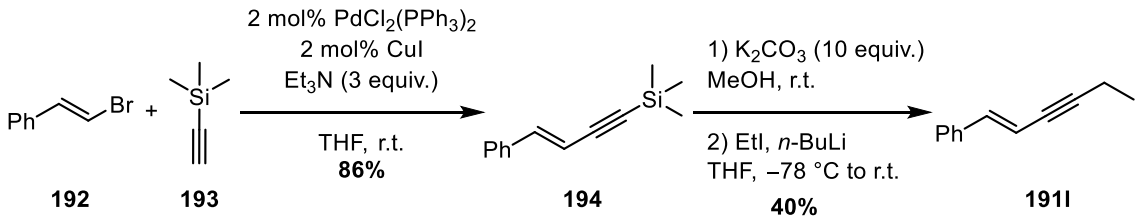

192 **193** **194** **191l**

Figure 60: Three steps synthesis to 191l

Finally, the tetra-substituted alkene **191m** was selected to assess whether a tetra-substituted alkene can still influence the regioselectivity of the insertion. Due to the extremely high cost of the brominated partner for a Sonogashira coupling, several alternative paths were proposed.

In 2006, Jung and Duclos showed that **195** could be converted to the hydrazine **196** and that its treatment with iodine followed by a base-mediated elimination could lead to the alkenyl iodide **197** in excellent yield over the two steps (Figure 61).[87]

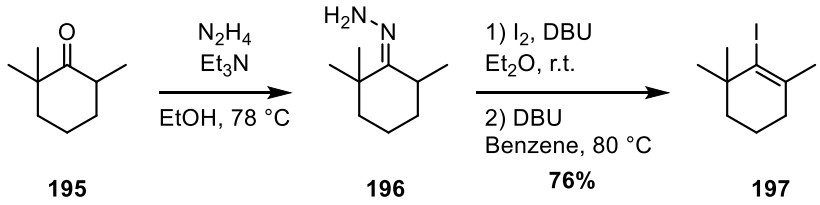

Figure 61: Regioselective synthesis of tetra-substituted iodoalkene

When applied to the cyclobutanone **198**, the reaction was unsuccessful and led to a complex mixture of products, of which none appeared to be a major component by ^{1}H NMR (Figure 62).

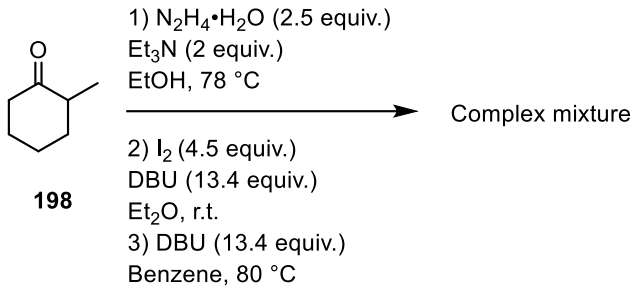

Figure 62: Attempt for the regioselective synthesis of tetra-substituted iodoalkene

Therefore, a second approach was considered with the key-step being a regioselective elimination. It was thought that after nucleophilic addition of an alkyne

onto the α-methylcyclohexanone **198**, the corresponding alcohol could be eliminated to afford the most stable tetra-substituted alkene **200** (Figure 63).

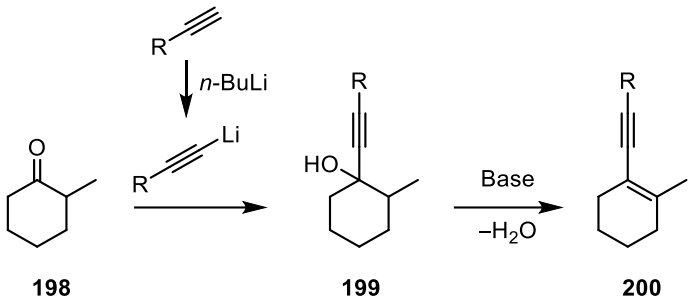

Figure 63: Alternative route to tetra-substituted alkene

The desired alcohol **202** was formed in moderate yield after addition of the corresponding lithiated cyclohexylacetylene, generated from **201** and *n*-BuLi, onto the cyclohexanone **198** (Figure 64). Extension of the stirring time did not increase the formation of the desired product but led to undesired by-products.

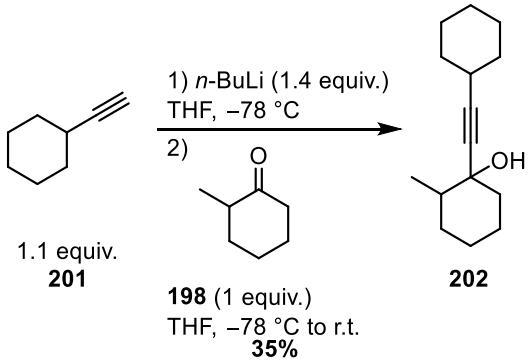

Figure 64: Alkynylation of α-substituted cyclobutanone

With the tertiary alcohol in hand, several conditions for the elimination were examined. Two sets were selected involving the activation of the hydroxyl group followed by a base-promoted elimination (Figure 65). Phosphoryl chloride and thionyl chloride were used based on published results on elimination reactions.[88, 89] A significant excess of phosphoryl chloride had to be used to reach full conversion of the

starting material and led to the formation of the corresponding eliminated product **191m** in poor yield and as a mixture of tetra- and tri-substituted alkene ($\Delta^{1\text{-}2}$/ $\Delta^{1\text{-}6}$) in a 2.3:1 ratio. Those isomers could not be separated by flash column chromatography. This result was improved with thionyl chloride, as only 5 equivalents of the activating agent were required and the produt was isolated in better yield, but still as a mixture of regioisomers with the same ratio.

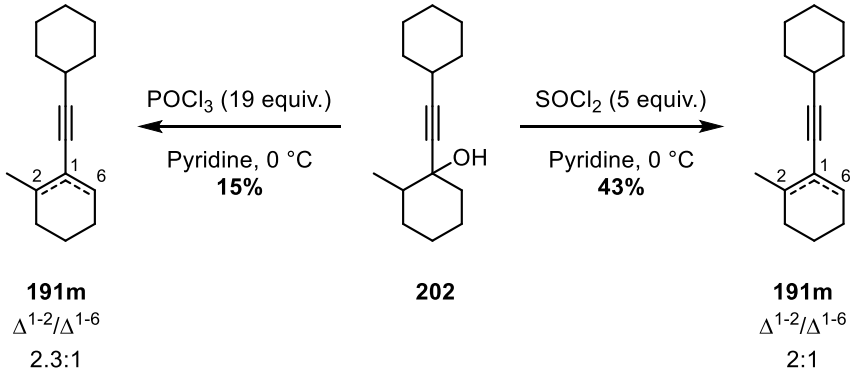

Figure 65: Regioselective elimination of the tetra-substituted alcohol 202

Due to the increased stability of a tetra-substituted over the tri-substituted isomer, it was believed that an isomerisation could resolve the mixture of product obtained in the previous step. Among possible isomerisation agents, hydrated rhodium chloride has been well studied and has proven to be extremely efficient with a wide functional group tolerance.[90] Unfortunately, when the mixture of alkenes was exposed to rhodium in ethanol at reflux, only decomposition of the starting material was observed (Figure 66).

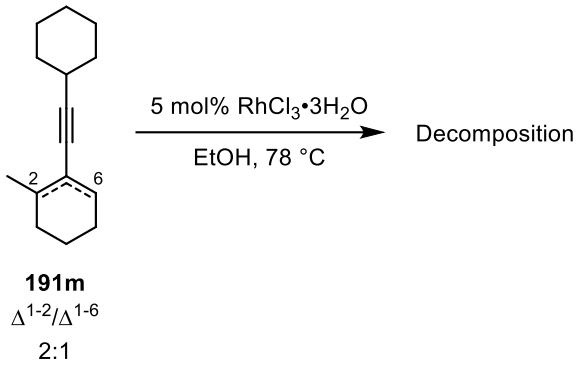

Figure 66: Attempt at the rhodium catalysed isomerisation of 191m

Due to time constraints, the mixture of regioisomers was used to examine the scope of the (4+2) cycloaddition of conjugated 1,3-enynes.

7.2 Optimisation of the reaction conditions

7.2.1 First generation of conditions

Previously optimised reaction conditions were used to assess the methodology on the 1,3-enynes **191c** and **191f** (Figure 67). Pleasingly, when **191f** was subjected to those conditions, **203f** was obtained in good yield as a single regioisomer observed by ^{1}H NMR. Unfortunately, when the same reaction conditions were used with **191c**, a complex mixture of products was recovered. Based on the crude NMR, insertion products were formed in a ratio of 90:10, and both products **203c** and **204c** were isolated in 40% and 8% respectively. The significant decrease of yield was explained by the formation of **205c** in 35%. This isomer arose from a C−H bond activation of **168** followed by attack on the triple bond of the enyne.

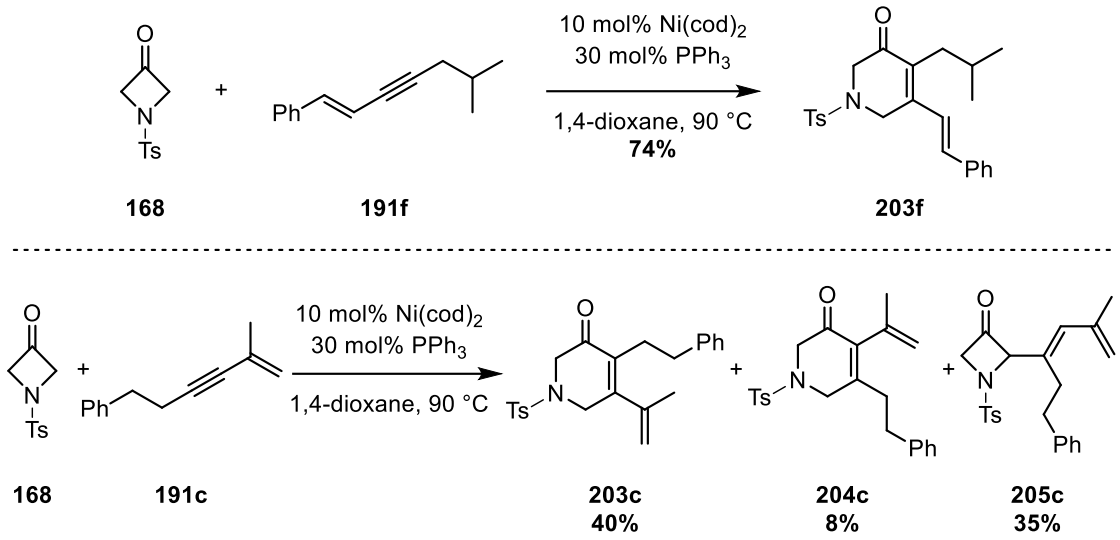

Figure 67 : Nickel catalysed (4+2) cycloaddition of 191f and 191c with 168 using reported conditions

7.2.2 Competition between C–C and C–H activation

The formation of **205c** was surprising as the conditions used in Figure 67 had been previously optimised in order to avoid this C–H bond activation process (Table 5). The optimisation of the reaction was reported by the Aïssa group in 2012.[44] When the Boc-protected azetidinone **53** was reacted with 1.5 equivalent of **131** in toluene at 110 °C, the cycloadduct **140a** and the azetidinone derivative **206** were obtained in a 1.4:1 ratio. The compound **140a** could be isolated in 55% (Table 5, Entry **1**). By changing the solvent to 1,4-dioxane at lower temperature with 1.1 equivalent of **131**, the authors were able to isolate **140a** in higher yield with an increased selectivity in favour of the cycloadduct (Table 5, entry **2**). Finally, decreasing the temperature to 90 °C with 30 mol% of PPh_3 led to the formation of **140a** only, in excellent yield (Table 5, entry **3**).

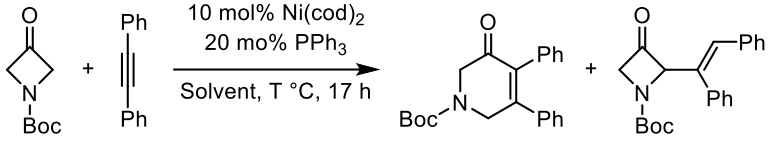

53 **131** **140a** **206**

Entry	Solvent	T (° C)	Ratio (140a/206)[a]	Yield [%][b]
1	Toluene	110	1.4:1	55
2 [c, d]	1,4-dioxane	100	5:1	77
3 [c, d]	1,4-dioxane	90	>20:1	90

a) Determined by ^{1}H NMR. *b)* Isolated yield. *c)* 1.1 equiv. of **131**. *d)* 30 mol% of PPh_3

Table 5: Reported optimisation of the nickel-catalysed (4+2) cycloaddition over the C−H activation

However, the formation of azetidinone derivatives such as **206** was limited to bis-aryl acetylenes and Boc-protected azetidinone **53**, and Tosyl-protected azetidinone gave only the desired (4+2) cycloadducts.

7.2.3 Second generation of conditions

When performing the reaction of **191c** with **168** at 60 °C instead of 90 °C, a slight increase of yield for the desired cycloadduct was observed (Table 6, entry **1** vs **2**). More importantly, the formation of the corresponding C−H activated product was almost prevented and the selectivity between **203c** and **204c** remained approximately the same. When the solvent was changed to toluene instead of 1,4-dioxane, no sign of **205c** was detected and **203c** was obtained in good yield from an 88:12 mixture of regioisomers (Table 6, Entry **2** vs **3**).

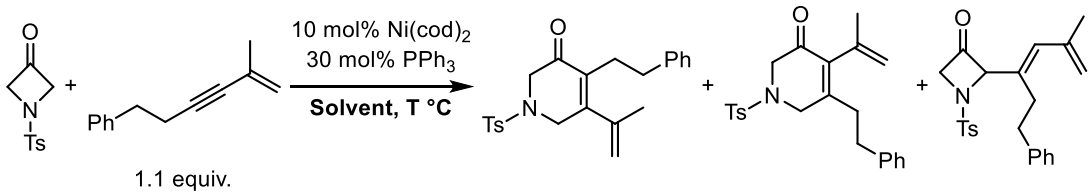

Entry	Solvent	Temperature (°C)	203c (%)[a]	204c (%)[a]	205c (%)[a]
1	1,4-dioxane	90	40	8	35
2	1,4-dioxane	60	47	8	8
3	Toluene	60	73	10	0

a) Isolated yield

Table 6 : Optimisation of the nickel-catalysed (4+2) cycloaddition of 191c with 168

When those new conditions were applied to the (4+2) cycloaddition of **191f** with **168**, **203f** was obtained in good yield as a single regioisomer, albeit traces of the other regioisomer **204f** could be seen by crude NMR (Figure 68).

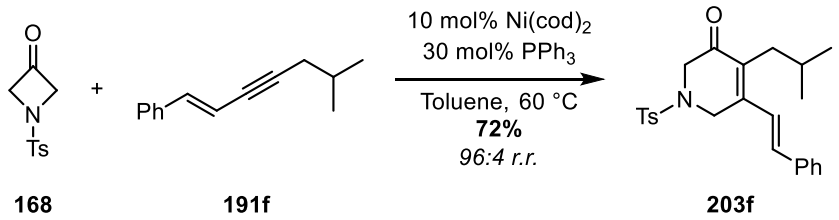

Figure 68 : Nickel-catalysed (4+2) cycloaddition of 191f with 168

As both regioselectivities and yields of the (4+2) cycloaddition were high, those conditions were kept, and the scope of the reaction could be investigated.

7.2.4 Product identification

All regioisomers obtained in this work were identified by HMBC. A correlation between the carbonyl and the alkyl chain could be seen for all major products (Figure 69).

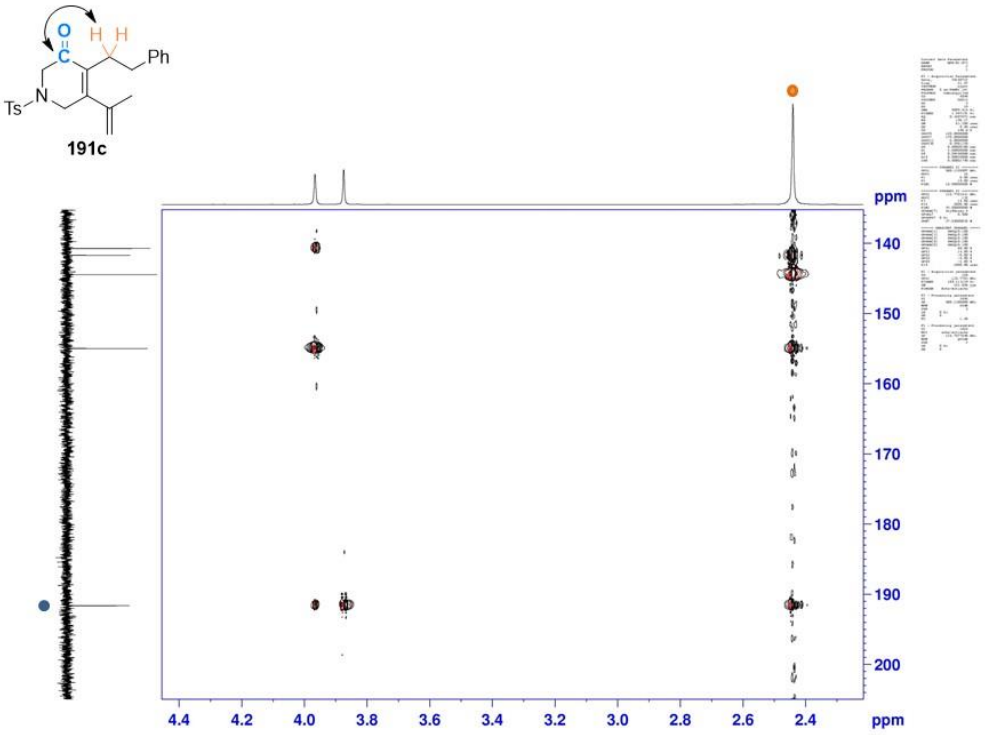

Figure 69: HMBC correlation of the carbonyl (*blue*) with the alkyl chain (*orange*)

7.3 Scope of the reaction

Pleasingly, when subjected to the optimised conditions, all selected 1,3-enynes gave the desired (4+2) adduct. It is noteworthy that in several cases, the phosphine loading could be reduced to 20 mol% without erosion of neither the efficiency nor the selectivity (Table 7**,** entry **2, 5, 6, 7** and **8**). When looking at the regioselectivity of this reaction, several conclusions can be drawn. Firstly, all enynes gave the same regioisomer as the major product. Secondly, the substitution of the double bond of the enynes **191a,c,e,g** did not affect the regioselectivity in a significant manner (Table 7**,** entry **1, 3, 5** and **7**). Similarly, the steric hindrance of the alkyl substituent on the alkyne did not have an impact on the yield or the selectivity in cases where the olefin was substituted with a phenyl group (Table 7**,** entry **2, 4, 6** and **8**). Conversely, the steric hindrance of the alkyl group on the alkyne led to a slight decrease of the regioselectivity when the olefin was substituted with other alkyl groups (Table 7, entry **1** *vs* **10** and **3** *vs* **9**). Moreover, with the enynes **191i** and **191j**, a decrease in yields were observed due to an increase of the steric hindrance around the triple bond, but synthetically useful regioselectivities were still observed (Table 7, entry **9** and **10**).

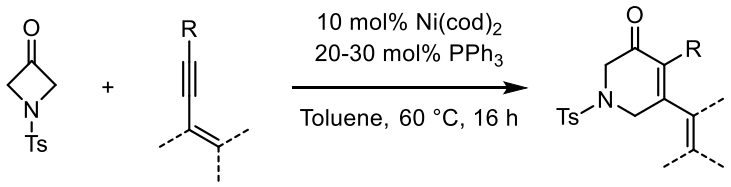

168 **191** **203**

Entry	Enyne	Yield[b]	Entry	Enyne	Yield[b]
1	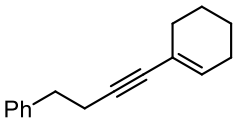 **191a**	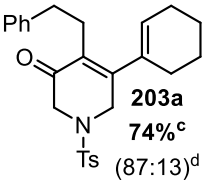 **203a** **74%**[c] (87:13)[d]	6	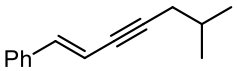 **191f**	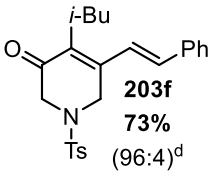 **203f** **73%** (96:4)[d]
2	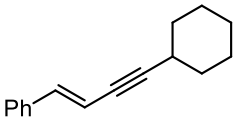 **191b**	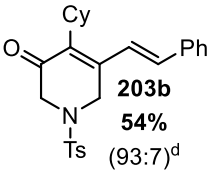 **203b** **54%** (93:7)[d]	7	 **191g**	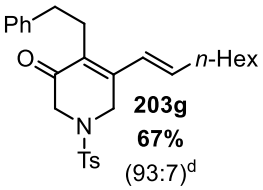 **203g** **67%** (93:7)[d]
3	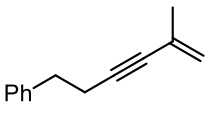 **191c**	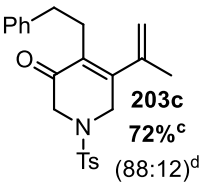 **203c** **72%**[c] (88:12)[d]	8	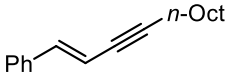 **191h**	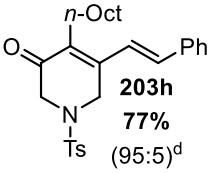 **203h** **77%** (95:5)[d]
4	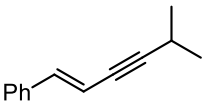 **191d**	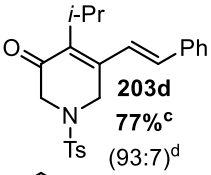 **203d** **77%**[c] (93:7)[d]	9	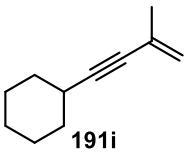 **191i**	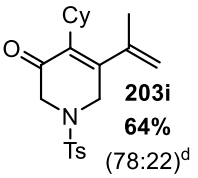 **203i** **64%** (78:22)[d]
5	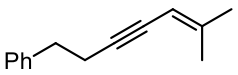 **191e**	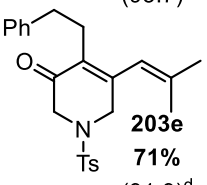 **203e** **71%** (91:9)[d]	10	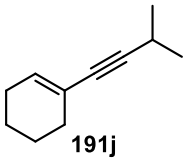 **191j**	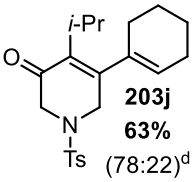 **203j** **63%** (78:22)[d]

a) All reactions were carried out with **168** (0.22 mmol), **191** (0.24 mmol), $Ni(cod)_2$ (0.022 mmol) and PPh_3 (0.044 mmol) except otherwise noted. *b)* Yield of isolated major isomer only, average of at least two experiments. *c)* 30 mol% PPh_3. *d)* From ^1H NMR of the crude mixture.

Table 7 : Nickel catalysed (4+2) cycloaddition of conjugated 1,3-enynes with tosyl-protected azetidinone

The 1,3-enyne **191m** could not be prepared as the pure tetra-substituted alkene form but was obtained as a mixture of tri/tetra-substituted in a 2:1 ratio, as discussed previously. When subjected to the optimised conditions, the desired cycloadduct was

obtained with good regioselectivity (83:17) but with a significant decrease in yield (Figure 70).

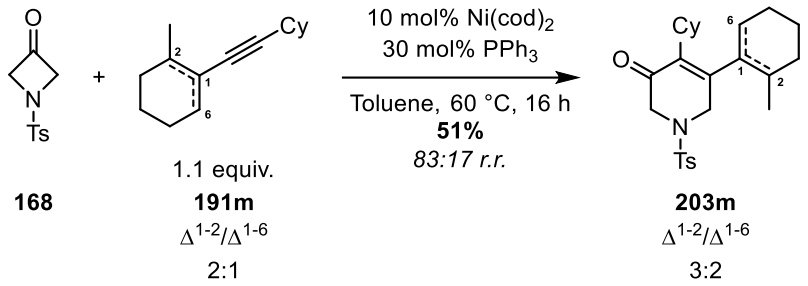

Figure 70: Nickel catalysed (4+2) cycloaddition of 1,3-enyne bearing a tetra-substituted alkene

Surprisingly, when the seemingly less challenging enyne **191k** was used with the optimised conditions, the reaction became sluggish and almost no product was isolated after 144 hours (Table 8, entry **1**). Optimisation of the reaction was attempted by extending the addition time of the enyne in the mixture with a syringe-pump. It was believed that due to the absence of steric hindrance around the alkene, the 1,3-enyne could saturate the catalyst and generate an unreactive species.[91] It was hypothesised that decreasing the concentration of **191k** over time could prevent this behaviour. Indeed, an increase in conversion was observed and an addition over 2.5 hours was the best compromise (Table 8, entry **2** and **3**). Increasing the addition time to overnight led to the same result (Table 8, entry **4**). Moreover, increasing the temperature of the reaction worsened the outcome, giving almost no conversion (Table 8, entry **5**). Finally, changing the stoichiometry by using an excess of **168** led to no reaction (Table 8, entry **6** and **7**).

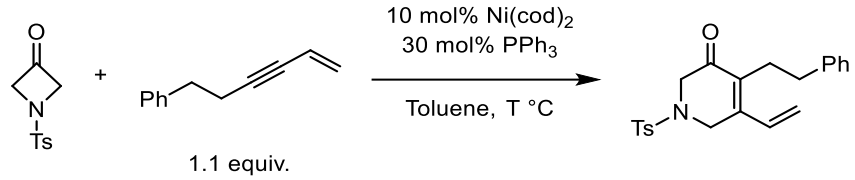

168 **191k** **203k**

Entry	Addition time of 191k (h)	Reaction time (h)	Temperature (°C)	Ratio (168/203k)[a]
1	0	144	60	3 : 1
2	2	18	60	9 : 1
3	2.5	18	60	1.5 : 1
4	Overnight	18	60	1.5 : 1
5	Overnight	72	90	9 : 1
6[b]	3	18	60	No reaction
7[c]	3	18	60	No reaction

a) Determined by ^{1}H NMR of the crude. *b)* **168** (2 equiv.), **191k** (1 equiv.). *c)* **168** (2 equiv.), **191k** (1 equiv.), without PPh_3

Table 8 : Optimisation of the nickel-catalysed (4+2) cycloaddition of 191k with 168

To circumvent the poor reactivity of the tosyl-azetidinone, the focus was placed on the more reactive Boc-protected equivalent **53**. Re-optimisation of the conditions was a necessity and both solvent and temperature were assessed. Changing the solvent back to 1,4-dioxane gave a good yield of 55% after stirring at 60 °C for 17 hours (Table 9, entry **1**). Both tetrahydrofuran and toluene gave lower yields (Table 9, entry **2** and **3**). It is interesting to point out that when toluene was used, the reaction time had to be extended to 40 hours in order to reach full conversion of the starting material. Increasing the temperature to 90 °C gave, overall, better results with a decent yield of

60% when the reaction was performed in 1,4-dioxane (Table 9, entry **4**). In all cases, **207k** was the only regioisomer seen by crude ^{1}H NMR.

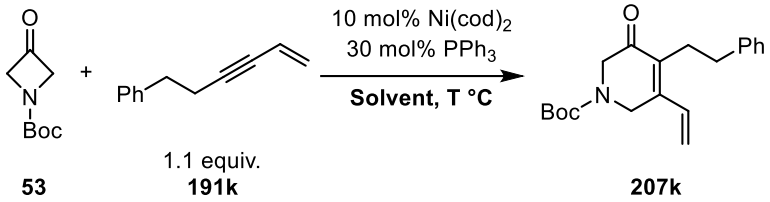

Entry	Solvent	Temperature (°C)	207k (%)[a]
1	1,4-dioxane	60	55
2	THF	60	34
3 [b]	Toluene	60	39
4	1,4-dioxane	90	60
5	THF	90	48
6	Toluene	90	41

a) Isolated yield. *b)* mixture stirred for 40 h.

Table 9: Nickel catalysed (4+2) cycloaddition of 191k with 53

Several reports have shown that the substitution of the azetidinone does not impede the insertion of alkynes.[44, 75, 76] Thus, when **208** was subjected to the optimised reaction conditions with the model substrate **176**, the 3-dihydropyridinone **209** was obtained as the single regioisomer in a slightly lower yield than that obtained with non-substituted azetidinone **168** (Figure 71).[44]

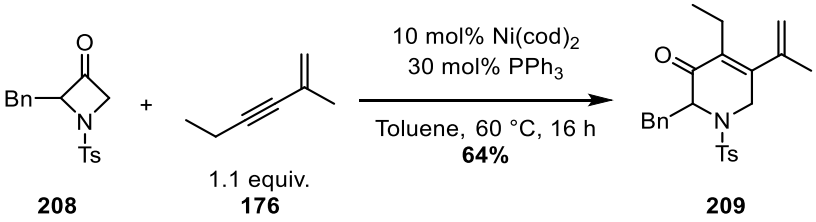

Figure 71 : Nickel catalysed (4+2) cycloaddition of 176 with the α-substituted tosyl-protected azetidinone

7.4 Hydrogenation/Re-aromatisation

7.4.1 Tosyl-protected 3-dihydropyridinones

As the aim of the project is to show the potency of 1,3-enynes as surrogates of unsymmetrical bis-alkyl-alkynes, it is necessary to develop a general process to convert the products **203**. To do so, the focus was placed on the most wide-ranging method, namely palladium on charcoal with hydrogen gas.[92] Several methods could be then used to re-aromatise the cycloadduct. As seen in the introduction, whilst working on the synthesis of 3-pyridinols through a ring closing metathesis, Donohoe *et al.* reported the re-aromatisation of tosyl-protected 3-dihydropyridinone with basic conditions in good yields.[42]

All cycloadducts previously formed by (4+2) cycloaddition were subjected to a sequence of hydrogenation with palladium on charcoal followed by base-mediated re-aromatisation. In all cases, the crude material obtained after hydrogenation was used without purification and all yields are reported for the overall two steps (Table 10).

Pleasingly, most 3-dihydropyridinones were transformed into pyridinols in high yields, with the hydrogenation step giving almost quantitative yields in many cases. Some issues where encountered during the hydrogenation of some of the examples. When **203g** was used, it was essential to stop the reaction after 5 hours to prevent hydrogenation of the endocyclic double bond (Table 10, entry **7**). Whilst **203b** underwent the sequence smoothly to give **210b** in good yield (Table 10, entry **2**), the corresponding regioisomer **203a** proved to be more challenging to hydrogenate. Conditions had to be modified due to the stability of endocyclic alkenes. Thus, the hydrogenation was carried out in a sonicating bath, leading to the desired intermediate in excellent yields (Table 10, entry **1**). It is believed that sonication can activate the

catalyst by changing the morphology of the metal particles.[93] *Via* this sequence, pyridinol **210a** was obtained in excellent yield of 80%. Finally, two interesting cases were **203i** and **203j**. Despite all efforts, their further transformation was impossible due to the uncontrolled reactivity towards hydrogenation, which is likely explained by the steric hindrance around the alkene.

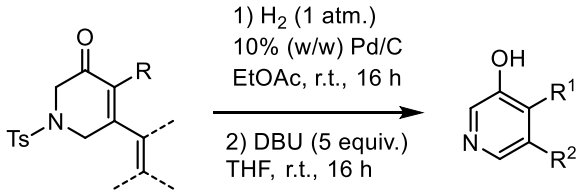

Entry	Cycloadduct	Yield[a]	Entry	Cycloadduct	Yield[a]
1	**203a**	**210a, 80%[b]**	6	**203f**	**210f, 70%**
2	**203b**	**210b, 78%**	7	**203g**	**210g, 54%**
3	**203c**	**210c, 69%**	8	**203h**	**210h, 56%**
4	**203d**	**210d, 60%**	9	**203i**	**NA**
5	**203e**	**210e, 65%**	10	**203j**	**NA**

a) Yield after two steps. *b)* Hydrogenation was done in a sonicating bath for 5 h.

Table 10: Hydrogenation/Re-aromatisation sequence

A comprehensive optimisation of the hydrogenation step was attempted in order to circumvent the limitation that **203j** brought to light. Firstly, using the optimised conditions, a complex mixture of compounds was obtained (Table 11, entry **1**). Subjecting this mixture to the re-aromatisation protocol did not give significant results. With an increase of both the catalyst loading and the temperature, some reactivity was observed but the reaction mixture obtained was too complex to proceed further (Table 11, entry **2**). The hydrogenation of endocyclic alkenes has been described using ethanol as a solvent, which is believed to increase the reactivity of the palladium towards reduction of the alkene.[83] However, either no reaction was observed, or another complex mixture of hydrogenated and deprotected products was recovered, when the temperature was increased (Table 11, entry **3** and **4**). As the problem of reactivity observed for **203a** could be solved using a sonicating bath, the same method was tried in this case, but no reactivity was observed neither at room temperature nor at 45 °C (Table 11, entry **5** and **6**). Performing the hydrogenation with a pressure of 5 bars of hydrogen in ethanol for twenty hours led to no reaction (Table 11, entry **7**). Finally, two other catalysts were tried, namely Raney nickel and rhodium supported on alumina, leading to the same outcome as observed previously (Table 11, entry **8** and **9**).[94, 95]

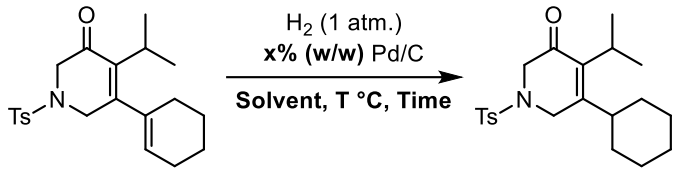

203j **210j-*int***

Entry	% (w/w) Pd/C	%w/w	T°C	Solvent	Time (h)	Result
1	10	10	r.t.	EtOAc	17	Complex mixture
2	10	20	80	EtOAc	17	≈20% conversion
3	5	20	80	EtOH	17	No Reaction
4[a]	5	20	r.t.	EtOH	48	Complex mixture; cleavage of tosyl
5[b]	10	10	r.t.	EtOAc	5	No Reaction
6[b]	10	10	r.t. to 45°C	EtOAc	7	No Reaction
7[c]	5	10	r.t.	EtOH	20	No Reaction
8	Ni Raney	NA	r.t.	MeOH	17	No Reaction
9[d]	Rh/Al_2O_3	NA	r.t.	EtOAc	17	No Reaction

a) A hydrogen bubbling was kept for 15 min. *b*) Using a sonicating bath. *c)* H_2, 5 bars. *d)* 100% (w/w).

Table 11 : Optimisation of the hydrogenation of 203j

Although this pair of enynes illustrates the limits of this methodology, eight highly functionalised pyridinols were successfully synthesised in good yields and high regioselectivities. As a result, four pairs of regioisomers have been obtained with conjugated 1,3-enynes working as unsymmetrical alkyl-alkyne surrogates.

7.4.2 Boc-protected 3-dihydropyridinone

The case of **207k** is slightly different as the starting azetidinone had to be changed for the reactive Boc-protected azetidinone. Therefore, the use of DBU for the final re-aromatisation step was not suitable.

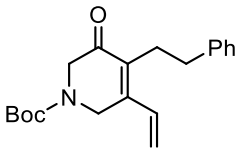

207k

It has been reported that when the 1,2-dihydroquinoline **211** was subjected to acidic conditions in the presence of silica and with a mild oxidising agent, the quinoline **212** was isolated in excellent yield (Figure 72).[96]

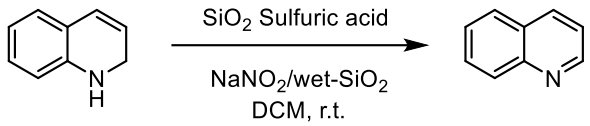

211 **212**

Figure 72: Re-aromatisation of 1,2-dihydroquinolines

Following a modified procedure based on this work and developed by a former PhD student from the group, the cycloadduct **207k** was successfully converted to the corresponding pyridinol **210k** (Figure 73).[44] After hydrogenation according to the optimised conditions, the Boc-protecting group was removed with TFA which subsequently acted as the acid needed for the re-aromatisation. By adding silica and sodium nitrite, the pyridinol could be obtained in a good yield within 2 hours. It is interesting to note that the three steps of the re-aromatisation were done as a one-pot sequence.

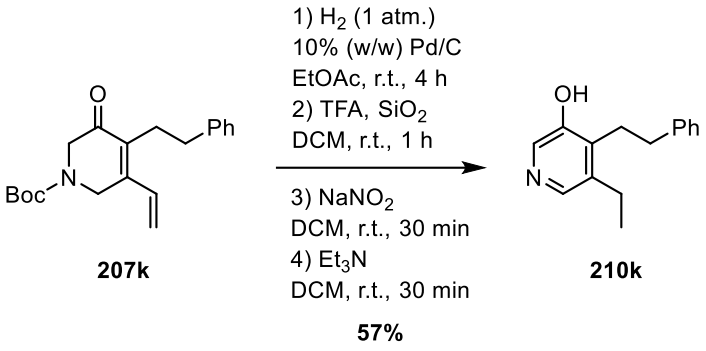

Figure 73: Hydrogenation/Re-aromatisation of 207k

7.4.3 Alternative re-aromatisation

Due to the toxicity of DBU, an alternative protocol to access pyridinol was developed using sodium bicarbonate. In 2005, Rault *et al.* reported the re-aromatisation of **213** to the corresponding quinolinol **214** in good yield using a mild base (Figure 74).[97] Despite harsher conditions, *i.e.* reflux overnight, this reaction remains significantly more advantageous and more feasible in a process than DBU in THF.

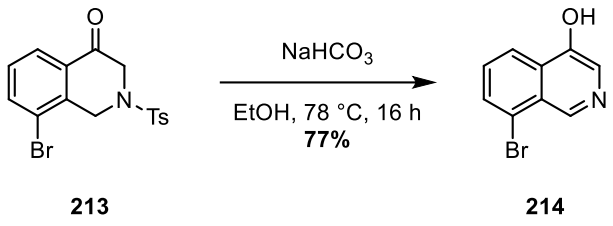

Figure 74: Deprotection and re-aromatisation with sodium bicarbonate

After the general hydrogenation procedure to remove the exocyclic double bond of **209**, the crude mixture was re-aromatised using Rault's conditions which pleasingly led to the pyridinol **215** in 56% yield over the two steps (Figure 75).

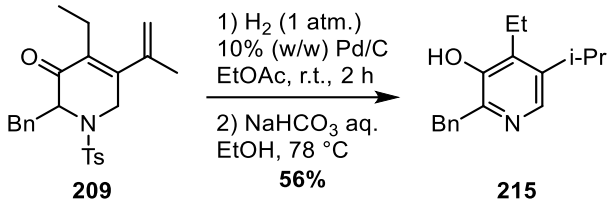

Figure 75: Hydrogenation/re-aromatisation of 209

7.5 Nickel (II) catalysis

The main issue arising from this new methodology comes from the pre-catalyst used. Nickel (0) is notorious for being highly sensitive to oxygen, thus requiring extreme care and a glovebox when setting up those reactions. Issues of reproducibility can be observed and scaling up the reaction seems hardly achievable.

However, nickel (II) complexes show increased stability and can be stored in air, making them good candidates to avoid this drawback. The nickel (0) catalyst can be generated *in situ* by reduction with a metal. The focus was placed on one type of nickel pre-catalyst, $NiBr_2(PPh_3)_2$, and three reductive agents, zinc, indium and manganese.

The conditions were optimised in the lab by a former PhD student and were tried on a model enyne in order to judge the potency of the pre-catalyst. Thankfully, both the regioselectivity and yield of the major compound were comparable to that with nickel (0), highlighting how efficient the new pre-catalyst can be (Figure 76).

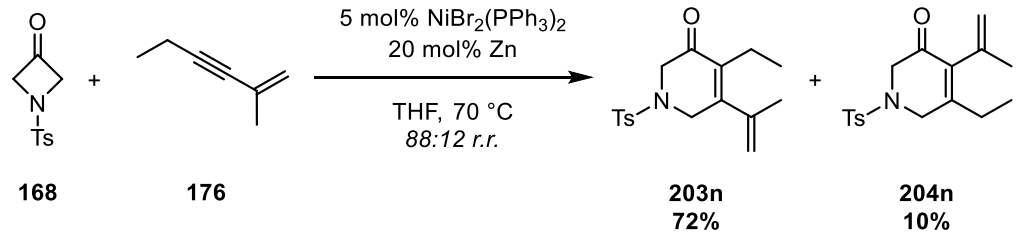

Figure 76 : Nickel catalysed (4+2) cycloaddition of 176 with 168 using a nickel (II) pre-catalyst

Encouraged by this result, the scope of enynes was examined under slightly modified conditions, whereby both catalytic charges of nickel and zinc were increased to 10% and 50% respectively in order to obtain decent conversions (Table 12). In all cases, except for entry 5, the reactivity decreased leading to a drop of at least 10% in yield, as compared to the previously reported nickel (0) catalysed insertion. Nonetheless, the high selectivities remained intact and in the same range as observed when using nickel (0).

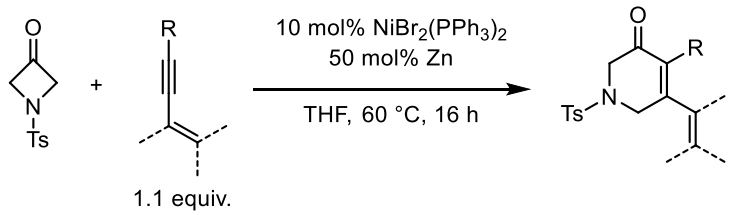

168 **191** **203**

Entry[a]	Enyne	Yield[b]	Ni(0)	Entry[a]	Enyne	Yield[b]	Ni(0)
1	191a	**203a** **66%** (85:15)[c]	**203a** **74%** (87:13)	5	191e	**203e** **69%** (87:3)[c]	**203e** **71%** (91:9)
2	191b	**203b** **31%** (91:9)[c]	**203b** **54%** (93:7)	6	191f	**203f** **54%** (94:6)[c]	**203f** **73%** (96:4)
3	191c	**203c** **51%** (85:15)[c]	**203c** **72%** (88:12)	7	191i	**203i** **44%** (88:12)[c]	**203i** **64%** (78:22)
4	191d	**203d** **59%** (91:9)[c]	**203d** **77%** (93:7)	8	191j	**203j** **52%** (78:22)[c]	**203j** **63%** (78:22)

a) All reactions were carried out with **168** (0.22 mmol), **191** (0.24 mmol), $NiBr_2(PPh_3)_2$ (0.022 mmol) and Zn (0.11 mmol) except otherwise noted. *b)* Yield of isolated major isomer only, average of at least two experiments. *c)* From ^1H NMR of the crude mixture.

Table 12: Nickel-catalysed (4+2) cycloaddition of conjugated 1,3-enynes with tosyl-protected azetidinone using a nickel (II) pre-catalyst

One plausible explanation to understand this decrease in yield comes from a side reaction. When **191f** was treated under the optimised condition, **216f** was obtained in 10% yield (Figure 77). Due to the presense of the Lewis acidic zinc bromide that is generated during the reduction of the pre-catalyst, an aldol reaction between the product and the activated starting material occurs.

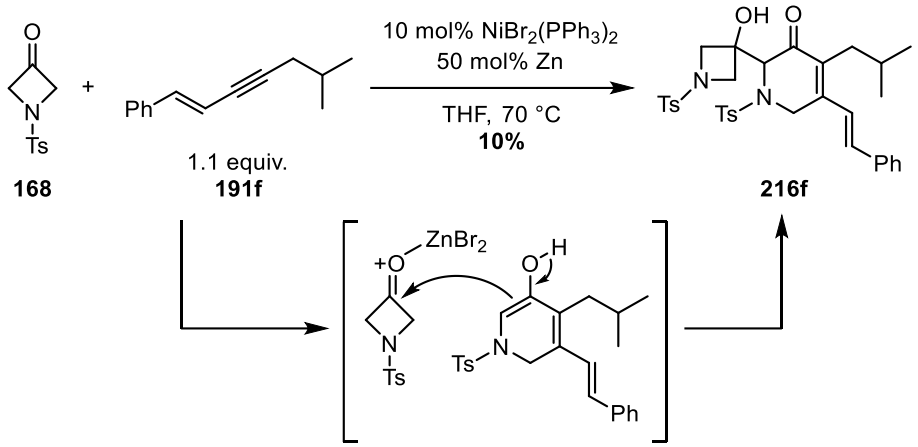

Figure 77: Aldol side-reaction of 191f with 168

From this unexpected reactivity, it is obvious that conditions can be optimised to avoid this side reaction. However, changing the reductant to indium or manganese did not improve the reaction. Another possibility would be to change the complex to alternative nickel (II) pre-catalysts which have been reported recently in the literature, which give unreactive by-products after the generation of the active catalyst.[98]

7.6 Late-stage Functionalisation

Extra substitution could be accessed from α-substitued azetidinones, *i.e.* **208** (Part **7.3**, Figure 71). However, a late-stage functionalisation of the pyridinol moiety seems more attractive and could resolve the small decrease of reactivity observed with

the substituted azetidinone. Several sequences were investigated to functionalise the pyridinol ring.

It is worth mentioning that all attempts of further functionalisation were done on the model substrate **203n**. In order to accumulate enough material, the sequence (4+2) cycloaddition/hydrogenation/re-aromatisation was scaled-up to 1 mmol and the catalyst loading was halved (Figure 78). Diminished reactivity was observed, and the reaction time had to be extended to 40 hours to reach a good yield. No erosion of the regioselectivity was observed in those attempts. Moreover, the alternative re-aromatisation procedure using sodium bicarbonate in refluxing ethanol was performed and gave **210n** in good yield and purity after recrystallisation.

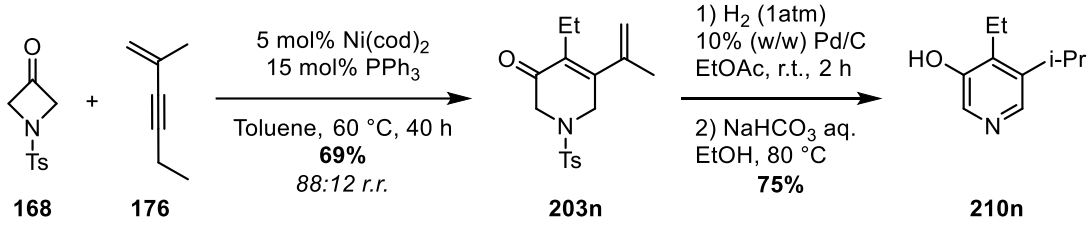

Figure 78: Large scale nickel-catalysed (4+2) cycloaddition/hydrogenation/re-aromatisation with 176 and 168

7.6.1 *Ortho*-lithiation

After protection of the alcohol with a methoxy-methyl ether (MOM), it was believed that the corresponding product could be deprotonated with a lithiated base and trapped with an electrophile.[99] Deprotonating the protected pyridinol **217** with *n*-BuLi and using butylbromide as the electrophile gave no reaction, even if TMEDA was used as an additive to improve the nucleophilicity of the lithiated species generated after deprotonation (Figure 79).

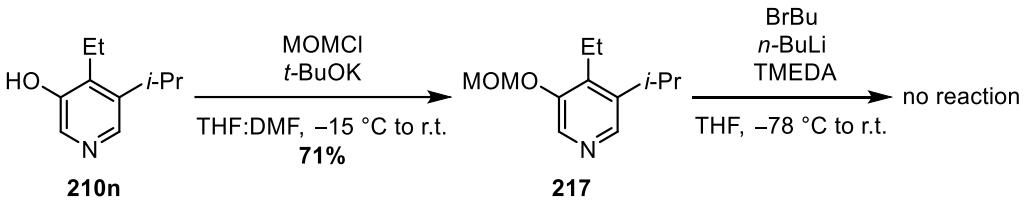

Figure 79: MOM-protection and attempt at the *ortho*-lithiation of 210n

Other protecting groups than MOM could be used. In 2011, Cossy *et al.* reported the selective ortholithiation of the 3-pyridinol **218** protected as a methyl ether (Figure 80).[100] After generation of the carbanion in position 2, they were able to trap it with iodine in an excellent yield. Functionalisation of the C-2 position with iodine is extremely interesting as it offers options for cross-coupling reactions.

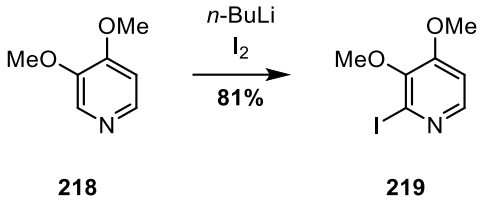

Figure 80: Iodination of 3-pyridinol

Those conditions were applied to **210n**. The transformation of the pyridinol to the corresponding methyl ether proved to be less trivial than initially believed. Sluggish reactions were observed in many cases when strong bases were used (Figure 81).

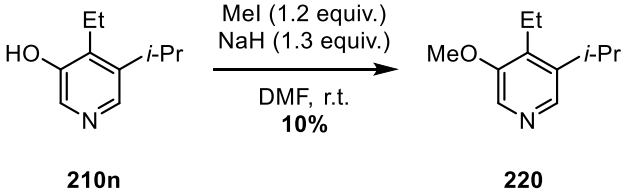

Figure 81: Protection of 210n to the methyl ether

Interestingly, when the relatively weak base K_2CO_3 was used, the activated pyridinium **221** was isolated in quantitative yield (Figure 82).

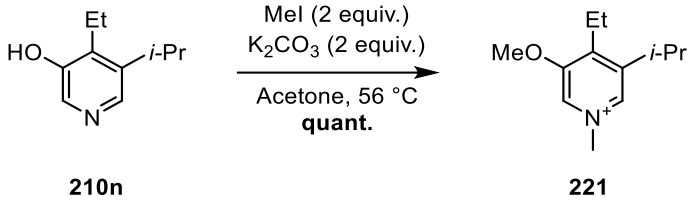

Figure 82: Methylation of 210n to the pyridinium salt

Although the formation of **221** was unexpected, an attempt of alkylation of this pyridinium was experimented.[101] Activation of the nitrogen atom should increase the electrophilicity, promoting the attack of a nucleophile in position 2 or 4. Methyl lithium was selected because of its small size (Figure 83). However, full decomposition of the starting material was observed after only 1 hour, thus, the *ortho*-lithiation strategy was resumed.

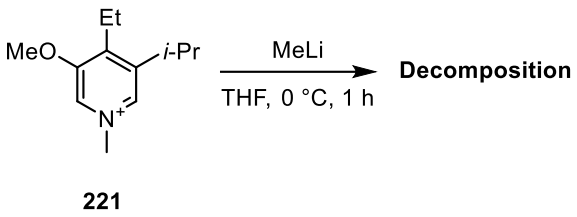

Figure 83: Direct methylation of the pyridinium salt 221

Changing the methylating agent from methyl iodide to TMS-diazomethane gave access to the desired protected pyridinol **220** in average yield (Figure 84).[102] However, when Cossy's conditions of *ortho*-lithiation were used, decomposition of the starting material occurred without observable traces of the expected functionalised pyridinol.

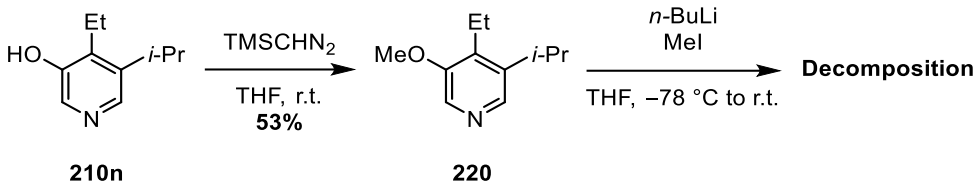

Figure 84: Protection of 210n and attempt at ortholithiation

7.6.2 Cyanation

As the direct functionalisation of the ring through *ortho*-lithiation revealed to be more difficult than anticipated, alternative routes were explored. As seen previously, activation of the nitrogen atom could enable the nucleophilic attack on position 2 and 4.[101] Among those activated species, *N*-oxides are well known. A particularly interesting example was published in 1983 by Krolikiewicz and Vorbrüggen, where a cyano group was added on a pyridinol ring after formation of the N-oxide **222**.[103] With trimethylsilyl cyanide, the authors were able to regioselectively access the functionalised pyridinol **224** (Figure 85). Interestingly, the alcohol was protected with TMS during the process and stirring in methanol was required to release the expected cyanated pyridinol **224** in 73% yield.

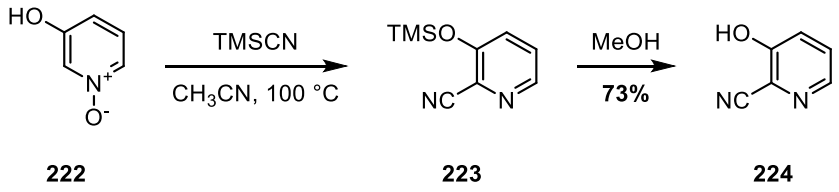

Figure 85: Direct cyanation of pyridinium N-oxide

Unfortunately, when the more substituted N-oxide **225** was subjected to the cyanation conditions, an unseparable mixture of compounds was recovered, showing how unapplicable this strategy was in this case (Figure 86).

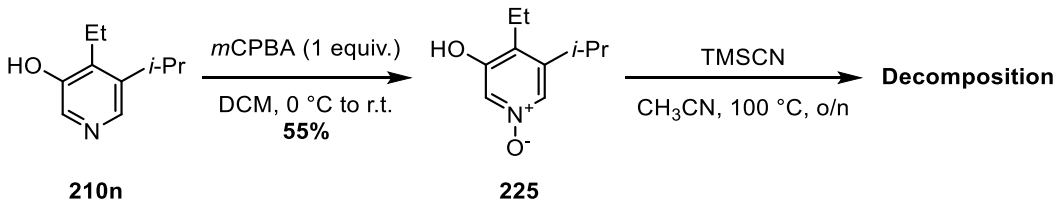

Figure 86: Synthesis of pyridinium N-Oxide and attempt at the direct cyanation

7.6.3 Iodination

The functionalisation of the pyridinol core to the iodo-cycloadduct is highly interesting as it could broaden the scope of possible further functionalisations. Cossy *et al.* showed the applicability of iodination of pyridinol ring.[100] However, harsh conditions seem detrimental for highly functionalised 3-pyridinols. The use of milder conditions could solve the issues of decomposition which were observed in all the examples. Koch's group managed to regioselectively access the iodinated pyridinol **227** in excellent yield with extremely mild conditions by using sodium carbonate and iodine (Figure 87).[104] A small fraction of the over-iodinated pyridinol **228** was obtained in the crude mixture. Moreover, the reaction was later scaled-up to several hundred of grams by Slaich's group with a significantly decreased yield.[105] The solvent was changed from water to dimethylformamide, and the reaction led to a mixture of C-2 and C-4 iodinated product, **227** and **228** respectively. The ratio between the two products was not reported.

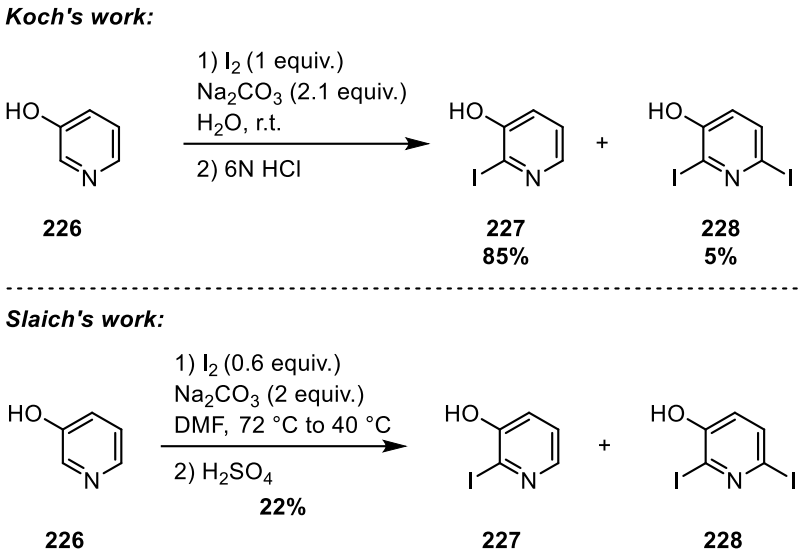

Figure 87: Direct iodination of 3-pyridinol

Applying Koch's optimised conditions to the prepared pyridinol **210n** enabled the direct iodination of C-2 in average yield (Figure 88).

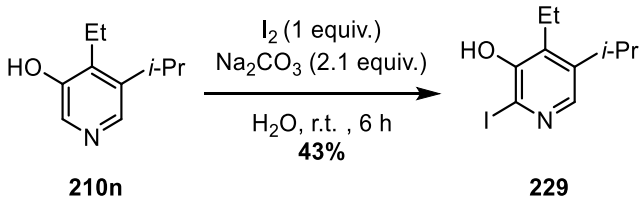

Figure 88: Direct iodination of 210n

Suprisingly, when the solvent was changed to a 1:1 mixture of water and tetrahydrofuran and the temperature was increased to 85 °C, the reaction proceeded in almost quantitative yields without traces of impurities (Figure 89).[106]

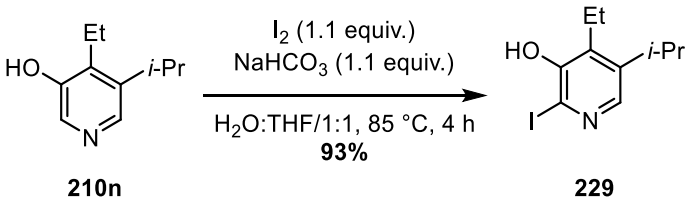

Figure 89: Improved iodination of 210n

In order to prove the usefulness of this functionalisation, the classical Sonogashira cross-coupling was attempted. Based on observations made during the synthesis of the 1,3-enynes (Part. I), palladium tetrakis-triphenylphosphine with piperidine was used and the starting material **229** was fully converted overnight (Figure 90). However, the expected product **231** was not observed, instead, the bicyclic product **232** was obtained in good yield.

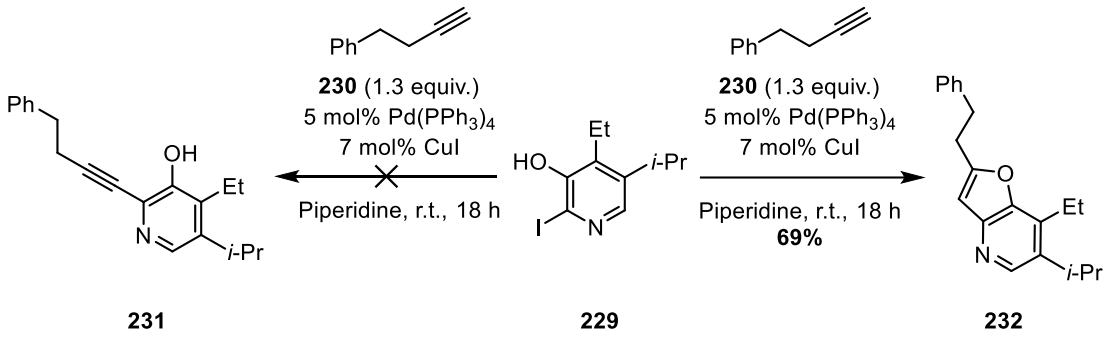

Figure 90: Sonogashira cross-coupling/cyclisation of 229

Manaba's group and Sekar's group have reported similar reactions catalysed by either copper or palladium.[107, 108] After formation of the Csp–Csp^2 bond, the copper or the palladium catalyst can activate the newly formed alkynyl product and trigger the cyclisation. Although unexpected, this iodination/Sonogashira sequence can be a valuable tool in synthesis.

7.6.4 Mannich reaction

In 1999, Park and coworkers reported the direct functionalisation of 3-pyridinol **226** *via* a one-pot Mannich reaction with secondary amines and paraformaldehyde (Figure 91).[109] They showed that pyridinol can undergo highly regioselective substitution with several amines in excellent yields.

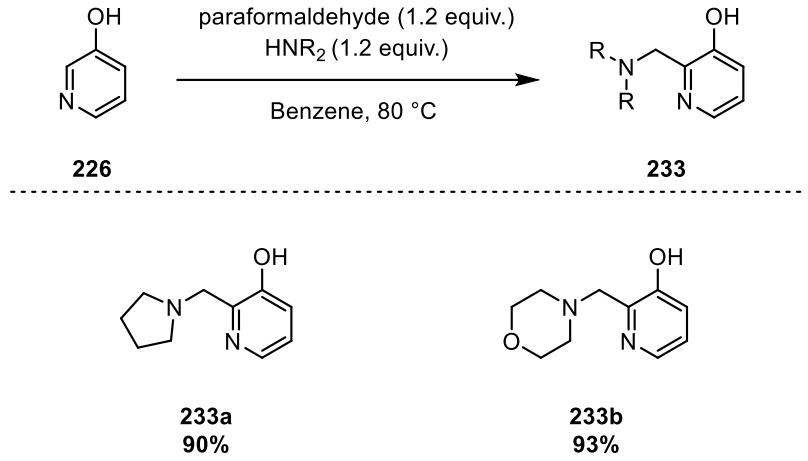

Figure 91: Regioselective functionalisation of 3-pyridinol through Mannich reaction

Thankfully, using their optimised conditions, the pyridinol **210n** was smoothly functionalised to the corresponding morpholine and pyrrole derivative **234** and **235**, in excellent yields (Figure 92). Since the use of benzene remains problematic due to the high toxicity of this solvent, toluene was used for the synthesis of **235**. A slight decrease of yield was observed in this case. Alkylation only occurred in position 2 and was confirmed through a series of selective NOEs.

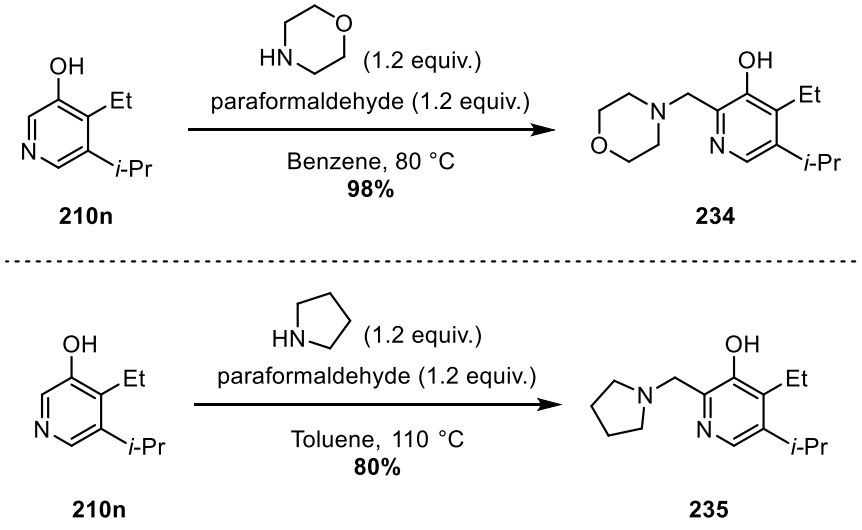

Figure 92: Regioselective functionalisation of 210n through a Mannich reaction

8 Conclusion & outlook

8.1 Summary

As a conclusion, we successfully addressed the regioselectivity issue observed with the nickel-catalysed (4+2) cycloddition of unsymmetrical alkynes by using conjugated 1,3-enynes as surrogates.

Fourteen 3-dihydropyridinones were synthesised in yields ranging from average to good (Figure 93). In all cases, high regioselectivities were observed with traces of the minor regioisomer in the crude reaction. Resolution of the regioisomeric mixture was possible with a classical column chromatography. Eleven of those 3-dihydropyridinones were successfully transformed into the corresponding pyridinols through a hydrogenation/re-aromatisation sequence. Three different re-aromatisation processes were reported allowing a better diversity in functional group tolerance. Unfortunately, the hydrogenation of two of the 3-dihydropyridinones failed due to the low reactivity of the alkene.

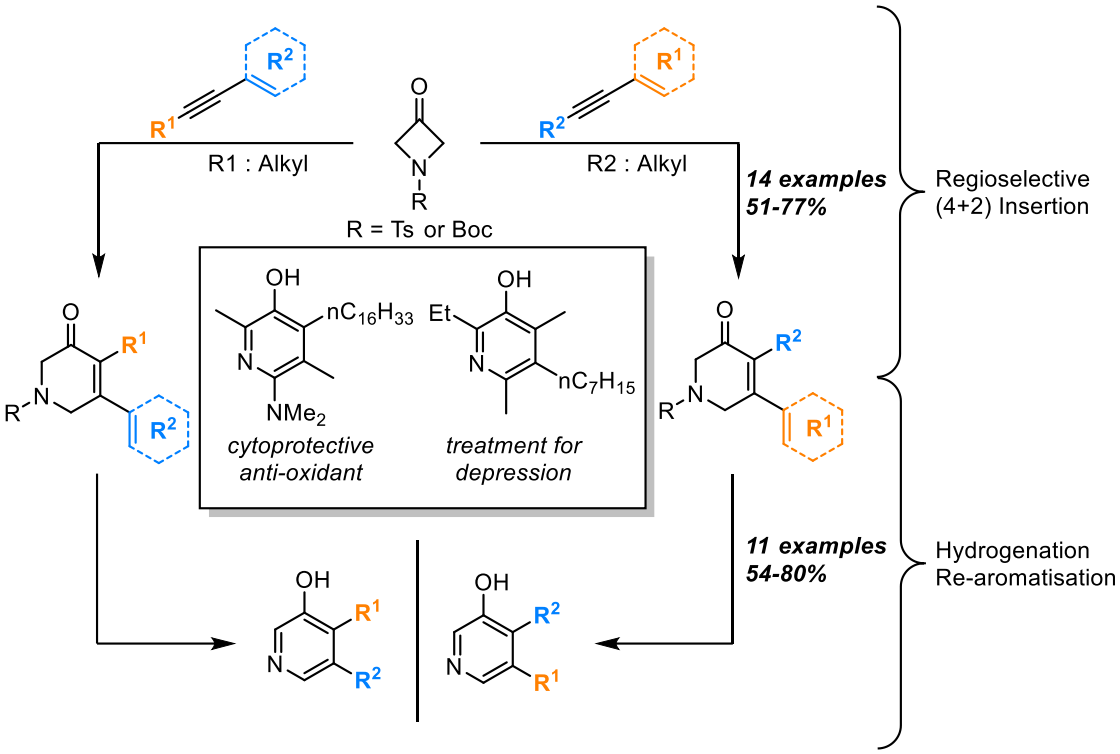

Figure 93: 1,3-enynes as unsymmetrical alkylalkynes surrogates in the regioselective synthesis of functionalised 3-pyridinols

The (4+2) cycloaddition could be expanded to the use of the air stable nickel (II) pre-catalyst without loss of selectivity (Figure 94). A side reaction was observed due to the generation of a Lewis acid during the process, diminishing the recovered yields.

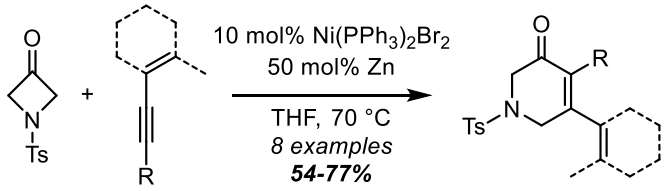

Figure 94: Nickel-catalysed (4+2) cycloaddition of conjugated 1,3-enynes with tosyl-protected azetidinone using a nickel (II) pre-catalyst

Further functionalisation of the pyridinol ring was possible (Figure 95). The selective addition of an iodine atom on the ring is highly interesting as the possibilities of functionalisation are high. A Sonogashira cross-coupling was attempted and led to

the unexpected bicyclic compound **178** after C−C bond formation and intramolecular cyclisation catalysed by copper or palladium. Moreover, a direct functionalisation of the 2-position on the pyridinol ring was reported with a Mannich type reaction. Excellent yields were obtained for this process.

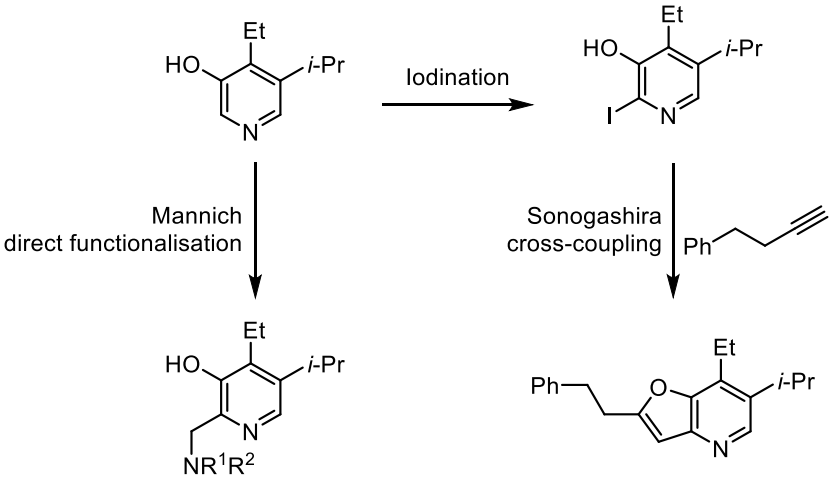

Figure 95: Summary of the late functionalisation

8.2 Outlook

This methodology proved to be powerful with protected-azetidinones, and an expansion to other strained rings such as the ones seen in the introduction, *i.e.* cyclobutanones, cyclobutenones, benzocyclobutenones and oxetanones, could prove to be a powerful tool in the synthesis of complex frameworks.

Moreover, the lack of regioselectivity is a common drawback in metal-catalysed cycloaddition, as depicted in the two examples below (Figure 96).[110, 111] The use of conjugated 1,3-enynes as alkyne surrogates in those reactions could enable a highly regioselective cycloaddtion, as seen in this chapter.

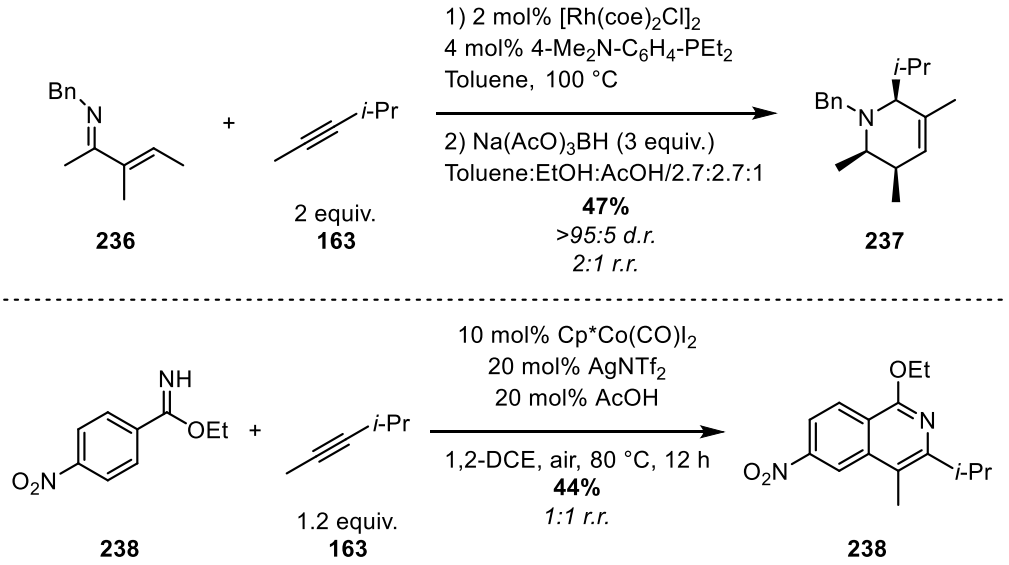

Figure 96: Regioselectivity issues in rhodium- and cobalt-catalysed (4+2) cycloadditions

9 Experimental Part

9.1 Synthesis of four-membered rings

Compound 53.

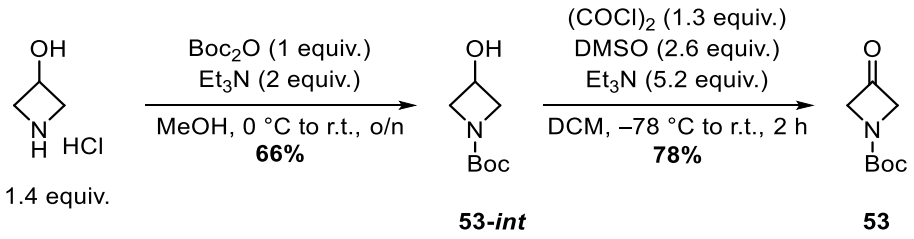

A round bottom flask was charged with 3-hydroxyazetidine hydrochloride (10.0 g, 91 mmol, 1.4 equiv.) and dissolved in methanol (91 mL) at 0 °C. Triethylamine (17.2 mL, 127 mmol, 2 equiv.) was added dropwise at 0 °C followed by di-*tert*-butyl decarbonate (13.9 g, 64 mmol, 1 equiv.). The mixture was stirred overnight at room temperature. The mixture was diluted with DCM and washed with H_2O. The organic layer was dried with $MgSO_4$ and concentrated to afford the **53-*int*** as a white solid (7.2 g, **66%**). The product was used without further purification.

Under N_2, at −78 °C, oxalyl chloride (4.7 mL, 55 mmol, 1.3 equiv.) was diluted in DCM (91 mL) and DMSO (7.8 mL, 109 mmol, 2.6 equiv.) was slowly added. The mixture was stirred for 15 min at −78 °C, then **53-*int*** (7.23 g, 42 mmol, 1 equiv.), diluted in DCM (53 mL), was added. The mixture was stirred for another 15 min at −78 °C, then triethylamine (29 mL, 218 mmol, 5.2 equiv.) was added. The mixture was stirred 2 h at room temperature, then the reaction was quenched with a saturated solution of NH_4Cl. The aqueous layer was extracted with diethyl ether. The gathered organic layer was washed with H_2O, brine, dried over $MgSO_4$, filtered and concentrated. Purification by flash chromatography (PE:EtOAc/2:1 to 1:1) afforded

53 as a white solid (5.6 g, **78%**). ^{1}H NMR (500 MHz, $CDCl_3$): δ 4.69 (s, 4H), 1.49 (s, 9H), *the NMR data is in accordance with that reported in the literature.*[112]

Compound 168.

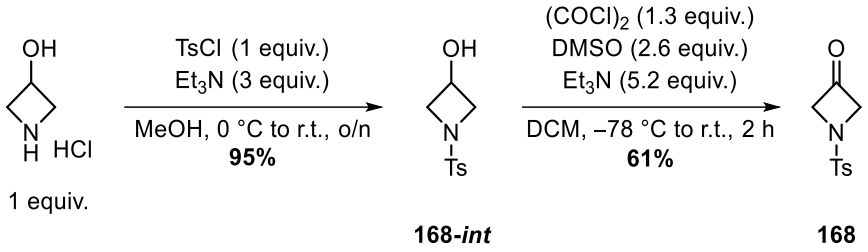

A round bottom flask was charged with 3-hydroxyazetidine hydrochloride (4.0 g, 37 mmol, 1 equiv.) and suspended in methanol (37 mL). Triethylamine (15 mL, 110 mmol, 3 equiv.) was added dropwise at 0 °C, then the clear mixture was allowed to stir at room temperature for 30 min. Afterwards, tosyl chloride (7.0 g, 37 mmol, 1 equiv.) was added portionwise at 0 °C. The mixture was stirred overnight at room temperature. Afterwards, all volatiles were evaporated and then partitioned between EtOAc and H_2O. The aqueous layer was extracted 3 times with EtOAc. The gathered organic layer was washed with H_2O, brine, dried over $MgSO_4$ filtered and concentrated to afford **168-*int*** as a white solid (7.9 g, **95%**). The product was used without further purification.

Under N_2, at −78 °C, oxalyl chloride (3.8 mL, 45 mmol, 1.3 equiv.) was diluted in DCM (78 mL) and DMSO (6.4 mL, 90 mmol, 2.6 equiv.) was slowly added. The mixture was stirred for 15 min at −78 °C, then a solution of **168-*int*** (7.9 g, 35 mmol, 1 equiv.) in DCM (43 mL), was added. The mixture was stirred for another 15 min at −78 °C, then triethylamine (25 mL, 180 mmol, 5.2 equiv.) was added. The mixture was stirred 2 h at room temperature, then the reaction was quenched with a saturated

solution of NH_4Cl. The aqueous layer was extracted with diethyl ether. The gathered organic layer was washed with H_2O, brine, dried over $MgSO_4$, filtered and concentrated. Purification by flash chromatography (PE:EtOAc/2:1 to 1:1) gave a yellow solid. The latter was washed in pentane then filtered to give **168** as white solid (5.0 g, **61%**). ^1H NMR (500 MHz, $CDCl_3$): δ 7.78 (d, *J* = 8.2 Hz, 2H), 7.40 (d, *J* = 8.2 Hz, 2H), 4.63 (s, 4H), 2.47 (s, 3H), *the NMR data is in accordance with that reported in the literature.*[113]

9.2 Synthesis of 1,3-enynes :

Method I : *Representative example for the synthesis of **191d.***

A flame dried schlenk was loaded with palladium dichloride (97 mg, 0.14 mmol, 0.05 equiv.) under nitrogen. The schlenk was vacuumed out for 15 min, then back filled with nitrogen. Dry THF (10 mL) was added, followed by triethylamine (1.1 mL, 8.3 mmol, 3 equiv.), copper iodide (37 mg, 0.19 mmol, 0.07 equiv.) and (*E*)-β-bromostyrene (350 µL, 2.75 mmol, 1 equiv.), in that order. A constant argon bubbling was kept during the set-up. The mixture was stirred 5 min at room temperature, then 3-methyl-1-butyne (400 µL, 3.6 mmol, 1.3 equiv.) was added. The mixture was stirred overnight. Then, the mixture was diluted with Et_2O and quenched with NH_4Cl. The aqueous layer was extracted with Et_2O. The combined organic layer was washed with H_2O, brine, dried with $MgSO_4$ and evaporated under vacuum. Purification by flash chromatography (PE: 100%) gave **191d** as a yellowish oil (0.42 g, **90%**).

Method II : *Representative example for the synthesis of **191c.***

Under nitrogen, $Pd(PPh_3)_4$ (89 mg, 0.08 mmol, 0.02 equiv.) was added to a flame dried schlenk followed 2-bromopropene (0.34 mL, 3.8 mmol, 1 equiv.) diluted in piperidine (3.8 mL). The mixture was stirred for 5 min, then, 4-phenyl-1-butyne (0.54 mL, 3.8 mmol, 1 equiv.) and copper iodide (51 mg, 0.27 mmol, 0.07 equiv.) were added. The mixture was stirred at room temperature overnight. Then, the mixture was diluted with Et_2O and quenched with NH_4Cl. The aqueous layer was extracted with Et_2O. The combined organic layer was washed with H_2O, brine, dried with $MgSO_4$ and evaporated under vacuum. Purification by flash chromatography (PE: 100%) gave **191c** as a colourless oil (0.6 g, **93%**).

Compound 191a. This product was obtained as a colourless oil (95 mg, **51%**) from

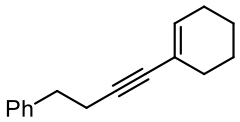

4-phenyl-1-butyne (124 µL, 0.9 mmol, 1.3 equiv.) and 1-cyclohexenyl trifluoromethanesulfonate (119 µL, 0.7 mmol, 1 equiv.) following method **I**. ^1H NMR (500 MHz, $CDCl_3$): δ 7.33 -7.27 (m, 2H), 7.25 -7.19 (m, 3H), 6.03 -5.99 (m, 1H), 2.85 (t, *J* = 7.7 Hz, 2H), 2.58 (t, *J* = 7.7 Hz, 2H), 2.13-2.03 (m, 4H), 1.66-1.51 (m, 4H); ^{13}C NMR (125 MHz, $CDCl_3$): δ 140.9 (e), 133.4 (o), 128.5 (o, 2C), 128.3 (o, 2C), 126.2 (o), 120.9 (e), 86.5 (e), 83.0 (e), 35.4 (e), 29.5 (e), 25.5 (e), 22.4 (e), 21.6 (e, 2C); IR (neat): ν = 3456 (w), 3026 (s), 2970 (s), 2927 (s), 2858 (m), 2838 (m), 1737 (vs), 1453 (s), 1366 (vs), 1228 (vs), 2076 (w), 917 (m), 840 (m), 799 (w), 747 (m), 696 (s); HRMS (CI (NH_3)) calcd for ($C_{16}H_{18}$ + H): 211.1481; found: 211.1489.

Compound 191b. This product was obtained as a yellow oil (492 mg, **85%**) from β-

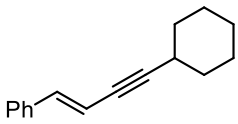

bromostyrene (0.35 mL, 2.8 mmol, 1 equiv.) and cyclohexylacetylene (0.47 mL, 3.6 mmol, 1.3 equiv.) following method **I**. ^{1}H NMR (500 MHz, $CDCl_3$): δ 7.38-7.34 (m, 2H), 7.33-7.29 (m, 2H), 7.27-7.23 (m, 1H), 6.87 (d, *J* = 16.3 Hz, 1H), 6.18 (dd, *J* = 16.2, 2.1 Hz, 1H), 2.58-2.50 (m, 1H), 1.90-1.82 (m, 2H), 1.78-1.70 (m, 2H), 1.59-1.43 (m, 3H), 1.39-1.28 (m, 3H); ^{13}C NMR (125 MHz, $CDCl_3$): δ 139.8 (o), 136.7 (e), 128.6 (o, 2C), 128.1 (o), 126.0 (o, 2C), 108.9 (o), 97.1 (e), 79.6 (e), 32.7 (e, 2C), 29.9 (o), 25.9 (e, 2C), 25.6 (e); IR (neat): ν = 3050 (w), 3027 (w), 2927 (vs), 2852 (s), 2206 (w), 1943 (w), 1789 (w), 1614 (w), 1597 (w), 1491 (m), 1447 (s), 1361 (w), 1349 (w), 1297 (m), 1233 (w), 950 (vs), 908 (m), 888 (w), 746 (vs), 690 (vs); HRMS (CI (NH_3)) calcd for ($C_{16}H_{18}$ + H): 211.1481; found: 211.1490.

Compound 191c. This product was obtained as a colourless oil (607 mg, **93%**) from

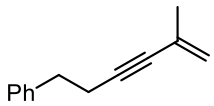

4-phenyl-1-butyne (0.54 mL, 3.8 mmol, 1 equiv.) and 2-bromopropene (0.34 mL, 3.8 mmol, 1 equiv.) following method **II**. ^{1}H NMR (500 MHz, $CDCl_3$): δ 7.32-7.28 (m, 2H), 7.25-7.19 (m, 3H), 5.20 (s, 1H), 5.14 (s, 1H), 2.85 (t, *J* = 7.7 Hz, 2H), 2.59 (t, *J* = 7.6 Hz, 2H), 1.86-1.85 (m, 3H); ^{13}C NMR (125MHz, $CDCl_3$) : δ 140.7 (e), 128.5 (o, 2C), 128.3 (o, 2C), 127.2 (e), 126.3 (o), 120.5 (e), 88.6 (e), 82.6 (e), 35.2 (e), 23.7 (o), 21.6 (e), *the NMR data is in accordance with that reported in the literature.*[114]

Compound 191d. This product was obtained as a yellowish oil (423 mg, **90%**) from

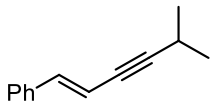

(*E*)-β-bromostyrene (0.35 mL, 2.8 mmol, 1 equiv.) and 3-methyl-1-butyne (0.37 mL, 3.6 mmol, 1.3 equiv.) following method **I**. ^{1}H

NMR (500 MHz, $CDCl_3$): δ 7.38-7.34 (m, 2H), 7.33-7.28 (m, 2H), 7.27-7.23 (m, 1H), 6.87 (d, *J* = 16.3 Hz, 1H), 6.16 (dd, *J* = 16.3, 2.1 Hz, 1H), 2.80-2.78 (m, 1H), 1.23 (d, *J* = 6.8 Hz, 6H); ^{13}C NMR (125 MHz, $CDCl_3$): δ 139.9 (o), 136.6 (e), 128.6 (o, 2C), 128.2 (o), 126.0 (o, 2C), 108.8 (o), 98.3 (e), 78.9 (e), 23.0 (o, 2C), 21.3 (o); IR (neat): ν= 3027 (w), 2968 (s), 2931 (m), 2870 (m), 2213 (w), 1792 (br), 1594 (w), 1494 (m), 1466 (m), 1446 (s), 1382 (m), 1362 (m), 1316 (s), 1270 (w), 1210 (w), 1185 (w), 1132 (w), 1103 (w), 1103 (w), 951 (vs), 908 (s), 746 (vs), 733 (vs), 690 (vs); HRMS (CI (NH_3)) calcd for ($C_{13}H_{14}$ + H): 171.1168; found: 171.1176.

Compound 191e. This product was obtained as a colourless oil (586 mg, **83%**) from

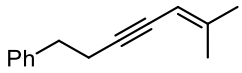

1-bromo-2-methyl-1-propene (0.39 mL, 3.8 mmol, 1 equiv.) and 4-phenyl-1-butyne (0.54 mL, 3.8 mmol, 1 equiv.) following method **II**. ^1H NMR (500 MHz, $CDCl_3$): δ 7.32-7.27 (m, 2H), 7.25-7.18 (m, 3H), 5.22 (s, 1H), 2.86 (t, *J* = 7.5 Hz, 2H), 2.63 (dt, *J* = 7.5, 2.3 Hz, 2H), 1.82 (s, 3H), 1.77 (s, 3H); ^{13}C NMR (125 MHz, $CDCl_3$): 147.1 (e), 140.9 (e), 128.5 (o, 2C), 128.3 (o, 2C), 126.2 (o), 105.2 (o), 91.2 (e), 79.1 (e), 35.5 (e), 24.6 (o), 21.7 (e), 20.7 (o), *the NMR data is in accordance with that reported in the literature.*[114]

Compound 191f. This product was obtained as a yellow oil (522 mg, **quant.**) from β-

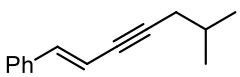

bromostyrene (0.35 mL, 2.8 mmol, 1 equiv.) and 4-methyl-1-pentyne (0.42 mL, 3.6 mmol, 1.3 equiv.) following method **I**. ^1H NMR (500 MHz, $CDCl_3$): δ 7.38-7.35 (m, 2H), 7.33-7.29 (m, 2H), 7.27-7.23 (m, 1H), 6.88 (d, *J* = 16.2 Hz, 1H), 6.18 (dt, *J* = 16.3, 2.2 Hz, 1H), 2.26 (dd, *J* = 6.5, 2.2 Hz, 2H), 1.87 (m, 1H), 1.03 (d, *J* = 6.7 Hz, 6H); ^{13}C NMR (125 MHz, $CDCl_3$): δ 139.9 (o),

136.6 (e), 128.6 (o, 2C), 128.2 (o), 126.0 (o, 2C), 108.9 (o), 92.0 (e), 80.6 (e), 28.8 (e), 28.2 (o), 22.0 (o, 2C); IR (neat): ν = 3027 (w), 2957 (s), 2898 (w), 2869 (w), 2828 (w), 2208 (w), 1789 (br), 1596 (m), 1490 (m), 1464 (m), 1448 (m), 1426 (w), 1384 (w), 1367 (w), 1343 (w), 1279 (s), 1167 (br), 951 (vs), 747 (vs), 690 (vs); HRMS (CI (NH_3)) calcd for ($C_{14}H_{16}$ + H): 185.325; found: 185.1334.

Compound 191g. This product was obtained as a colourless oil (106 mg, **77%**) from

trans-1-iodo-1-octene (80 µL, 0.6 mmol, 1 equiv.) and 4-phenyl-1-butyne (147 µL, 0.6 mmol, 1 equiv.) following method **II**. ^{1}H NMR (500 MHz, $CDCl_3$): δ 7.32-7.27 (m, 2H), 7.24-7.19 (m, 3H), 6.06 (dt, *J* = 15.7, 7.2 Hz, 1H), 5.47-5.41 (m, 1H), 2.86 (t, *J* = 7.7 Hz, 2H), 2.58 (dt, *J* = 7.8, 1.9 Hz, 2H), 2.08 (q, *J* = 7.5 Hz, 2H), 1.41-1.22 (m, 8H), 0.90 (t, *J* = 6.7 Hz, 3H); ^{13}C NMR (125 MHz, $CDCl_3$): δ 143.8 (o), 140.8 (e), 128.4 (o, 2C), 128.3 (o, 2C), 126.2 (o), 109.6 (o), 87.7 (e), 79.9 (e), 35.3 (e), 33.0 (e), 31.7 (e), 28.8 (e, 2C), 22.6 (e), 21.6 (e), 14.1 (o); IR (neat): ν = 3026 (w), 2955 (m), 2925 (vs), 2855 (s), 1944 (w), 1604 (w), 1496 (m), 1454 (s), 1377 (w), 1340 (w), 1305 (w), 1259 (w), 1165 (w), 1076 (w), 953 (vs), 909 (s), 734 (vs), 697 (vs); HRMS (CI (NH_3)) calcd for ($C_{18}H_{24}$ + H): 241.1951; found: 241.1958.

Compound 191h. This product was obtained as a yellow oil (558 mg, **85%**) from β-

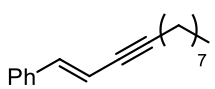

bromostyrene (0.35 mL, 2.8 mmol, 1 equiv.) and 1-decyne (0.6 mL, 3.6 mmol, 1.3 equiv.) following method **I**. ^{1}H NMR (500 MHz, $CDCl_3$): δ 7.38-7.34 (m, 2H), 7.34-7.29 (m, 2H), 7.37-7.23 (m, 1H), 6.87 (d, *J* = 16.3 Hz, 1H), 6.16 (d, *J* = 16.5 Hz, 1H), 2.37 (dt, *J* = 7.2, 2.2 Hz, 2H), 1.57 (quint, *J* = 7.2 Hz, 2H), 1.46-1.39 (m, 2H), 1.36-1.22 (m, 8H), 0.92-0.86 (m, 3H); ^{13}C NMR (125

MHz, $CDCl_3$): δ 140.0 (o), 136.6 (e), 128.6 (o, 2C), 128.2 (o), 126.0 (o, 2C), 108.9 (o), 93.1 (e), 79.7 (e), 31.9 (e), 29.2 (e), 29.2 (e), 29.0 (e), 28.8 (e), 22.7 (e), 19.7 (e), 14.1 (o); IR (neat): ν = 3027 (w), 2924 (vs), 2854 (s), 2211 (w), 1465 (m), 1448 (m), 950 (vs), 745 (vs), 722 (m), 689 (vs); HRMS (CI (NH_3)) calcd for ($C_{18}H_{24}$ + H): 241.1951; found: 241.1952.

Compound 191i. This product was obtained as a yellow oil (423 mg, **62%**) from 2-

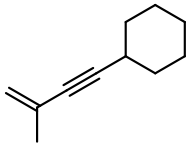

bromopropene (0.53 mL, 6 mmol, 1.3 equiv.) and cyclohexylacetylene (0.6 mL, 4.6 mmol, 1 equiv.) following method **I**. ^{1}H NMR (500 MHz, $CDCl_3$): δ 5.20-5.18 (m, 1H), 5.14-5.11 (m, 1H), 2.5-2.43 (m, 1H), 1.87 (s, 3H), 1.84-1.67 (m, 4H), 1.53-1.40 (m, 3H), 1.37-1.26 (m, 3H); ^{13}C NMR (125 MHz, $CDCl_3$): δ 127.4 (e), 120.5 (e), 93.5 (e), 82.3 (e), 32.7 (e, 2C), 29.5 (o), 25.9 (e, 2C), 24.9 (e), 24.0 (o); IR (neat): ν = 2927 (vs), 2854 (s), 2219 (w), 1785 (w), 1614 (m), 1448 (s), 1372 (m), 1318 (w), 1302 (m), 1284 (m), 1233 (w), 1134 (w), 1011 (w), 986 (w), 887 (vs), 861 (w), 844 (w), 791 (w); HRMS (CI (NH_3)) calcd for ($C_{11}H_{16}$ + H): 149.1325; found: 149.1330.

Compound 191j. This product was obtained as a colourless oil (206 mg, **70%**) from

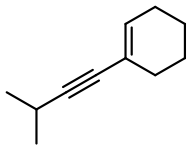

1-cyclohexenyl trifluoromethanesulfonate (0.35 mL, 2 mmol, 1 equiv.) and 3-methyl-1-butyne (0.27 mL, 2.6 mmol, 1.3 equiv.) following method **I**. ^{1}H NMR (500 MHz, $CDCl_3$): δ 6.02-5.99 (m, 1H), 2.66 (sept, *J* = 6.9 Hz, 1H), 2.12-2.02 (m, 4H), 1.65-1.53 (m, 4H), 1.18 (d, *J* = 6.9 Hz, 6H) ; ^{13}C NMR (125 MHz, $CDCl_3$): δ 133.2 (o), 120.9 (e), 91.9 (e), 81.4 (e), 29.7 (e), 25.6 (e), 23.2 (o, 2C), 22.4 (e), 21.6 (e), 21.0 (o); IR (neat): ν = 3028 (w), 2968 (m), 2929 (s), 2870 (m), 1634 (w), 1448 (m), 1436 (m), 1381 (w), 1360 (w), 1342 (w), 1319 (s), 1269 (w), 1239

(w), 1214 (w), 1135 (w), 1104 (w), 1077 (w), 1045 (w), 977 (w), 970 (vs), 856 (w), 840 (m), 804 (w), 732 (vs); HRMS (CI (NH_3)) calcd for ($C_{11}H_{16}$ + H): 149.1325; found: 149.1331.

Compound 191k. This product was obtained as a yellow oil (580 mg, **97%**) from 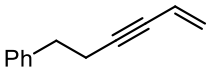 vinyl bromide (12 mL, 1.6 M in THF, 19 mmol, 5 equiv.) and 4-phenyl-1-butyne (648 µL, 3.8 mmol, 1 equiv.) following method **I**. ^{1}H NMR (500 MHz, $CDCl_3$): δ 7.33-7.28 (m, 2H), 7.25-7.19 (m, 3H), 5.78 (dt, *J* = 11.0, 2.0 Hz, 1H), 5.55 (dd, *J* = 17.8, 2.0 Hz, 1H), 5.39 (dd, *J* = 11.0, 2.0 Hz, 1H), 2.86 (t, *J* = 7.5 Hz, 2H), 2.60 (dt, *J* = 7.6, 1.9 Hz, 2H); ^{13}C NMR (125 MHz, $CDCl_3$): δ 140.6 (e), 128.4 (o, 2C), 128.3 (o, 2C), 126.3 (o), 125.7 (e), 117.5 (o), 90.2 (e), 80.0 (e), 35.1 (e), 21.5 (e), *the NMR data is in accordance with that reported in the literature.* [115]

Compound 191l.

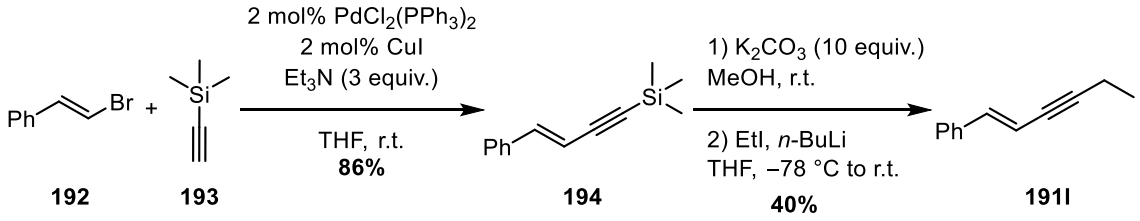

A flame dried schlenk was loaded with palladium dichloride (77 mg, 0.1 mmol, 0.03 equiv.) under nitrogen. The schlenk was vacuumed out for 15 min, then back filled with nitrogen. Dry THF (20 mL) was added, followed by triethylamine (2.2 mL, 16.6 mmol, 4.3 equiv.), copper iodide (21 mg, 0.1 mmol, 0.03 equiv.) and (*E*)-β-bromostyrene (496 µL, 3.9 mmol, 1 equiv.), in that order. A constant argon bubbling was kept during the set-up. The mixture was stirred 5 min at room temperature,

then trimethylsilylacetylene (1 mL, 7.2 mmol, 1.8 equiv.) was added. The mixture was stirred overnight. Then, the mixture was diluted with Et_2O and quenched with NH_4Cl. The aqueous layer was extracted with Et_2O. The combined organic layer was washed with H_2O, brine, dried with $MgSO_4$ and evaporated under vacuum. Purification by flash chromatography (PE: 100%) gave **194** as a colourless oil (675 mg, **87%**).

To a mixture of **194** (675 mg, 3.4 mmol, 1 equiv.) in methanol (10 mL) at room temperature was added potassium carbonate (4.7 g, 33.8 mmol, 10 equiv.) and the mixture was stirred overnight. All volatiles were evaporated and the crude mixture was partitioned between Et_2O and H_2O. The aqueous layer was extracted 3 more times with Et_2O. The gathered organic layer was washed with H_2O, brine, dried over $MgSO_4$ filtered and concentrated to afford the deprotected terminal alkyne as a colourless oil (304 mg, **70%**). The product was used without purification

Under N_2, at −78 °C, *n*-BuLi (1.2 mL, 2.5 M in Hexanes, 3.1 mmol, 1.3 equiv.) was added dropwise to the residue (304 mg, 2.4 mmol, 1 equiv.) in THF (10 mL). The mixture was warmed up to room temperature and iodoethane (0.2 mL, 2.4 mmol, 1 equiv.) was added. The mixture was stirred at room temperature overnight. Then, the mixture was diluted with Et_2O and quenched with NH_4Cl. The aqueous layer was extracted with Et_2O. The combined organic layer was washed with H_2O, brine, dried with $MgSO_4$ and evaporated under vacuum. Purification by flash chromatography (PE: 100%) afforded **191l** as a yellowish oil (0.157 g, **42%**) as a mixture of *E/Z* isomers in a 80:20 ratio. *E*-isomer: ^{1}H NMR (500 MHz, $CDCl_3$): δ 7.38-7.29 (m, 5H), 6.88 (d, *J* = 16.4 Hz, 1H), 6.16 (dt, *J* = 16.3, 2.2 Hz, 1H), 2.39 (dq, *J* = 7.7, 2.1 Hz, 2H), 1.21 (t, *J* = 7.6 Hz, 3H) ; *Z*-isomer: ^{1}H NMR (500 MHz, $CDCl_3$): δ 7.87 (d, *J* = 7.34 Hz, 2H), 7.29-7.20 (m, 3H), 6.56 (d, *J* = 11.9 Hz, 1H), 5.70 (dt, *J* = 12.0, 2.4, 1H), 2.47 (dq, *J*

= 7.6, 2.5, 2H), 1.25 (t, *J* = 7.6 Hz, 3H), *the NMR data is in accordance with that reported in the literature.*[116]

Compound 191m.

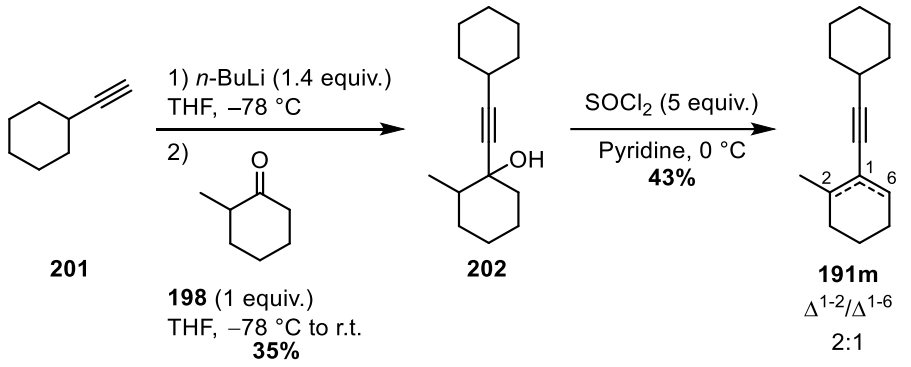

A flame-dried round bottom flask, under nitrogen was loaded with **201** (1.5 mL, 11.5 mmol, 1.1 equiv.) and THF (25 mL). The mixture was cooled to −78 °C and *n*-BuLi (4.6 mL, 2.5M in hexanes, 11.5 mmol, 1.1 equiv.) was added dropwise. The mixture was stirred at −78 °C for 15 min with a vigorous stirring. Then, **198** (1.1 mL, 8.2 mol, 1 equiv.) in THF (8 mL) was added. The mixture was stirred at room temperature for 4 hours. The reaction was quenched with sat. NH_4Cl and the aqueous layer was extracted with Et_2O. The gathered organic layer was washed with water and brine, was dried with $MgSO_4$ and evaporated under vacuum. Purification by flash chromatography (PE/EtOAc:95/5) afforded **202** as a colourless oil (626 mg, **35%**).

202 (300 mg, 1.4 mmol, 1 equiv.) was dissolved in pyridine (5.6 mL). The mixture was cooled to 0 °C and $SOCl_2$ (0.5 mL, 6.9 mmol, 5 equiv.) was added dropwise. The mixture was stirred at 0 °C for another 1 h before the reaction was quenched with sat. $NaHCO_3$ and the aqueous layer was extracted with Et_2O. The gathered organic layer was thoroughly washed with water, brine, dried with $MgSO_4$ and evaporated under

vacuum. Purification by flash chromatography (PE: 100%) gave **191m** as a 2:1 mixture of isomers as a colourless oil (117 mg, **43%**). ^{1}H NMR (500 MHz, $CDCl_3$): δ 6.00 (dt, J = 4.0, 1.8 Hz, 0.5H, min.), 2.58-2.45 (m, 1.4H, maj.+min.), 2.26-2.16 (m, 0.6H, min.), 2.14-2.07 (m, 2H, maj.), 2.06-1.95 (m, 3H, maj.), 1.85 (s, 3H, maj.), 1.84-1.66 (m, 6.6H, maj.+min.), 1.62-1.55 (m, 4H, maj.), 1.53-1.41 (m, 4.8H, maj.+min.), 1.38-1.25 (m, 5.1H, maj.+min.), 1.13 (d, J = 7.1 Hz, 1.6 H, min.); ^{13}C NMR (125 MHz, $CDCl_3$): δ 139.8 (e, maj.), 133.0 (o, min.), 126.5 (e, min.), 114.4 (e, maj.), 96.0 (e, maj.), 92.6 (e, min.), 81.2 (e, min.), 81.1 (e, maj.), 33.1 (e), 32.9 (e), 32.9 (o), 32.9 (e), 31.1 (e), 30.8 (e), 30.3 (e), 29.8 (o), 26.0 (e), 26.0 (e), 25.9 (e), 24.9 (e), 22.6 (e), 22.0 (o), 20.4 (o), 19.9 (e); IR (neat): ν = 2925 (vs), 2852 (s), 1447 (s), 1361 (m), 1297 (w), 1234 (w), 1139 (w), 1111 (w), 1001 (w), 932 (w), 887 (m), 811 (m), 602 (m); HRMS (CI (NH_3)) calcd for ($C_{15}H_{22}$ + H): 203.1794; found: 203.1800.

9.3 Nickel-catalysed (4+2) cycloaddition

Method **III**: *Representative example for the synthesis of **203c***.

Inside a glovebox, a Teflon-screw flame-dried Schlenk equipped with a small stirrer bar was charged with $Ni(cod)_2$ (6.1 mg, 0.022 mmol, 0.1 equiv.), sealed and taken out of the glovebox. Under N_2, PPh_3 (17.3 mg, 0.066 mmol, 0.3 equiv.) is added with toluene (0.2 mL). The mixture was stirred at room temperature for 10 min, then, **168** (50 mg, 0.22 mmol, 1 equiv.) was added followed by **191c** (42 mg, 0.024 mmol, 1.1 equiv.) diluted in toluene (0.8 mL). Then, the tube was sealed and the mixture was stirred at 60 °C overnight and filtered through a small plug of silica. Purification by flash chromatography (PE:EtOAc/95:5 to 90:10) afforded **203c** as a colourless paste (64 mg, **73%**).

Method **IV**: Same procedure as before but **0.2 equiv.** of PPh_3 were used.

Method **V**: *Representative example for the synthesis of **203f**.*

A flame-dried Schlenk tube equipped with a small stirrer, under N_2, was charged with $NiBr_2(PPh_3)_2$ (33 mg, 0.044 mmol, 0.1 equiv.), zinc (14 mg, 0.22 mol, 0.5 equiv.), **168** (100 mg, 0.44 mmol, 1 equiv.), **191f** (90 mg, 0.49 mmol, 1.1 equiv.) and THF (1.6 mL). Then the flask was sealed and the mixture was stirred at 70 °C overnight. Afterwards, the mixture was cooled down and filtered through a plug of silica before evaporation. Purification by flash chromatography (PE:EtOAc/95:5 to 90:10) afforded **203f** as a colourless paste (97 mg, **54%**).

All the results obtained with method **III**, **IV** and **V** are compiled in the table below. Most attempts were reproduced, and the yields presented previously are averages of those duplicates. The Boc-protected azetidinone **53** was used with **191k** (Table 13, entry **12**). The α-substituted tosyl-protected azetidinone **208** was used with **176** (Table 13, entry **15**).

Entry	**Enyne**	**Yield of the isolated major isomer (%)**		
		Method **III**	Method **IV**	Method **V**
1	191a	**79/71**	**72/67**	**66**
2	191b	**54/54**	**43/53/40**	**31**
3	191c	**78/73/67**	**64/60**	**51**
4	191d	**79/76**	**67/75**	**59**
5	191e	**75/78**	**72/70**	**69**
6	191f	**72/70**	**76/70**	**54/47**
7	191g	/	**65/69**	/

8	191h	/	**77/77**	/
9	191i	**64/65**	**63/50**	/
10	191j	**62/65**	**61/53**	/
11	191k	**69**	/	**69/64**
12	53+191k	**60/55**	/	/
13	191m	**51**	/	/
14	176	**69**	/	/
15	208+176n	**64/64**	/	/

Table 13 : Summary of the resulsts for the (4+2) insertion of 1,3-enynes in azetidinone

The analytical data for **203a-n**, **207k** and **209** are compiled below:

Compound 203a. Colourless oil. (method **III**: first attempt: 76 mg (**79%**), second attempt: 69 mg (**71%**)). ^{1}H NMR (500 MHz, $CDCl_3$): δ 7.69-7.65 (m, 2H), 7.34 (d, *J* = 8.0 Hz, 2H), 7.28-7.23 (m, 2H), 7.19-7.13 (m, 1H), 7.10-7.07 (m, 2H), 5.40-5.35 (m, 1H), 3.89 (s, 2H), 3.81 (s, 2H), 2.48-2.37 (m, 7H), 2.09-2.04 (m, 2H), 1.92-1.88 (m, 2H), 1.69-1.57 (m, 4H); ^{13}C NMR (125 MHz, $CDCl_3$): δ 191.8 (e), 155.9 (e), 144.2 (e), 141.8 (e), 134.2 (e), 133.2 (e), 132.9 (e), 130.0 (o, 2C), 128.3 (o, 4C), 127.7 (o, 2C), 127.3 (o), 125.9 (o), 52.6 (e), 48.0 (e), 35.5 (e), 28.3 (e), 27.3 (e), 24.9 (e), 22.3 (e), 21.6 (e), 21.5 (o); IR (neat): ν = 3026 (w), 2926 (m), 2857 (w), 2256 (w), 1674 (s), 1598 (m), 1495 (m), 1438 (m), 1400 (w), 1350 (s), 1305 (w), 1291 (w), 1268 (w), 1234 (w), 1210 (w), 1180 (vs), 1137 (w), 1118 (m), 1088 (s), 991 (w), 961 (m), 909 (m), 880 (w), 847 (w), 814 (m), 802 (w), 780 (w), 754 (w), 729 (vs), 693 (s), 674 (m), 660 (w); HRMS (ESI) calcd for ($C_{26}H_{29}NO_3S$ + Na): 458.1766; found: 458.1757.

Compound 203b. Yellow solid. (method **III**: first attempt: 52 mg (**54%**), second attempt: 52 mg (**54%**)). ***170*** *and* ***193b*** *were added as a solution*. m.p.: 178-182 °C; ^{1}H NMR (500 MHz, $CDCl_3$): δ 7.67 (d, *J* = 8.2 Hz, 2H), 7.50 (d, *J* = 7.4 Hz, 2H), 7.42 (t, *J* = 7.2 Hz, 2H), 7.39-7.34 (m, 1H), 7.32 (d, *J* = 8.3 Hz, 2H), 7.24 (d, *J* = 16.5 Hz, 1H), 6.96 (d, *J* = 16.4 Hz, 1H), 4.26 (s, 2H), 3.80 (s, 2H), 2.72-2.64 (m, 1H), 2.41 (s, 3H), 1.84-1.64 (m, 5H), 1.31-1.21 (m, 5H); ^{13}C NMR (125 MHz, $CDCl_3$): δ 191.5 (e), 145.0 (e), 144.2 (e), 139.4 (e), 135.9 (e), 135.5 (o), 133.3 (e), 130.0 (o, 2C), 129.4 (o), 129.0 (o, 2C), 127.6 (o, 2C), 127.2 (o, 2C), 123.0 (o), 53.2 (e), 45.2 (e), 37.8 (o), 30.1 (e, 2C), 27.0 (e, 2C), 25.8 (e), 21.4 (o); IR (neat): ν = 2927 (m), 2853 (m), 1661 (vs), 1607 (s), 1576 (m), 1557 (m), 1494 (m), 1442 (s), 1392 (m), 1342 (vs), 1324 (s), 1303 (s), 1264 (w), 1243 (m), 1226 (w), 1160 (vs), 1121 (m), 1089 (s), 1051 (s), 981 (s), 956 (s), 860 (s), 842 (m), 814 (m), 806 (m), 751 (s), 730 (s), 707 (m), 684 (s); HRMS (ESI) calcd for ($C_{26}H_{29}NO_3S$ + Na): 458.1766; found: 458.1759; elemental analysis (%) calcd for $C_{26}H_{29}NO_3S$: C 71.7, H 6.7, N 3.2, S 7.4; found C 70.77, H 6.86, N 2.88, S 6.71.

Compound 203c. Colourless paste. (method **III**: first attempt: 68 mg (**78%**), second attempt: 64 mg (**73%**)). ^{1}H NMR (500 MHz, $CDCl_3$): δ 7.68 (d, *J* = 8.2 Hz, 2H), 7.34 (d, *J* = 8.0 Hz, 2H), 7.27-7.23 (m, 2H), 7.16 (tt, *J* = 7.3, 1.4 Hz, 1H), 7.12-7.08 (m, 2H), 5.09 (br s, 1H), 4.69 (br s, 1H), 3.94 (s, 2H), 3.85 (s, 2H), 2.42 (s, 7H), 1.79 (s, 3H); ^{13}C NMR (125 MHz, $CDCl_3$): δ 191.5 (e), 154.9 (e), 144.3 (e), 141.6 (e), 140.6 (e), 133.2 (e), 132.9 (e), 130.0 (o, 2C), 128.3 (o, 3C), 127.7 (o, 2C), 126.0 (o, 2C), 115.8 (e), 52.6 (e), 47.6 (e), 35.4 (e), 28.2 (e), 21.6 (o), 21.5 (o); IR (neat): ν = 3343 (br), 3060 (w), 3028 (w), 2923 (w), 1681 (s), 1620 (w), 1598 (m), 1496 (m), 1440 (m), 1400 (w), 1346 (s), 1305 (w),

1292 (w), 1263 (m), 1234 (w), 1180 (vs), 1122 (m), 1090 (m), 1029 (m), 1002 (w), 961 (m), 908 (m), 886 (w), 816 (m), 755 (m), 733(m), 700 (s), 665 (vs); HRMS (ESI) calcd for ($C_{23}H_{25}NO_3S$ + Na): 418.1453; found: 418.1457.

Compound 203d. Yellow solid. (method **III**: first attempt: 69 mg (**79%**), second attempt: 67 mg (**76%**)). m.p.: 138-140 °C; ^{1}H NMR (500 MHz, $CDCl_3$): δ 7.68 (d, *J* = 8.3 Hz, 2H), 7.53-7.48 (m, 2H), 7.43-7.38 (m, 2H), 7.38-7.34 (m, 1H), 7.32 (d, *J* = 8.3 Hz, 2H), 7.21 (d, *J* = 16.3 Hz, 1H), 6.97 (d, *J* = 16.6 Hz, 1H), 4.27 (s, 2H), 3.81 (s, 2H), 3.09 (sept, *J* = 7.5 Hz, 1H), 2.40 (s, 3H), 1.1 (d, *J* = 7.08 Hz, 6H); ^{13}C NMR (125 MHz, $CDCl_3$): δ 191.3 (e), 144.6 (e), 144.2 (e), 140.0 (e), 135.8 (e), 135.6 (o), 133.3 (e), 130.0 (o, 2C), 129.5 (o), 129.0 (o, 2C), 127.6 (o, 2C), 127.3 (o, 2C), 122.6 (o), 53.1 (e), 45.1 (e), 26.6 (o), 21.4 (o), 20.6 (o, 2C); IR (neat): ν = 2961(w), 2926 (w), 2871 (w), 1662 (vs), 1609 (m), 1576 (w), 1564 (w), 1495 (w), 1446 (m), 1340 (vs), 1321 (s), 1304 (m), 1238 (w), 1173 (m), 1180 (vs), 1130 (w), 1099 (s), 1020 (w), 998 (s), 971 (m), 956 (s), 930 (w), 884 (w), 860 (w), 841 (s), 812 (s), 752 (s), 711 (s), 687 (vs), 659 (vs); HRMS (ESI) calcd for ($C_{23}H_{25}NO_3S$ + Na): 418.1453; found: 418.1445; elemental analysis (%) calcd for $C_{23}H_{25}NO_3S$: C 69.8, H 6.3, N 3.5, S 8.1; found C 67.83, H 6.30, N 3.26, S 7.31.

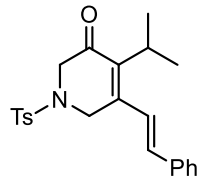

Compound 203e. Colourless paste. (method **III**: first attempt: 68 mg (**75%**), second attempt: 71 mg (**78%**)). ^{1}H NMR (500 MHz, $CDCl_3$): δ 7.67 (d, *J* = 8.4 Hz, 2H), 7.34 (d, *J* = 8.4 Hz, 2H), 7.26-7.22 (m, 2H), 7.16 (t, *J* = 7.7 Hz, 1H), 7.12-7.08 (m, 2H), 5.55 (s, 1H), 3.85 (s, 2H), 3.78 (s, 2H), 2.42 (s, 7H), 1.81 (s, 3H), 1.58 (s, 3H); ^{13}C NMR (125 MHz, $CDCl_3$): δ

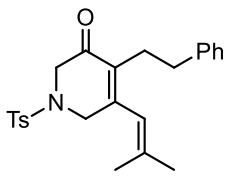

191.4 (e), 150.7 (e), 144.3 (e), 141.7 (e), 141.0 (e), 134.3 (e), 132.0 (e), 130.0 (o, 2C), 128.4 (o, 2C), 128.3 (o, 2C), 127.7 (o, 2C), 125.9 (o), 120.4 (o), 52.8 (e), 48.2 (e), 34.4 (e), 27.7 (e), 26.2 (o), 21.6 (o), 20.3 (o); IR (neat): ν = 3026 (w), 2928 (m), 2859 (w), 2254 (w), 1672 (vs), 1598 (m), 1495 (m), 1442 (m), 1378 (w), 1349 (vs), 1316 (m), 1291 (w), 1234 (m), 1185 (w), 1163 (vs), 1118 (m), 1088 (m), 1024 (s), 961 (s), 910 (m), 853 (m), 814 (s), 751 (w), 731 (s), 698 (s), 678 (m); HRMS (ESI) calcd for ($C_{24}H_{27}NO_3S$ + Na): 432.1609; found: 432.1601; elemental analysis (%) calcd for $C_{24}H_{27}NO_3S$: C 70.4, H 6.60, N 3.42, S 7.84; found C 66.22, H 6.28, N 3.11, S 7.08.

Compound 203f. Yellow solid. (method **IV**: first attempt: 69 mg (**76%**), second attempt: 63 mg (**70%**)). m.p.: 154-158 °C; ^{1}H NMR (500 MHz, $CDCl_3$): δ 7.70 (d, *J* = 8.3Hz, 2H), 7.50 (d, *J* = 7.5 Hz, 2H), 7.43-7.39 (m, 2H), 7.38-7.35 (m, 1H), 7.34 (d, *J* = 8.3 Hz, 2H), 7.14 (d, *J* = 16.6 Hz, 1H), 6.95 (d, *J* = 16.4 Hz, 1H), 4.28 (s, 2H), 3.84 (s, 2H), 2.43 (s, 3H), 2.30 (d, *J* = 7.0 Hz, 2H), 1.61 (sept, *J* = 6.8 Hz, 1H), 0.82 (d, *J* = 6.6 Hz, 6H); ^{13}C NMR (125 MHz, $CDCl_3$): δ 191.4 (e), 145.7 (e), 144.3 (e), 136.0 (e), 135.4 (o), 135.0 (e), 133.0 (e), 130.0 (o, 2C), 129.5 (o), 129.0 (o, 2C), 127.6 (o, 2C), 127.3 (o, 2C), 123.3 (o), 52.6 (e), 44.6 (e), 32.6 (e), 29.1 (o), 22.5 (o, 2C), 21.5 (o); IR (neat): ν = 2947 (m), 2865 (w), 1662 (s), 1613 (m), 1597 (m), 1582 (m), 1495 (w), 1465 (w), 1447 (m), 1396 (w), 1382 (w), 1367 (w), 1343 (s), 1330 (s), 1305 (m), 1283 (w), 1246 (m), 1224 (w), 1202 (w), 1182 (w), 1180 (vs), 1124 (m), 1088 (m), 1026 (m), 960 (s), 865 (m), 848 (m), 839 (m), 812 (m), 753 (m), 709 (m), 692 (m), 675 (s); HRMS (ESI) calcd for ($C_{24}H_{27}NO_3S$ + Na): 432.1609; found: 432.1606.

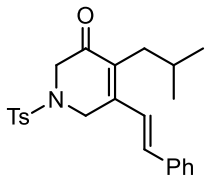

Compound 203g. Yellow paste. (method **IV**: first attempt: 71 mg (**69%**), second attempt: 69 mg (**71%**)). ^{1}H NMR (500 MHz, $CDCl_3$): δ 7.66 (d, *J* = 8.3 Hz, 2H), 7.32 (d, *J* = 8.3 Hz, 2H), 7.29-7.23 (m, 2H), 7.19-7.11 (m, 3H), 6.26 (d, *J* = 16.0 Hz, 1H), 6.16 (dt, *J* = 15.8, 6.9 Hz, 1H), 4.11 (s, 2H), 3.83 (s, 2H), 2.56-2.50 (m, 2H), 2.44-2.37 (m, 5H), 2.18 (q, *J* = 7.2 Hz, 2H), 1.47-1.39 (m, 2H), 1.38-1.27 (m, 6H), 0.91 (t, *J* = 7.1 Hz, 3H); ^{13}C NMR (125 MHz, $CDCl_3$): δ 191.4 (e), 146.0 (e), 144.2 (e), 141.4 (e), 140.5 (o), 133.3 (e), 132.8 (e), 130.0 (o, 2C), 128.3 (o, 4C), 127.6 (o, 2C), 126.0 (o), 125.0 (o), 52.6 (e), 44.7 (e), 35.1 (e), 33.9 (e), 31.6 (e), 28.9 (e), 28.7 (e), 26.1 (e), 22.6 (e), 21.5 (o), 14.1 (o); IR (neat): ν = 3028 (w), 2926 (s), 2855 (m), 1670 (s), 1627 (m), 1597 (m), 1545 (w), 1495 (m), 1454 (m), 1350 (s), 1306 (m), 1238 (w), 1163 (vs), 1121 (m), 1088 (m), 1031 (m), 1009 (m), 962 (s), 846 (w), 813 (s), 752 (m), 699 (s), 677 (s); HRMS (ESI) calcd for ($C_{28}H_{35}NO_3S$ + Na): 488.2235; found: 488.2230; elemental analysis (%) calcd for $C_{28}H_{35}NO_3S$: C 72.22, H 7.52, N 3.00, S 6.89; found C 71.34, H 7.53, N 2.87, S 6.62.

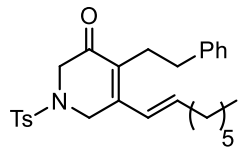

Compound 203h. Yellowish foam. (method **IV**: first attempt: 160 mg (**77%**), second attempt: 80 mg (**77%**)). ^{1}H NMR (500 MHz, $CDCl_3$): δ 7.68 (d, *J* = 8.6 Hz, 2H), 7.53-7.49 (m, 2H), 7.44-7.34 (m, 3H), 7.32 (d, *J* = 8.4 Hz, 2H), 7.10 (d, *J* = 16.3 Hz, 1H), 6.96 (d, *J* = 16.4 Hz, 1H), 4.29 (s, 2H), 3.87 (s, 2H), 2.41 (s, 3H), 2.37-2.31 (m, 2H), 1.34-1.20 (m, 10H), 1.18-1.09 (m, 2H), 0.87 (t, *J* = 6.7 Hz, 3H); ^{13}C NMR (125 MHz, $CDCl_3$): δ 191.2 (e), 144.7 (e), 144.2 (e), 135.9 (e), 135.8 (e), 135.7 (o), 133.4 (e), 130.0 (o, 2C), 129.5 (o), 129.0 (o, 2C), 127.6 (o, 2C), 127.3 (o, 2C), 122.9 (o), 52.6 (e), 44.6 (e), 31.8 (e), 29.7 (e), 29.6 (e), 29.3 (e), 29.2 (e), 24.0 (e), 22.6 (e), 21.5 (o), 14.1 (o); IR (neat): ν = 2923 (s), 2853

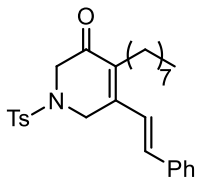

(m), 1720 (w), 1664 (vs), 1613 (m), 1581 (w), 1494 (w),1448 (m), 1342 (vs), 1306 (m), 1243 (m), 1161 (vs), 1121 (m), 1089 (m), 1024 (m), 958 (s), 862 (w), 815 (m), 751 (m), 680 (s); HRMS (ESI) calcd for ($C_{28}H_{35}NO_3S$ + Na): 488.2235; found: 488.2233.

Compound 203i. Colourless paste. (method **III**: first attempt: 54 mg (**65%**), second attempt: 53 mg (**64%**)). ^{1}H NMR (500 MHz, $CDCl_3$): δ 7.64 (d, *J* = 8.3 Hz, 2H), 7.32 (d, *J* = 8.3 Hz, 2H), 5.07 (s, 1H), 4.72 (s, 1H), 3.89 (s, 2H), 3.74 (s, 2H), 2.41 (s, 3H), 2.22 (tt, *J* = 11.9, 3.11 Hz, 1H), 1.87 (s, 3H), 1.81-1.55 (m, 5H), 1.18-1.04 (m, 5H); ^{13}C NMR (125 MHz, $CDCl_3$): δ 191.4 (e), 154.1 (e), 144.2 (e), 141.1 (e), 137.2 (e), 133.1 (e), 130.0 (o, 2C), 127.6 (o, 2C), 115.1 (e), 53.3 (e), 47.9 (e), 39.8 (o), 29.9 (e, 2C), 26.7 (e, 2C), 25.6 (e), 22.0 (o), 21.4 (o); IR (neat): ν = 2925 (s), 2852 (m), 1670 (vs), 1597 (m), 1494 (w), 1444 (s), 1345 (vs), 1306 (m), 1272 (m), 1242 (m), 1190 (vs), 1088 (s), 1044 (m), 1012 (w), 982 (m), 960 (vs), 926 (s), 917 (m), 901 (m), 886 (w), 842 (w), 822 (m), 812 (m), 802 (s), 790 (s), 734 (s), 707 (m), 682 (vs), 654 (s); HRMS (ESI) calcd for ($C_{21}H_{27}NO_3S$ + Na): 396.1609; found: 396.1601.

Compound 203j. White solid. (method **III**: first attempt: 51 mg (**62%**), second attempt: 54 mg (**65%**)). m.p.: 102-106 °C; ^{1}H NMR (500 MHz, $CDCl_3$): δ 7.65 (d, *J* = 8.4 Hz, 2H), 7.32 (d, *J* = 8.3 Hz, 2H), 5.47-5.43 (m, 1H), 3.86 (s, 2H), 3.73 (s, 2H), 2.60 (sept, *J* = 7.0 Hz, 1H), 2.42 (s, 3H), 2.11-2.05 (m, 2H), 2.03-1.97 (m, 2H), 1.73-1.67 (m, 2H), 1.65-1.59 (m, 2H), 0.99 (d, *J* = 7.0 Hz, 6H); ^{13}C NMR (125 MHz, $CDCl_3$): δ 191.5 (e), 154.5 (e), 144.1 (e), 137.8 (e), 134.6 (e), 133.1 (e), 129.9 (o, 2C), 127.6 (o, 2C), 126.3 (o), 53.3

(e), 48.2 (e), 28.8 (o), 27.4 (e), 24.7 (e), 22.2 (e), 21.4 (e), 21.4 (o), 20.6 (o, 2C); IR (neat): ν = 2929 (m), 2875 (w), 2838 (w), 1675 (vs), 1598 (m), 1448 (m), 1346 (vs), 1317 (s), 1297 (m), 1237 (w), 1162 (vs), 1091 (s), 989 (s), 966 (s), 891 (m), 844 (m), 804 (s), 777 (m), 696 (s); HRMS (ESI) calcd for ($C_{21}H_{27}NO_3S$ + Na): 396.1609; found: 396.1605.

Compound 203m. White foam (method **III**: 48 mg (**51%**), 52 mg (**54%**)). ^{1}H NMR

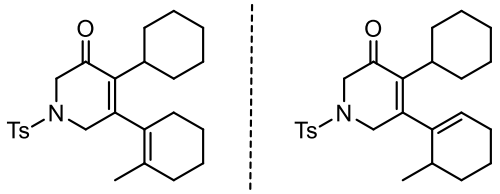

(500 MHz, $CDCl_3$): δ 7.65 (d, *J* = 8.3 Hz, 3.2H, *maj.*+*min.*), 7.34-7.30 (m, 3.2H, *maj.*+*min.*), 5.45-5.40 (m, 0.6H, *min.*), 4.05 (d, *J* = 18.0 Hz, 0.6H, *min.*), 3.90 (dd, *J* = 16.4, 1.4Hz, 0.6H, *min.*), 3.88 (dd, *J* = 18.0, 1.7Hz, 1H, *maj.*), 3.76 (dd, *J* = 16.3, 1.7 Hz, 1H, *maj.*), 3.70 (dd, *J* = 17.9, 1.7 Hz, 1H, *maj.*), 3.64 (dd, *J* = 16.3, 1.7 Hz, 1H, *maj.*), 3.51 (d, *J* = 17.9 Hz, 0.6H, *min.*), 3.42 (dd, *J* = 16.5, 1.5 Hz, 0.6H, *min.*), 2.42 (s, 4.9H, *maj.*+*min.*), 2.39-2.24 (m, 1.3H, *min.*), 2.14 (tt, *J* = 12.2, 3.1 Hz, 1H, *maj.*), 2.10-1.96 (m, 4.4H, *maj.*+*min.*), 1.91-1.53 (m, 16.5H, *maj.*+*min.*), 1.46 (s, 3H, *maj.*), 1.43-1.31 (m, 1H, *maj.*), 1.29-1.02 (m, 9.7H, *maj.*+*min.*), 0.91 (d, *J* = 7.1 Hz, 2H, *min.*); ^{13}C NMR (125 MHz, $CDCl_3$): δ 191.7 (e, *min.*), 191.5 (e, *maj.*), 155.1 (e, *maj.*), 154.9 (e, *min.*), 144.2 (e, *min.*), 144.1 (*maj.*), 139.6 (e, *min.*), 138.2 (e, *min.*), 137.8 (e, *maj.*), 133.0 (e, *maj.*), 132.8 (e, *min.*), 130.3 (e, *maj.*), 129.9 (o, 2C, *min.*), 129.9 (o, 2C, *maj.*), 128.0 (e, *maj.*), 127.7 (o, 4C, *maj.*+*min.*), 126.9 (o, *min.*), 53.5 (e, *min.*), 53.4 (e, *maj.*), 48.5 (e, *min.*), 47.5 (e, *maj.*), 40.4 (o, *min.*), 40.3 (o, *maj.*), 31.5 (o, *min.*), 31.2 (e, *maj.*), 30.5 (e, *maj.*), 30.4 (e, *min.*), 30.3 (e, *maj.*), 29.2 (e, *min.*), 29.4 (e, *maj.*), 28.9 (e, *maj.*), 27.1 (e, *maj.*), 27.0 (e, *maj.*), 27.0 (e, *min.*), 26.9 (e, *min.*), 25.8 (e, *maj.*), 25.7 (e, *min.*), 25.3 (e, *min.*), 22.7 (e, *min.*), 22.6 (e, *maj.*), 21.5 (o, *maj.*+*min.*), 20.6 (o, *maj.*), 20.0 (e, *min.*), 19.7 (o, *min.*); IR

(neat): ν = 2924 (s), 2853 (m), 1674 (s), 1598 (m), 1494 (w), 1449 (m), 1350 (s), 1305 (m), 1241 (w), 1162 (vs), 1121 (w), 1090 (m), 1046 (m), 978 (m), 965 (m), 888 (w), 837 (w), 813 (m), 753 (w), 732 (m), 677(s); HRMS (ESI) calcd for ($C_{25}H_{33}NO_3S$ + Na): 450.2079; found: 450.2067.

Compound 203n. This product was obtained as a white solid (486 mg, **69%**) from

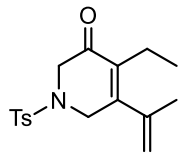

168 (500 mg, 2.2 mmol, 1 equiv.) and **176** (303 µL, 2.4 mmol, 1.1 equiv.). m.p.: 90-92 °C; ^{1}H NMR (500 MHz, $CDCl_3$): δ 7.66 (d, *J* = 8.2 Hz, 2H), 7.32 (d, *J* = 8.2 Hz, 2H), 5.13-5.09 (m, 1H), 4.79-4.76 (m, 1H), 3.94 (s, 2H), 3.82 (s, 2H), 2.42 (s, 3H), 2.13 (q, *J* = 7.2 Hz, 2H), 1.88 (s, 3H), 0.77 (t, *J* = 7.4 Hz, 3H); ^{13}C NMR (125 MHz, $CDCl_3$): δ 191.5 (e), 153.8 (e), 144.3 (e), 140.7 (e), 135.2 (e), 133.3 (e), 130.0 (o, 2C), 127.8 (o, 2C), 115.7 (e), 52.7 (e), 47.6 (e), 21.8 (o), 21.5 (o), 19.2 (e), 14.0 (e); IR (neat): ν = 3675 (m), 2973 (s), 2901 (s), 2818 (w), 1676 (s), 1614 (m), 1597 (m), 1494 (w), 1438 (s), 1404 (m), 1345 (s), 1321 (w), 1255 (m), 1226 (w), 1180 (vs), 1088 (br s), 1026 (vs), 980 (s), 907 (s), 812 (vs), 769 (m), 708 (m), 677 (s); HRMS (ESI) calcd for ($C_{17}H_{21}NO_3S$ + Na): 342.1140; found: 342.1135.

Compound 207k. Yellowish paste. (method **III**: first attempt: 40 mg (**5%**), second

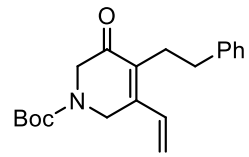

attempt: 44 mg (**60%**)). ^{1}H NMR (500 MHz, $CDCl_3$): δ 7.30-7.25 (m, 2H), 7.22-7.16 (m, 3H), 6.72 (dd, *J* = 17.8, 11.0 Hz, 1H), 5.68 (br, 1H), 5.49 (d, *J* = 11.0 Hz, 1H), 4.37 (s br, 2H), 4.11 (s, 2H), 2.76-2.71 (m, 2H), 2.67-2.61 (m, 2H), 1.49 (s, 9H); ^{13}C NMR (125 MHz, $CDCl_3$): δ 193.5, 154.2, 147.5, 141.4, 134.5, 131.7, 128.5 (2C), 128.4 (2C), 126.0, 121.4, 80.97, 51.6, 42.4, 35.5, 28.4 (3C), 26.3; IR (neat): ν = 3375 (w), 3026 (w), 2974 (m), 2929

(m), 2869 (m), 1698 (vs), 1671 (vs), 1620 (w), 1583 (w), 1496 (w), 1453 (m), 1417 (s), 1366 (vs), 1281 (m), 1243 (s), 1163 (vs), 1125 (vs), 1084 (m), 1029 (w), 984 (w), 924 (w), 894 (m), 857 (w), 748 (m), 699 (s); HRMS (ESI) calcd for ($C_{21}H_{27}NO_3S$ + Na): 350.1732; found: 350.1726; elemental analysis (%) calcd for $C_{20}H_{25}NO_3$: C 73.35, H 7.64, N 4.28; found C 73.29, H 7.72, N 3.80.

Compound 209. White paste. (method **III**: first attempt: 58 mg (**64%**), second attempt: 58 mg (**64%**)). ^{1}H NMR (500 MHz, $CDCl_3$): δ 7.53 (d, *J* = 8.2 Hz, 2H), 7.30-7.14 (m, 7H), 5.04-5.00 (m, 1H), 4.67 (t, *J*= 6.62 Hz, 1H), 4.56 (s, 1H), 4.25 (d, *J* = 20.2 Hz, 1H), 3.81 (d, *J* = 20.2 Hz, 1H), 3.09-3.00 (m, 2H), 2.36 (s, 3H), 2.09-1.89 (m, 2H), 1.72 (s, 3H), 0.61 (t, *J* = 7.3 Hz, 3H); ^{13}C NMR (125 MHz, $CDCl_3$): δ 194.2 (e), 153.0 (e), 143.8 (e), 140.4 (e), 136.5 (e), 136.2 (e), 134.1 (e), 129.8 (o, 2C), 129.4 (o, 2C), 128.4 (o, 2C), 127.0 (o, 2C), 127.0 (o), 115.4 (e), 61.9 (o), 44.6 (e), 37.5 (e), 21.8 (o), 21.4 (o), 19.2 (e), 13.4 (o); IR (neat): ν = 3086 (w), 2963 (m), 1671 (s), 1618 (m), 1598 (m), 1494 (m), 1456 (m), 1435 (m), 1348 (s), 1339 (s), 1307 (m), 1288 (w), 1260 (w), 1180 (vs), 1120 (m), 1089 (m), 987 (m), 951 (m), 936 (m), 907 (s), 873 (m), 847 (m), 914 (s), 799 (m), 740 (s), 704 (s), 675 (s); HRMS (CI (NH_3)) calcd for ($C_{24}H_{27}NO_3S$ + H): 410.1784; found : 410.1801.

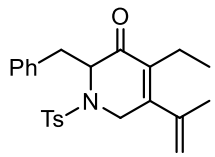

9.4 Hydrogenation/Re-aromatisation

Method **VI**: *Representative example for the synthesis of **210b***.

A flame-dried Schlenk was charged with 10% Pd/C (10 % w/w) and **203b** (76 mg, 0.2 mmol, 1 equiv.) dissolved in EtOAc (2 mL). The mixture was frozen with liquid nitrogen and the Schlenk was evacuated, then back filled with a balloon of hydrogen.

This process was repeated 3 times. 1 atmosphere of hydrogen was kept with a balloon and the mixture was stirred vigorously for 16 h. Afterwards, the mixture was filtered through a small plug of celite and the mixture was concentrated, affording the hydrogenated residue (76 mg, **quant.**). The residue (64 mg, 0.15 mmol, 1 equiv.) was dissolved in THF (290 μL) and DBU (110 μL, 0.73 mmol, 5 equiv.) was added. The mixture was stirred overnight, then all volatiles were removed and the residue was loaded on top of a silica column. Purification by flash chromatography (DCM:MeOH/98:2 to 95:5) afforded **210b** as a white solid (32 mg, **78%**).

The -OH proton was not observed in ^{1}H NMR in compounds 210a-n, 215, 234 and 235.

Compound 210a. Beige amorphous solid (19 mg, **80%**) from of **203a** (35 mg, 0.08 mmol, 1 equiv.) using method **VI** (5% Pd/C; 10% w/w; stirred for 7 h) in a sonicating bath. ^{1}H NMR (500 MHz, $CDCl_3$): δ 8.22 (s, 1H), 7.97 (s, 1H), 7.31-7.26 (m, 2H), 7.23-7.17 (m, 3H), 3.08-3.02 (m, 2H), 2.93-2.87 (m, 2H), 2.59-2.50 (m, 1H), 1.86-1.60 (m, 5H), 1.42 (q, *J* = 12.3 Hz, 2H), 1.36-1.19 (m, 3H); ^{13}C NMR (125 MHz, $CDCl_3$): δ 153.8 (e), 143.0 (e), 141.8 (e), 137.2 (e), 136.9 (o), 132.3 (o), 128.5 (o, 2C), 128.4 (o, 2C), 126.0 (o), 38.6 (o), 35.2 (e), 34.0 (e, 2C), 27.6 (e), 27.0 (e, 2C), 26.0 (e); IR (neat): ν = 2922 (s), 2848 (m), 2518 (br), 1803 (br), 1567 (m), 1495 (m), 1428 (vs), 1382 (m), 1290 (vs), 1190 (s), 1146 (s), 1123 (m), 994 (m), 865 (s), 752 (s), 699 (vs); HRMS (CI (CH_4)) calcd for ($C_{19}H_{23}NO$ + H): 282.1852; found: 282.1859.

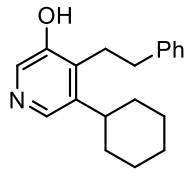

Compound 210b. White solid (32 mg, **78%**) from **203b** (76 mg, 0.17 mmol, 1 equiv.)

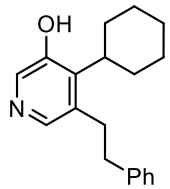

using method **VI** (10% Pd/C; 10% w/w; stirred for 16 h). m.p.: 179-180 °C; ^{1}H NMR (500 MHz, $CDCl_3$): δ 8.18 (s, 1H), 7.83 (s, 1H), 7.32 (t, *J* = 7.7 Hz, 2H), 7.25-7.19 (m, 3H), 2.99-2.81 (m, 5H), 2.44-2.30 (m, 2H), 1.91-1.83 (m, 2H), 1.80-1.73 (m, 1H), 1.62-1.54 (m, 2H), 1.44-1.31 (m, 3H); ^{13}C NMR (125 MHz, $CDCl_3$) : δ 154.6, 142.7, 141.1, 139.5, 136.5, 134.6, 128.6 (2C), 128.3 (2C), 126.2, 38.9, 38.0, 33.5, 29.9 (2C), 27.1 (2C), 25.9; IR (neat): ν = 3022 (w), 2929 (s), 2913 (s), 2850 (m), 2512 (br), 1801 (br), 1588 (m), 1563 (m), 1495 (m), 1462 (w), 1450 (m), 1422 (vs), 1365 (w), 1335 w), 1292 (vs), 1227 (m), 1188 (m), 1155 (s), 1129 (m), 1073 (m), 1028 (s), 893 (m), 862 (vs), 839 (w), 827 (w), 789 (m), 752 (s), 720 (m), 698 (vs); HRMS (CI (CH_4)) calcd for ($C_{19}H_{23}NO$ + H): 282.1852; found: 282.1859.

Compound 210c. Off-white solid (39 mg, **69%**) from of **203c** (93 mg, 0.24 mmol)

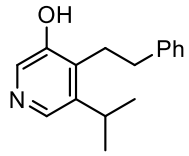

using method **VI** (10% Pd/C; 10% w/w; stirred for 16 h). m.p.: 125-127 °C; ^{1}H NMR (500 MHz, $CDCl_3$): δ 8.23 (s, 1H), 8.03 (s, 1H), 7.32-7.22 (m, 4H), 7.22-7.18 (m, 1H), 3.11-3.03 (m, 3H), 2.95-2.89 (m, 2H), 1.21 (d, *J* = 6.9Hz, 6H); ^{13}C NMR (125 MHz, $CDCl_3$): δ 153.7 (e), 143.8 (e), 141.8 (e), 136.8 (e), 136.7 (o), 132.6 (o), 128.5 (o, 2C), 128.3 (o, 2C), 126.0 (o), 35.2 (e), 27.9 (o), 27.5 (e), 23.7 (o, 2C); IR (neat): ν = 3061 (w), 3026 (w), 2963 (m), 2928 (m), 2866 (m), 2534 (br), 1762 (br), 1599 (m), 1567 (s), 1494 (m), 1427 (vs), 1391 (m), 1364 (w), 1292 (vs), 1192 (m), 1157 (m), 1137 (w), 1078 (w), 1016 (s), 907 (m), 877 (w), 863 (vs), 805 (m), 762 (s), 749 (vs), 701 (vs), 690 (vs); HRMS (CI (CH_4)) calcd for ($C_{16}H_{19}NO$ + H): 242.1539; found: 242.1549.

Compound 210d. White solid (24 mg, **60%**) from **203d** (65 mg, 0.17 mmol) using

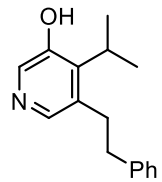

method **VI** (10% Pd/C; 10% w/w; stirred for 16 h). m.p.: 175-179 °C; ^{1}H NMR (500 MHz, $CDCl_3$): δ 8.18 (s, 1H), 7.82 (s, 1H), 7.30 (t, *J* = 7.3 Hz, 2H), 7.24-7.18 (m, 3H), 3.28 (sept, *J* = 6.9 Hz, 1H), 2.99-2.92 (m, 2H), 2.89-2.83 (m, 2H), 1.43 (d, *J* = 7Hz, 6H); ^{13}C NMR (125 MHz, $CDCl_3$): δ 154.4 (e), 142.9 (e), 141.1 (e), 140.2 (o), 136.0 (e), 135.1 (o), 128.5 (o, 2C), 128.3 (o, 2C), 126.2 (o), 37.9 (e), 33.1 (e), 28.5 (o), 19.9 (o, 2C); IR (neat): ν = 3061 (w), 3026 (w), 2963 (m), 2928 (w), 2866 (w), 2534 (br), 1762 (br), 1599 (m), 1567 (s), 1494 (m), 1453 (w), 1427 (vs), 1391 (s), 1364 (m), 1292 (vs), 1192 (m), 1157 (m), 1016 (s), 907 (m), 863 (vs), 805 (m), 762 (m), 749 (vs), 701 (vs), 690 (s); HRMS (CI (CH_4)) calcd for ($C_{16}H_{19}NO$ + H): 242.1539; found: 242.1542.

Compound 210e. Off-white solid (26 mg, **71%**) from **203e** (64 mg, 0.16 mmol) using

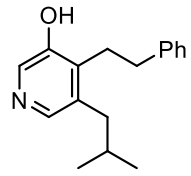

method **VI** (10% Pd/C; 10% w/w; stirred for 16 h). m.p.: 162-164 °C; ^{1}H NMR (500 MHz, $CDCl_3$): δ 8.24 (s, 1H), 7.88 (s, 1H), 7.33-7.19 (m, 5H), 3.05-2.99 (m, 2H), 2.94-2.88 (m, 2H), 2.41 (d, *J* = 7.4 Hz, 2H), 1.84 (sept, *J* = 6.8 Hz, 1H), 0.94 (d, *J* = 6.7 Hz, 6H); ^{13}C NMR (125 MHz, $CDCl_3$): δ 154.0 (e), 142.0 (e), 140.4 (o), 138.1 (e), 137.0 (e), 133.1 (o), 128.4 (o, 2C), 128.3 (o, 2C), 126.0 (o), 39.2 (e), 34.8 (e), 29.7 (o), 28.6 (e), 22.5 (o, 2C); IR (neat): ν = 3064 (w), 3026 (w), 2953 (m), 2926 (w), 2494 (br), 1804 (br), 1589 (m), 1563 (s), 1495 (m), 1464 (m), 1422 (vs), 1366 (s), 1298 (vs), 1266 (m), 1165 (m), 1146 (s), 1031 (m), 906 (m), 874 (s), 763 (s), 747 (s), 660 (vs); HRMS (CI (CH_4)) calcd for ($C_{17}H_{21}NO$ + H): 256.1707; found: 256.1696.

Compound 210f. Off-white solid (71 mg, **70%**) from **203f** (165 mg, 0.4 mmol) using

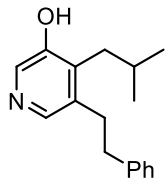

method **VI** (10% Pd/C; 10% w/w; stirred for 16 h). m.p.: 169-171 °C; ^{1}H NMR (500 MHz, $CDCl_3$): δ 8.19 (s, 1H), 7.92 (s, 1H), 7.31 (t, *J* = 7.3 Hz, 2H), 7.25-7.18 (m, 3H), 2.97-2.92 (m, 2H), 2.91-2.85 (m, 2H), 2.63 (d, *J* = 7.4 Hz, 2H), 2.07 (sept, *J* = 6.8 Hz, 1H), 0.97 (d, *J* = 6.7 Hz, 6H); ^{13}C NMR (125 MHz, $CDCl_3$): δ 154.0 (e), 141.2 (e), 139.5 (o), 138.0 (e), 137.5 (e), 133.3 (o), 128.6 (o, 2C), 128.3 (o, 2C), 126.2 (o), 37.4 (e), 34.5 (e), 32.4 (e), 28.5 (o), 22.7 (o, 2C); IR (neat): ν = 3030 (w), 2961 (m), 2945 (w), 2925 (w), 2863 (m), 2481 (br), 1761 (br), 1595 (m), 1564 (s), 1494 (m), 1463 (m), 1423 (vs), 1381 (s), 1366 (s), 1337 (m), 1297 (vs), 1260 (m), 1220 (w), 1191 (w), 1161 (s), 1127 (m), 1112 (m), 1073 (m), 1027 (w), 985 (w), 935 (m), 869 (vs), 847 (m), 818 (w), 756 (s), 747 (vs), 719 (s), 690 (vs); HRMS (CI (CH_4)) calcd for ($C_{17}H_{21}NO$ + H): 256.1696; found: 256.1706.

Compound 210g. Brown paste (12 mg, **54%**) from **203g** (42 mg, 0.09 mmol) using

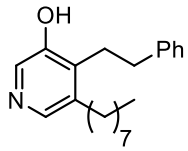

method **VI** (5% Pd/C; 10% w/w; stirred for 7.5 h). ^{1}H NMR (500 MHz, $CDCl_3$): δ 8.21 (s, 1H), 7.91 (s, 1H), 7.32-7.18 (m, 5H), 3.04-2.98 (m, 2H), 2.93-2.87 (m, 2H), 2.54-2.48 (m, 2H), 1.54 (quint, *J* = 7.1 Hz, 2H), 1.38-1.22 (m, 10H), 0.88 (t, *J* = 7.1 Hz, 3H); ^{13}C NMR (125 MHz, $CDCl_3$): δ 153.8 (e), 142.0 (e), 139.7 (o), 138.2 (e), 137.7 (e), 133.1 (o), 128.4 (o, 2C), 128.4 (o, 2C), 126.0 (o), 34.9 (e), 31.8 (e), 31.1 (e), 30.1 (e), 29.7 (e), 29.4 (e), 29.2 (e), 28.4 (e), 22.6 (e), 14.1 (o); IR (neat): ν = 2956 (m), 2917 (s), 2617 (br), 1602 (m), 1572 (s), 1495 (m), 1451 (s), 1431 (vs), 1379 (m), 1312 (vs), 1201 (m), 1147 (m), 1029 (m), 905 (w), 751 (s), 695 (vs); HRMS (CI (CH_4)) calcd for ($C_{21}H_{29}NO$ + H): 312.2322; found: 312.2328.

Compound 210h. Beige solid (28 mg, **56%**) from **203h** (75 mg, 0.16 mmol) using

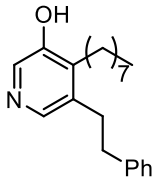

method **VI** (10% Pd/C; 10% w/w; 5 h). m.p.: 79-82 °C; ^{1}H NMR (500 MHz, $CDCl_3$): δ 8.17 (s, 1H), 7.91 (s, 1H), 7.34-7.28 (m, 2H), 7.25-7.18 (m, 3H), 2.96-2.85 (m, 4H), 2.75-2.67 (m, 2H), 1.64-1.52 (m, 2H), 1.48-1.39 (m, 2H), 1.38-1.22 (m, 8H), 0.92-0.83 (m, 3H); ^{13}C NMR (125 MHz, $CDCl_3$): δ 153.7 (e), 141.2 (e), 139.7 (o), 139.1 (e), 136.8 (e), 133.4 (o), 128.5 (o, 2C), 128.3 (o, 2C), 126.2 (o), 37.6 (e), 32.4 (e), 31.9 (e), 30.1 (e), 29.5 (e), 29.3 (e), 29.1 (e), 26.0 (e), 22.7 (e), 14.1 (o); IR (neat): ν = 2954 (w), 2922 (s), 2852 (m), 2539 (br), 1565 (s), 1495 (m), 1463 (m), 1422 (vs), 1366 (s), 1298 (vs), 1262 (m), 1165 (s), 1119 (s), 1072 (m), 749 (s), 695 (vs); HRMS (CI (CH_4)) calcd for ($C_{21}H_{29}NO$ + H): 312.2322; found: 312.2327.

Compound 210k. A flame-dried Schlenk was charged with 10% Pd/C (10 % w/w)

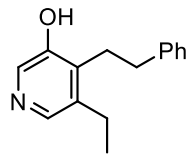

and **207k** (30 mg, 0.09 mmol, 1 equiv.) dissolved in EtOAc (1 mL). The mixture was frozen with liquid nitrogen and the Schlenk was evacuated, then back filled with hydrogen. The process was repeated 3 times. 1 atmosphere of hydrogen was kept with a balloon and the mixture was stirred vigorously for 4 h. Afterwards, the mixture was filtered through celite and was concentrated, affording the hydrogenated residue (30 mg, **99%**). Under air, a suspension of the residue (25 mg, 0.08 mmol, 1 equiv.), SiO_2 (25 mg) and TFA (76 μL, 0.1 mmol, 1.3 equiv.) in DCM (271 μL) was stirred at room temperature for 1 h. $NaNO_2$ (8 mg, 0.11 mmol, 1.5 equiv.) was then added and the suspension was stirred 30 min. Afterwards, Et_3N (271 μL, 0.2 mmol, 2.7 equiv.) was added and the suspension was stirred for another 30 min. Finally, all volatiles were removed *in vacuo*. The residue was loaded on a column and purified by flash chromatography

(DCM:MeOH/98:2), affording **210k** as a beige foam (10 mg, **57%**). ^{1}H NMR (500 MHz, $CDCl_3$): δ 8.24 (s, 1H), 7.94 (s, 1H), 7.32-7.27 (m, 2H), 7.26-7.18 (m, 3H), 3.06-2.99 (m, 2H), 2.94-2.87 (m, 2H), 2.58 (q, *J* = 7.7 Hz, 2H), 1.20 (t, *J* = 7.6 Hz, 3H); ^{13}C NMR (125 MHz, $CDCl_3$): δ 154.0 (e), 141.8 (e), 139.7 (e), 138.7 (e), 138.0 (o) 132.2 (o), 128.5 (o, 2C), 128.4 (o, 2C), 126.1 (o), 34.7 (e), 28.3 (e), 23.2 (e), 15.2 (o); IR (neat): ν = 3027 (w), 2965 (w), 2932 (w), 2525 (br), 1820 (br), 1599 (m), 1568 (s), 1495 (m), 1458 (m), 1424 (vs), 1376 (m), 1299 (vs), 1193 (m), 1147 (s), 1056 (w), 1029 (m), 867 (s), 814 (m), 751 (s), 698 (vs); HRMS (CI (CH_4)) calcd for ($C_{15}H_{17}NO$ + H): 228.1383; found: 228.1392.

Compound 215. A flame-dried Schlenk was charged with 10% Pd/C (10 % w/w) and

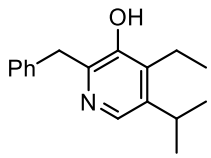

209 (58 mg, 0.14 mmol, 1 equiv.) dissolved in EtOAc (1.4 mL). The mixture was frozen with liquid nitrogen and the Schlenk was evacuated, then back filled with hydrogen. The process was repeated 3 times. 1 atmosphere of hydrogen was kept with a balloon and the mixture was stirred vigorously for 2 h. Afterwards, the mixture was filtered through celite and was concentrated, affording the hydrogenated residue (55 mg, **95%**). The residue (55 mg, 0.13 mmol, 1 equiv.) was dissolved in EtOH (0.7 mL) and a saturated solution of $NaHCO_3$ (4 mL) was added. The mixture was stirred under reflux overnight. The volume of the reaction mixture was reduced by half under vacuum and was extracted 3 times with EtOAc. The combined organic layer was washed with brine, dried over $MgSO_4$, filtered and concentrated under reduced pressure. Purification by flash chromatography (DCM:MeOH/98:2 to 95:5) afforded **215** as a yellow paste (20 mg, **59%**). ^{1}H NMR (500 MHz, $CDCl_3$): δ 8.06 (s, 1H), 7.29 (d, *J* = 4.5 Hz, 4H), 7.25-7.20 (m, 1H), 4.20 (s, 2H), 3.08 (sept, *J* = 6.8 Hz, 1H), 2.66 (q, *J* = 7.6 Hz, 2H), 1.28 (d, *J*

= 6.8 Hz, 6H), 1.12 (t, *J* = 7.6 Hz, 3H); ^{13}C NMR (125 MHz, $CDCl_3$): δ 148.6 (e), 144.0 (e), 141.4 (e), 138.6 (e), 138.2 (o), 137.7 (e), 128.9 (o, 2C), 128.7 (o, 2C), 126.8 (o), 39.6 (e), 27.6 (o), 23.8 (o, 2C), 18.5 (e), 13.8 (o); IR (neat): ν = 3065 (m), 2959 (s), 2930 (m), 2870 (br), 1595 (m), 1551 (m), 1494 (m), 1453 (m), 1417 (s), 1372 (w), 1338 (w), 1318 (w), 1273 (m), 1231 (m), 1185 (vs), 1166 (s), 1149 (s), 1109 (m) 1060 (m), 1012 (s), 962 (m), 890 (s), 867 (m), 716 (vs), 693 (vs), 656 (m); HRMS (ESI) calcd for ($C_{17}H_{21}NO$ + H): 256.1701; found: 256.1696.

Compound 210n. A flame-dried Schlenk was charged with 10% Pd/C (10 % w/w) and **203n** (246 mg, 0.78 mmol, 1 equiv.) dissolved in EtOAc (7.8 mL). The mixture was frozen with liquid nitrogen and the Schlenk was evacuated, then back filled with hydrogen. The process was repeated 3 times. 1 atmosphere of hydrogen was kept with a balloon and the mixture was stirred vigorously for 2 h. Afterwards, the mixture was filtered through celite and was concentrated affording the hydrogenated residue (246 mg, **97%**). The residue (246 mg, 0.76 mmol, 1 equiv.) was dissolved in EtOH (4 mL) and a saturated solution of $NaHCO_3$ (20 mL) was added. The mixture was stirred under reflux overnight. The volume of the reaction mixture was reduced by half under vacuum and was extracted 3 times with EtOAc. The combined organic layer was washed with brine, dried over $MgSO_4$, filtered and concentrated under reduced pressure. Purification by flash chromatography (DCM:MeOH/98:2 to 95:5) afforded **210n** as a white solid (93 mg, **73%**). Instead of using a flash chromatography, the crude mixture could be recrystallised from EtOAc (80 mg, **63%**). m.p.: 164-165 °C; ^{1}H NMR (500 MHz, $CDCl_3$): δ 8.18 (s, 1H), 8.01 (s, 1H), 3.18 (sept, *J* = 6.9 Hz, 1H), 2.78 (q, *J* = 7.4 Hz, 2H), 1.29 (d, *J* = 6.8 Hz, 6H), 1.20 (t, *J* = 7.6 Hz, 3H); ^{13}C NMR (125 MHz, $CDCl_3$):

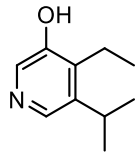

δ 153.4 (o), 143.4 (o), 139.3 (o), 136.8 (e), 132.6 (e), 27.6 (o), 23.8 (o, 2C), 18.6 (e), 13.8 (o); IR (neat): ν = 2970 (s), 2936 (m), 2874 (w), 2508 (br), 1781 (br), 1591 (m), 1562 (s), 1466 (m), 1422 (vs), 1368 (s), 1320 (w), 1282 (vs), 1192 (m), 1168 (m), 1152 (m), 1050 (s), 908 (s), 871 (s), 807 (s), 770 (m), 672 (m); HRMS (CI (CH_4)) calcd for ($C_{19}H_{23}NO$ + H): 166.1226; found: 166.1228; elemental analysis (%) calcd for $C_{10}H_{15}NO$: C 72.67, H 9.08, N 8.48; found C 72.68, H 9.08, N 8.44.

9.5 Functionalisation

Compound 229. Under nitrogen, **210n** (50 mg, 0.3 mmol, 1 equiv.) was added to an oven dried Schlenk tube. A 1:1 mixture of distilled water and THF (3 mL) was added at room temperature, followed by I_2 (85 mg, 0.33 mmol, 1.1 equiv.) and $NaHCO_3$ (140 mg, 0.33 mmol, 1.1 equiv.). The mixture was stirred at 85 °C for 4 h. Then, the reaction mixture was cooled down to room temperature and the excess of iodine was quenched with a 10% solution of Na_2SO_3. The aqueous layer was extracted with DCM, the gathered organic layer was dried with $MgSO_4$ and all volatiles were removed *in vacuo* to afford **229** as a yellowish solid (81 mg, **93%**). The product was used for the next step without further purification. m.p.: 83-86 °C; ^{1}H NMR (500 MHz, $CDCl_3$): δ 7.89 (s, 1H), 5.3 (s, 1H), 3.10 (sept, *J* = 7.0 Hz, 1H), 2.75 (q, *J* = 7.6 Hz, 2H), 1.27 (d, *J* = 7.0 Hz, 6H), 1.15 (t, *J* = 7.6 Hz, 3H); ^{13}C NMR (125 MHz, $CDCl_3$): δ 149.5 (e), 143.2 (e), 141.5 (o), 136.4 (e), 108.7 (e), 27.2 (o), 23.7 (o, 2C), 19.9 (e), 16.5 (o); IR (neat): ν = 2963 (s), 2927 (m), 2867 (m), 2541 (br), 1566 (m), 1540 (w), 1458 (m), 1381 (vs), 1324 (s), 1284 (m), 1262 (m), 1210 (vs), 1152 (s), 1054 (s), 962 (m), 904 (m), 835 (vs), 787 (m), 674 (m); HRMS (CI (CH_4)) calcd for ($C_{10}H_{14}NIO$ + H): 292.0193; found: 292.0190.

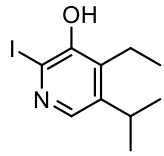

Compound 232. Under nitrogen, $Pd(PPh_3)_4$ (2 mg, 0.02 mmol, 0.05 equiv.) was added

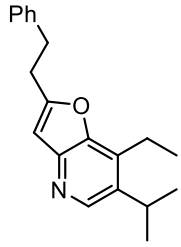

to a flame dried Schlenk tube followed by **229** (100 mg, 0.3 mmol, 1 equiv.) in piperidine (1 mL). The mixture was stirred for 5 min, then, 4-phenyl-1-butyne (49 µL, 0.3 mmol, 1 equiv.) and copper iodide (5 mg, 0.02 mmol, 0.07 equiv.) were added. The mixture was stirred at room temperature overnight. Then, the mixture was diluted with Et_2O and quenched with NH_4Cl. The aqueous layer was extracted with Et_2O. The combined organic layer was washed with H_2O, brine, dried with $MgSO_4$ and evaporated under vacuum. Purification by flash chromatography (PE:EtOAc/90:10) aforded **232** as a yellow solid (67 mg, **69%**). m.p.: 64-66 °C; ^{1}H NMR (500 MHz, $CDCl_3$): δ 8.37 (s, 1H), 7.32-7.27 (m, 2H), 7.24-7.19 (m, 3H), 6.53 (s, 1H), 3.23 (sept, *J* = 7.0 Hz, 1H), 3.16-3.05 (m, 4H), 2.94 (q, *J* = 7.6 Hz, 2H), 1.34 (d, *J* = 7 Hz, 6H), 1.28 (t, *J* = 7.6 Hz, 3H); ^{13}C NMR (125 MHz, $CDCl_3$): δ 161.6, 146.9, 145.7, 143,7, 140.6, 136.5, 132.3, 128.5 (2C), 128.3 (2C), 126.2, 103.7, 33.8, 30.6, 27.4, 24.3 (2C), 18.8, 14.4; IR (neat): ν = 2960 (s), 2924 (m), 2866 (m), 1615 (m), 1594 (s), 1560 (w), 1495 (m), 1473 (w), 1450 (s), 1383 (vs), 1303 (w), 1269 (w), 1238 (s), 1197 (s), 1049 (m), 966 (m), 933 (s), 871 (w), 808 (s), 785 (m), 765 (w), 747 (s), 698 (vs); HRMS (CI (CH_4)) calcd for ($C_{20}H_{23}NO$ + H): 294.1852; found: 294.1855.

Compound 234. A flame-dried Schlenk tube, under nitrogen, was charged with a solution of **210n** (50 mg, 0.3 mmol, 1 equiv.) in benzene (0.3 mL). Paraformaldehyde (11 mg, 0.4 mmol, 1.2 equiv.) and morpholine (31 µL, 0.4 mmol, 1.2 equiv.) were added at room temperature. The mixture was stirred at 80 °C for 24 h. Afterwards, all volatiles were removed *in vacuo*. Purification by flash chromatography (DCM:MeOH/98:2) afforded **234** as a white solid (78 mg, **98%**). m.p.: 43-45 °C; ^{1}H NMR (500 MHz, $CDCl_3$): δ 7.94 (s, 1H), 3.90 (s, 2H), 3.77 (br s, 4 H), 3.11 (sept, *J* = 7.0 Hz, 1H), 2.70 (q, *J* = 7.6 Hz, 2H), 2.63 (br s, 4H), 1.27 (d, *J* = 7.0 Hz, 6H), 1.15 (t, *J* = 7.5 Hz, 3H); ^{13}C NMR (125 MHz, $CDCl_3$): δ 151.7 (e), 142.1 (e), 137.5 (e), 137.4 (o), 137.2 (e), 66.7 (e, 2C), 63.6 (e), 53.0 (e, 2C), 27.5 (o), 23.8 (o, 2C), 18.2 (e), 13.8 (o); IR (neat): ν = 2961 (s), 2930 (m), 2878 (m), 2849 (s), 2757 (w), 1556 (m), 1498 (w), 1453 (s), 1407 (vs), 1364 (m), 1347 (m), 1270 (s), 1213 (m), 1114 (vs), 1069 (s), 1023 (s), 979 (m), 954 (w), 913 (m), 890 (s), 863 (vs), 808 (s), 734 (s), 665 (w); HRMS (CI (NH_3)) calcd for ($C_{15}H_{25}N_2O_2$ + H): 265.1911; found: 265.1915; elemental analysis (%) calcd for $C_{15}H_{24}N_2O_2$: C 68.14, H 9.08, N 10.60; found C 67.92, H 9.13, N 10.24.

Compound 235. A flame-dried Schlenk tube, under nitrogen, was charged with a solution of **210n** (50 mg, 0.3 mmol, 1 equiv.) in toluene (0.3 mL). Paraformaldehyde (11 mg, 0.4 mmol, 1.2 equiv.) and pyrrrolidine (31 µL, 0.4 mmol, 1.2 equiv.) were added at room temperature. The mixture was stirred at 80 °C for 24 h. Afterwards, all volatiles are removed *in vacuo*. Purification by flash chromatography (DCM:MeOH/98:2) afforded **235** as a colourless paste (60 mg, **80%**). ^{1}H NMR (500 MHz, $CDCl_3$): δ 7.91 (s, 1H), 4.00 (s, 2H), 3.09 (sept, *J* = 6.9 Hz, 1H), 2.85-2.63 (m, 6H), 1.95-1.82 (m, 4H), 1.27

(d, J = 6.9 Hz, 6H), 1.15 (t, J = 7.5 Hz, 3H); ^{13}C NMR (125 MHz, $CDCl_3$): δ 151.9 (e), 141.5 (e), 139.2 (e), 137.3 (o), 136.4 (e), 60.9 (e), 53.6 (e, 2C), 27.5 (o), 23.9 (o, 2C), 23.7 (e, 2C), 18.2 (e), 13.9 (o); IR (neat): ν = 2970 (s), 2874 (m), 1740 (vs), 1555 (w), 1461 (m), 1407 (s), 1366 (vs), 1274 (m), 1216 (vs), 1120 (m), 900 (s), 730 (s); HRMS (ESI) calcd for ($C_{15}H_{24}N_2O$ + H): 249.1967; found: 249.1962.

10 References

1 A. Schmidt, *Curr. Org. Chem.,* **2004**, *8*, 653–670.

2 NIH, Office of dietary supplements. Dietary Supplement Fact Sheet: Vitamin B6 (2013-01-10). http://ods.od.nih.gov/factsheets/VitaminB6-HealthProfessional/.

3 D. E. Metzler, M. Ikawa, E. E. Snell, *J. Am. Chem. Soc.*, **1954**, *76*, 648.

4 M. D. Toney, *Biochim. Biophys. Acta.*, **2011**, *11*, 1407.

5 G. Saposnik *et* al., *Stroke,* **2009**, *40*, 1365.

6 Y. Murakami, J. Kikuchi, Y. Hisaeda, O. Hayashida, *Chem. Rev.*, **1996**, *96*, 721.

7 L. Liu, R. Breslow, *Bioorg. Med. Chem.,* **2004**, *12,* 3277.

8 G. Moine, H.-P. Hohmann, R. Kurth, J. Paust, W. Hahnlien, H. Pauling, B.-J. Weimann, B. Kaesler, *Ullmann's Encyclopedia of Industrial Chemistry*, **2011**, 234.

9 M. Wijtmans, D. A. Pratt, L. Valgimigli, G. A. DiLabio, G. F. Pedulli, N. A. Porter, *Angew. Chem. Int. Ed.,* **2003**, *42*, 4370.

10 J. Natera, W. Massad, N. A. García, *Photochem. Photobiiol. Sci.*, **2012**, *11*, 938.

11 L. Valgimigli, D. Bartolomei, R. Amorati, E. Haidasz, J. J. Hanthorn, S. J. Nara, J. Brinkhorst, D. A. Pratt, *Beilstein J. Org. Chem.*, **2013**, *9*, 2781.

12 V. P. Singh, J.-F. Poon, L. Engman, *J. Org. Chem.*, **2013**, *78*, 1478.

13 D. Bok, *J. Cell. Sci. Suppl.*, **1993**, *17*, 189.

14 I. Bhutto, G. Lutty, *Mol. Aspects Med.*, **2012**, *33*, 295.

15 D. Bae, J. Gautam, H. Jang, S. Banskota, S. Y. Lee, M.-J. Jeong, A.-S. Kim, H. C. Kim, I.-H. Lee, T.-G. Nam, J.-A. Kim, B.-S. Jeong, *Bioorg. Med. Chem. Lett.*, **2018**, *28*, 107.

16 M. P. Alam, O. M. Khdour, P. M. Arce, Y. Chen, B. Roy, W. G. Johnson, S. Dey, S. M. Hecht, *Bioorg. Med. Chem.*, **2014**, *22*, 4935.

17 W. Risau, I. Flamme, *Annu. Rev. Cell Dev. Biol.*, **1995**, *11*, 73.

18 A. M. Byrne, D. J. Bouchier-Hayes, J. H. Harmey, *J. Cell. Mol. Med.*, **2005**, *9*, 777.

19 D.-G. Kim, Y. Kang, H. Lee, E. K. Lee, T.-G. Nam, J.-A. Kim, B.-S. Jeong, *Eur. J. Med. Chem.*, **2014**, *78*, 126.

20 H. Lee, S. Banskota, D.-G. Kim, J.-H. Been, Y.-J. Jin, J. Gautam, H. Jang, T.-G. Nam, J.-A. Kim, B.-S. Jeong, *Bioorg. Med. Chem. Lett.*, **2014**, *24*, 3131.

21 H. Lee, D.-G. Kim, S. Banskota, Y. K. Lee, T.-G. Nam, J.-A. Kim, B.-S. Jeong, *Org. Biomol. Chem.*, **2014**, *12*, 8702.

22 R. P. Moerschell, Y. Hosokawa, S. Tsunasawa, F. Sherman, *J. Biol. Chem.*, **1990**, *265*, 19638.

23 Q.-L. Luo, J.-Y. Li, Z.-Y. Liu, L.-L. Chen, J. Li, Z. Qian, Q. Shen, Y. Li, G. H. Lushington, Q.-Z. Ye, F.-J. Nan, *J. Med. Chem.*, **2003**, *46*, 2631.

24 T. Hakki, R. Bernhardt, *Pharmacol. Ther.*, **2006**, *111*, 27.

25 M. J Young, C. D. Clyne, T. J. Cole, J. W. Cardiac, *J. Clin. Endrocinol. Metab.*, **2001**, *86*, 5121.

26 M. A. E. P.-B. Mendieta, Q. Hu, M. Engel, R. W. Hartmann, *J. Med. Chem.*, **2013**, *56*, 6101.

27 M. D. Houslay, P. Schafer, K. Y. J. Zhang, *Drug Discovery Today*, **2005**, *10*, 1503.

28 M. Kawasaki, A. Fusano, T. Nigo, S. Nakamura, M. N. Ito, Y. Teranishi, S. Matsumoto, N. Nomura, T. Sumiyoshi, *Bioorg. Med. Chem. Lett.*, **2014**, *24*, 2689.

29 Y. Shi, F. Lan, C. Matson, P. Mulligan, J. R. Whestine, P. A. Cole, R. A. Casero, Y. Shi, *Cell*, **2004**, *119*, 941.

30 F. Wu, C. Zhou, Y. Yao, L. Wei, Z. Feng, L. Deng, Y. Song, *J. Med. Chem.*, **2016**, *59*, 253.

31 E. E. Harris, R. A. Fireston, K. Pfirster, R. R. Boettcher, F. J. Cross, R. B. Currie, M. Monaco, E. R. Petterson, W. Reuter, *J. Org. Chem.*, **1962**, *27*, 2705.

32 Y. Zou, X. Shi, G. Zhang, Z. Li, C. Jin, W. Su, *Org. Process. Res. Dev.*, **2013**, *17*, 1498.

33 C. Sabot, E. Oueis, X. Brune, P.-Y. Renard, *Chemm. Commun.*, **2011**, *48*, 768.

34 L.-A. Jouanno, C. Sabot, P.-Y. Renard, *J. Org. Chem.*, **2012**, *77*, 8549.

35 L.-A. Jouanno, V. Tognetti, L. Joubert, C. Sabot, P.-Y. Renard, *Org. Lett.*, **2013**, *15*, 2530.

36 L.-A. Jouanno, V. Di Mascio, V. Tognetti, L. Joubert, C. Sabot, P.-Y. Renard, *J. Org. Chem.*, **2014**, *79*, 1303.

37 J.-Y. Lu, H.-D. Arndt, *J. Org. Chem.*, **2007**, *72*, 4205.

38 J.-Y. Lu, J. A. Keith, W.-Z. Shen, M. Schurmann, H. Preut, T. Jacob, H.-D. Arndt, *J. Am. Chem. Soc.*, **2008**, *130*, 13219.

39 P. Allevi, A. Longo, M. Anastisia, *Chem. Commun.*, **1999**, *0*, 559.

40 N. A. Nedolya, L. Brandsma, N. I. Slyakhtina, S. V. Fedorov, *Chem. Heterocycl. Compd.*, **2002**, *38*, 622.

41 K. Yoshida, F. Kawagoe, K. Hayashi, S. Horiuchi, T. Imamoto, A. Yanagisawa, *Org. Lett.*, **2009**, *3*, 515.

42 T. Donohoe, J. F. Bower, J. A. Basutto, L. P, Fishlock, P. A., Procopiou, C. K. A. Callens, *Tetrahedron*, **2009**, *65*, 8969.

43 H. Liu, L. Wang, X. Tong, *Chem. Commun.*, **2011**, *47*, 12206.

44 K. Y. T. Ho, C. Aïssa, *Chem. Eur. J.*, **2012**, *18*, 3486.

45 M. Murakami, S Ashida, T. Matsuda, *J. Am. Chem. Soc.*, **2005**, *127*, 6932.

46 S. Ashida, M. Murakami, *Bull. Chem. Soc. Jpn.*, **2008**, *82*, 885.

47 M. Murakami, S. Ashida, *Chem. Commun.*, **2006**, 4599.

48 L. Liu, N. Ishida, M. Murakami, *Angew. Chem. Int. Ed.*, **2012**, *51*, 2485.

49 M. Murakami, T. Itahashi, Y. Ito, *J. Am. Chem. Soc.*, **2002**, *124*, 13976.

50 T. Matsuda, A. Fujimoto, M. Ishibashi, M. Murakami, *Chem. Lett.*, **2004**, *33*, 876.

51 L. Souillard, E. Parker, N. Cramer, *Angew. Chem. Int. Ed.*, **2014**, *53*, 3001.

52 P. A. Wender, A. G. Correa, Y. Sato, R. Sun, *J. Am. Chem. Soc.*, **2000**, *122*, 7815.

53 M. Murakami, H. Amii, K. Shigeto, Y. Ito, *J. Am. Chem. Soc.*, **1996**, *118*, 8285.

54 H. M. Ko, G. Dong, *Nat. Chem.*, **2014**, *6*, 739.

55 X. Zhou, H. M. Ko, G. Dong, *Angew. Chem. Int. Ed.*, **2016**, *55*, 13867.

56 X. Zhou, G. Dong, *J. Am. Chem. Soc.*, **2015**, *137*, 13715.

57 N Ishida, W. Ikemoto, M. Murakami, *J. Am. Chem. Soc.*, **2014**, *136*, 5912.

58 E. V. Anslyn, M. B. Sponsler, *Modern Organic Chemistry*, **2005**, *University Science Book.*

59 M. A. Huffman, L. S. Liebeskind, *J. Am. Chem. Soc.*, **1990**, *113*, 2771.

60 A. Cammers-Goodwin, *J. Org. Chem.*, **1993**, *58*, 7619.

61 A.-L. Aauvinet, J. P. A. Harrity, *Angew. Chem. Int. Ed.*, **2011**, *50*, 2769.

62 T. Stalling, W. R. R. Harker, A.-L. Auvinet, E. J. Cornel, J. P. A. Harrity, *Chem. Eur. J.*, **2015**, *21*, 2701.

63 T Kondo, Y. Taguchi, Y. Kaneko, M. Niimi, T.-A. Mitsudo, *Angew. Chem. Int. Ed.*, **2004**, *43*, 5369.

64 T. Kondo, M. Niimi, M. Nomura, K. Wada, T.-A. Mitsudo, *Tetrahedron Lett.*, **2007**, *48*, 2837.

65 M. A. Huffman, L. S. Liebeskind, *J. Am. Chem. Soc.*, **1990**, *112*, 8617.

66 M. A. Huffman, L. S. Liebeskind, *Organometallics*, **1990**, *9*, 2194.

67 D. N. Hickman, K. J. Hodgetts, P. S. Mackman, T. W. Wallace, J. M. Wardleworth, *Tetrahedron*, **1996**, *52*, 2235.

68 F. Juliá-Hernández, A. Ziadi, A. Nishimura, R. Martin, *Angew. Chem. Int. Ed.*, **2015**, *54*, 9537.

69 a) T. Xu, G. Dong, *Angew. Chem. Int. Ed.*, **2012**, *124*, 7685; b) T. Xu, H. M. Ko, N. A. Savage, G. Dong, *J. Am. Chem. Soc.*, **2012**, *134*, 20005.

70 P.-H. Chen, T. Xu, G. Dong, *Angew. Chem. Int. Ed*, **2014**, *53*, 1674.

71 L. Deng, T. Xu, H. Li, G. Dong, *J. Am. Chem. Soc.*, **2016**, *138*, 369.

72 T. Xu, H. M. Ko, N. A. Savage, G. Dong, *J. Am. Chem. Soc.*, **2012**, *134*, 20005.

73 L. Deng, M. Che, G. Dong, *J. Am. Chem. Soc.*, **2018**, DOI: 0.1021/jacs.8b05549 (Article just accepted during the writing of this thesis).

74 Z. Zhu, X. Li, S. Chen, P.-H. Chen, B. A. Billett, Z. Huang, G. Dong, *ACS Catal.*, **2018**, *8*, 845.

75 P. Kumar, J. Louie, *Org. Lett.*, **2012**, *14*, 2026.

76 N. Ishida, T. Yuhki, M. Murakami, *Org. Lett.*, **2012**, *14*, 3898.

77 P. Kumar, K. Zhang, J. Louie, *Angew. Chem. Int. Ed.*, **2012**, *51*, 8602.

78 A. Thakur, M. E. Facer, J. Louie, *Angew. Chem. Int. Ed.*, **2013**, *52*, 12161.

79 S. Ogoshi, M. Ueta, T. Arai, H. Kurosawa, *J. Am. Chem. Soc.*, **2005**, *127*, 12810.

80 M. Ohashi, H. Saijo, T. Arai, S. Ogoshi, *Organometallics*, **2010**, *29*, 6534.

81 Y. Li, Z. Lin, *Organometallics*, **2013**, *32*, 3003.

82 D. R. Stuart, M. Bertrand-Laperle, K. M. N. Burgess, K. Fagnou, *J. Am. Chem. Soc*. **2008**, *130*, 16474.

83 M. P. Huestis, L. Chan, D. R. Stuart, K. Fagnou, *Angew. Chem. Int. Ed*., **2011**, *50*, 1338.

84 K. M. Miller, T. Luanphaisarnnont, C. Molinaro, T. F. Jamison, *J. Am. Chem. Soc.*, **2004**, *126*, 4130.

85 G. M. Mahandru, G. Liu, J. Mongomery, *J. Am. Chem. Soc.*, **2004**, *126*, 3698.

86 P. Liu, P. McCarren, P. H.-Y. Cheong, T. F. Jamison, K. N. Houk, *J. Am. Chem. Soc.*, **2010**, *132*, 2050.

87 M. E. Jung, B. A. Duclos, *Tetrahedron*, **2006**, *62*, 9321.

88 J.-L. Giner, G. H. Wikfors, *Phytochemistry*, **2011**, *72*, 1896.

89 M. Tori, N. Uchida, A. Sumida, H. Furuta, Y. Asakawa, *J. Chem. Soc. Perkin Trans.*, **1995**, *1*, 1513.

90 P. Metz, S. Bertels, R. Frohlich, *J. Am. Chem. Soc.*, **1993**, *115*, 12595.

91 Y. Mori, G. Onodera, M. Kimura, *Chem. Lett.*, **2014**, *43*, 97.

92 A. Tungler, T. Tarnai, L. Hegedus, K. Fodor, T. Mathé, *Platinum Metals Rev.*, **1998**, *42*, 108.

93 P. W. Cains, L. J. McCausland, D. M. Bates, T. J. Mason, *Ulrason. Sonochem.*, **1994**, *1*, 45.

94 T.-K. Yang, D.-S. Lee, J. Haas, *Encyclopedia of Reagents in Organic Chemistry*, **2006**.

95 S. Siegel, *Encyclopedia of Reagents in Organic Chemistry*, **2001**.

96 K. Niknam, B. Karami, M. A. Zolfigol, *Catal. Commun.*, **2007**, *8*, 1427.

97 I. Andreu, N. Cabedo, F. Fabis, D. Cortes, S. Rault, *Tetrahedron*, **2005**, *61*, 8282.

98 a) E. A. Standley, T. F. Jamison, *J. Am. Chem. Soc.*, **2013**, *135*, 1585; b) N. H. Park, G. Teverovskiy, S. L. Buchwald, *Org. Lett.*, **2014**, *16*, 220; c) J. D. Shields, E. F. Gray, A. G. Doyle, *Org. Lett.*, **2015**, *17*, 2166.

99 R. C. Ronald, M. R. Winkle, *Tetrahedron*, **1983**, *39*, 2031.

100 J. Dash, B. Melillo, S. Arseniyadis, J. Cossy, *Tetrahedron Lett.*, **2011**, *52*, 2246.

101 N. B Eddy, J. G. Murphy, E. L. May, *J. Org. Chem.*, **1957**, *22*, 1370.

102 Y. Liu, J. B. Friesen, L. L. Klein, J. B McAlpine, D. C. Lankin, G. F. Pauli, S.-N. Chen, *J. Chromatogr. A.*, **2015**, *1426*, 248.

103 H. Vorbruggen, K. Krolikiewicz, *Synthesis*, **1983**, 316.

104 V. Koch, S. Schnatterer, *Synthesis*, **1990**, 497.

105 P. W. Sheldrake, L.C. Powling, P. K. Slaich, *J. Org. Chem.*, **1997**, *62*, 3008.

106 M. Casalino, V. De Felice, N. Fraldi, A. Panunzi, F. Ruffo, *Inorg. Chem.*, **2009**, *48*, 5913.

107 E. A. Jaseer, D. J. C. Prasad, G. Sekar, *Tetrahedron*, **2010**, *66*, 2077.

108 M. Yamaguchi, H. Katsumata, K. Manaba, *J. Org. Chem.*, **2013**, *78*, 9270.

109 K.-W. Chi, Y. S. Ahn, K. T. Shim, T. H. Park, J. S. Ahn, *Bull. Korean. Chem. Soc.*, **1999**, *20*, 973.

110 S. Duttwyler, C. Lu, A. L. Rheingold, R. G. Bergman, J. A. Ellman, *J. Am. Chem. Soc.*, **2012**, *134*, 4064.

111 S. Gong, W. Xi, Z. Ding, H. Sun, *J. Org. Chem.*, **2017**, *82*, 7643.

112 J. A. Steves, Y. Preger, J. R. Martinelli, C. J. Welch, T. W. Root, J. M. Hawkins, S. S. Stahl, *Org. Process. Res. Dev.*, **2015**, *19*, 1548.

113 T. Axenrod, C. Watnick, H. Yazdekhasti, *J. Org. Chem.*, **1995**, *60*, 1959.

114 Y. Sasaki, Y. Horita, C. Zhong, M. Sawamura, H. Ito, *Angew. Chem. Int. Ed.*, **2011**, *50*, 2778.

115 S. Kujawa, D. Best, D. J. Burns, H. W. Lam, *Chem. Eur J.*, **2014**, *20*, 8599.

116 R. A. Aitken, C. Boeters, J. J. Morrison, *J. Chem. Soc., Perkin Trans. 1*, **1994**, *0*, 2473.

Cross-coupling of α-carbonyl sulfoxonium ylides with C–H bonds

1 Introduction

Sulfoxonium and sulfonium ylides are stable carbene precursors which were discovered in the 1960's and 30's respectively.[1,2] Sulfur-based ylides have become a great tool in organic chemistry, providing robust alternatives for the synthesis of small rings such as epoxides and cyclopropanes.[3,4,5] Another substantial part of the reactivity of sulfonium ylides is dedicated to the (2,3) rearrangement of allylic sulfoniums which has been extended to the asymmetric version.

In 1966, Trost reported the copper-catalysed cyclopropanation of cyclohexene with sulfonium ylides.[6] Since this report, many metals have been used in collaboration with sulfonium ylides, such as rhodium, palladium, iridium, gold and iron.[7,8,9,10,11] Those species have also been used in the metal-catalysed epoxidation, cyclisation and C–H bond insertion reactions.

Although sulfoxonium ylides share some resemblance with sulfonium ylides a more indepth study of the former is required to gain an understanding to rival that of sulfonium ylides. Thus, a thorough review on the chemistry involving sulfoxonium ylides, and their application when coupled with a metal-catalysts, will be presented hereafter.

2 Sulfoxonium ylides reactivity

2.1 Dimethyl sulfoxonium methylide

2.1.1 Epoxidation

The simplest sulfoxonium ylide is dimethyl sulfoxonium methylide **2**. It was identified and used for the first time by Corey and Chaykovsky in 1962.[1] This species

was generated from trimethylsulfoxonium chloride **1** upon deprotonation with sodium hydride (Figure 1). The ylide was used as a solution in THF for epoxidation reactions. Numerous epoxides were thus accessed from ketones and aldehydes in excellent yields.[12] However, several ketones such as desoxybenzoin **6** and Δ^4-cholestenone **7** proved to be inert under these conditions.

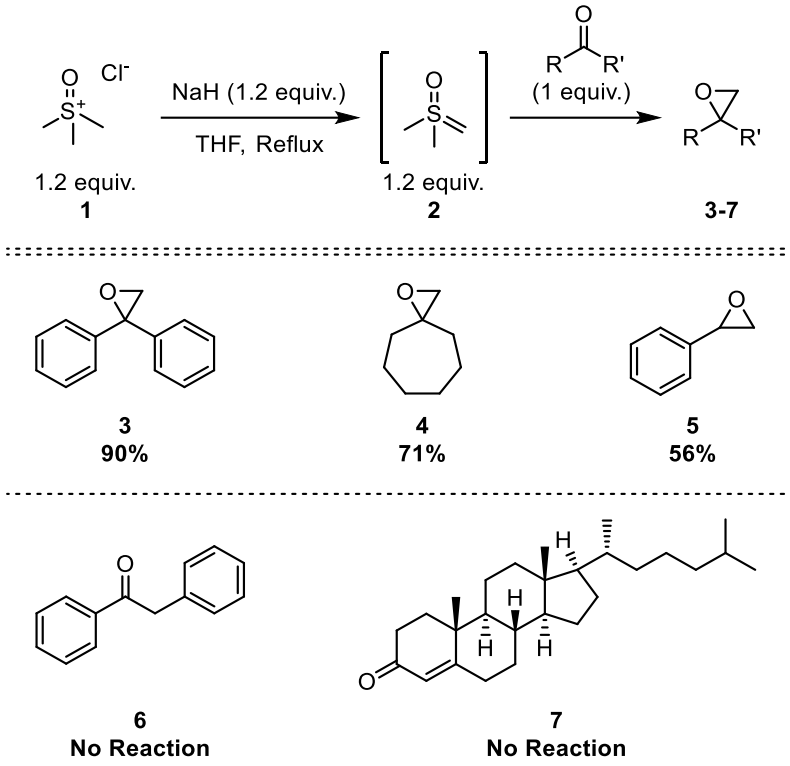

Figure 1: Epoxidation of ketones and aldehydes using dimethylsulfoxonium methylide

Since this work, epoxidation conditions have been refined allowing access to chiral frameworks. In 2008, Shibasaki and his group reported the epoxidation of the ketone **8** in excellent yield and enantiomeric excess (Figure 2).[13] Interestingly, the combination of the chiral lanthanide **9** and a catalytic amount of the phosphine oxide was required to obtain good levels of stereoselectivity.

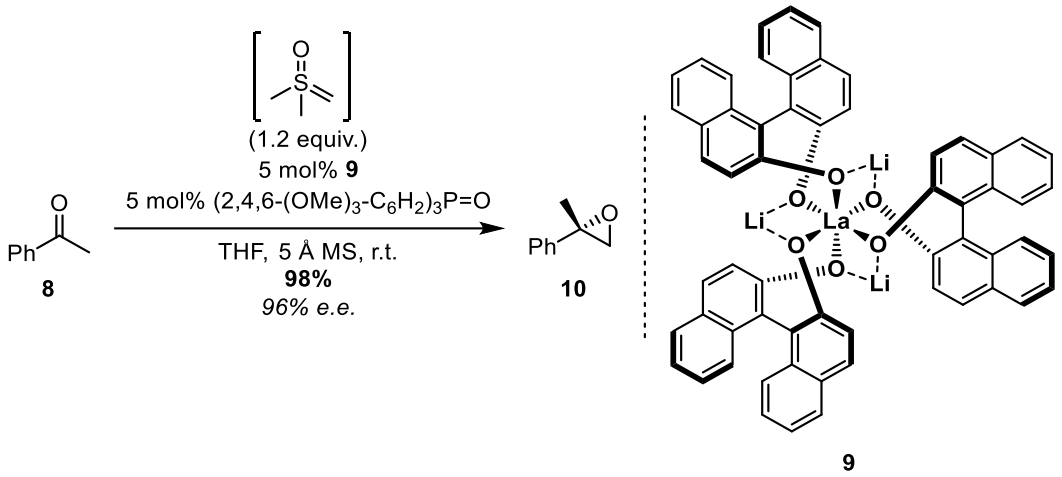

Figure 2: Enantioselective epoxidation of ketones using dimethylsulfoxonium methylide

2.1.2 Cyclopropanation

As seen previously, dimethylsulfoxonium methylide is an excellent methylene donor. Shortly after Corey and Chaykovsky's pioneering work, Izzo *et al.* were able to carry out the cyclopropanation of three unsaturated maleimides **11a-c** with yields ranging from low to excellent (Figure 3).[14]

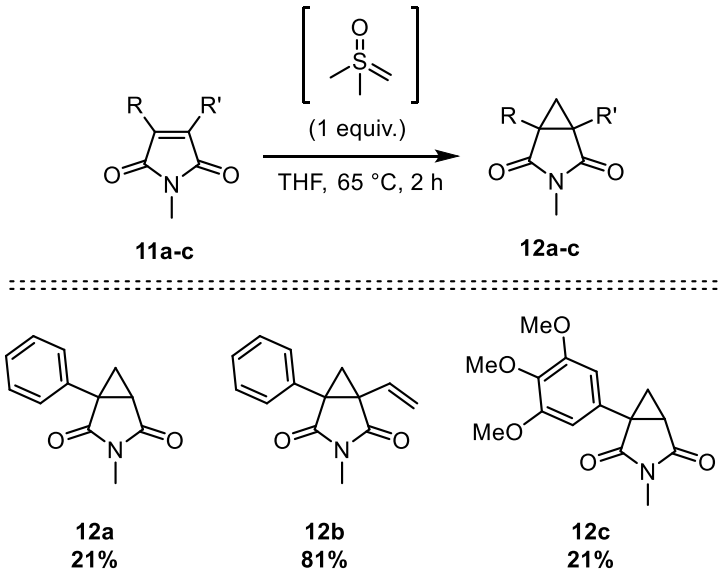

Figure 3: Cyclopropanation of maleimides using dimethylsulfoxonium methylide

The cyclopropanation of α,β-unsaturated ketones was further investigated by Corey and Chaykovsky.[12] The authors demonstrated that the cyclopropanation of α,β-unsaturated ketones was preferred over the epoxidation, thus, eucarvone **13** gave the bicylic compound **14** selectively and in excellent yield (Figure 4). Recently, Ledingham and co-workers confirmed that stabilised ylides, such as sulfoxonium ylides, gave cyclopropanated products whilst less stable sulfonium ylides led to the corresponding epoxide.[15]

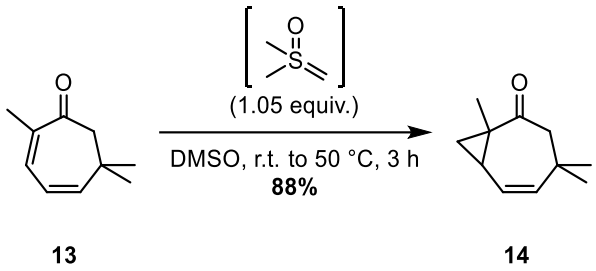

Figure 4: Cyclopropanation of eucarvone using dimethylsulfoxonium methylide

Cyclopropanation with sulfoxonium methylide has been of great interest to the scientific community. Similar to the epoxidation, control of the chemoselectivity and stereoselectivity was improved. A representative example of stereocontrolled cyclopropanation was reported by Ellison and Marshall. The authors obtained the diastereoisomer **16** as the major product when subjecting the 4-substituted α,β-unsaturated cyclohexanone **15** to dimethylsulfoxonium methylide (Figure 5).[16]

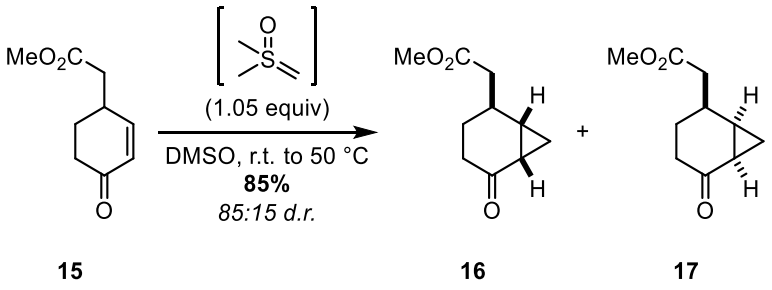

Figure 5: Diastereospecific cyclopropanation using dimethylsulfoxonium methylide

Furthermore, chiral α,β-unsaturated esters have proven to be suitable for the stereoselective cyclopropanation (Figure 6). The chiral cyclopropane **19** was obtained in excellent yield when the sulfoxide **18** was subjected to the cyclopropanation with dimethylsulfoxonium methylide.[17] Even the unprotected terpenoid **21** underwent cyclopropanation of the activated alkene to give **22** in excellent yield.[18]

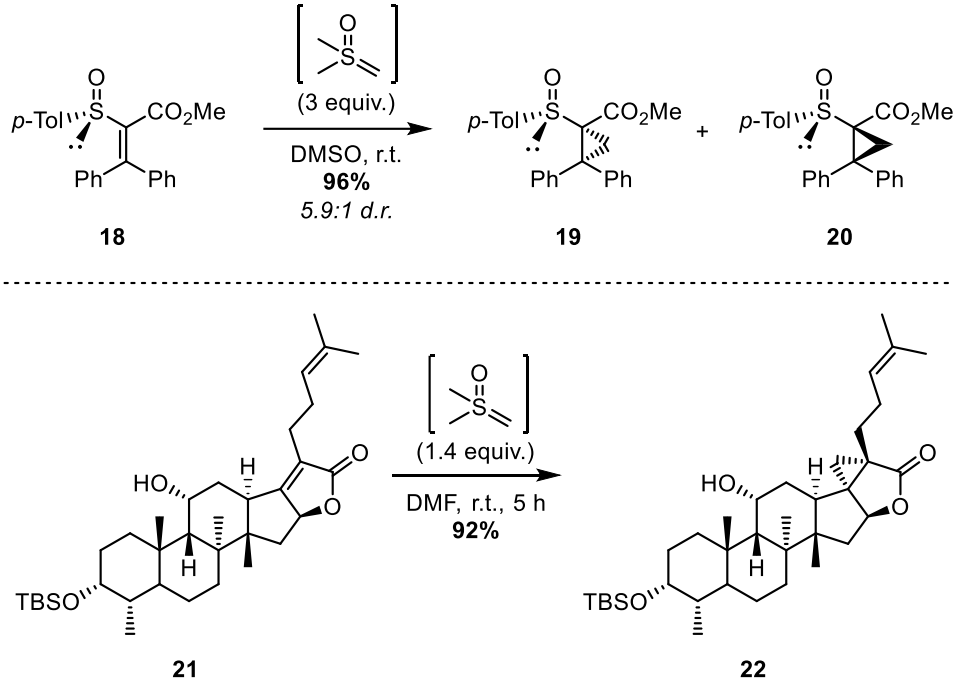

Figure 6: Stereoselective cyclopropanation of α,β-unsaturated esters using dimethylsulfoxonium methylide

2.1.3 Ring expansion

Another important application of dimethylsulfoxonium methylide is the ring expansion of small rings. Nadir and co-workers reported the stereospecific transformation of the aziridines **23** and **25** to the azetidines **24** and **26** in good yields (Figure 7).[19] An inversion of configuration was observed on the attacked carbon centre during the reaction.

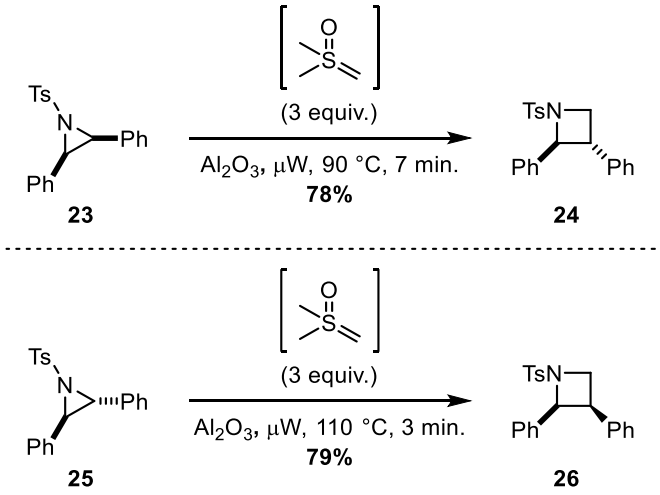

Figure 7: Stereospecific ring expansion from aziridines to azetidines using dimethylsulfoxonium methylide

Following their work on the enantioselective epoxidation of ketones, Shibasaki *et al.* reported the conversion of the epoxide **27** into the oxetane **28** in excellent yield and enantioselectivity (Figure 8).[20] The chiral ligand **9** acted as a chiral amplificator and allowed the access to highly enantiorich products. It is noteworthy that the authors reported the one-pot sequence from ketones to oxetanes in good to excellent yields. Interestingly, the access to oxetanes was limited to terminal epoxides.

Moreover, Fokin and his group showed that the chiral oxetane **29** could be converted to the functionalised tetrahydrofuran **30** in a stereospecific fashion in good yield.[21]

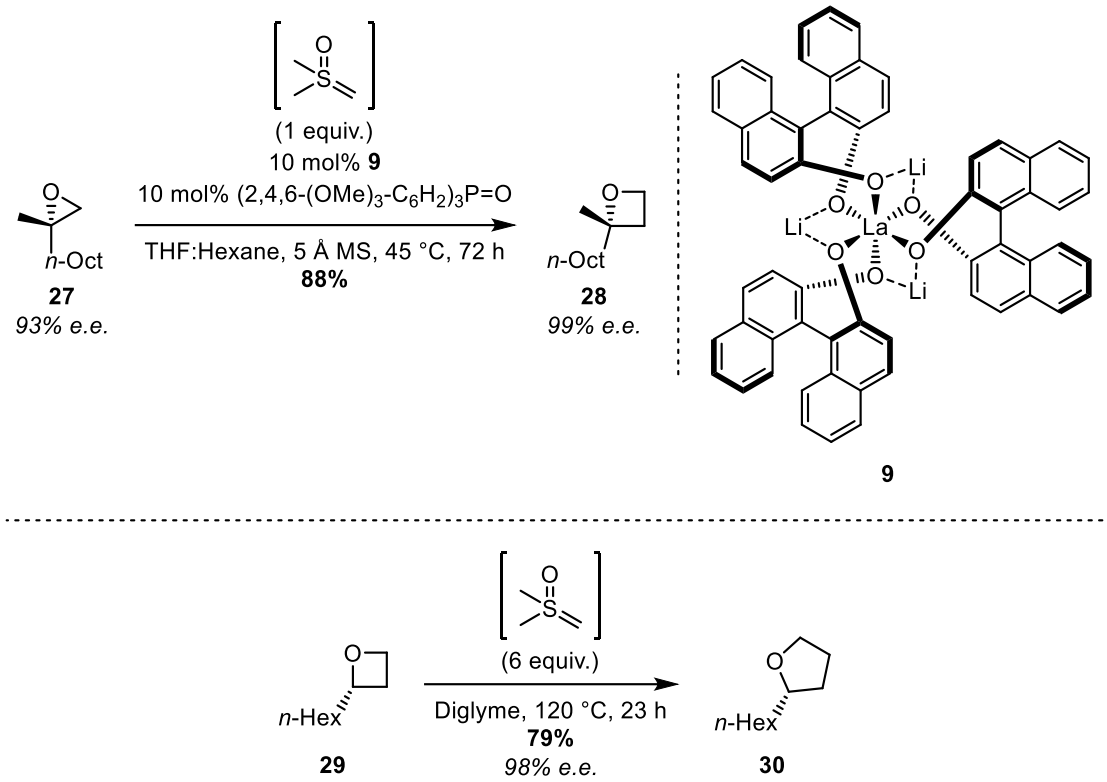

Figure 8: Enantioselective ring expansion of epoxide to oxetane using dimethyl sulfoxonium methylide / ring expansion from oxetane to tetrahydrofuran using dimethyl sulfoxonium methylide

Recently, Xu and Dong reported that the thiirane **31** could give the corresponding thietane **32** in excellent yield (Figure 9).[22] However, the same limitation as with epoxides seems to apply to thiiranes as only terminal thietanes could be generated.

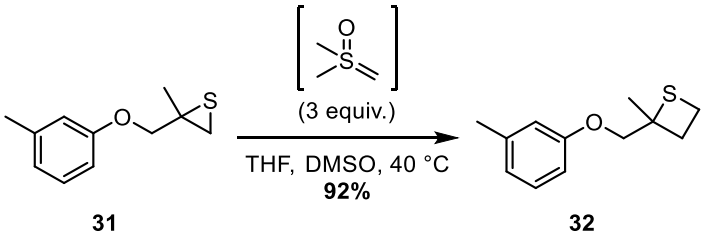

Figure 9: Ring expansion from thiirane to thietane using dimethylsulfoxonium methylide

2.1.4 S–S bond cleavage

In 1977, Field and Chu reported that when the disulphide **33** was reacted with dimethylsulfoxonium methylide, a mixture of three products was obtained, amongst which, the product of interest was the dithiol **34** (Figure 10).[23] However, this reaction could not be optimised and only low yield of **34** was obtained under the best conditions.

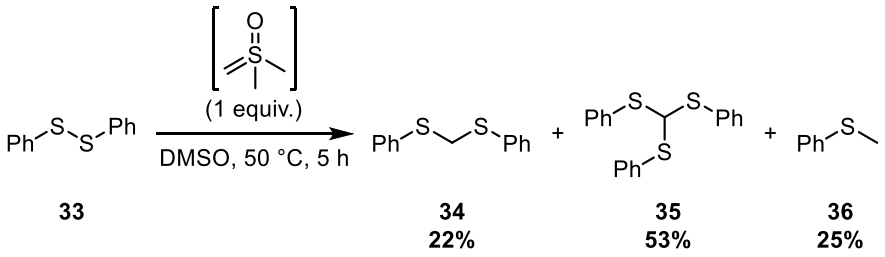

Figure 10: Non-selective S–S bond cleavage using dimethylsulfoxonium methylide

In 1996, Tazaki and Yamada reported the homologation of the 1,2-dithiolane **37** into the 1,3-dithiane **38** with dimethylsulfoxonium methylide in excellent yield (Figure 11).[24] In this case, the S–S bond cleavage was extremely selective and only traces of impurities were observed.

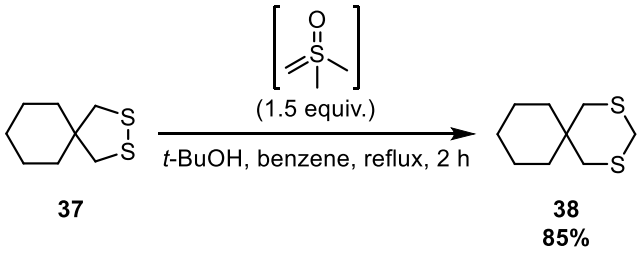

Figure 11: S–S bond cleavage of dithiolane using dimethylsulfoxonium methylide

2.1.5 Polymerisation

In 2002, Shea and co-workers developed an access to the long-chain alcohol **41** by mixing triethyl borane **39** with dimethylsulfoxonium methylide. Upon oxidation of the intermediate **40**, the corresponding alcohol was obtained in 78% yield (Figure 12).[25] By applying the same methodology to the heptacyclo-thexyl-borane **42**, the authors were able to synthesise the macrocycle **43** which was then converted to the linear diol **44** in excellent yield.[26]

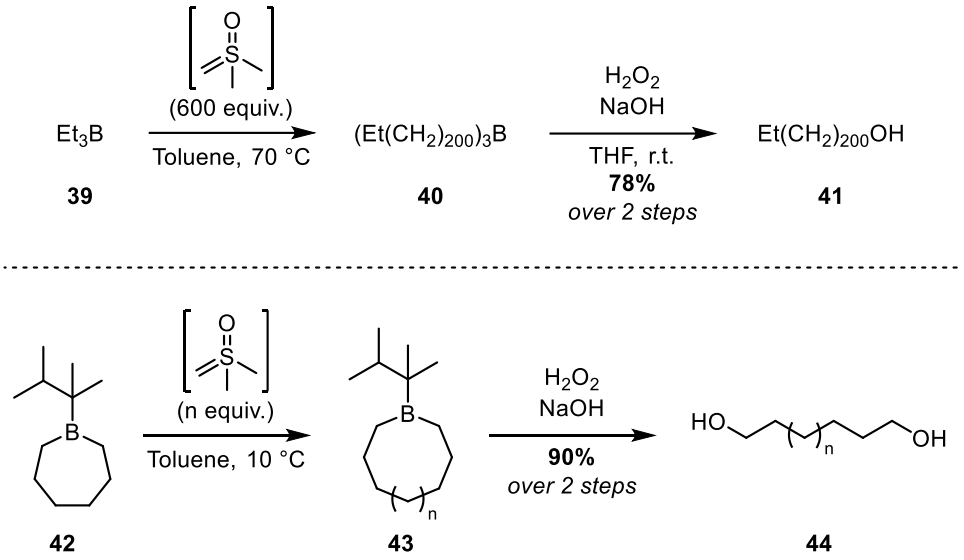

Figure 12: Polymerisation of triethylborane using dimethylsulfoxonium methylide / polymerisation of heptacyclo-thexyl-borane using dimethylsulfoxonium methylide

2.1.6 Formation of complex sulfoxonium ylides

Dimethylsulfoxonium methylide can also be used to generate more complex sulfoxonium ylides when reacted with a suitable electrophile. After the generation of the dimethylsulfoxonium methylide **A** with a base, the attack of the carbene onto the electrophile occurs to give **B**. As an excess of methylide is used, a second equivalent can deprotonate the intermediate to form the desired sulfoxonium ylide **C** along with trimethylsulfoxonium salt (Figure 13).

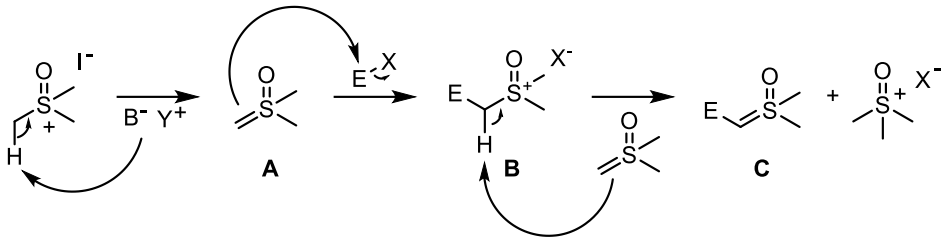

Figure 13: Mechanism for the synthesis of substituted sulfoxonium ylides

Acyl chloride **45**, ester **47** and isocyanate **49** have been successfully used (Figure 14).[27, 28, 29] Although methyl esters have proven to be efficient in some cases, *p*-nitrophenyl esters remain more robust.[30]

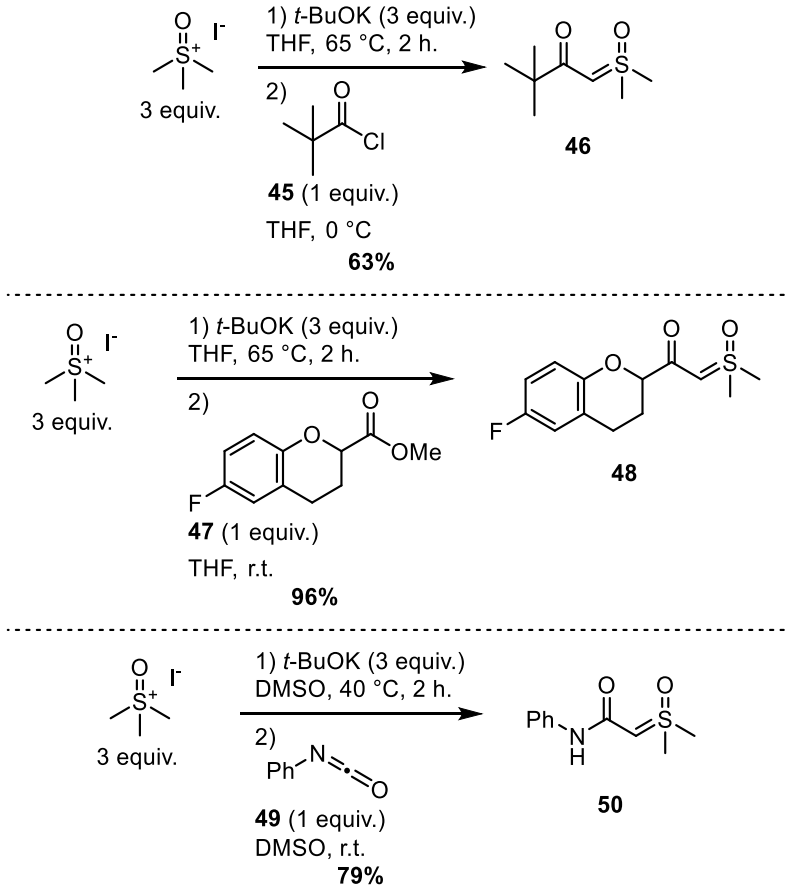

Figure 14: Synthesis of α-carbonylsulfoxonium ylides

Aromatic electrophiles that are prone to undergo nucleophilic aromatic substitution are also suitable reagents to prepare functionalised sulfoxonium ylides

(Figure 15). For example, dimethylchloropyrimidine **51** could be converted to the desired sulfoxonium ylide **52** in good yield. The highly functionalised sulfoxonium ylide **54** was obtained in good yield when **52** was reacted with acetyl chloride.[31]

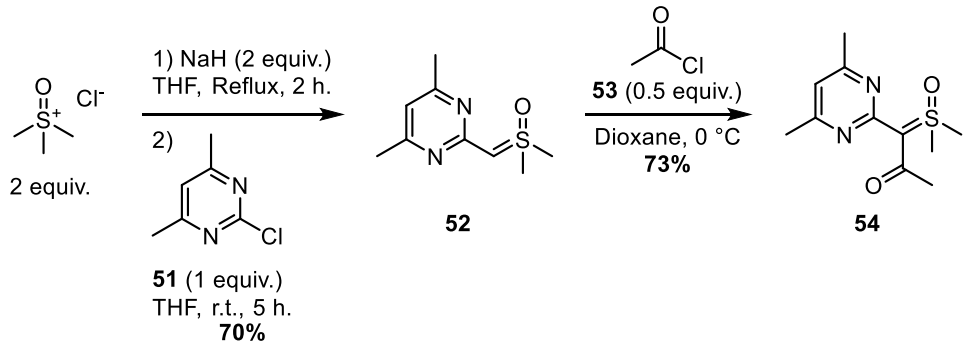

Figure 15: Synthesis of α-pyrimidylsulfoxonium ylide and further substitution

Finally, various other electrophiles have given access to sulfoxonium ylides bearing heteroatoms on the methylene centre such as **56** and **58** (Figure 16).[32, 33]

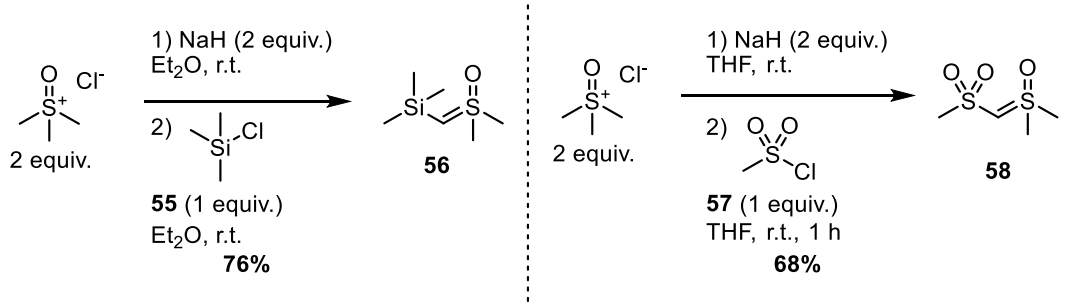

Figure 16: Synthesis of sulfoxonium ylides bearing heteroatoms

2.2 Application of functionalised sulfoxonium ylides

2.2.1 Non-metal catalysed reactions

2.2.1.1 Hydrolysis of sulfoxonium ylides

In 1965, Metzger and König reported the hydrolysis of the α-carbonylsulfoxonium ylide **50** with hydrochloric acid in quantitative yield (Figure 17).[29]

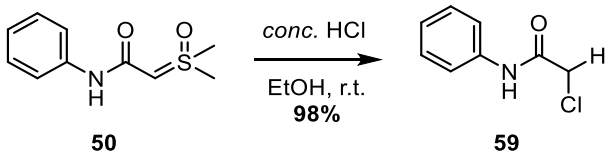

Figure 17: Hydrolysis of α-carbonylsulfoxonium ylide

In 2003, Nugent and co-workers used another type of hydrolysis to access the corresponding chloroketone derivatives **61a-c** from α-ketosulfoxonium ylides **60a-c**.[34] Those species are useful building blocks for the synthesis of *N*-protected α-amino epoxides which can be used as protease inhibitors and HIV treatment.[35] The sulfoxonium ylides **60a-c** were generated from three different Boc- or Cbz-protected amino-acids without loss of the enantiomeric purity. Under mild conditions the authors obtained the desired α-chloroketones in good yields (Table 1, entry **1-3**). Gratifyingly, the protecting group was left intact with those conditions.

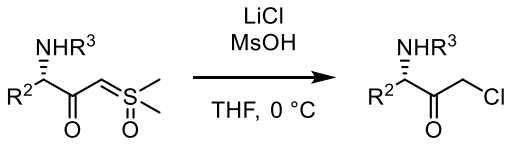

60a-c 61a-c

Entry	R^2	R^3	Yield (%)	*e.e.* (%)
1	Bn	Boc	81	>99
2	Me	Cbz	70	>99
3	*i*-Pr	Cbz	75	>99

Table 1: Hydrolysis of α-ketosulfoxonium ylide derived from amino-acids

2.2.1.2 Formation of thioethers

In addition to the hydrolysis of sulfoxonium ylides, Metzger and König showed that the β-carbonyl-thioether **63** could be isolated in almost quantitative yield when the sulfoxonium ylide **50** was reacted with the thiophenol **62** (Figure 18).[29]

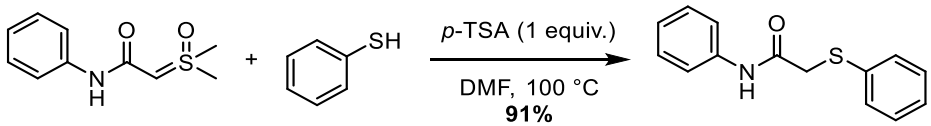

50 **62** **63**

Figure 18: Synthesis of β-carbonyl-thioether using sulfoxonium ylide

In 2016, Burtoloso and his group revisited this work and reported that, along with aromatic thiols, the aliphatic thiol **65** could undergo the reaction smoothly to give **66** in good yield (Figure 19).[36] Treatment of the ketone **67** with a Brønsted acid allowed the synthesis of the benzothiophene **68** in 78% yield.

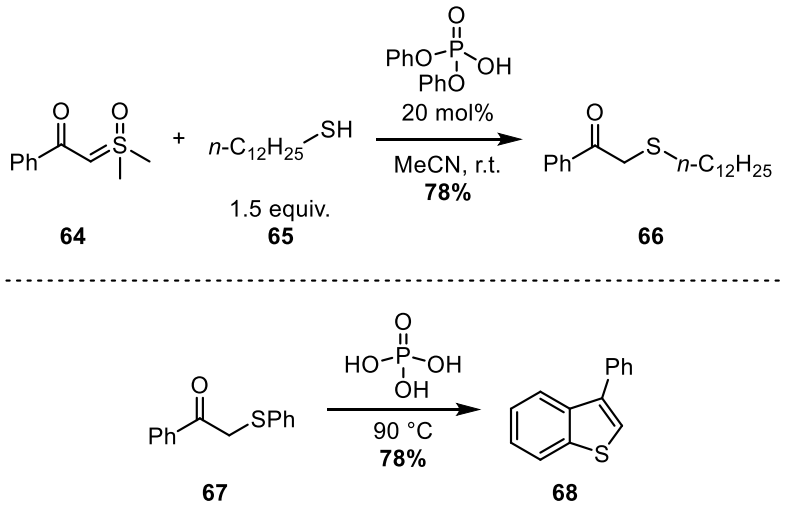

Figure 19: Synthesis of β-keto-thioether using sulfoxonium ylide / access to benzothiophene

2.2.1.3 Difunctionalisation of sulfoxonium ylides

Metzger and König also reported in 1965 the reactivity of sulfoxonium ylides when mixed with halogenoalkane (Figure 20).[29] When the sulfoxonium ylide **50** was treated with methyl iodide, the authors obtained the corresponding *gem*-methyl-iodide-amide **69** in low yield.

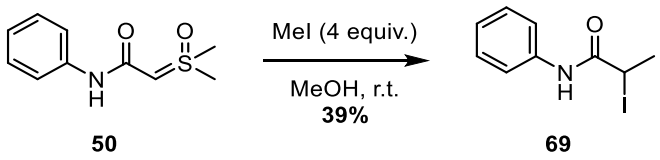

Figure 20: Difunctionalisation of sulfoxonium ylide with methyl iodide

Recently, Burtoloso *et al.* expanded the scope of halogenoalkanes suitable for this reaction.[27] The α-bromoketone **71** was obtained in good yield when the sulfoxonium ylide **70** was reacted with benzyl bromide (Figure 21). Moreover, electrophilic halogen sources such as Selectfluor were tolerated in this reaction, giving the corresponding *gem*-dihalogenated ketone **73** in 72% yield.

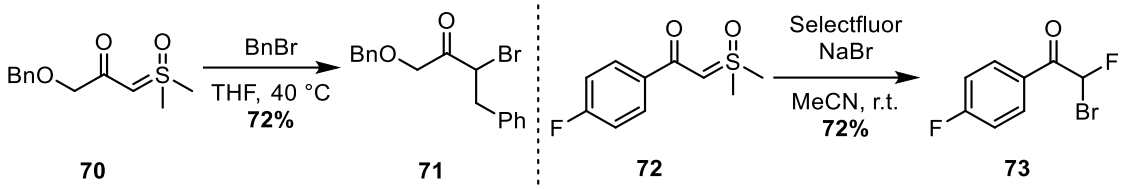

Figure 21: Difunctionalisation of sulfoxonium ylide with benzyl bromide or selectfluor

2.2.2 Metal-catalysed reactions

2.2.2.1 Carbon–heteroatom bond formation

Surprisingly, metal catalysed reactions with sulfoxonium ylides is far less explored. In 1993, Baldwin and co-workers reported the formation of the pyrrolidinone and piperidinone, **75** and **77** respectively, from the corresponding linear sulfoxonium ylide in the presence of a rhodium (II) catalyst (Figure 22).[37] Moderate to good yields of the cycloadduct were obtained.

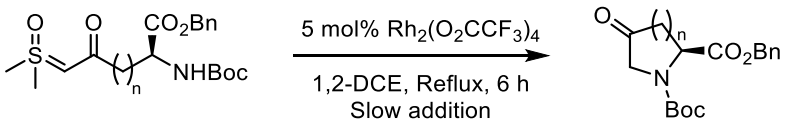

74, (n=1)
76, (n=2)

75, (n=1), **77%**
77, (n=2), **51%**

Figure 22: Rhodium-catalysed cyclisation of sulfoxonium ylides

Later, investigation of the mechanism hinted towards the generation of a metal-carbene species **A** (Figure 23).[38] Attack of the carbene centre by the amine to give **B** followed by proto-demetalation can regenerate the catalyst alongside the product.

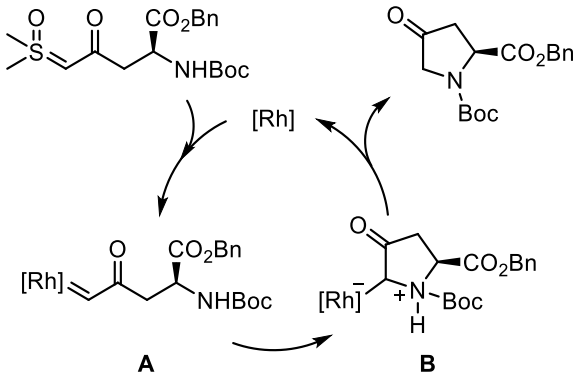

Figure 23: Catalytic cycle of the rhodium-catalysed cyclisation of sulfoxonium ylides

Although highly interesting, no improvement on this carbene chemistry was reported until 2009. Huffman and co-workers showed that the reaction scope could be broadened and both intra- and intermolecular carbon-heteroatom bond formation were described.[39] The optimisation of the reaction showed that iridium (I) was a better catalyst than rhodium (II) for this transformation, with a loading as low as 1 mol% at room temperature. Amines, alcohols and thiols reacted smoothly in those conditions. When a secondary amine was used, the temperature had to be increased to 70 °C, and the solvent was thus changed to 1,2-DCE (Table 2, Entry **2**). To access ethers, the corresponding alcohol was used as the solvent (Table 2, Entry **3**).

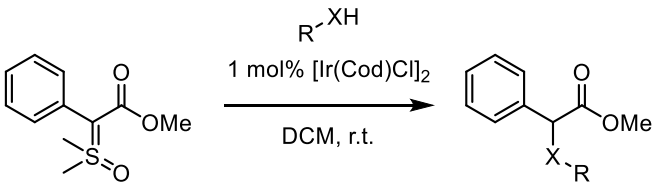

78 79a-d

Entry	R	X	Yield (%)
1	Ph	NH	91
2[a]	Ph	NMe	89
3[b,c]	Et	O	86
4	Ph	S	80

a) at 70 °C. *b)* at 35 °C. *c)* neat EtOH.

Table 2: Iridium-catalysed C–heteroatom bond formation using sulfoxonium ylides

Five-, six- and seven-membered rings, **81**, **83** and **85** respectively, were synthesised after cyclisation of the corresponding sulfoxonium ylides (Figure 24). All reactions were performed at 70 °C in 1,2-DCE and gave the desired cycloadduct in good yields.

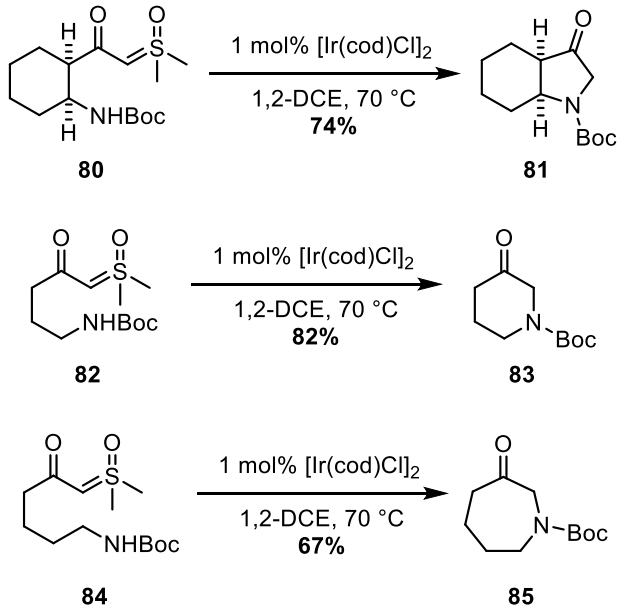

Figure 24: Iridium-catalysed cyclisation of sulfoxonium ylides

The same authors demonstrated that gold catalysts were also potent for the carbon-heteroatom bond formation with sulfoxonium ylides (Table 3).[38] A slight increase in yield was observed as compared to iridium complexes. Platinum, as well as silver catalysts, proved to be less efficient.

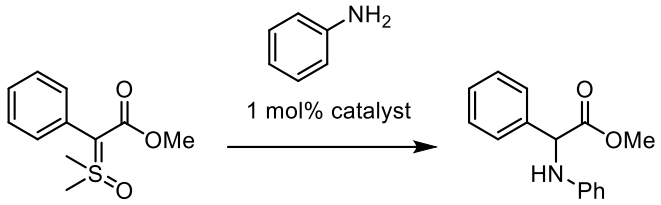

78 **79a**

Entry	Catalyst	Yield (%)
1	$[Ir(cod)Cl]_2$	91
2[a]	$[Cp^*IrCl_2]_2$	88
3[b]	AgCN	24
4[c]	$Pt(cod)Cl_2$	81
5	AuCl	30
6	$AuCl_3$	78
7	$AuCl(SMe_2)$	94

a) 3 mol% of $[IrCp^*Cl_2]_2$. *b)* 3 mol% of AgCN. *c)* 3 mol% of $Pt(cod)Cl_2$

Table 3: Optimisation of the metal-catalysed cyclisation of sulfoxonium ylides

Interestingly, when this new catalyst was used for the cyclisation of **82**, the desired piperidinone **83** was obtained in extremely low yield when compared to the results obtained with the iridium (I) catalyst (Figure 25).

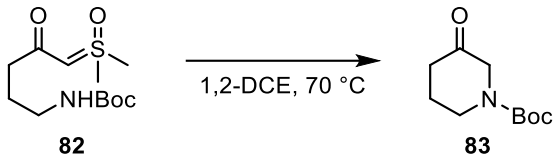

82 **83**

1 mol%, $[Ir(cod)Cl]_2$: **82%**
1 mol%, $AuCl(SMe)_2$: **7%**

Figure 25: Iridium- and gold-catalysed cyclisation of sulfoxonium ylides

Gratifyingly, this methodology was used by Merck in their synthesis of two potent drugs: MK-7655 and MK-7246 (Figure 26).[40, 41]

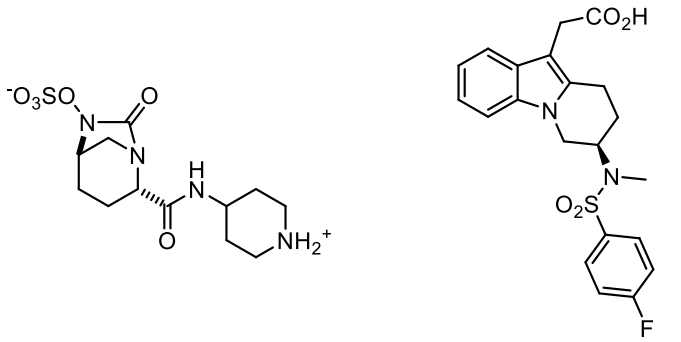

MK-7655 **MK-7246**

Figure 26: Structure of MK-7655 and MK-7246

The opening of the Boc-protected pyroglutamic acid **86** to the sulfoxonium ylide **87**, followed by an iridium catalysed cyclisation, gave the desired piperidinone **88** in good yield (Figure 27). More importantly, the protocol was used on multi-kilogram scale.

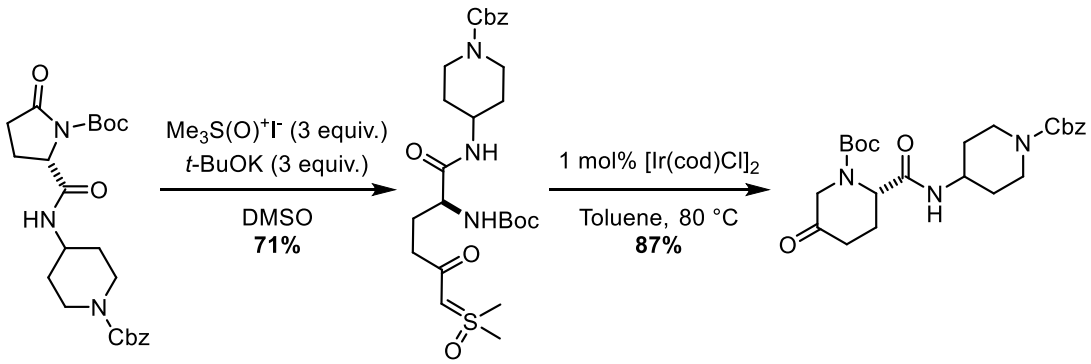

86 **87** **88**

Figure 27: Ring opening of pyroglutamic acid and iridium-catalysed cyclisation with sulfoxonium ylides to access MK-7655

The same metal-catalysed C–N bond formation was employed to access MK-7246. The opening of the five-membered lactam **89** followed by an iridium-catalysed cyclisation gave the 3-piperidinone **91** (Figure 28). Changing the solvent to a mixture

of toluene and DMF did not decrease the reactivity and gave the desired piperdinone in 83% yield. Similarly to their previous synthesis, this pathway was used in pilot-plant on production scale to produce more than a hundred kilograms of **91**.

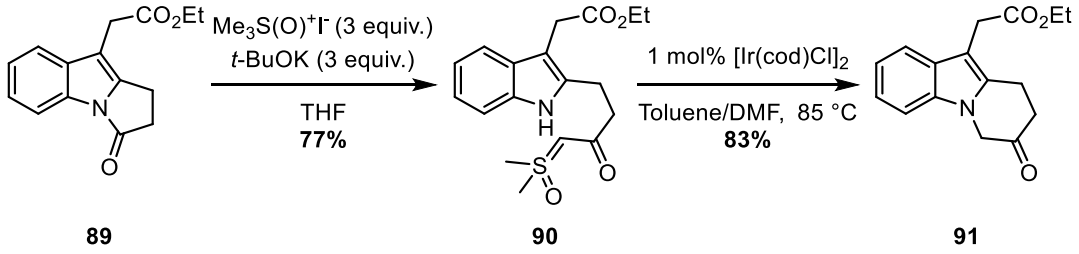

Figure 28: Ring opening of five-membered β-lactam and iridium-catalysed cyclisation with sulfoxonium ylides to access MK-7246

Interestingly, a decreased yield was observed when O'Shea and his team tried the same iridium catalysed cyclisation with the corresponding diazo intermediate **92**, even with 10 mol% of rhodium (Figure 29). This last result shows that, in some cases, sulfoxonium ylides can be more reactive than other carbene precursors.

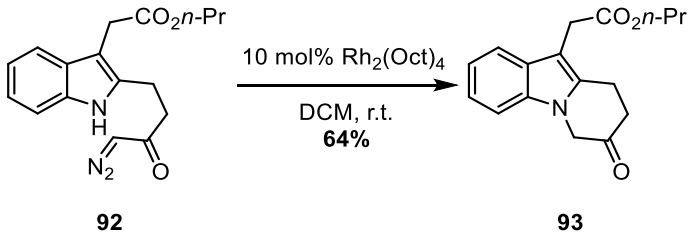

Figure 29: Rhodium-catalysed cyclisation using diazo-compound

In 2016, Shekhar *et al.* showed that sulfoxonium ylides could be used in the synthesis of either 7- or 8-substituted-imidazopyrrolopyrazines, depending on the tandem Catalyst/Ligand used (Figure 30).[42] When the iridium catalyst was used without external ligands, the C–N bond formation was observed without further cyclisation, to give **95** as the major isomer in low yield. However, if phenanthroline

was added to the reaction pot, along with sodium triflate, the reaction gave selectively the cyclised heterocycle **96** in 60% yield.

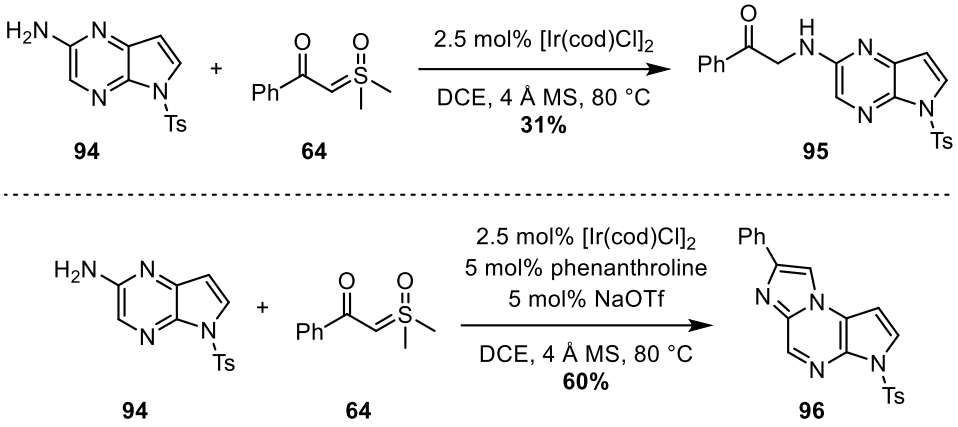

Figure 30: Iridium-catalysed formation of 7-or 8-substituted imidazopyrrolopyrazines

Using NMR and mass spectrometry, the authors were able to track the iridium catalyst throughout the reaction. With the iridium (I) catalyst alone, they proposed that coordination of the pyrazine ring occurs prior to the carbene formation to give intermediate **A** (Figure 31). Formation of the carbene **B** followed by the nucleophilic attack of the amine leads to the intermediate **C**. Proto-demetalation of the complex affords the functionalised azole and regenerates the active species.

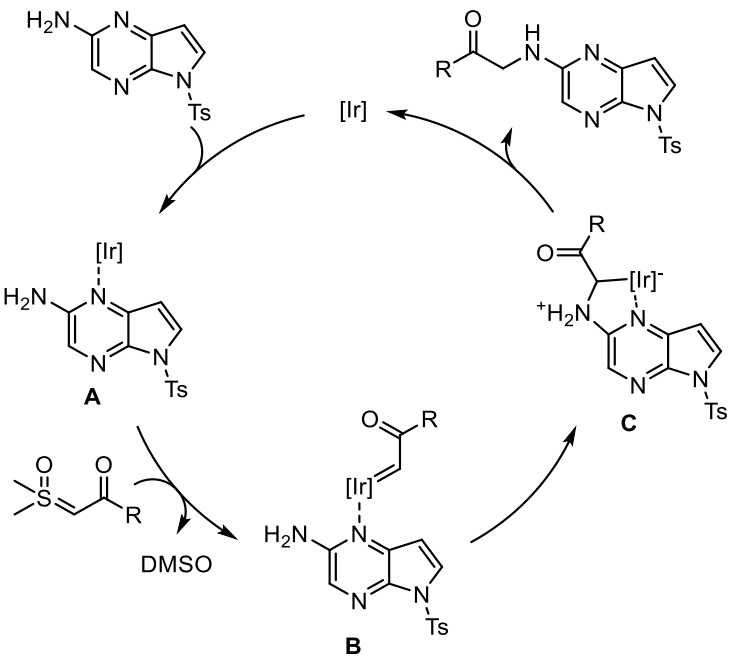

Figure 31: Mechanism for the iridium-catalysed synthesis of the 7-substituted imidazopyrrolopyrazine

When NaOTf and phenanthroline are added to the reaction, coordination of the phenanthroline occurs rapidly, favouring the formation of the carbene **A** (Figure 32). Intermolecular attack of the starting material to form the pyrazinium **B** proceeds in a second step. Delocalisation of the lone-pair of electrons of the amine into the ring affords the intermediate **C**, which gives **D** upon proto-demetalation of the iridium catalyst. The product is obtained after cyclisation and elimination of water.

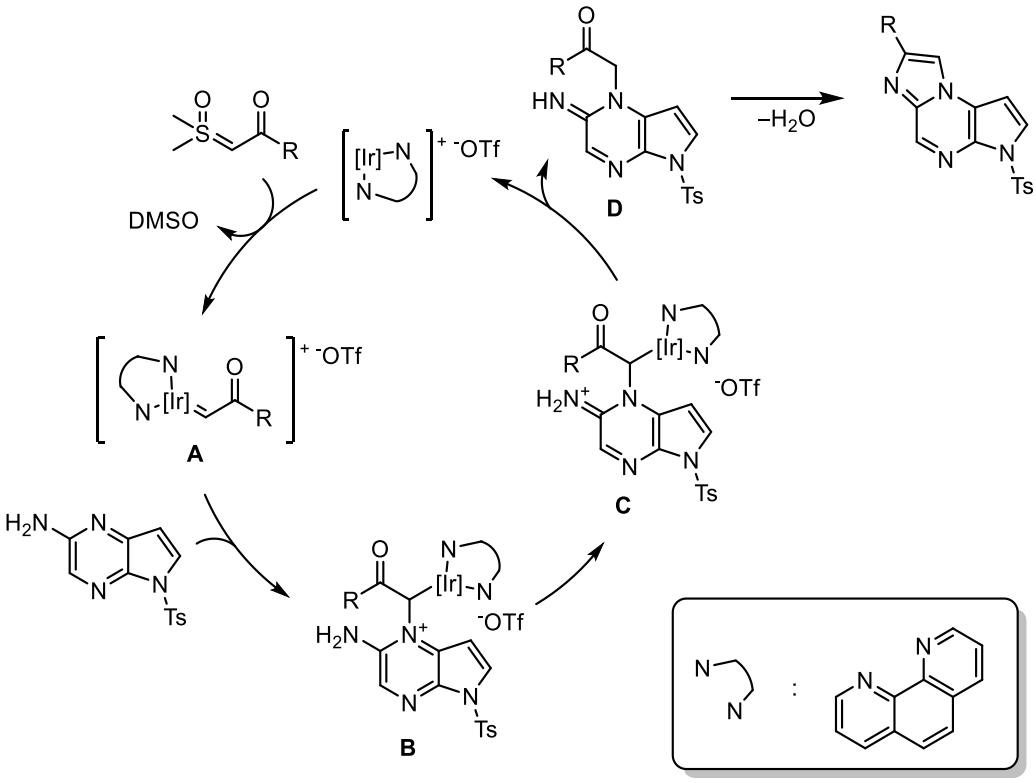

Figure 32: Mechanism for the iridium-catalysed synthesis of the 8-substituted imidazopyrrolopyrazine

2.2.2.2 Polymerisation

De Bruin and co-workers used dimethylsulfoxonium methylide in rhodium-catalysed polymerisation reactions (Figure 33).[43] The authors also used a combination of the ethyl diazoacetate **98** with dimethylsulfoxonium methylide to form co-polymers such as **99** in low yield.

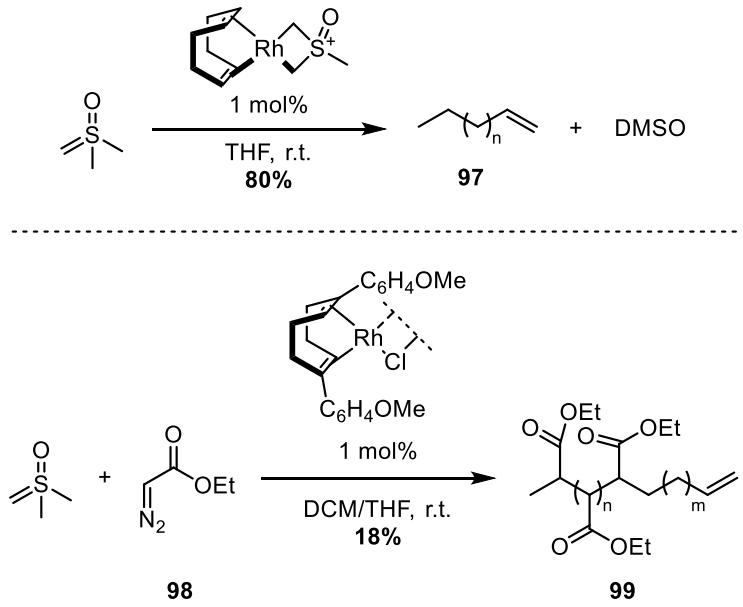

Figure 33: Rhodium-catalysed polymerisation of dimethylsulfoxonium methylide / rhodium catalysed co-polymerisation of dimethylsulfoxonium methylide and diazo-compound

2.2.2.3 Carbon-carbon bond formation

In 2012, an example of intramolecular carbon-carbon bond formation catalysed by iridium was reported in a patent.[44] Cyclisation of the pyrrole derivative **100** with an alkyltether chain carrying the sulfoxonium ylide, gave the bicyclic compound **101** in moderate yield (Figure 34).

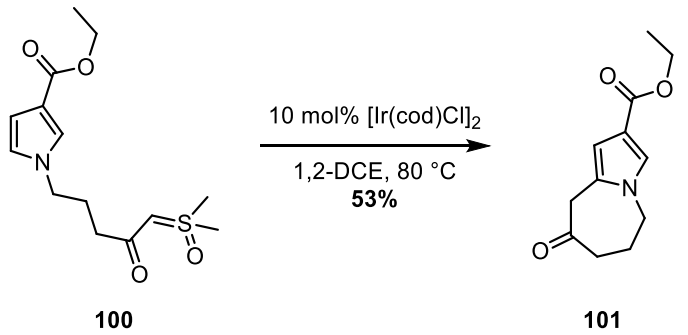

Figure 34: Iridium-catalysed cyclisation *via* C–C bond formation with sulfoxonium ylide

3 Aims and objectives

As seen in this introduction, although sulfoxonium ylides have great potential as bench stable carbene precursors, transition-metal catalysed reactions with those species are scarce. Moreover, all those reactions involve the formation of a metal-carbene species as the first elementary step, which can react to generate a C–C or C–X bond. This methodology requires the use of an activated coupling partner and can not be applied to the functionalisation of inert C–H bond.

Recently, the metal-catalysed C–H bond functionalisation with carbenes has raised a tremendous interest for the rapid formation of complex frameworks. Selected examples are presented hereafter to showcase the great scope of possible transformations brought by this methodology.

3.1 Carbenes generated from diazo-compounds

3.1.1 Previous work

The first example of metal-catalysed C–H bond functionalisation using carbenes and a rhodium (III) catalyst was reported in 2012 by Yu.[45] The authors reported the rhodium-catalysed functionalisation of the *O*-methyloxime **102** with the diazomalonate **103** (Figure 35). Aside from methylated oximes, the authors demonstrated that the carboxylic acid **105** was suitable as a directing group and obtained the functionalised naphthyl **106** in excellent yield.

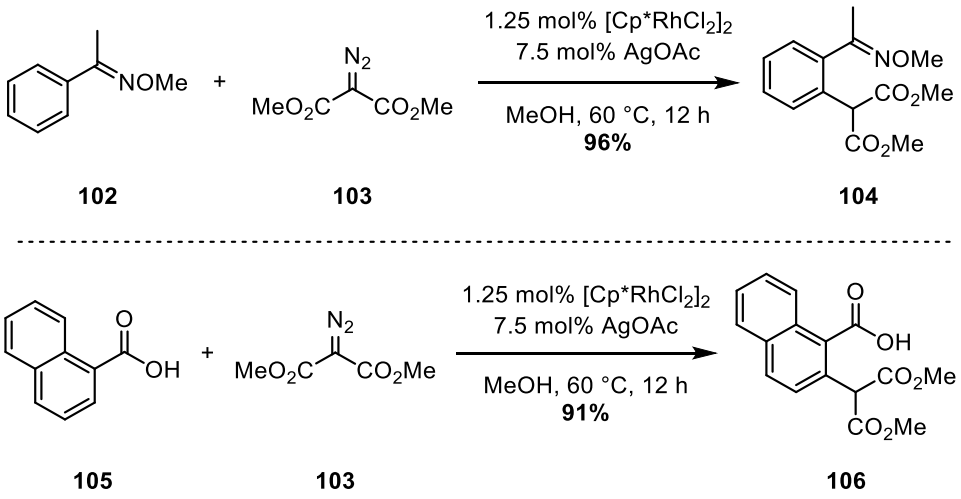

Figure 35: Rhodium-catalysed Csp^2–H bond functionalisation with diazomalonate and methyloximes/carboxylic acids

Rovis *et al.* complemented this work by using the hydroxamate **107** to obtain the isoindolone **109** in 81% yield through a rhodium-catalysed (4+1) cyclisation (Figure 36).[46] Later, Cramer and co-workers reported the enantioselective version of this reaction and obtained **111** in good yield and excellent enantioselectivity when the chiral Cp ligand was used.[47]

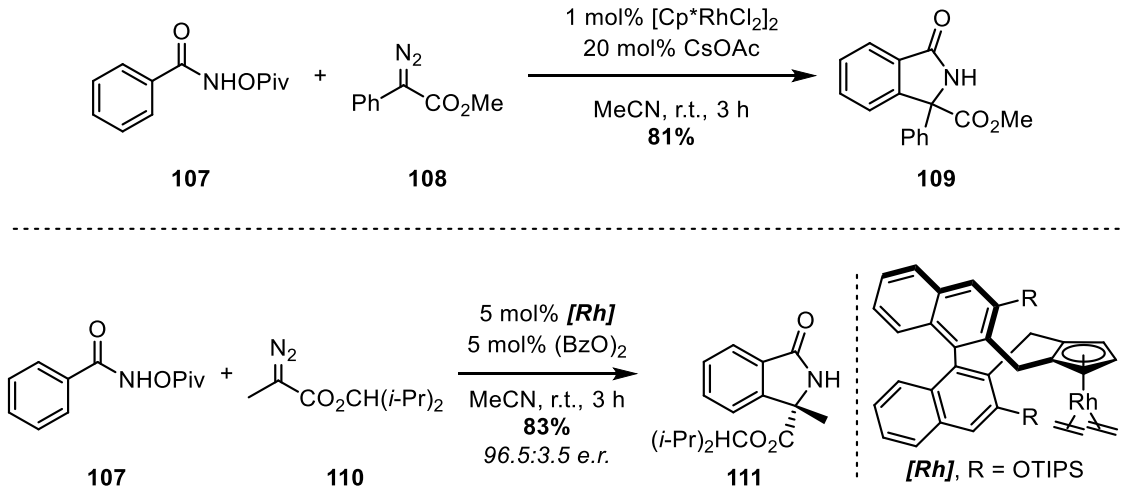

Figure 36: Racemic and enantioselective rhodium-catalysed Csp^2–H bond functionalisation with diazo-compounds and hydroxamate

Glorius and his group reported the functionalisation of the unprotected oxime **112** to yield the quinoline *N*-oxide **114** in quantitative yield (Figure 37).[48]

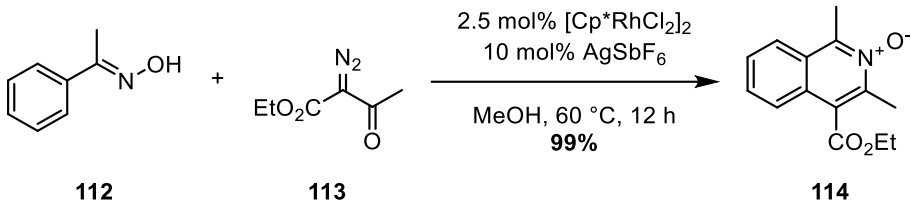

Figure 37: Rhodium-catalysed Csp^2–H bond functionalisation and cyclisation with diazo-compounds and oximes

Finally, Li and co-workers showed that pyrrazoles, pyrimidines, pyridines and benzoxazoles could be used as directing group with the diazomalonate **103**, to give the corresponding products in yields ranging from good to excellent (Figure 38).[49] It is noteworthy that the *ortho*-substitution of the arene was needed to prevent bis-functionalisation with the pyrimidine **116** and the benzoxazole **118**.

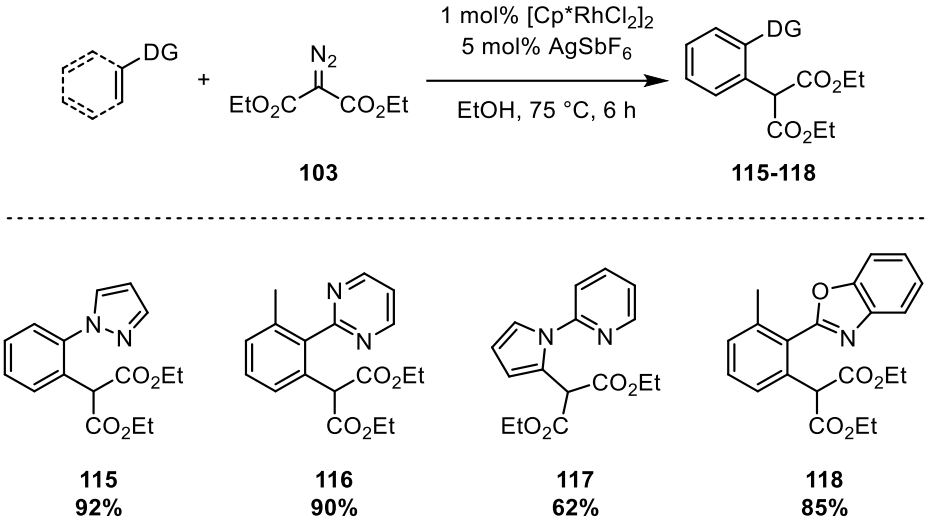

Figure 38: Rhodium-catalysed Csp^2–H bond functionalisation with diazo-compounds and various *N*-containing directing groups

An extensive effort has been made following those works, and a large variety of directing groups have been utilised in the C–H bond functionalisation, *i.e.* secondary amines, sulfoximines, diazenes, alcohols and quinolines.[45, 49, 50, 51, 52]

Moreover, Glorius and co-workers reported the cobalt-catalysed activation of olefinic C–H bonds (Figure 39).[53] Annulation of the vinyl pyridine **119** gave the fully aromatic bicyclic compound **120** in moderate yield.

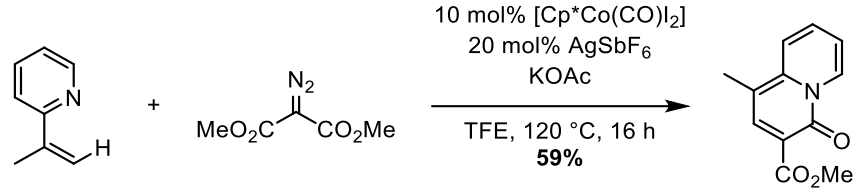

119 **103** **120**

Figure 39: Cobalt-catalysed Csp^2–H bond functionalisation of olefins with diazo-compounds

Only two examples of Csp^3–H functionalisation using diazo-compounds have been described in the literature. In 2016, Zhou and co-workers reported the rhodium-catalysed functionalisation of the quinoline **121** with the diazo-compound **122** in quantitative yield (Figure 40).[54]

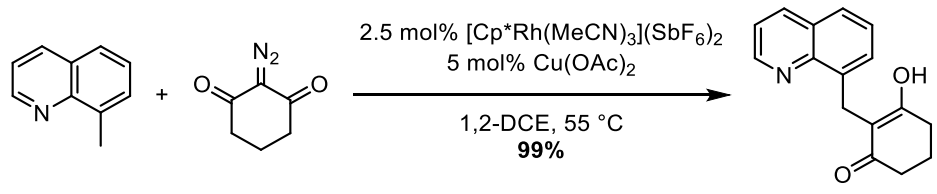

121 **122** **123**

Figure 40: Rhodium-catalysed Csp^3–H bond functionalisation with diazo-compounds

However, no reaction was observed, neither with the monocarbonyl diazo-compound **108**, nor with any Csp^3–H other than primary such as **124** and **125** (Figure 41).

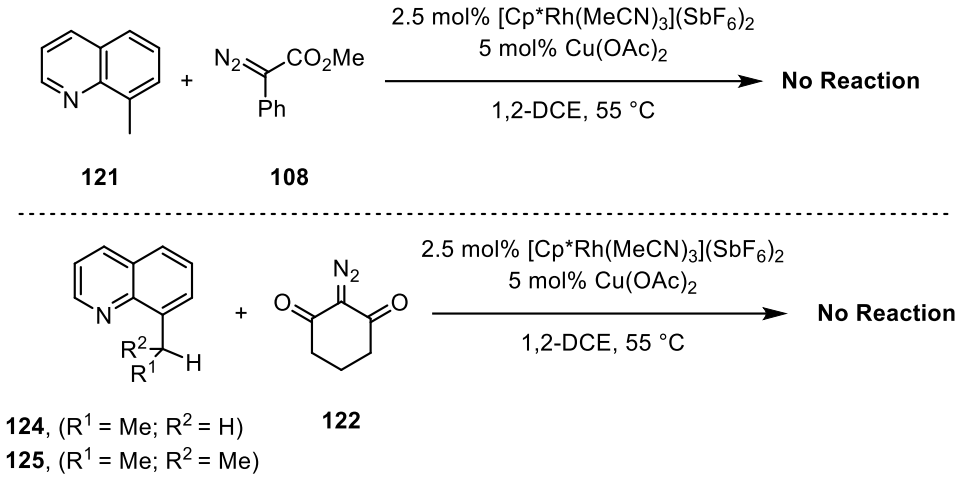

Figure 41: Limitations of the rhodium-catalysed Csp^3–H bond functionalsiation with diazo-compounds

Recently, a similar approach was investigated with a cobalt catalyst and the same limitations were observed.[55]

3.1.2 Proposed mechanism

The C–H activation/functionalisation mechanism can be summarised as depicted below (Figure 42).[56] Coordination of the catalyst to the directing group affords the complex **A** which is converted to **B** upon a concerted metallation/deprotonation (CMD). Nucleophilic attack of the diazo-compound forms the diazonium intermediate **C** which is converted to the carbene species **D** upon release of nitrogen. After migratory insertion to give **E**, the proto-demetalation of this intermediate releases the product along with the active catalyst.

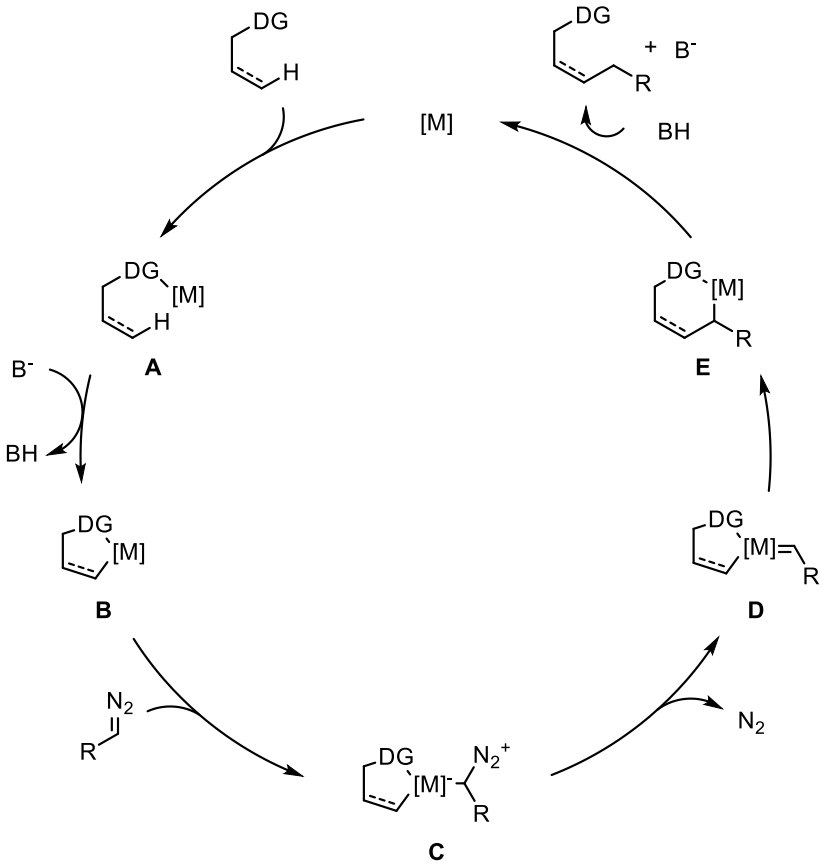

Figure 42: Proposed mechanism for the metal-catalysed C–H bond functionalisation with diazo-compounds

3.2 Alternatives

Although incredibly versatile and useful synthons, diazo-compounds are notorious for being unstable. Thus, alternatives have been studied in order to circumvent this drawback.[57]

3.2.1 Triazoles

In 2015, Glorius *et al*. investigated the use of pyridotriazoles as a new class of stable carbene precursors.[58] Triazoles have been mainly used in C–H functionalisation as directing groups.[59] Pyridotriazoles are in equilibrium with the α-diazopyridine form,

as depicted with **126** and **127**, thus the same reactivity as described previously can be expected (Figure 43).[60]

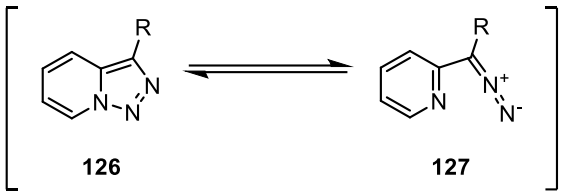

Figure 43: Equilibrium between the triazole and the α-diazopyridine

This property was successfully applied to the rhodium catalysed C–H activation of phenyl pyridine **128** (Figure 44). The authors reported the synthesis of the highly conjugated heterocycle **130** in quantitative yield.

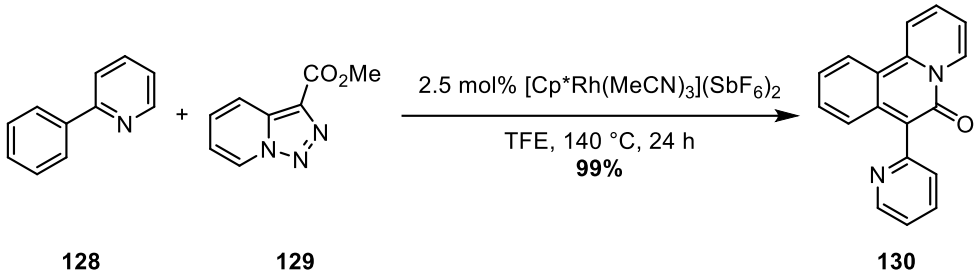

Figure 44: Rhodium-catalysed Csp^2–H Bond functionalisation/cyclisation with triazoles

The same reagent was used by Lee and his group for the functionalisation of the sulfoximine **131** to the benzothiazine **133** in 83% yield (Figure 45).[61] The product with the *anti*-relationship between the methyl and the pyridyl group was the major diastereoisomer.

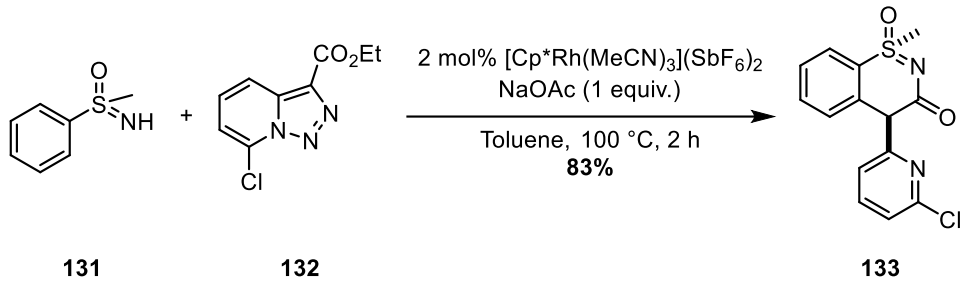

Figure 45: Rhodium-catalysed Csp^2–H bond functionalisation/cyclisation with triazoles and sulfoximines

3.2.2 Tosyl-hydrazones

Similar to the previous reagent, tosyl-hydrazones are used as stable diazo precursors. When subjected to basic conditions, a loss of tosylate occurs to generate the desired diazo-compound **136** (Figure 46).[62]

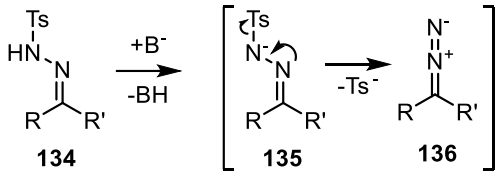

Figure 46: Mechanism for the generation of diazo-compounds from tosyl-hydrazones

Although more studied than triazoles as carbene precursors, the C–H activation with tosyl-hydrazones generally involves a copper, nickel or cobalt catalyst. Wang and co-workers focused on the copper catalysed C–H bond functionalisation.[63] The authors reported the alkylation of the benzoxazole **137** with the tosyl-hydrazone **138** (Figure 47). Aside from benzoxazoles, the benzothiazole **140** and the 1,2,4,5-tetrafluorobenzene **142** gave the corresponding products **141** and **143** respectively, in good to moderate yield. Both the temperature and the amount of catalyst had to be increased and the solvent changed to 1,4-dioxane for those substrates.

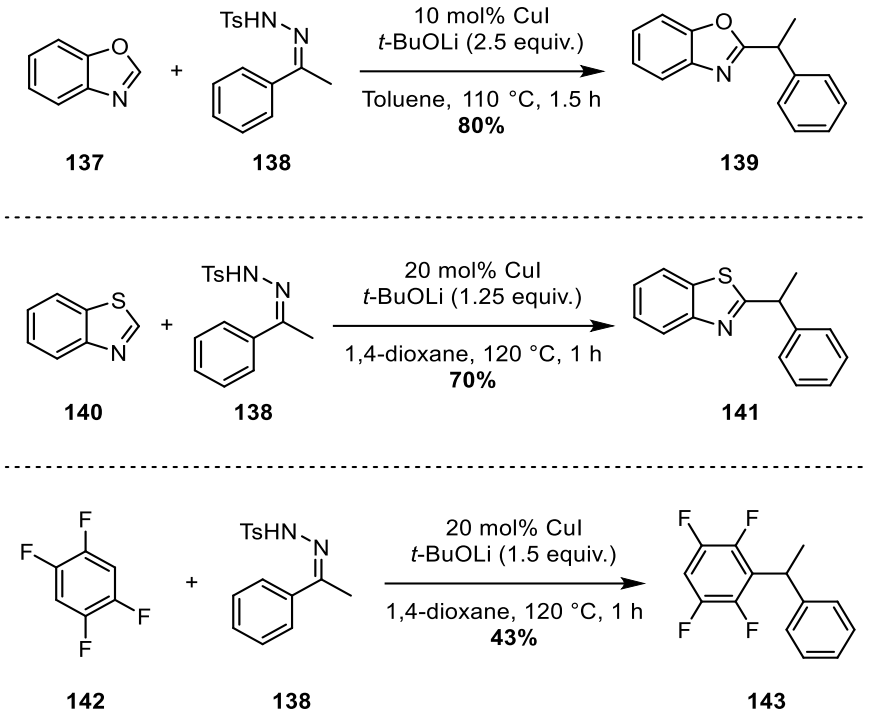

Figure 47: Copper-catalysed Csp^2–H bond functionalisation with tosyl-hydrazones

Shortly after, Hirano and Miura reported the same reaction with either a nickel or cobalt catalyst (Figure 48).[64] Both the benzoxazole **144** and phenyloxazole **147** were functionalised in good yields, but only 1,3-azoles were investigated.

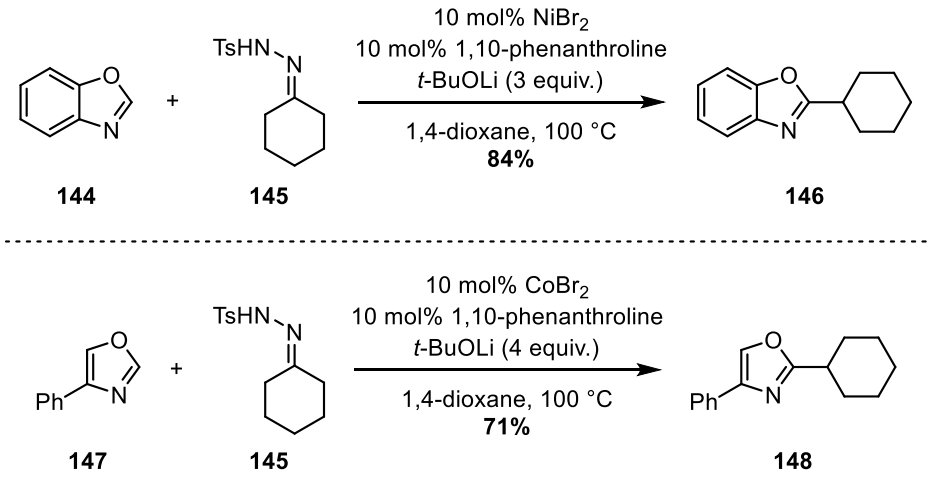

Figure 48: Nickel- and cobalt-catalysed Csp^2–H bond functionalisation with tosyl-hydrazones

Only two examples of rhodium-catalysed C–H bond functionalisation with tosyl-hydrazones were reported, both by Wang and his group in 2013 and 2014. In their first paper, the authors used Wilkinson's catalyst to activate the quinolinylmethanone **149** and synthesise the α,β-unsaturated ketone **151** in good yield (Figure 49).[65]

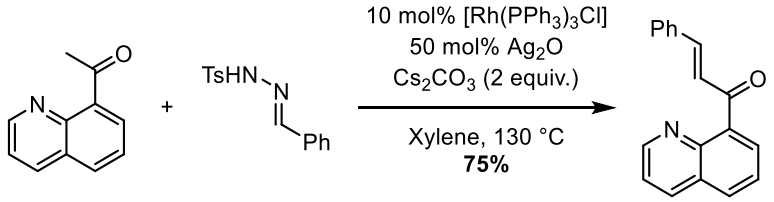

Figure 49: Rhodium-catalysed Csp^3–H functionalisation with tosyl-hydrazones

A year later, the same group reported the rhodium-catalysed functionalisation of the oxyacetimide **152** to the phenol **153** in 83% yield (Figure 50).[66]

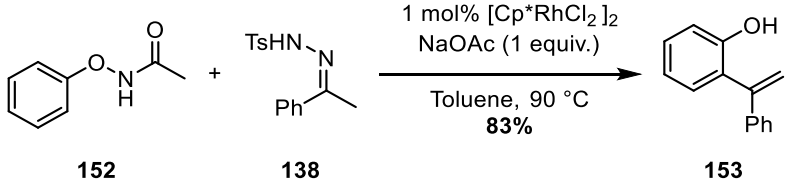

Figure 50: Rhodium-catalysed Csp^2–H bond functionalisation with tosyl-hydrazones

3.2.3 Enynones

Recently, Chang *et al.* reported the use of enynones as possible carbene precursors, and their application in the functionalisation of the *N*-functionalised benzamide **107** (Figure 51).[67] With the appropriate Cp ligand, the authors could direct the reaction towards the (4+2) or the (4+1) cycloadduct, **155** and **156** respectively.

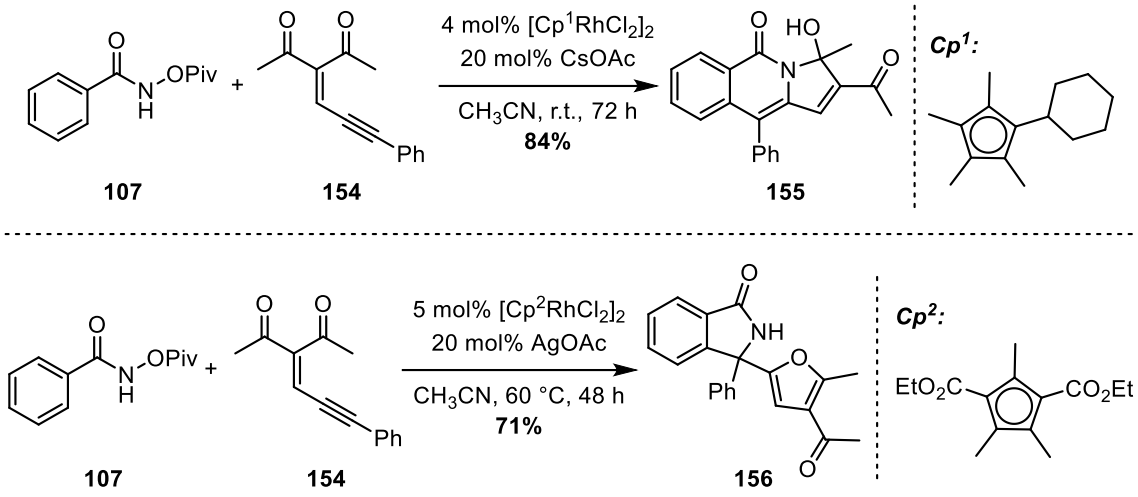

Figure 51: Rhodium-catalysed Csp^2–H functionalisation with enynones

The authors proposed that the formation of **155** involves a series of cyclisations after the first C–H bond functionalisation, as opposed to **156** which proceeds through the generation of a rhodium-carbene species.

After the generation of the pentarhodacycle **A**, the coordination of the enynone **154** affords the complex **B** (Figure 52). The nucleophilic attack of one of the oxygens gives the zwitterionic intermediate **C** which rearranges into the rhodium-carbene **D**. The furan **156** is released, along with the active catalyst, upon migratory insertion and reductive elimination of the metal.

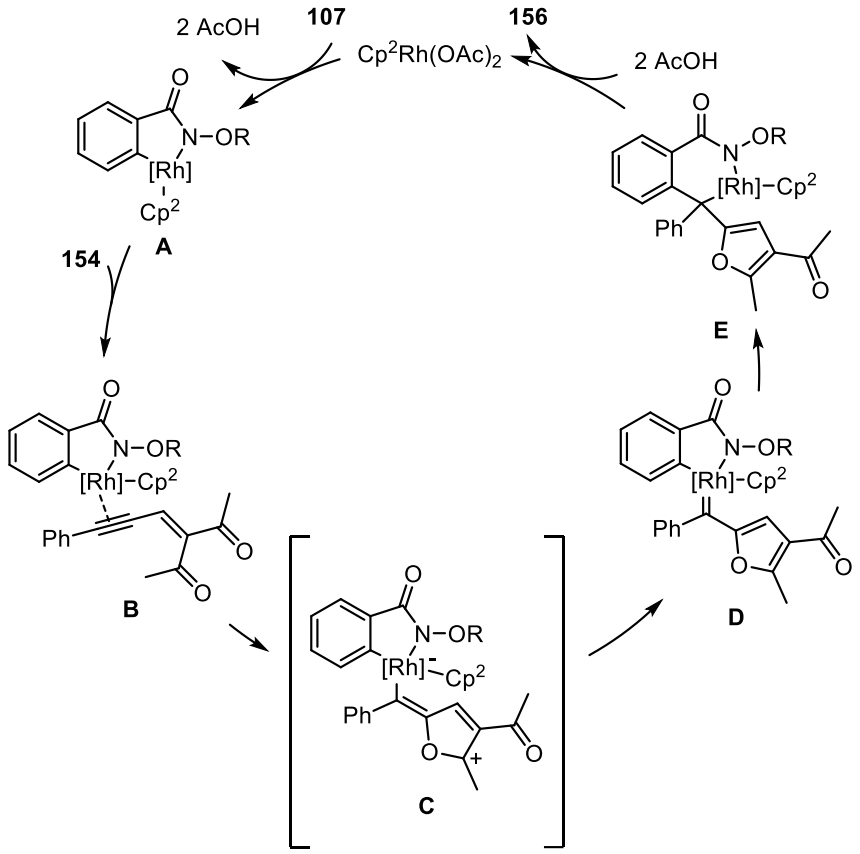

Figure 52: Mechanism for the rhodium-catalysed (4+1) cycloaddition with enynones

3.3 Hypothesis

The chemistry around sulfoxonium ylides has been well studied and those species have been used in various reactions. However, all metal catalysed reactions with sulfoxonium ylides relied on the generation of a metal-carbene species **A**, as depicted in the example below (Figure 53). Recently, Vaitla and co-workers reported the synthesis of the functionalised indole **158** through the iridium-catalysed C–N bond formation with sulfoxonium ylides.[68] Addition of aniline on the iridium-carbene intermediate **A**, gives the zwitterrionic intermediate **B** which transforms to **C** upon proto-demetalation. After generation of **D** with a second equivalent of aniline, the desired indole is obtained through a cyclisation/re-aromatisation sequence.

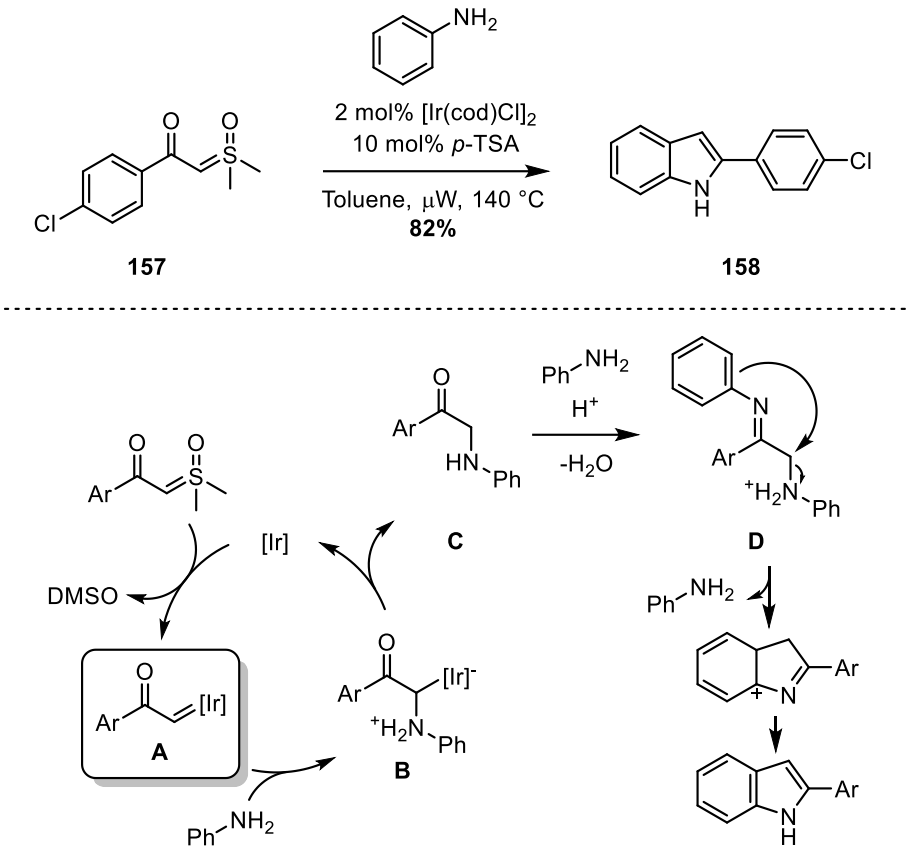

Figure 53: Iridium-catalysed synthesis of a functionalised indole

Although efficient and elegant, this methodology was expanded to the synthesis of pyrroles, it requires the use of activated coupling partners and is limited to C–N bond formation. As the direct functionalisation of Csp^2–H was not reported, we wanted to show that sulfoxonium ylides could be used for the rhodium (III)-catalysed cross-coupling reaction with C–H bonds, in a similar mechanism to the one described with diazo-compounds, triazoles and tosyl-hydrazones.

4 Cross coupling of sulfoxonium ylides with C–H bonds

4.1 Synthesis of sulfoxonium ylides

4.1.1 From esters

4.1.1.1 Sulfoxonium ylides synthesis from methyl esters

A seen in the introduction (Part 2.1.6), several α-ketosulfoxonium ylides have been prepared by reacting dimethylsulfoxonium methylide with a methyl ester. The carbene can be generated from either trimethylsulfoxonium chloride or the iodide salt. The latter shows decreased reactivity but is significantly cheaper than the chloride salt.

When the procedure was applied to selected ketosulfoxonium ylides, results did not appear as promising in comparison to those reported in the literature (Table 4). Traces of the pyridine derivative **167** were obtained, giving the sulfoxonium ylide in 3% yield (Table 4, entry **1**). A Boc-protected piperidine **168** was obtained in a significantly better yield of 26% (Table 4, entry **2**). The *gem*-diphenyl sulfoxonium ylide **169** was synthesised in average yield (Table 4, entry **3**). However, when α-β-unsaturated esters **162** and **164** were used, a complex mixture was obtained without significant traces of the desired product (Table 4, entry **4** and **6**). The same results were observed with the furyl ester **163** and the 1,4-ketoester **165** (Table 4, entry **5** and **7**). No reactivity was observed when the sulfonyl ester **166** was used (Table 4, entry **8**).

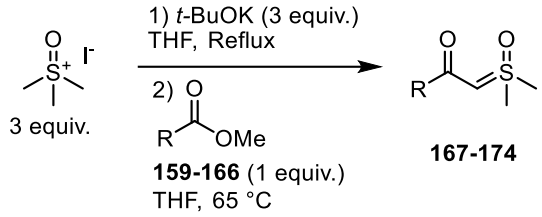

Entry	Ester	Yield	Entry	Ester	Yield
1	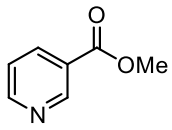 **159**	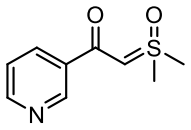 **167** **3%**	5	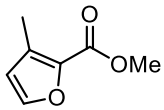 **163**	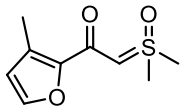 **171** **Decomposition**
2	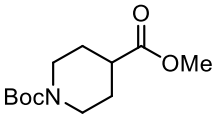 **160**	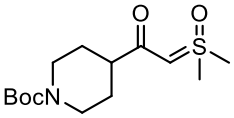 **168** **26%**	6	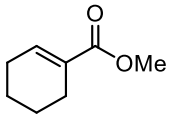 **164**	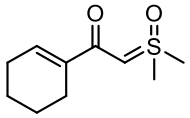 **172** **Decomposition**
3	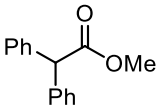 **161**	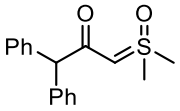 **169** **40%**	7	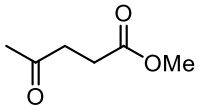 **165**	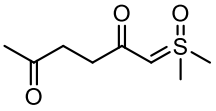 **173** **Decomposition**
4	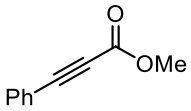 **162**	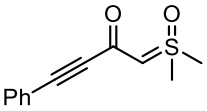 **170** **Decomposition**	8	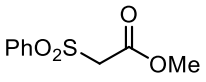 **166**	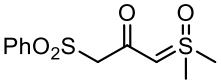 **174** **No Reaction**

Table 4: Synthesis of α-ketosulfoxonium ylides using methyl esters

It is worth mentioning that no reaction was observed when the ethyl ester **175** was reacted with dimethyl sulfoxonium methylide, even at elevated temperature (Figure 54).

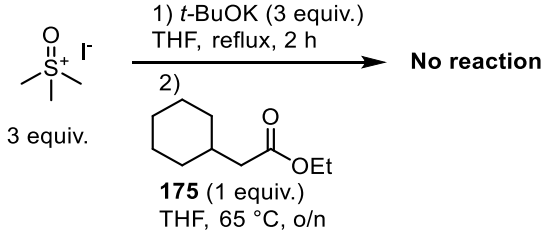

Figure 54: Synthesis of α-ketosulfoxonium ylides using an ethyl ester

4.1.1.2 Sulfoxonium ylides synthesis from *p*-nitrophenyl ester

In order to solve the issues of low reactivity often encountered with methyl esters, *para*-nitrophenyl esters have been used as an alternative.[30]

The better leaving group allowed the synthesis of various sulfoxonium ylides (Table 5). The esterification of the carboxylic acids gave the corresponding esters in good yields in all cases. The purification of those esters proved to be difficult in some cases, giving a mixture of the *p*-nitrophenol and the ester. Aromatic compounds were tolerated and gave **64**, **185** and **186** in 44%, 27% and 36% yield respectively, over the two steps (Table 5, entry **1**, **2** and **3**). Aliphatic groups could be transformed to the corresponding sulfoxonium ylides **187** and **188** in 71% and 66% yield (Table 5, entry **4** and **5**). The cyclopropane derivative **181** gave the desired sulfoxonium ylide **189** in 32% yield (Table 5, entry **6**). A benzylic group such as in **182** was well tolerated and afforded **190** in 70% yield (Table 5, entry **7**). Finally, the conjugated alkynyl substrate **183**, as well as the heterocycle **184**, gave complex mixtures without traces of the desired products (Table 5, entry **8** and **9**).

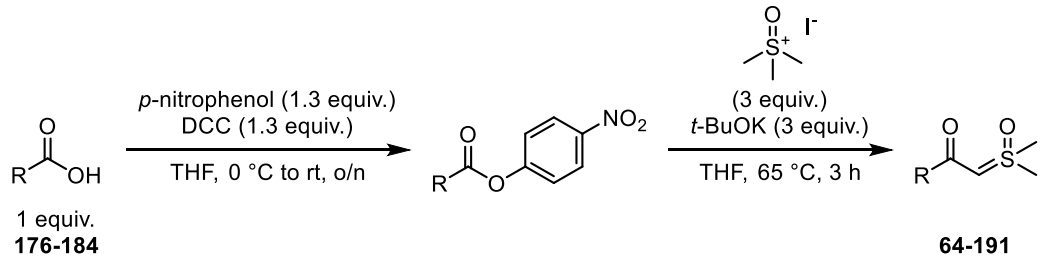

Entry	Carboxylic acid	Yield[a]	Entry	Carboxylic acid	Yield[a]
1	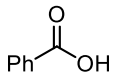	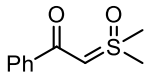	6	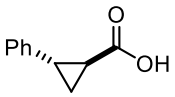	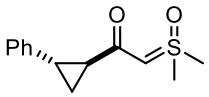
	176	**64** **44%**		**181**	**189** **32%**
2	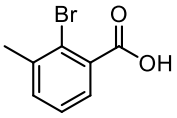	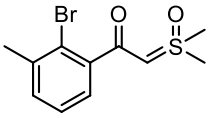	7	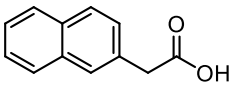	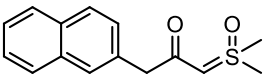
	177	**185** **27%**		**182**	**190** **70%**
3	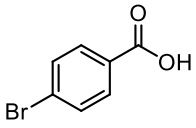	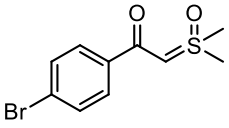	8	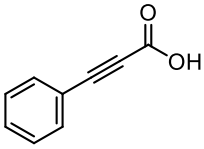	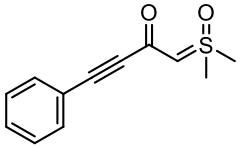
	178	**186** **36%**		**183**	**170** **Decomposition**
4	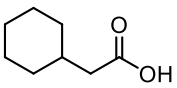	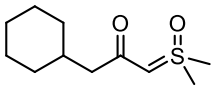	9	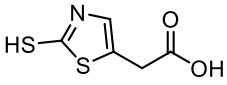	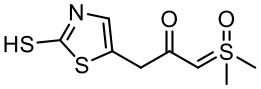
	179	**187** **71%**		**184**	**191** **Decomposition**
5	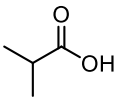	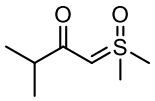			
	180	**188** **66%**			

a) Yields reported for the 2 steps.

Table 5: Synthesis of α-ketosulfoxonium ylides using *p*-nitrophenyl esters

4.1.2 From acyl chlorides

A possible alternative for the synthesis of sulfoxonium ylides is to start with the corresponding acyl chloride. Numerous acyl chlorides are commercially available,

often at low cost, allowing the rapid construction of a great library of sulfoxonium ylides. Finally, due to the great reactivity of acyl chlorides, the formation of the desired sulfoxonium ylide often requires only ten minutes as opposed to the reactions starting from *p*-nitrophenylesters (Table 6).

Thus, an interesting array of sulfoxonium ylides was obtained with acyl chlorides with among them, four other aromatic compounds. *Para*-substitution of the benzene ring with an eletron-donating functional group led to the synthesis of **203** in 19% yield (Table 6, entry **1**). It is worth mentioning that in this case, sodium *tert*-butoxide was used instead of the potassium salt. A chloro substituent in *ortho*-position of the benzene ring did not impede the reaction and the desired ylide **204** was isolated in 80% yield (Table 6, entry **2**). Moreover, bis-meta substituted acyl chlorides bearing electron withdrawing groups led to the corresponding sulfoxonium ylides **205** and **206** in 50% and 89% yield (Table 6, entry **3** and **4**). In order to assess the effect of the steric hindrance in the subsequent C–H bond activation, the bulky adamantyl derivative **207** was synthesised in almost quantitative yield (Table 6, entry **5**). Heteroaromatic acyl chlorides were well tolerated in this reaction and gave the furyl **208** and the thiophenyl **209** in good yields (Table 6, entry **6** and **7**). Surprisingly, the isoxazole **199** gave the corresponding ylide **210** in significantly lower results and the reaction of **200** led to the decomposition of the starting material without traces of the desired compound in the crude mixture (Table 6, entry **8** and **9**). The benzyl protected alcohol **201** was converted into the corresponding product **70** in good yield (Table 6, entry **10**). Finally, the chloroamide **202** led to no reaction upon treatment with the optimised conditions (Table 6, entry **11**).

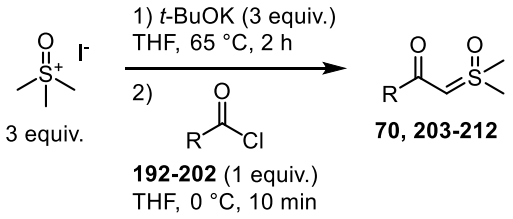

Entry	Acyl chloride	Yield	Entry	Acyl chloride	Yield
1	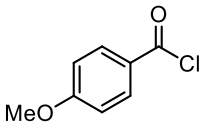 **192**	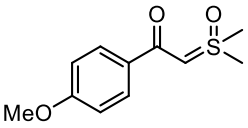 **203** **19%**	7	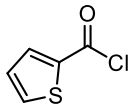 **198**	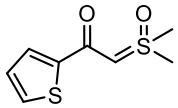 **209** **80%**
2	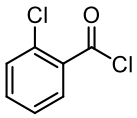 **193**	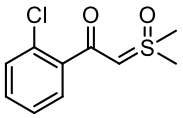 **204** **80%**	8	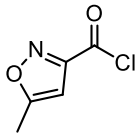 **199**	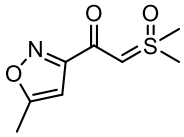 **210** **38%**
3	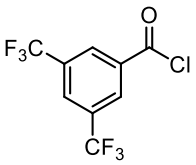 **194**	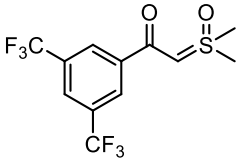 **205** **50%**	9	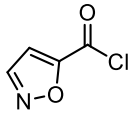 **200**	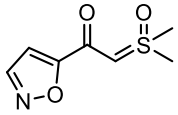 **211** **Decomposition**
4	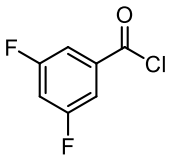 **195**	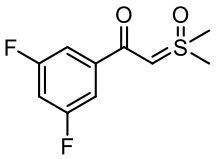 **206** **89%**	10	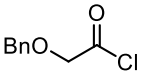 **201**	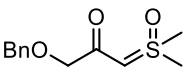 **70** **54%**
5	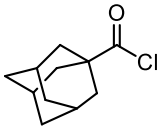 **196**	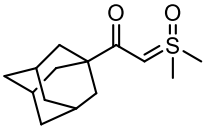 **207** **93%**	11	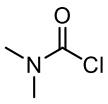 **202**	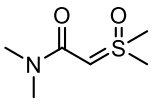 **212** **Decomposition**
6	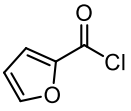 **197**	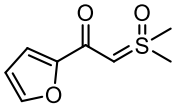 **208** **71%**			

Table 6: Synthesis of α-ketosulfoxonium ylides using acyl chlorides

4.1.3 Miscellaneous

In some cases, the use of other electrophiles was synthetically advantageous. Thus, acetic anhydride **213** gave the sulfoxonium ylide **214** in good yield (Figure 55).

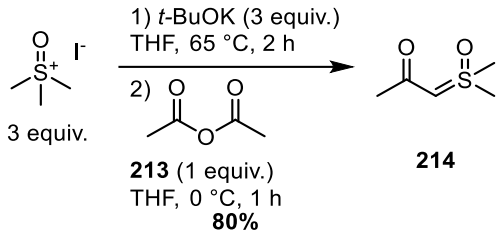

Figure 55: Synthesis of an α-ketosulfoxonium ylide using acetic anhydride

By reacting the phosphine oxide **215** in the classical conditions, the sulfoxonium ylide **216** bearing a phosphorus atom was synthesised in 25% yield (Figure 56). This example shows versatility of those carbene precursors.

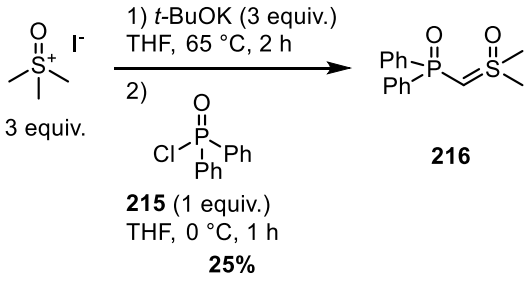

Figure 56: Synthesis of an α-phosphinylsulfoxonium ylide using a chloro-phosphine oxide

As seen in the introduction, pyrimidines have been used as electrophiles to generate several sulfoxonium ylides.[31] Those results could be reproduced to get **52** in average yield (Figure 57).

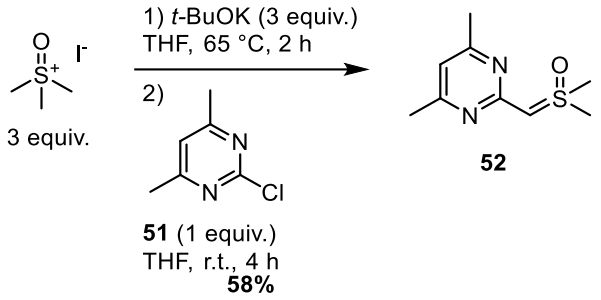

Figure 57: Synthesis of an of α-pyrimidylsulfoxonium ylide from a chloro-pyrimidine

4.1.4 Bis-substituted sulfoxonium ylides

When the pyrimidine sulfoxonium ylide **52** was reacted with the acyl chloride **217**, the chloroformate 2**19** or the isocyanate **49**, the corresponding highly substituted sulfoxonium ylides were recovered in low to good yield (Figure 58). The lack of reactivity observed with the isocyanate could be explained by the poor state of the starting material used.

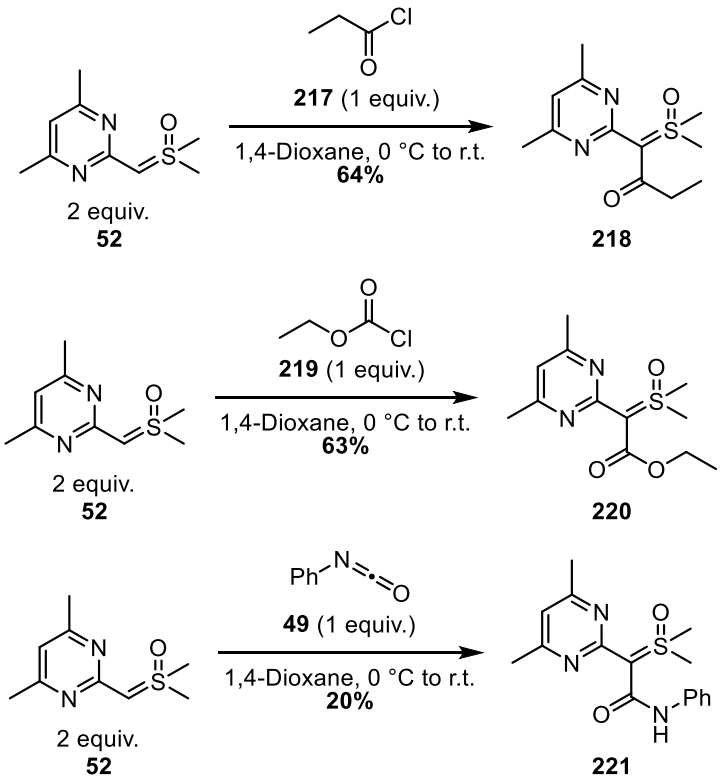

Figure 58: Bis-functionalisation of α-pyrimidylsulfoxonium ylides

As shown by the group groups of Metzger and Burtoloso, the direct alkylation of the methylide centre of a sulfoxonium ylide is not possible and leads instead to the formation of the *gem*-difunctionalised product **69**.[29] Thus, an alternative route had to be developed for the synthesis of alkyl-substituted α-ketosulfoxonium ylides.

Shea and Zhao reported the synthesis and application of diethylsulfoxonium ethylide **223** in the synthesis of co-polymers (Figure 59).[69]

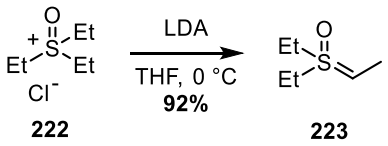

Figure 59: Synthesis of diethylsulfoxonium ethylide

We assured that the substituted sulfoxonium ylide **226** could be obtained upon reaction of diethylsulfoxonium ethylide **223** and the electrophile **192** (Figure 61). The synthesis of the triethylsulfoxonium chloride was completed in three steps starting from the diethyl sulfur **224** (Figure 60). Thus, triethylsulfur chloride **225** was obtained in quantitative yield after a nucleophilic attack of diethyl sulfur **224** on iodoethane followed by a halogen exchange with tri-butylbenzylammonium chloride. Oxidation with *m*-CPBA in basic media afforded the triethyl sulfoxonium ylide **222** in moderate yield.

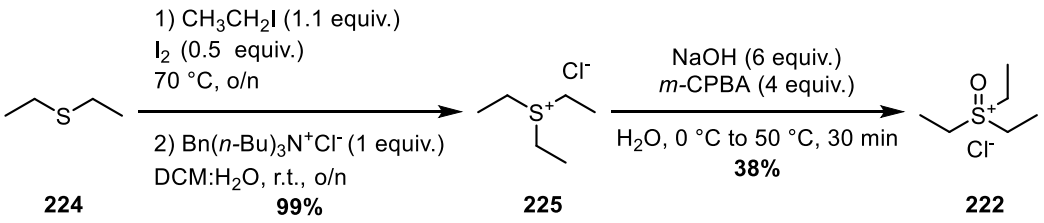

Figure 60: 3-steps synthesis of triethylsulfoxonium chloride

Following the general conditions developed with acyl chlorides, the diethylsulfoxonium ethylide **223** was generated *in-situ* with potassium *tert*-butoxide in THF at reflux (Figure 61). Slow addition of the *p*-methoxybenzoyl chloride **192** at low temperature gave the sulfoxonium ylide **226** in excellent yield.

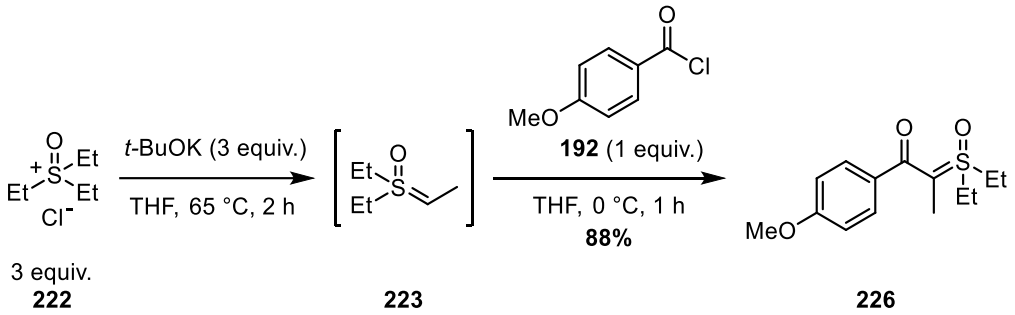

Figure 61: Synthesis of methyl-substituted sulfoxonium ylide

4.2 Transition-metal catalysed C–H bond functionalisation

4.2.1 Optimisation of the reaction conditions

4.2.1.1 Catalytic attempt

The investigation into the rhodium-catalysed C–H bond functionalisation using sulfoxonium ylides began by using Bolm's conditions with slight changes.[50] The hexarhodacycle **227** was obtained in 15% yield, based on the starting rhodium complex, when the sulfoxonium ylide **187** was treated with **128**, NaOAc, $[Cp^*RhCl_2]_2$ and AgOAc in 1,2-DCE (Figure 62). The complex **227** was characterised by ^1H NMR and ^{13}C NMR and the diastereomeric ratio was calculated based on the crude ^1H NMR.

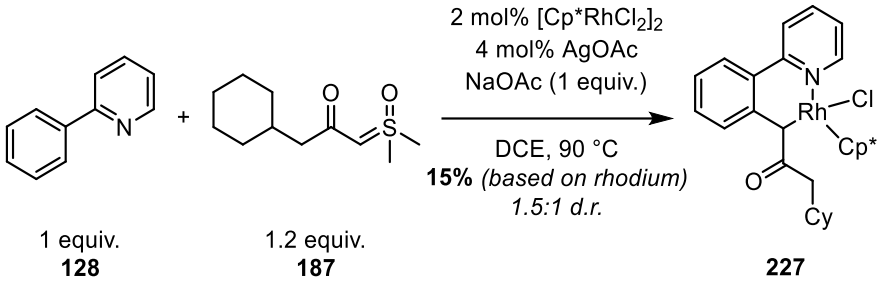

Figure 62: Catalytic attempt at the rhodium catalysed Csp^2–H bond functionalisation of phenylpyridine with a sulfoxonium ylide

This result was encouraging as it confirmed that the targeted C–C bond formation had occurred. However, the reaction was clearly not catalytic, and changes had to be made in order to close the catalytic cycle.

4.2.1.2 Stoichiometric attempts

In order to improve the understanding of the reaction, a step-wise approach of the mechanism was investigated. The C–H activated metallacycle **228** was prepared assuring that the lack of reactivity observed was not imputable to the first C–H activation. The desired pentarhodacycle was prepared in good yield upon reaction of the $[Cp^*RhCl_2]_2$ with the model substrate **128** in DCM with sodium acetate (Figure 63).[70]

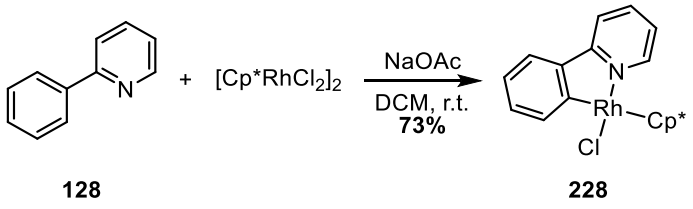

Figure 63: Synthesis of the five-membered rhodacycle with phenylpyridine

When the pentarhodacycle **228** was treated with the cyclohexyl sulfoxonium ylide **187** in 1,2-DCE, the hexarhodacycle **227** was isolated in low yield (Figure 64).

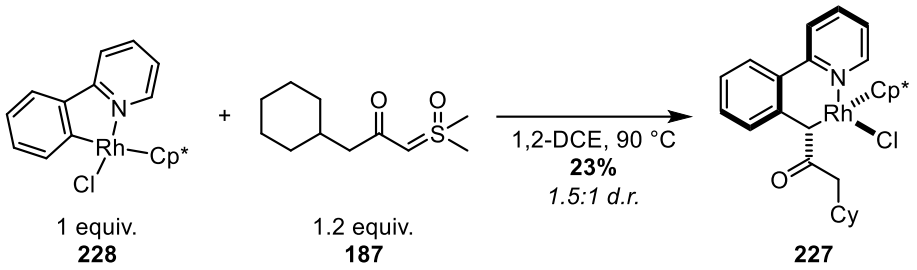

Figure 64: Stoichiometric attempt at the rhodium-catalyed Csp²–H bond functionalisiation of phenylpyridine with a sulfoxonium ylide

By looking at the proposed mechanisms of transition-metal catalysed C–H functionalisation using carbenes (See Figure 42, Section 3.1.1.2), one can understand that the problem observed in those attempts arises from the final catalytic step converting **E** to the desired product with regeneration of the active catalyst upon proto-demetalation (Figure 65).

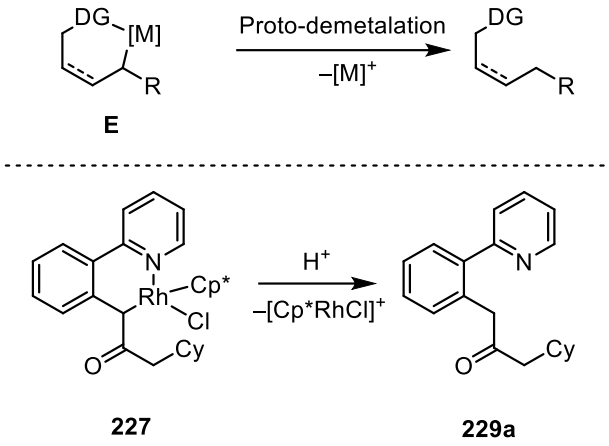

Figure 65: Hypothesis of the key-role of the solvent in the proto-demetalation elementary step

It was hypothesised that a proton source was needed in order to close the catalytic cycle. Acidic additives and protic solvents were investigated to induce a catalytic turnover.

4.2.1.3 Effect of the solvent

Unfortunately, nor the addition of trifluoroacetic acid (TFA), nor acetic acid, promoted the formation of the desired product (Table 7, entry **1** and **2**). It was hypothesised that ethanol at higher temperature could help the formation of the desired product. Indeed, traces of the functionalised phenyl pyridine were observed in the crude mixture, validating that protic solvent could close the catalytic cycle (Table 7, entry **3**). Thus, fluorinated solvent with better protic properties were investigated. The conversion increased to 37% when trifluoroethanol (TFE; pKa = 12.3) was used as the solvent (Table 7, entry **4**). [71] Changing the base from sodium acetate to potassium pivalate induced a decrease of conversion (Table 7, entry **5**). Finally, the best conversion was observed by using hexafluoroisopropanol (HFIP; pKa = 9.3) (Table 7, entry **6**). [72]

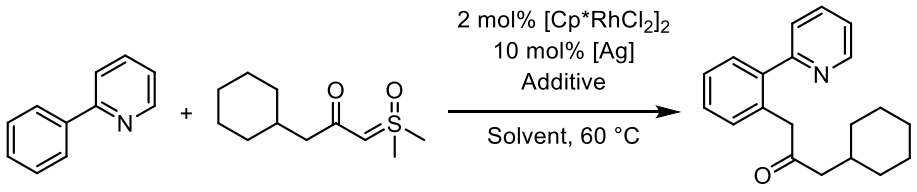

Entry[a]	Solvent	Co-catalyst	Additive	Conversion (%)[b]
1	DCE	10 mol% AgTFA	TFA (1 equiv.)	0
2	DCE	10 mol% $AgSbF_6$	AcOH (1 equiv.)	0
3[c]	EtOH	10 mol% $AgSbF_6$	/	7
4	TFE	10 mol% $AgSbF_6$	NaOAc (1 equiv.)	37
5	TFE	10 mol% $AgSbF_6$	PivOK (1 equiv.)	29
6	HFIP	10 mol%, AgOAc	NaOAc (1 equiv.)	63

a) All reactions were carried out with **128** (0.2 mmol), **187** (0.2 mmol), $[Cp^*RhCl_2]_2$ (0.004 mmol) except noted otherwise. *b)* determined by ^1H NMR of the crude mixture. *c*) using 2.5 mol% of $[Cp^*RhCl_2]_2$ at 100 °C.

Table 7: Solvent screening for the rhodium-catalysed Csp^2–H bond functionalisation of phenylpyridine with a sulfoxonium ylide

4.2.1.4 Effect of the silver co-catalyst

With the optimal solvent in hand, our focus was placed on the silver additive used to promote the formation of the active rhodium monomer. Following reaction conditions reported by Zhou and co-workers, a mixture of two silver sources was used, leading to similar results as those obtained with silver acetate (Table 8, entry **1** and **2**).[73] A significant increase of conversion was obtained using either silver tetrafluoroborate or hexafluoroantimonate (Table 8, entry **3** and **4**). Silver hexafluoroantimonate was used due to the availability of this additive in the laboratory.

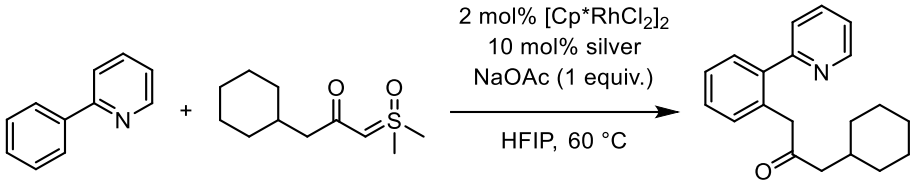

Entry[a]	Silver	Conversion (%)[b]
1	AgOAc	63
2[c]	$AgOAc/AgNTf_2$	64
3	$AgBF_4$	73
4	$AgSbF_6$	72

a) All reactions were carried out with **128** (0.2 mmol), **187** (0.2 mmol), $[Cp^*RhCl_2]_2$ (0.004 mmol) and NaOAc (0.2 mmol) in HFIP at 60 °C except noted otherwise. *b)* determined by ^1H NMR of the crude mixture. *c*) using 10 mol% of AgOAc and 10 mol% of $AgNTf_2$.

Table 8: Silver co-catalyst screening for the rhodium-catalysed Csp^2–H bond functionalisation of phenylpyridine with a sulfoxonium ylide

4.2.1.5 Effect of the stoichiometry

Although relatively high conversions were obtained in HFIP with silver hexafluoroantimonate, a significant part of unreacted starting material was recovered (Table 9, entry **1**). Interestingly, an almost linear increase of conversion was observed with the increase of the amount of sulfoxonium ylide, with 1.7 equivalent giving the optimum result (Table 9, entry **1**-**6**). Moreover, an inert atmosphere was not required to carry out the reaction to full conversion (Table 9, entry **7**). Finally, inverting the stoichiometry by using 2 equivalents of **128** for 1 equivalent of the sulfoxonium ylide **187** gave lower yield (Table 9, entry **8**).

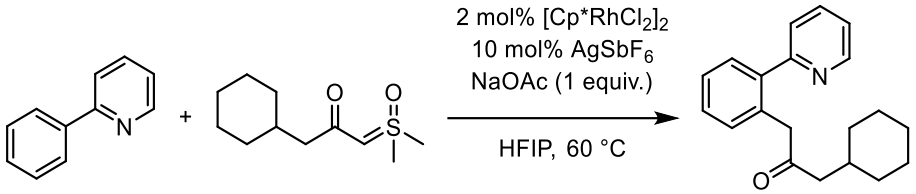

Entry[a]	X (equiv.)	Conversion (%)[b]
1	1	72
2	1.1	75
3	1.2	84
4	1.5	88
5	1.7	>99
6	2	>99
7[c]	1.7	>99
8[d]	1	70[e]

a) All reactions were carried out with **128** (0.2 mmol), $[Cp^*RhCl_2]_2$ (0.004 mmol), $AgSbF_6$ (0.02 mmol) and NaOAc (0.2 mmol) in HFIP at 60 °C except noted otherwise. *b)* determined by ^1H NMR of the crude mixture. *c*) under air. *d*) with **128** (0.4 mmol) and **187** (0.2 mmol). *e*) isolated yield.

Table 9: Effect of the stoichiometry on the rhodium-catalysed Csp^2–H bond functionalisation of phenylpyridine with a sulfoxonium ylide

4.2.1.6 Effect of the base

As reported previously the use of a base can have a significant impact on the outcome of the reaction. When potassium pivalate was used instead of sodium acetate the conversion significantly decreased (see Table 7 entry **4** and **5**). Thus, the effect of the base loading was investigated with three different sulfoxonium ylides **187**, **188** and **64**. In the case of the cyclohexyl-substituted sulfoxonium ylide **187**, no effect of the base on the conversion was observed (Table 10, **1** and **2**). However, an increase of

conversion was seen with the increase of the amount of sodium acetate used in the case of **188** (Table 10, entry **3**, **4**, and **5**). Finally, no significant effect of the base on the reaction was observed with the phenyl-substituted sulfoxonium ylide **64** and excellent conversions were thus obtained with or without sodium acetate (Table 10, entry **6** and **7**).

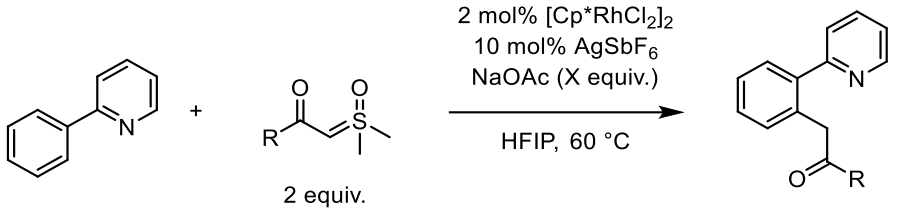

128

187 (R = CH_2Cy)
188 (R = *i*-Pr)
64 (R = Ph)

229a (R = CH_2Cy)
229b (R = *i*-Pr)
229c (R = Ph)

Entry[a]	Sulfoxonium ylide	X (equiv.)	Yield (%)[b]
1[c]	**187**	1	99
2[c]	**187**	0	99
3	**188**	1	77
4	**188**	0.2	61
5	**188**	0.5	71
6[c]	**64**	1	99
7[c]	**64**	0	95

a) All reactions were carried out with **128** (0.2 mmol), **sulfoxonium ylide** (0.4 mmol), $[Cp^*RhCl_2]_2$ (0.004 mmol), $AgSbF_6$ (0.02 mmol) in HFIP at 60 °C except noted otherwise. *b)* isolated yield. *c*) 1.7 equiv. of **sulfoxonium ylide**.

Table 10: Base screening for the rhodium-catalysed Csp^2–H bond functionalisation of phenylpyridine with sulfoxonium ylides

4.2.1.7 Control experiments

Finally, a series of control experiments were run in order to prove that all species were required for the direct C–H functionalisation of phenyl pyridine **128** with the sulfoxonium ylide **187**. Removing the silver co-catalyst from the reaction decreased significantly the isolated yield, but good conversion was still obtained (Table 11, entry **1**). Moreover, decreasing the amount of rhodium and silver catalysts almost halved the conversion (Table 11, entry **2**). Removing the catalyst completely stopped the reaction, which shows that it is indeed catalysed by rhodium (Table 11, entry **3**). Finally, changing the rhodium catalyst for an iridium, a cobalt or a ruthenium catalyst did not give any reactivity (Table 11, entry **4**, **5**, **6** and **7**).

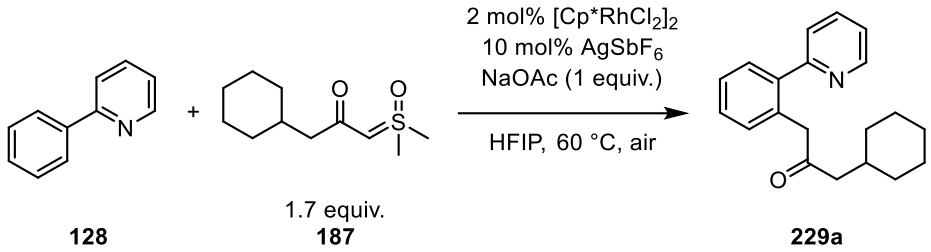

Entry[a]	Variations to standard conditions	Conversion (%)[b]
1	No $AgSbF_6$	81
2	1 mol% [Rh], 5 mol% Ag	58
3	No $[Cp^*RhCl_2]_2$	0
4	$[Cp^*IrCl_2]_2$ instead of [Rh]	0
5	$[Cp^*CoI_2]_2$ instead of [Rh]	0
6	$[Cp^*Co(CO)_2I]_2$ instead of [Rh]	0
7	$[Ru(p\text{-cymene})Cl_2]_2$ instead of [Rh]	0

a) All reactions were carried out with **128** (0.2 mmol), **187** (0.4 mmol), $[Cp^*RhCl_2]_2$ (0.004 mmol), $AgSbF_6$ (0.02 mmol) and NaOAc (0.2 mmol) in HFIP at 60 °C except noted otherwise. *b)* determined by ^1H NMR of the crude mixture.

Table 11: Control experiments for the rhodium-catalysed Csp^2–H bond functionalisation of phenylpyridine with a sulfoxonium ylide

Those optimised conditions were used with all the prepared sulfoxonium ylides in order to assess the scope of the cross-coupling of C–H bonds with sulfoxonium ylides.

4.2.2 Scope of the reaction

4.2.2.1 Sulfoxonium ylide

Pleasingly, excellent yields were obtained with many sulfoxonium ylides (Figure 66). The cyclopropyl derivative **229a** was obtained in quantitative yield while the bulkier isopropyl coumpound **229b** was isolated in lower yield. Moreover, in this case the amount of sulfoxonium ylide had to be increased to 2 equivalents in order to reach full conversion of the phenyl pyridine. *Para*-substituted arenes with both an electron-withdrawing or an electron-donating group underwent the reaction smoothly to give **229d** and **229e**, respectively. However, electron-poor arenes gave slightly decreased yield and the amount of sulfoxonium ylide had to be increased to 2 equivalents, as observed with **229f**. Heteroarene sulfoxonium ylides could undergo the reaction well when an extended reaction time was applied, as shown with **229g** and **229h**. Finally, the cyclopropane derivative **229i**, the adamantyl **229j** and the Boc-protected piperidine **229k** afforded the desired products in 90%, 89% and 86% yield respectively.

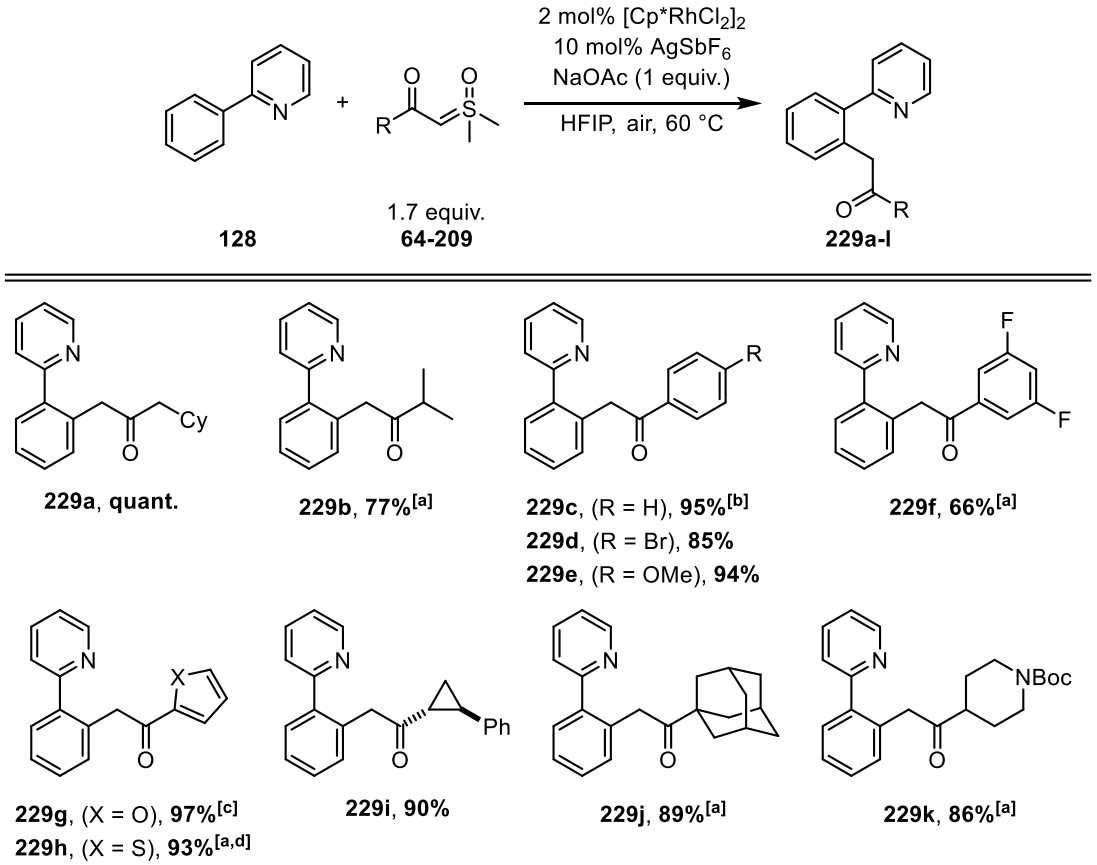

All reactions were carried out with **128** (0.2 mmol), **sulfoxonium ylide** (0.34 mmol), $[Cp^*RhCl_2]_2$ (0.004 mmol), $AgSbF_6$ (0.02 mmol) and NaOAc (0.2 mmol) in HFIP at 60 °C under air except noted otherwise. All the yields are for isolated products. *a*) 2 equiv. of **sulfoxonium ylide** were used. *b)* No NaOAc. *c)* Reaction stirred for 48 h. *d)* Reaction stirred for 24 h.

Figure 66: Scope of the rhodium-catalysed Csp^2–H bond functionalisation of phenylpyridine with sulfoxonium ylides

Interestingly, when the sulfoxonium ylide **190** was used, no traces of the desired functionalised phenyl pyridine were obtained, and **230** was recovered in low yield as the sole regioisomer (Figure 67). The same outcome was observed with **169** which gave traces of the functionalised pyridine **229l** and the cycloadduct **231** as the major product.

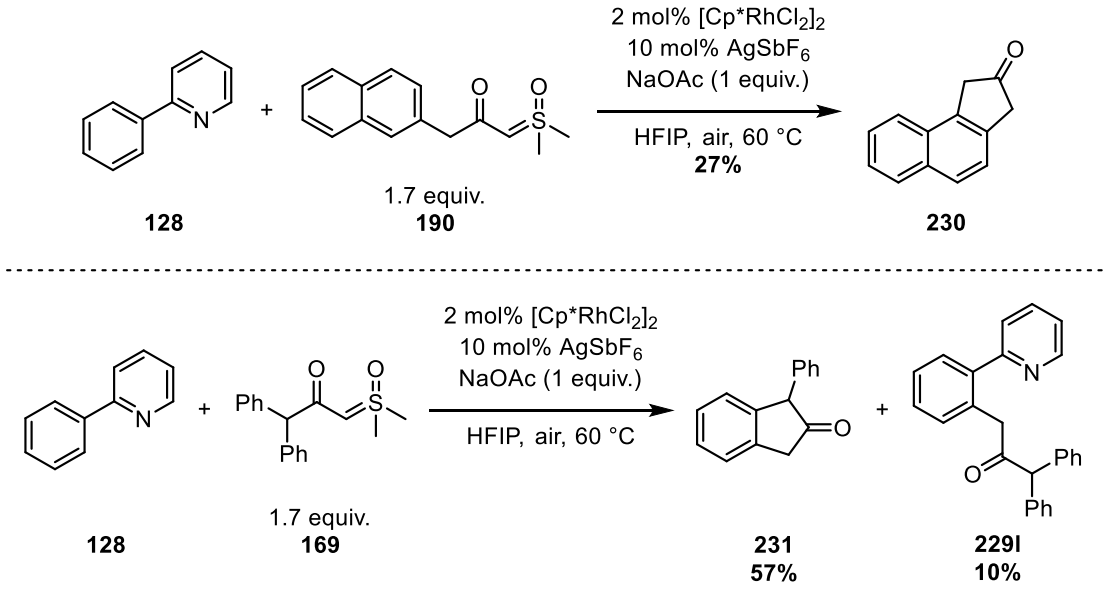

Figure 67: Cyclisation of sulfoxonium ylides

Although unexpected, this reaction was interesting and further investigation in the optimisation of the reaction conditions was started (Figure 68). Removing both catalysts, as well as the phenyl pyridine, gave the bicyclic compound **231** in 70% yield. This project was given to another student from the group for further optimisation.

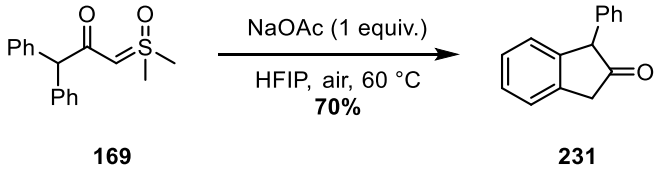

Figure 68: Optimisation of the rhodium-catalysed cyclisation of sulfoxonium ylides

Unfortunately, several sulfoxonium ylides were not suitable for the C–H functionalisation reaction. *Ortho*-substitution of the arene ring with a halogen atom was detrimental and no reaction was observed with the two sulfoxonium ylides **185** and **204** (Figure 69). The two heteroaromatic rings bearing a nitrogen atom, **167** and **210**, led to the same outcome, probably due to an inhibiting coordination from the nitrogen atom to the metal. Reacting the phosphosulfoxonium ylide **216** also led to no

reaction. Finally, both the keto- and ester-substituted sulfoxonium ylides with a pyrimidine group **218** and **220** gave no reaction under the optimised conditions.

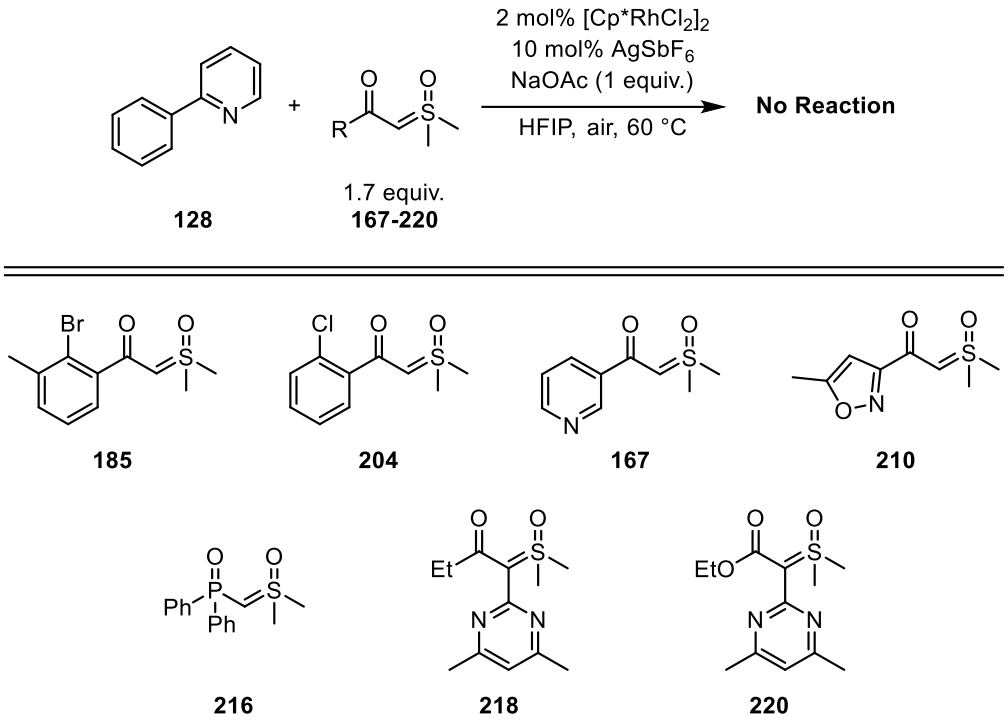

All reactions were carried out with **128** (0.2 mmol), **sulfoxonium ylide** (0.34 mmol), $[Cp^*RhCl_2]_2$ (0.004 mmol), $AgSbF_6$ (0.02 mmol) and NaOAc (0.2 mmol) in HFIP at 60 °C under air except noted otherwise.

Figure 69: Limitations regarding the scope of sulfoxonium ylides suitable for the rhodium-catalysed Csp^2–H bond functionalisation

As opposed to the two pyrimidine sulfoxonium ylides **218** and **220**, the substituted amide sulfoxonium ylide **221** gave the fully aromatic tetracyclic compound **232** in low yield (Figure 70). After a first C–H bond functionalisation, a cyclisation occurs to release **232**, along with aniline. This reaction relates to that reported by Glorius *et al.* on their work with triazoles as carbene precursors.[58] However, regardless of all efforts the yield of this cyclisation remained low.

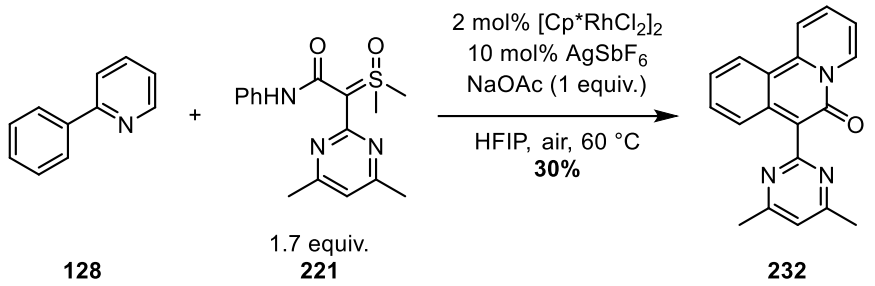

Figure 70: Rhodium-catalysed Csp^2–H bond functionalsiation/cyclisation of phenylpyridine with a α-pyrimidyl-α-amidosulfoxonium ylide

The methyl substituted sulfoxonium ylide **226** generated from the diethylsulfoxonium ethylide reacted with the phenylpyridine to give the corresponding cycloadduct **229m** in average yield (Figure 71). Moreover, the amount of sulfoxonium ylide, the temperature and the reaction time had to be increased in order to obtain full conversion, leading to the formation of a lot of side-products. A pure fraction of the product could not be isolated, thus the reported yield was based on ^{1}H NMR with an internal standard.

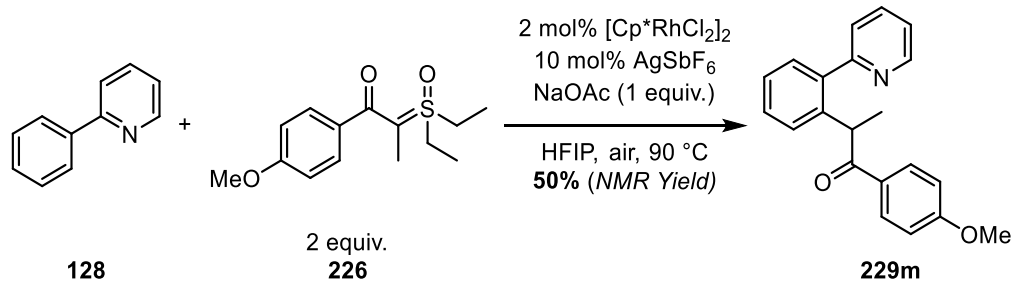

Figure 71: Rhodium-catalysed Csp^2–H bond functionalisaiton of phenylpyridine with a methyl-substituted sulfoxonium ylide

4.2.2.2 Csp^2–H bond scope

Whilst the conditions proved to be general with respect to the sulfoxonium ylide, the functionalisation of other Csp^2–H bonds was investigated (Figure 72). The first attempts were directed towards substituted arenes bearing electron-donating or -withdrawing groups. Interestingly, a mixture of unseparable regioisomers **233a** and **233b** were obtained with the methoxy-substituted arene in a 2.5:1 ratio. However, a completely regioselective functionalisation occurred with the electron-poor arene and **234** was isolated in good yield with two equivalents of sulfoxonium ylide at 90 °C. Increasing both the temperature and the amount of sulfoxonium ylide did not allow the improvement of the results obtained with electron-rich arenes.

Heteroaromatic rings were well tolerated in the reaction and the functionalised indole **235** was isolated in good yield. The pyrrole derivative was successfully functionalised with the isopropyl-substituted sulfoxonium and **236** was recovered in 75% yield. However, a mixture of mono- and bis-substituted pyrrole, **237** and **238**, was obtained with the furyl-substituted sulfoxonium. Surprisingly, the cross-coupled furylpyridine **239** was recovered in good yield as the sole regioisomer. Finally, the functionalised pyridinone **240** was isolated in 71% yield at higher temperature when using the pre-formed rhodium catalyst [Cp*Rh$(OAc)_2$•H_2O].

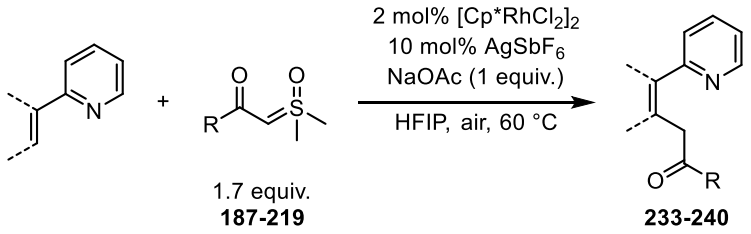

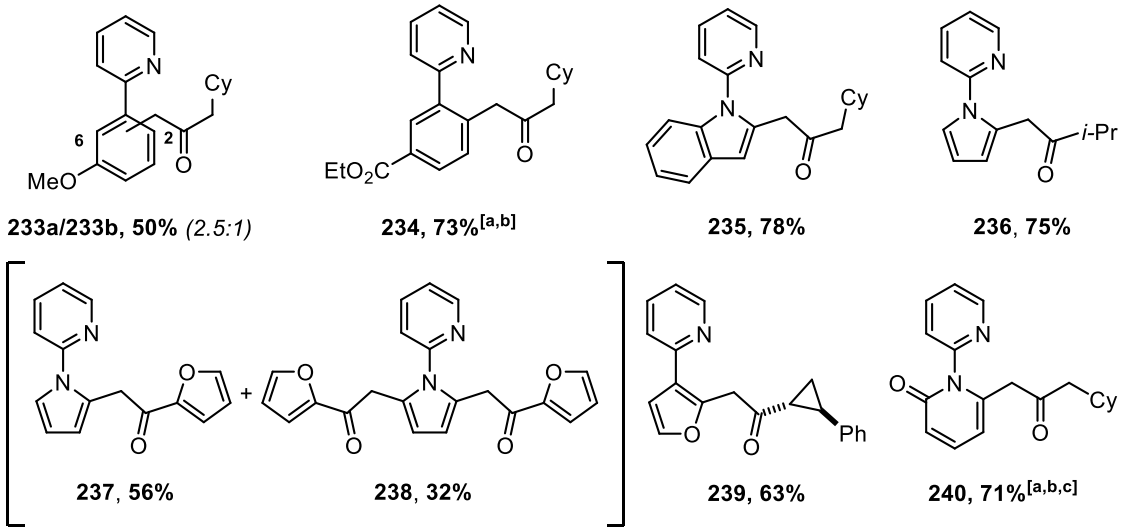

All reactions were carried out with **substrate** (0.2 mmol), **sulfoxonium ylide** (0.34 mmol), $[Cp^*RhCl_2]_2$ (0.004 mmol), $AgSbF_6$ (0.02 mmol) and NaOAc (0.2 mmol) in HFIP at 60 °C under air except noted otherwise. All the yields are for isolated products. *a*) 2 equiv. of ylide were used. *b)* at 90 °C. *c*) 8 mol% of $[Cp^*Rh(OAc)_2 \cdot H_2O]$ were used.

Figure 72: Scope of the rhodium-catalysed Csp^2–H bond functionalisation of pyridyl-arenes with sulfoxonium ylides

4.2.2.3 Directing groups

4.2.2.3.1 Quinoline

Although highly interesting as model substrates in order to optimise reaction conditions, pyridine is not the most useful directing group with respect to a possible application of the products of C–H functionalisation in synthesis. Thus, the investigation of other functionalities capable of directing the C–H activation was required. The quinoline **241** proved to be efficient in the reaction and gave the desired functionalised product in good to quantitative yields (Figure 73). Interestingly, whilst

242b and **242c** were obtained quantitatively, a significant decrease of yield was observed with the cyclohexyl-substituted sulfoxonium ylide **187**, as compared to the result obtained with phenylpyridine **128**.

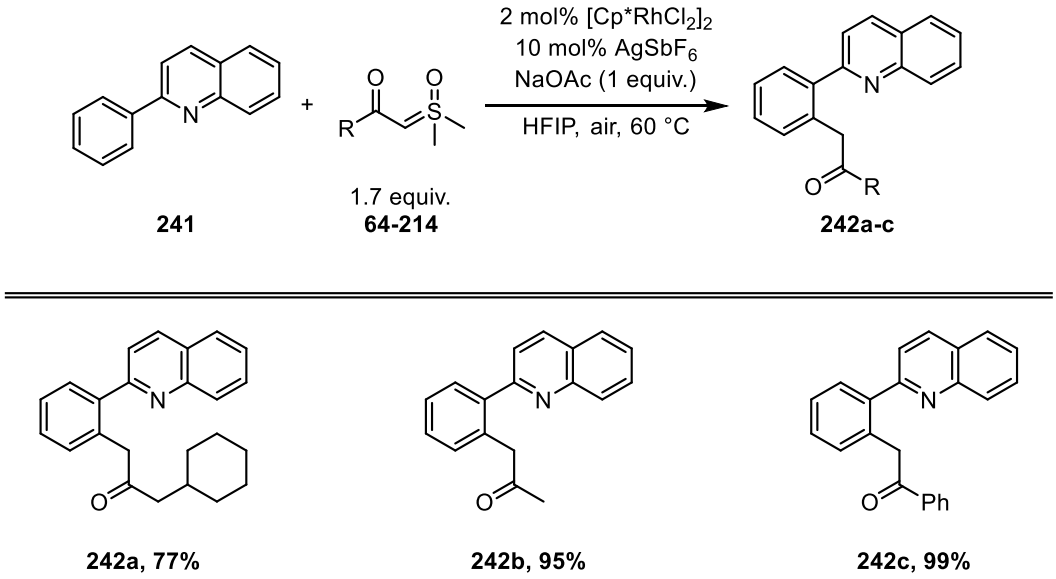

All reactions were carried out with **241** (0.2 mmol), **sulfoxonium ylide** (0.34 mmol), $[Cp^*RhCl_2]_2$ (0.004 mmol), $AgSbF_6$ (0.02 mmol) and NaOAc (0.2 mmol) in HFIP at 60 °C under air except noted otherwise. All the yields are for isolated products.

Figure 73: Scope of the rhodium-catalysed Csp²–H bond functionalisation of quinolinyl-arenes with sulfoxonium ylides

4.2.2.3.2 N-methoxybenzamide

N-functionalised-benzamides have been extensively used as directing groups in metal-catalysed C–H activation.[46] After a C–H functionalisation of the *ortho*-position, a cyclisation can occur leading to the formation of substituted isoquinolinones (Figure 74). Unfortunately, no reaction occurred when the optimised conditions were used. However, moderate yields were obtained when the pre-made rhodium acetate monomer was used as catalyst. Whilst the sulfoxonium ylide **187** gave the corresponding isoquinolinone **244a** in 59% yield as the only product,

chemoselectivity issues arised with the phenyl derivative **64**. In this case, both the isoquinolinone **244b** and the isocoumarin **245** were isolated.

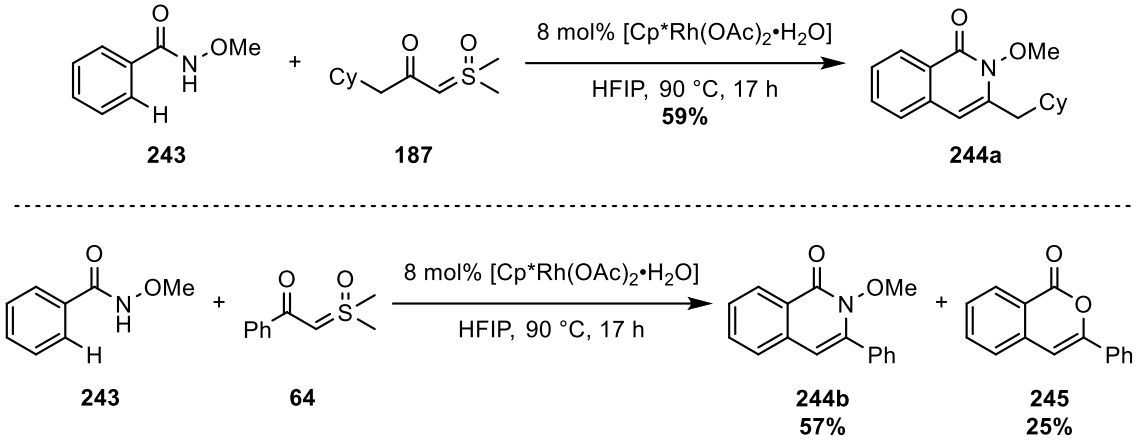

Figure 74: Rhodium-catalysed Csp^2–H bond functionalisation of *N*-methoxybenzamide with sulfoxonium ylides

Regardless of this selectivity issue, both products are interesting heterocycles with possible biological properties (Figure 75). The isoquinolinone **246** has been reported to have anti-viral activity, while the isocoumarin **247** showed great MptpB inhibition properties which is key in the treatment of tuberculosis.[74, 75, 76]

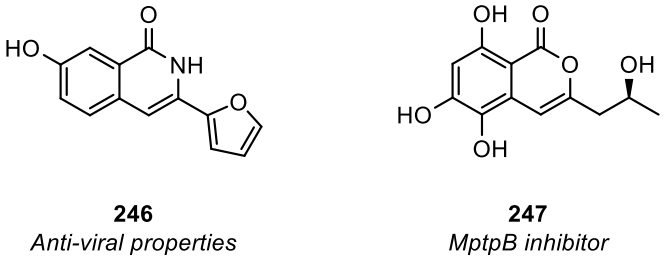

246
Anti-viral properties

247
MptpB inhibitor

Figure 75: Biological properties of isoquinolinone and isocoumarin

4.2.2.3.3 O-*methyloximes*

In their pioneering work on metal-catalysed C–H bond functionalisation with carbenoids, Yu and co-workers showed that methylated oxymes can efficiently direct the reaction.[45] As was the case with the *N*-methoxybenzamide **243**, no reaction was

observed when subjecting the methyl oxime **102** to the optimised conditions. The same outcome was obtained with the [Cp*Rh(OAc)$_2$•H$_2$O]. Changing to the cationic rhodium monomer, [Cp*Rh(MeCN)$_3$](SbF$_6$)$_2$, allowed the synthesis of **248** in excellent yield (Figure 76).

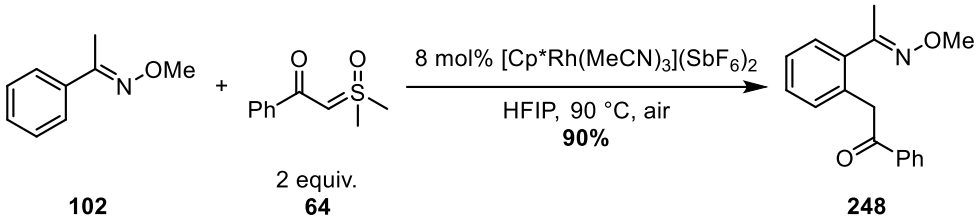

Figure 76: Rhodium-catalysed Csp^2–H bond functionalisation of *N*-methoxybenzamide with sulfoxonium ylide

4.2.2.4 Limitations

As seen in this section, the extension of the reaction to other directing groups was not as trivial as expected and led in many cases to a complete absence of reactivity. All the directing groups that failed to promote the reaction are depicted below (Figure 77).

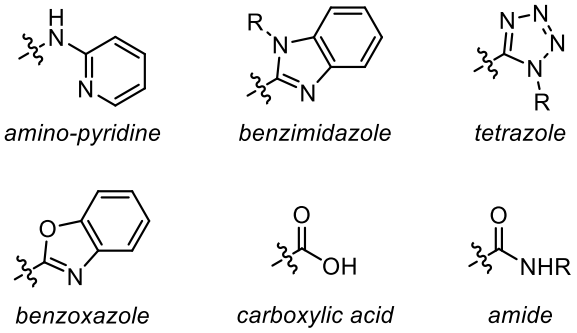

Figure 77: Limitations regarding the scope of directing groups suitable for the rhodium-catalysed Csp^2–H bond functionalisation with sulfoxonium ylides

However, another student from the group showed that pyrimidines and pyrazoles were suitable for this reaction when both the amount of sulfoxonium ylide

and the temperature were increased (Figure 78). Average to quantitative yields were obtained and the scope was thus extended.

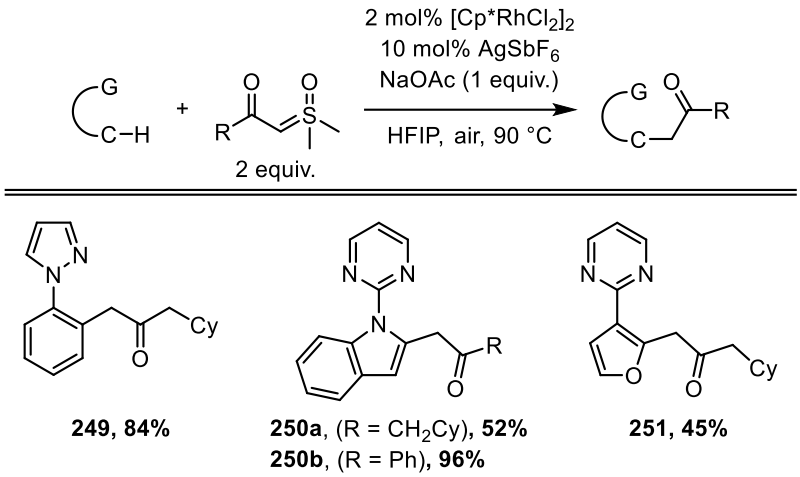

Figure 78: Rhodium-catalysed Csp^2–H bond functionalisation with pyrazyl-/pyrimidyl-arenes and sulfoxonium ylides

4.3 Further functionalisation

4.3.1 Cleavage of the directing group

As mentioned previously, pyridine groups are not the most interesting functional groups for synthetic applications. Thus, cleavage of the directing group was required to offer new possibilities of functionalisation.

Ackermann and co-workers have reported the straightforward cleavage of pyridine from indoles.[77] By reacting the *N*-functionalised indole **252** with methyltriflate, the authors could generate the pyridinium species **253** which could undergo a platinum-catalysed hydrogenolysis with ammonium formate as the hydrogen source (Figure 79). No purification was required between the two steps and the cleaved product **254** was obtained in excellent yield.

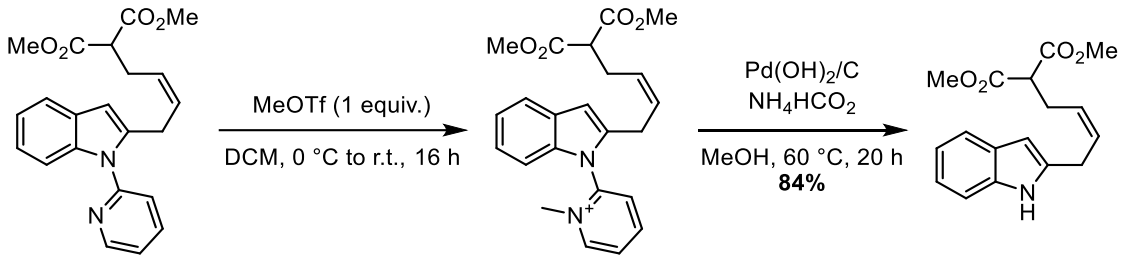

Figure 79: Cleavage of the pyridyl directing group *via* quaternisation/hydrogenolysis

Unfortunately, only traces of the desired cleaved pyridine **255** were isolated when those conditions were applied to the pyrrole **236** (Figure 80). As the crude mixture showed a significant amount of impurities, an attempt at room temperature was carried out, which led to the same outcome.

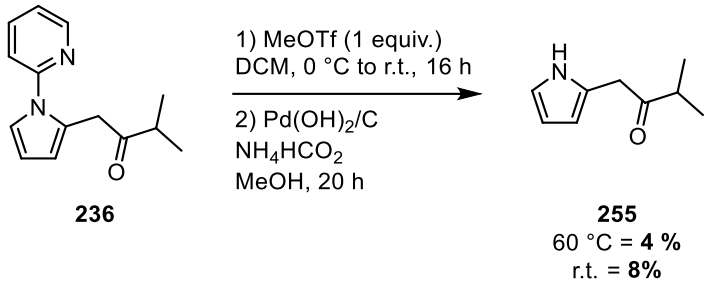

Figure 80: Attempts at the cleavage of the pyridyl directing group *via* quaternarisation/hydrogenolysis

A similar approach to the cleavage of pyridine was reported by Maes *et al.* whereby the quaternarised pyridine **257** could be removed by action of sodium borohydride (Figure 81).[78] The piperidine **258** was obtained in 77% yield in this one-pot sequence.

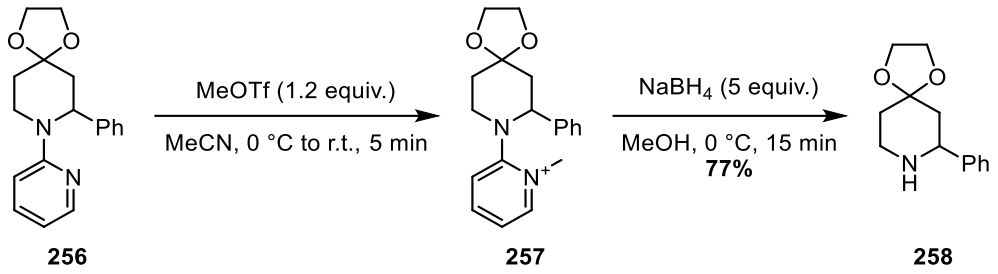

Figure 81: Cleavage of the pyridyl directing group *via* quaternisation/hydrogenolysis

When those conditions were applied to the protected indole **259**, the cleaved product **260** was obtained in low yield (Figure 82).

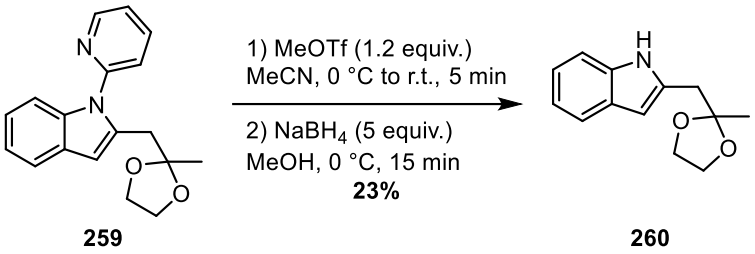

Figure 82: Attempts at the cleavage of the pyridyl directing group *via* quaternarisation/hydrogenolysis

The cleavage of the pyridine failed in our hand, thus, the incorporation of the directing group into the final product was investigated.

4.3.2 Hydrogenation

Logothetis reported the transformation of the pyridine **261** into the tetracycle **262** in 81% yield after hydrogenation of the aromatic ring to the piperidine (Figure 83).[79] Interestingly, protection of the carbonyl was not required.

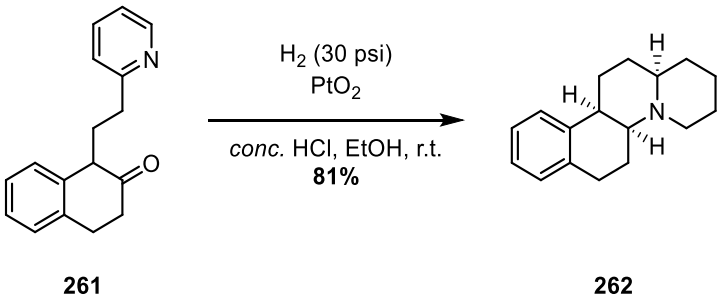

261 **262**

Figure 83: Platinum-catalysed hydrogenation of a pyridine ring followed by cyclisation

Applying this methodology to the functionalised phenyl pyridines could give access to interesting tricyclic compounds. However, no traces of the desired product were observed when the cyclohexyl **229a**, the isopropyl **229b** or the methyl **229n** derivatives were sujected to the hydrogenation (Figure 84).

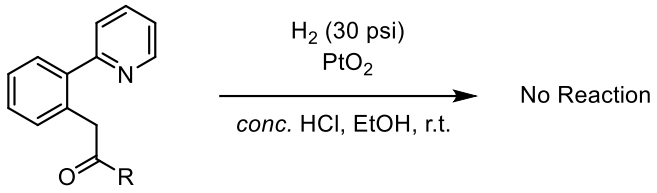

229a, (R = CH_2Cy)
229b, (R = *i*-Pr)
229n, (R = Me)

Figure 84: Attempt at the platinum-catalysed hydrogenation of pyridine rings followed by cyclisation

When those conditions were applied to the hydrogenation of the quinoline derivative **242b**, the 4,5,6,7-tetrahydroquinoline **263** was obtained in 47% yield (Figure 85). The ketone was also reduced to the corresponding alcohol during the reaction. This process proved not to be synthetically useful due to the lack of control.

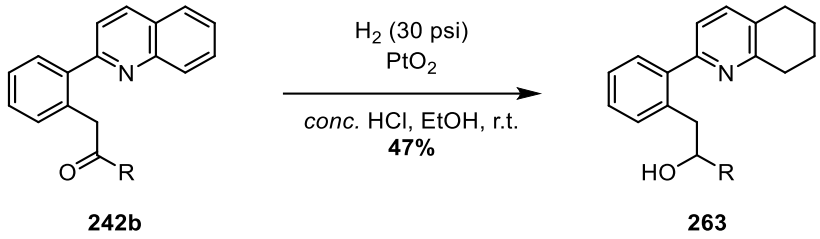

Figure 85: Attempt at the platinum-catalysed hydrogenation of the quinoline ring

Such a reactivity was reported by McEachern and co-workers where the hydrogenation of the substituted quinoline **264** led to the corresponding 1,2,3,4- and 4,5,6,7-tetrahydroquinolines **265** and **266** respectively (Figure 86).[80] In all their example the 4,5,6,7-tetrahydroquinoline **266** was the major product.

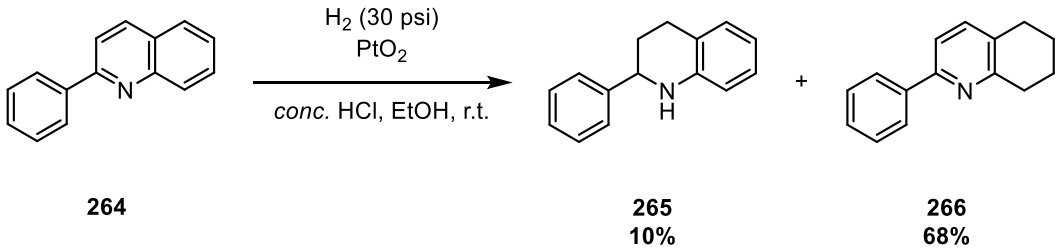

Figure 86: Selectivity of the platinum-catalysed hydrogenation of quinolines

As none of the hydrogenation conditions proved to be adequate for further functionalisation, another methodology was investigated.

4.3.3 Nickel-catalysed hydride transfer

In 2011, Knochel and his group used a nickel-catalysed transfer of hydrides to access the 1,2,3,4-tetrahydroquinoline **268** that bears an alcohol group (Figure 87).[81] By mixing nickel chloride with an excess of sodium borohydride, the authors isolated **268** in excellent yield. Moreover, Li and co-workers used the same approach to

transform the quinoline **269** with a carbonyl group to the tricyclic compound **270** in good yield.[82] The alcohol **271** was also recovered as a side product in low yield.

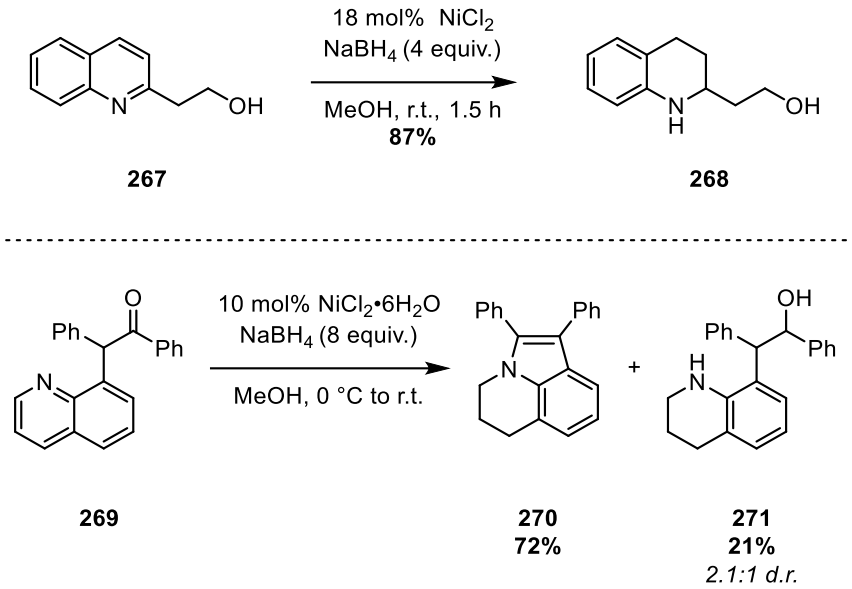

Figure 87: Nickel-catalysed hydrogenation of quinoline / Nickel-catalysed hydrogenation followed by cyclisation

These conditions were applied to the cyclisation of the two quinoline derivatives **242a** and **242b** (Figure 88). A complex mixture of products was obtained with the cyclohexyl starting material **242a**. However, when **242b** was treated under the same conditions, the desired tetracyclic product **272** was obtained in traces amount. Unfortunately, the yield could not be improved, and other functionalisation procedures were investigated.

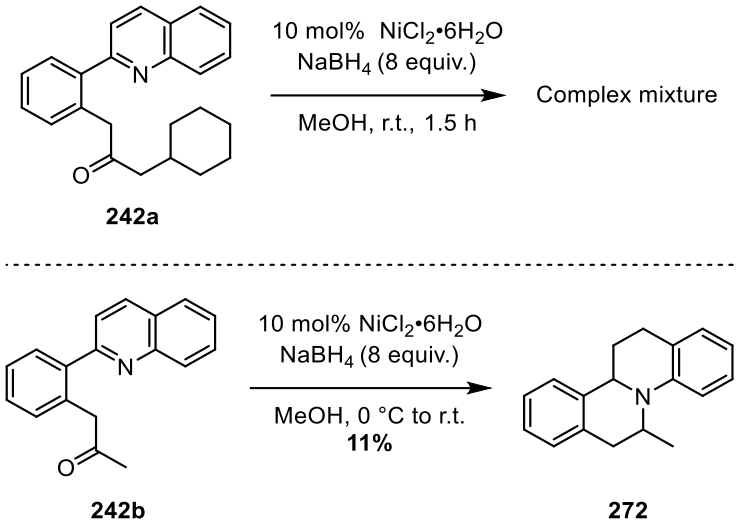

Figure 88: Attempts at the nickel-catalysed hydrogenation of quinolines

4.3.4 Hydrogen-transfer

In 2011, Rueping and Hubener described the organo-catalysed hydrogen transfer to form the tricyclic compound **277** from the quinoline **273**.[83] Using the Hantzsch dihydropyriridine **274** as the hydride donor and the BINOL-derived phosphate **275** as the catalyst, the authors isolated a mixture of both saturated and unsaturated cyclised intermediate **276** (Figure 89). Hydrogenation of the mixture over iridium supported on carbon nanotubes afforded the desired 1,2,3,4-tetrahydroquinoline **277** in excellent yield and enantiomeric excess.

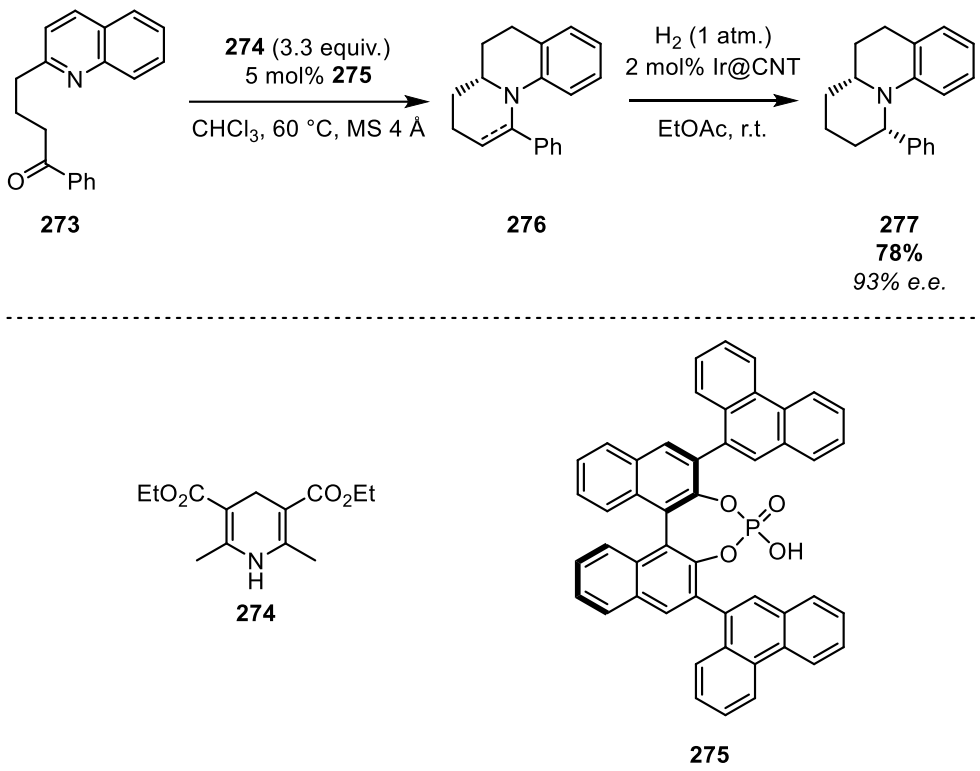

Figure 89: Hydrogenation of quinolines *via* an organo-catalysed hydrogen transfer

Application of those conditions to the methyl quinoline derivative **242b** gave the unexpected C-3 cyclisation, leading to the tetracyclic compound **278** in moderate yield (Figure 90). A proposed mechanism to explain this cyclisation invokes a first 1,4-hydrogen transfer onto the isoquinole ring giving the enamide **A** which can then attack the carbonyl to give the intermediate **B**. Elimination of water followed by the re-aromatisation of the naphthyl group affords the dihydrobenzo[c]acridine **278**.

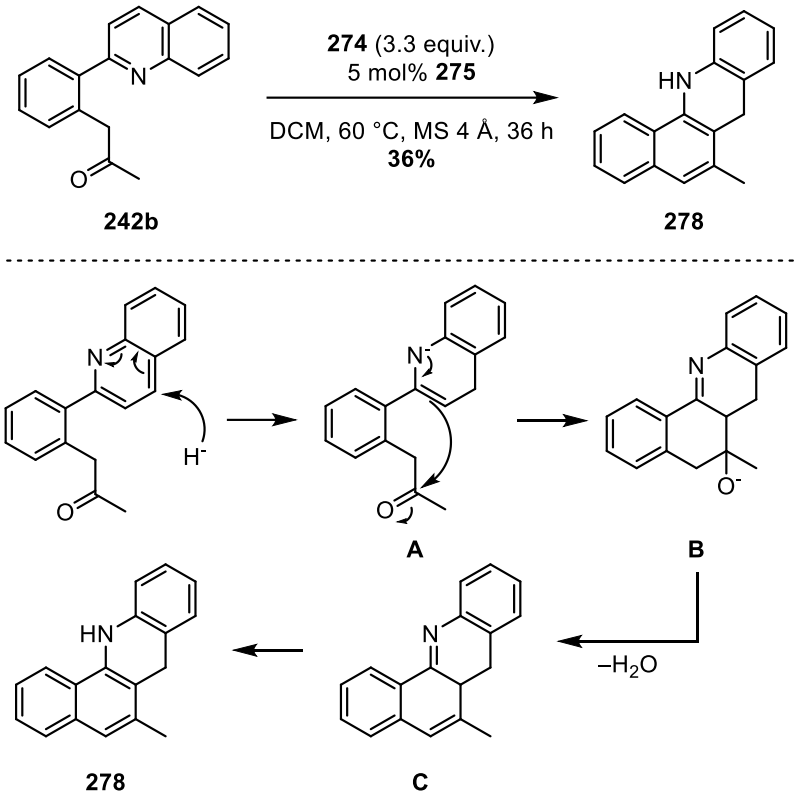

Figure 90: Formation of dihydrobenzo[c]acridine *via* an organocatalysed hydrogen transfer / Proposed mechanism

Yamagushi and co-workers reported the hydrogenation of the quinoline **279** to the 1,2,3,4-tetrahydroquinoline **280** *via* an iridium-catalysed hydrogen transfer (Figure 91).[84] The reaction afforded the desired product in excellent yield using a mixture of isopropanol and water with a catalytic amount of hydrogen perchlorate.

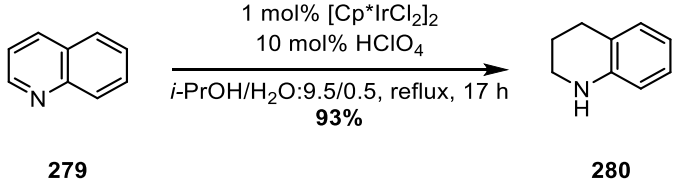

Figure 91: Hydrogenation of quinolines *via* an iridium-catalysed hydrogen transfer

Thus, those conditions were applied to the transformation of the methylquinoline derivative **242b** (Figure 92). The reproducibility of the reaction

proved to be challenging and the benz[c]acridine **281b** was isolated in yields ranging from low to quantitative. In this case, the fully aromatic benz[c]acridine was isolated after the reaction.

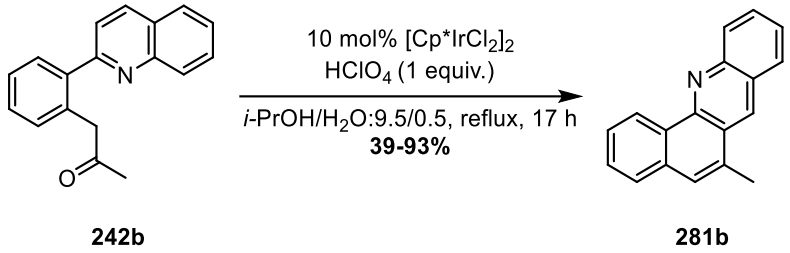

Figure 92: Formation of benz[c]acridine *via* an iridium-catalysed hydrogen transfer

Upon optimisation of the reaction, it was shown that hydrogen perchlorate was not needed to obtain the benz[c]acridine in good yield. Three benz[c]acridines could be formed in moderate yields from the cyclohexyl, methyl and phenyl derivatives **242a**, **242b** and **242c** respectively (Figure 93). Interestingly, in all cases a mixture of the benz[c]acridine and the corresponding dihydrobenzo[c]acridine was recovered after the reaction. However, exposing the mixture of products to air overnight, led to the conversion of the dihydrobenzo[c]cacridine into the desired benz[c]acridine.

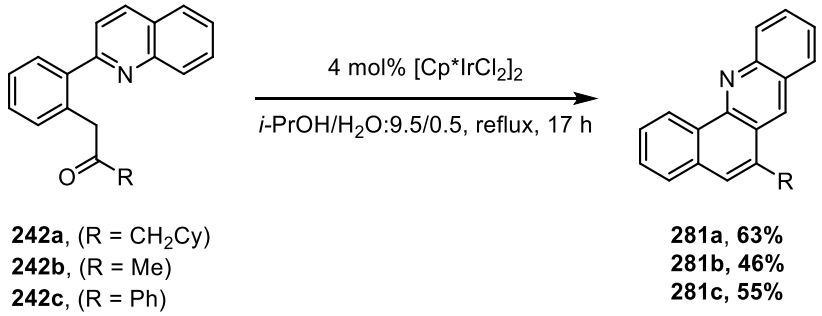

Figure 93: Scope of the iridium-catalysed hydrogen transfer

Benz[c]acridine is a well-known motif and has been used as fluorescent sensors.[85] Gryko and Piechowska have reported on the use of functionalised

benz[c]acridine as 10-hydrobenzo[h]quinoline (HBQ) replacement (Figure 94).[86] They reported the synthesis of eight different acridines with six of them exhibiting similar fluorophore properties as HBQ.

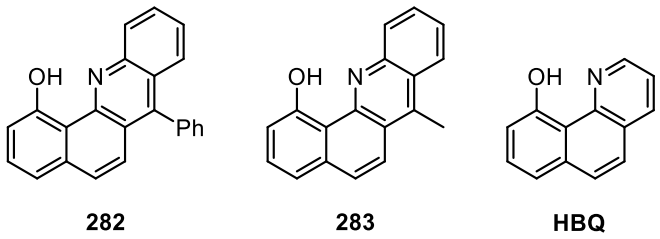

282 **283** **HBQ**

Figure 94: Structure of two benz[c]acridine with fluorophore properties / structure of HBQ

Despite being potentially interesting, the synthesis of benz[c]acridines oftens require extremely harsh conditions (Figure 95). The intermediate **286**, precursor of **282**, was obtained by heating **284** and benzoic acid at 200 °C with zinc chloride without any solvent.

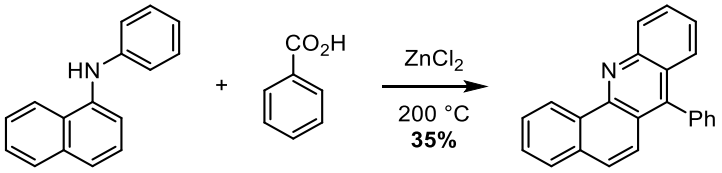

284 **285** **286**

Figure 95: Synthesis of benz[c]acridine

In this context, the new access to functionalised benz[c]acridine observed in our case could improve on the development and applications of such a framework.

4.4 Mechanistic study

4.4.1 Reversibility of the C–H bond cleavage

As seen previously, the rhodacycle formed prior to proto-demetalation was recovered when a non-protic solvent was used for the cross-coupling reaction. Based

on this result it was hypothesised that the first C–H functionalisation was not likely to be the rate determining step. Thus, when the phenyl pyridine **128** was treated with the sulfoxonium ylide **187** in the optimised conditions with a mixture of 1,2-dichlorobenzene and deuterated HFIP, the reaction was significantly slower and deuterium incorporation in the starting material and the product was observed (Figure 96). Interestingly, a significant scrambling of the deuterium label was observed and more than two third of hydrogen atoms in *ortho*-position of the phenyl pyridine were exchanged. Hence, the C–H bond functionalisation leading to the rhodium complex **228** must be reversible. Moreover, no deuterium exchange was observed at this position when the rhodium catalyst was not present in the solution.

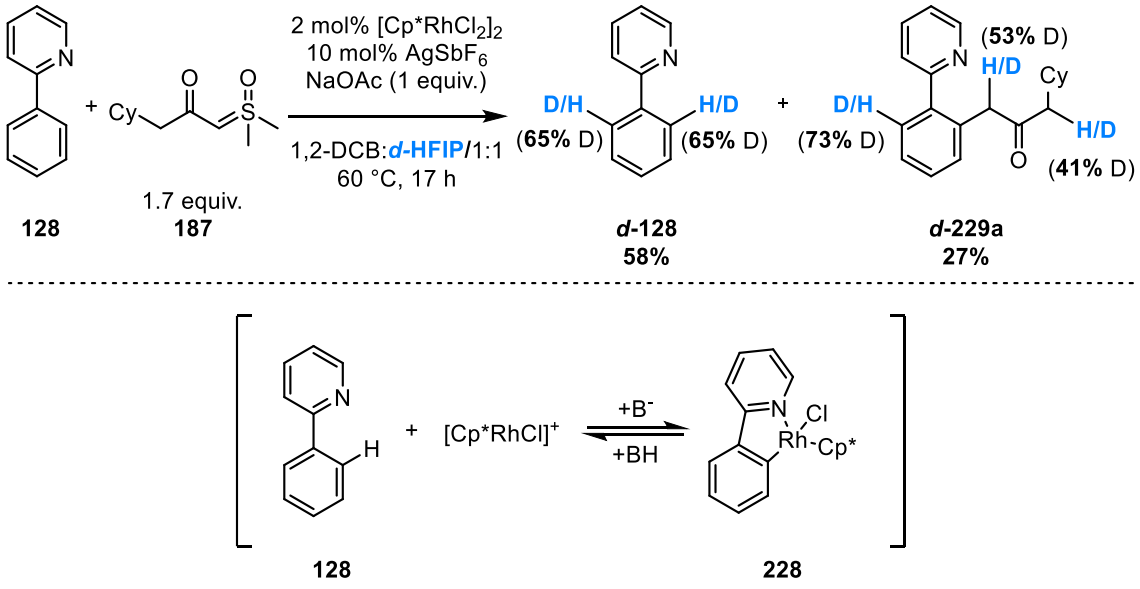

Figure 96: Reversibility of the C–H bond cleavage

Moreover, incorporation of deuterium in the *ortho*-position as well as at the two methylene positions next to the carbonyl was observed when the product **229a** was subjected to the standard conditions (Figure 97). Surprisingly, when the product **229a** was treated with *d*-HFIP, deuterium was observed in α-positions of the carbonyl.

Those experiments show that the solvent has a great impact on the outcome and is likely to play a key role in the proto-demetalation.

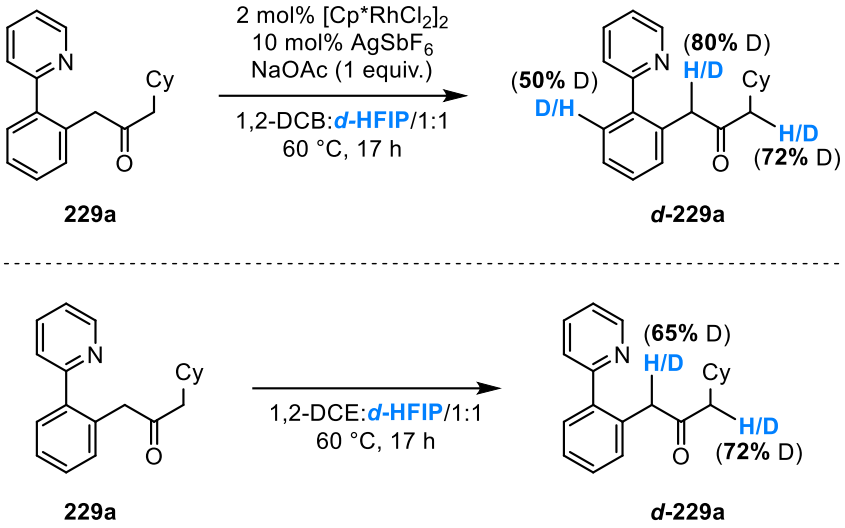

Figure 97: Deuterium scrambling on the product

4.4.2 Deuterium-labelling experiment

A series of experiments based around a deuterium-labelled starting material were designed to understand the relative rate of the first C–H activation. Firstly, when the mono-deuterated phenyl pyridine ***d*-128** was set to react in the optimised conditions without any sulfoxonium ylide, no traces of deuterium were seen on the recovered starting material (Figure 98).

Figure 98: Rhodium-catalysed deuterium exchange with HFIP

Secondly, no incorporation of the deuterium atom was observed in the product **229** when the standard conditions were used with the model sulfoxonium ylide **187** and deuterated phenyl pyridine ***d*-128** (Figure 99). Moreover, only traces of deuterium were found on the starting material after only 2 hours.

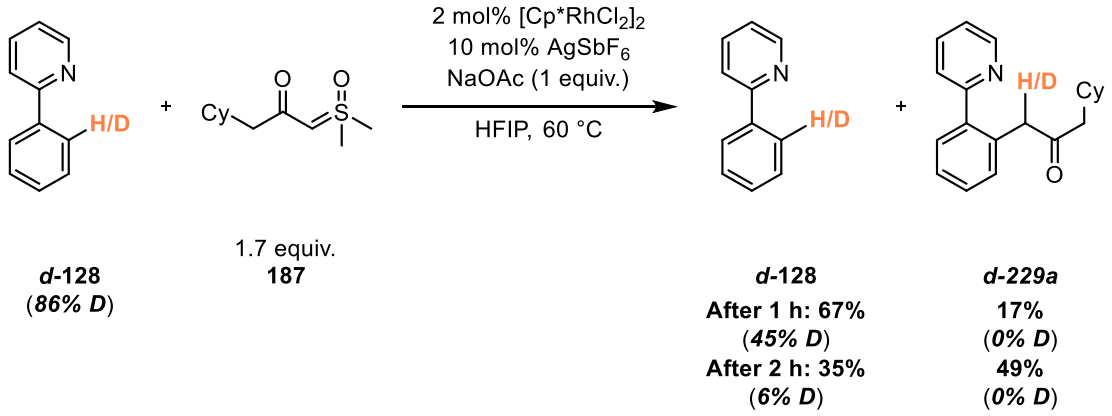

Figure 99: Deuterium exchange with HFIP

This experiment confirms that the C–H bond activation is not only reversible but occurs faster than the formation of the product.

4.4.3 Kinetic isotope effect

Through those experiments we can say that the rate determining step is not the C–H bond cleavage. Since the hypothesis was that the proto-demetalation could be the key event of the catalytic cycle, thus making the solvent the most important entity in the release of the desired product, a series of experiments with *d*-HFIP were ran. Due to the high cost of *d*-HFIP, a mixture of 1,2-DCE and *d*-HFIP was used. It is noteworthy that the yield obtained after seventeen hours in those conditions was significantly decreased as compared to those in only HFIP (Figure 100). Nonetheless, almost half of the product was recovered after 12 hours with non-deuterated solvents

(Orange plot). However, a significant decrease of rate was observed when deuterated HFIP was used (Blue plot).

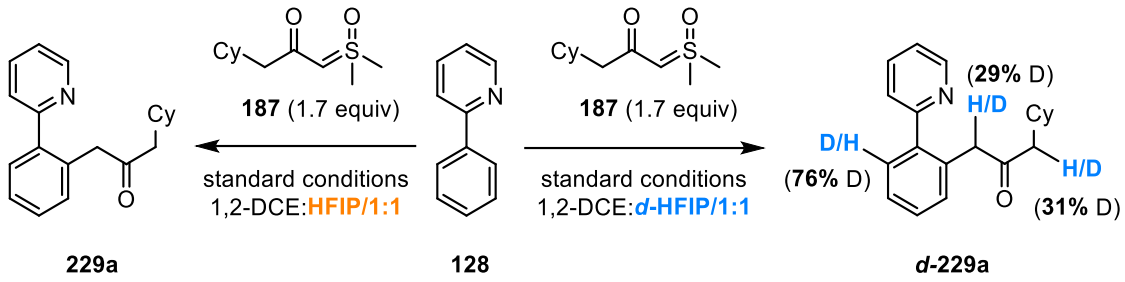

229a **128** ***d*-229a**

KIE = 2.6

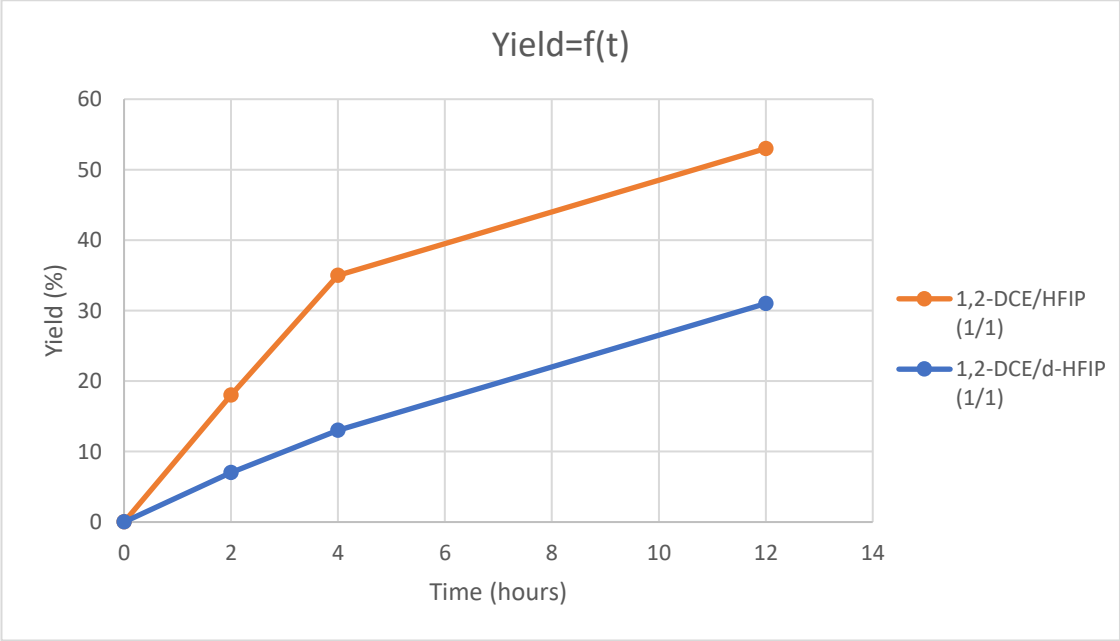

Figure 100: KIE experiment

Based on the isolated yield of products after 2 h, we could estimate the KIE (k_H/k_D) to be around 2.6, thus validating the hypothesis of the proto-demetalation being the rate determining step along with the fact that HFIP is key to close the catalytic cycle.

4.4.4 Determination of the rate-law *via* NMR monitoring

In 2016, Burés reported the use of the variable time normalisation in the elucidation of the rate law of reactions.[87, 88] By changing the concentration of one reagent at a time from a reference condition, the effect of this change could be seen by overlaying the concentration profile. The two reaction profiles obtained can only overlap when the concentration of the investigated species is raised to the correct power, enabling the elucidation of the rate order in this species. This method involves the time normalisation between two data points by averaging the concentration of the observed species between those points according to the following formula.

$$\int_{t=0}^{t=n} [A]^{\alpha} \mathrm{d}t = \sum_{i=1}^{n} \left(\frac{[A]_i + [A]_{i-1}}{2} \right)^{\alpha} (t_i - t_{i-1})$$

This normalisation removes the kinetic effect of the observed species on the reaction profile. This method allows a quick access to the reaction order of each species present in the reaction.

The reaction conditions had to be changed in order to be applicable with this method of analysis. Due to the presence of silver salts in the mixture, an NMR monitoring would not be possible. Thus, the pre-formed rhodium acetate monomer was used as the catalyst. A control experiment showed that this catalyst was potent in the reaction and a similar yield of product was obtained (Figure 101). Moreover, a mixture of deuterated toluene and HFIP was used for the reaction to avoid the use of deuterated HFIP. Acceptable conversions were obtained with a one to one mixture of toluene and HFIP, thus this mixture was kept for the study. Finally, since the base had a relatively low impact on the reaction outcome, it was removed from the mixture.

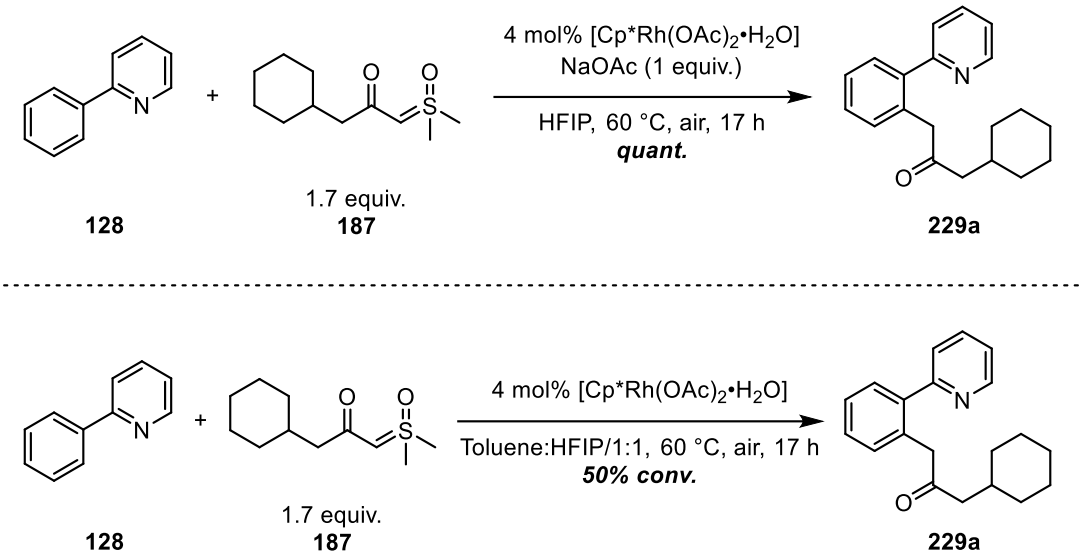

Figure 101: Control experiments

The optimised conditions were used as the reference for the study. Every concentration was changed one at a time in order to complete the variable time normalisation analysis (Figure 102).

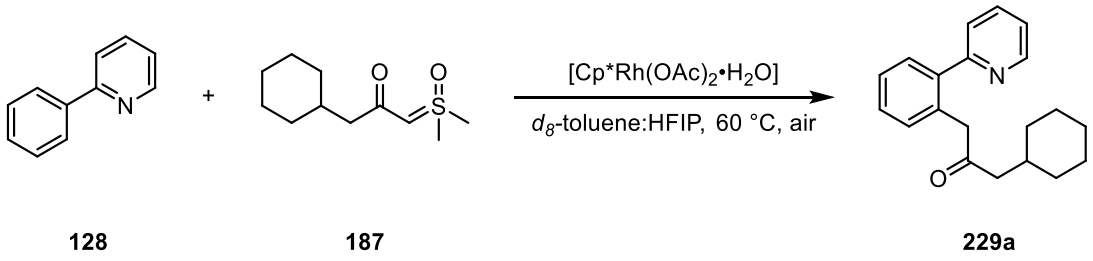

Ref : [128] = 0.27 M; [187] = 0.45 M; [Rh] = 0.01 M; [HFIP] = 9.5 M
[128] = 0.27 M; [187] = 0.45 M; [Rh] = 0.01 M; ***[HFIP] = 4.1 M***
[128] = 0.27 M; [187] = 0.45 M; ***[Rh] = 0.02 M***; [HFIP] = 9.5 M
[128] = 0.27 M; ***[187] = 0.35 M***; [Rh] = 0.01 M; [HFIP] = 9.5 M
[128] = 0.35 M; [187] = 0.45 M; [Rh] = 0.01 M; [HFIP] = 9.5 M

Figure 102: Concentrations used for the time normalisation

Below, are reported all the results obtained after a single attempt at varying the concentrations.

Firstly, the concentration of HFIP was changed and gave the first six graphs. In orange are the plots for the attempts with the new concentration of HFIP while the

plots in black are for the reference reaction (Figure 103). As expected the reaction was slower when less HFIP was added to the mixture. Changing the power of the HFIP concentration to one did not fully overlap the reference (in grey) with the new plot (in orange). The best overlap was obtained with the power of 0.7 or 0.8. From this result it is clear that the HFIP is involved in the rate-determining step, although the proto-demetalation proceeds *via* a complex mechanism explaining the non-integer value of the rate order.

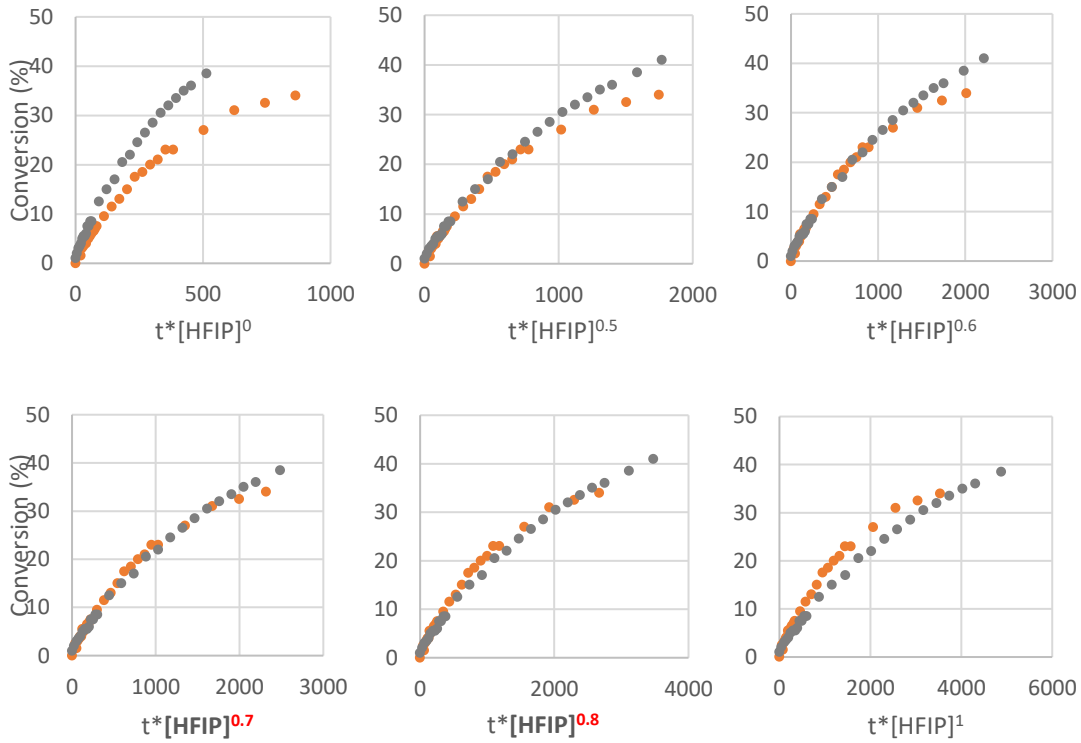

Figure 103: Plots obtained for the determination of the order in HFIP (Orange: modified concentration/ Grey: reference)

Secondly, the focus was placed on the concentration of the rhodium catalyst. In this case the concentration was increased as compared to the reference and a significant increase of rate was observed as depicted by the blue plot (Figure 104). When the concentration was raised to the power of two, a good overlap between the

two plots was obtained. Thus, a dimer of rhodium must be involved in the rate determining step.

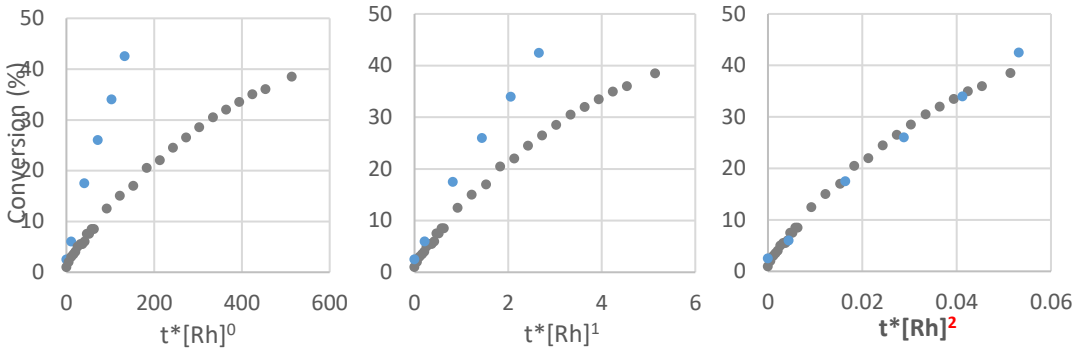

Figure 104: Plots obtained for the determination of the order in rhodium catalyst (Blue: modified concentration/Grey: reference)

Surprisingly, the decrease of the concentration in sulfoxonium ylide did not affect the reaction rate (Figure 105). The reaction presents a zero-order dependence in sulfoxonium ylide, and it is believed that the excess needed for the reaction to reach full conversion is due to the decomposition of a part of this reagent during the course of the reaction.

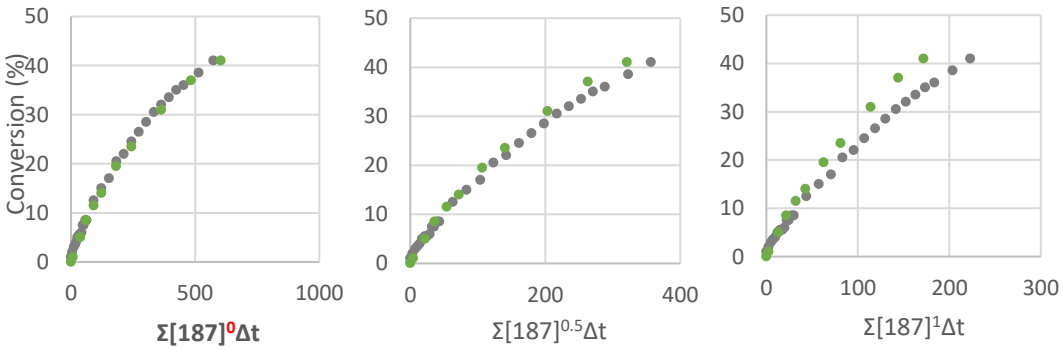

Figure 105: Plots obtained for the determination of the order in sulfoxonium ylide (Green: modified concentration/Grey: reference)

Increasing the concentration of phenyl pyridine, in purple, as compared to the reference experiment led to an increase in rate (Figure 106). The best overlap was obtained with the concentration raised to the power of 1.5. Similarly to the

concentration of HFIP, a non-integer value for the kinetic order was obtained, pointing to a complex mechanism for the rate determining step involving most probably two molecules of phenyl pyridine.

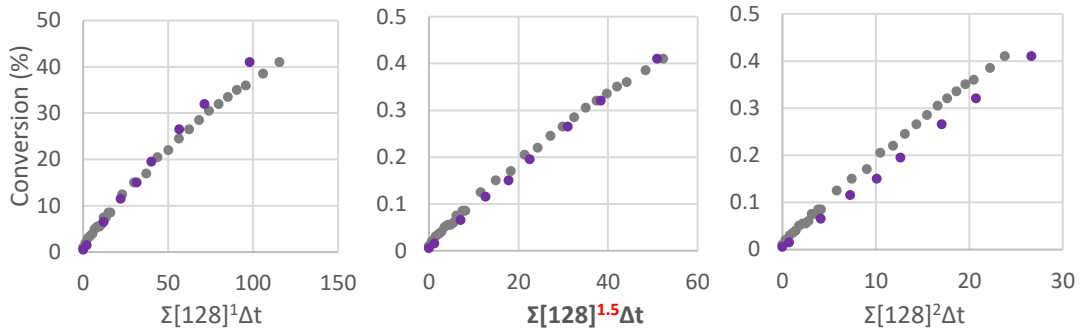

Figure 106: Plots obtained for the determination of the order in phenylpyridine (Purple: modified concentration/Grey: reference)

Finally, by merging all those results into one plot with all the best rate orders found earlier, a linear plot with the five curves overlayed was obtained, validating all the reaction orders (Figure 107). To summarise, the reaction presents a zero-order dependence in sulfoxonium ylide, and a second order in the rhodium catalyst. The order-dependence in starting material **128** and HFIP would be 1.5 and 0.7-0.8, respectively.

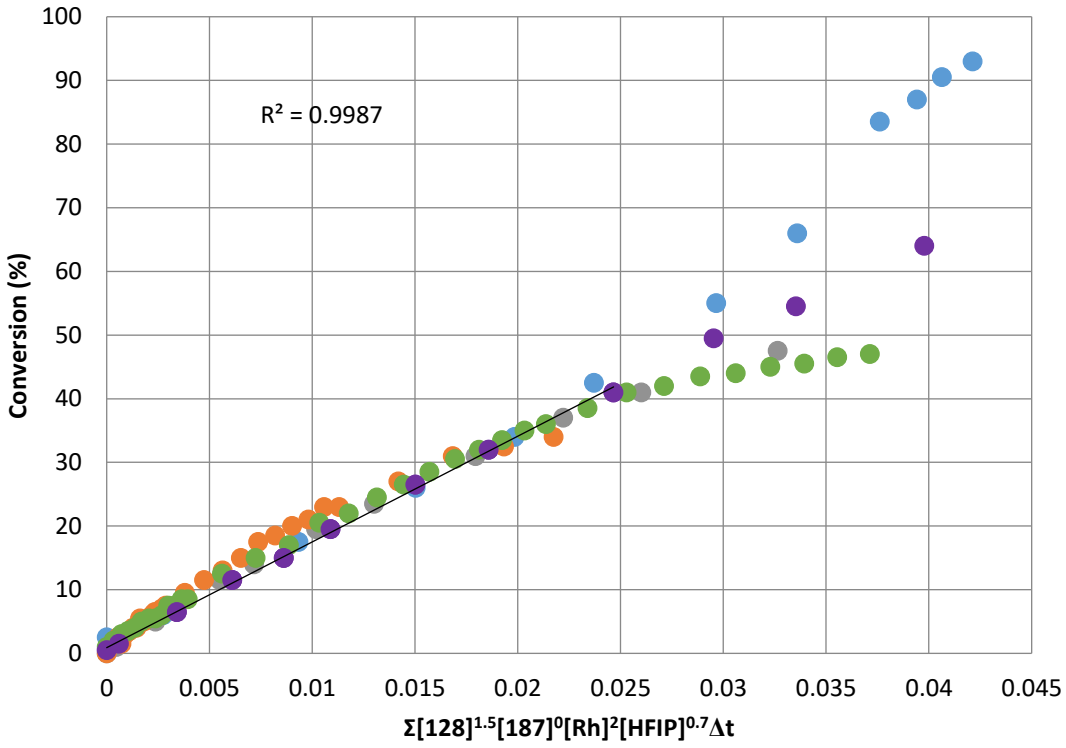

Figure 107: Time normalised analysis

It is worth mentioning that in this case the conversion was kept below 40% in order to obtain reliable results. Beyond this conversion, an inflection point can be observed with the five plots diverging from each other. This same observation has been reported by Gade *et al.*, showing that the global order of the mechanism is likely to change in the late stage of their manganese-catalysed hydroboration due to the low concentration of starting material, or a potential deactivation of some of the active species.[89] In our case, a possible product inhibition could be hypothesised along with the deactivation of the catalyst by the release of DMSO.[39]

A monitoring of the catalyst concentration would show any decomposition of the catalyst over the reaction time. Moreover, a product inhibition could be assessed by adding a known concentration of product from the beginning. Any difference from

the original plot would indicate that the product has an influence on the reaction, thus explaining the deviation observed beyond a certain conversion.

4.4.5 Proposed mechanism

Nonetheless, a refined mechanism for this reaction can be proposed with all the results gained with the mechanistic study (Figure 108).

The generation of the active cationic rhodium species **A** can occur *via* the release of an acetate ligand.[90] Coordination of the catalyst to the pyridine followed by abstraction of the *ortho* C–H bond *via* a CMD mechanism gives the pentarhodacycle **B** and releases acetic acid.[91] Through the deuterium labelling experiments we have shown that this species is in rapid equilibrium with the starting phenyl pyridine **128**. This rhodacycle is converted to the intermediate **C** upon nucleophilic attack of the sulfoxonium ylide onto the eletronically deficient rhodium atom. Further elimination of dimethylsulfoxide gives the rhodium carbene species **D** which is converted to **E** after a migratory insertion step. It is noteworthy that Cramer and Qu have shown through DFT calculation that the leaving-group elimination/ C–C bond formation can be written as a concerted mechanism if the leaving group is in *anti*- position to the formed C–C bond.[92] The proto-demetalation, assisted by HFIP, can release the desired functionalised pyridine along with the active catalyst. Thanks to the kinetic isotope effect experiments using catalytic conditions or stoichiometric conditions we have shown that this last step is likely to be the rate-determining step of the catalytic cycle.

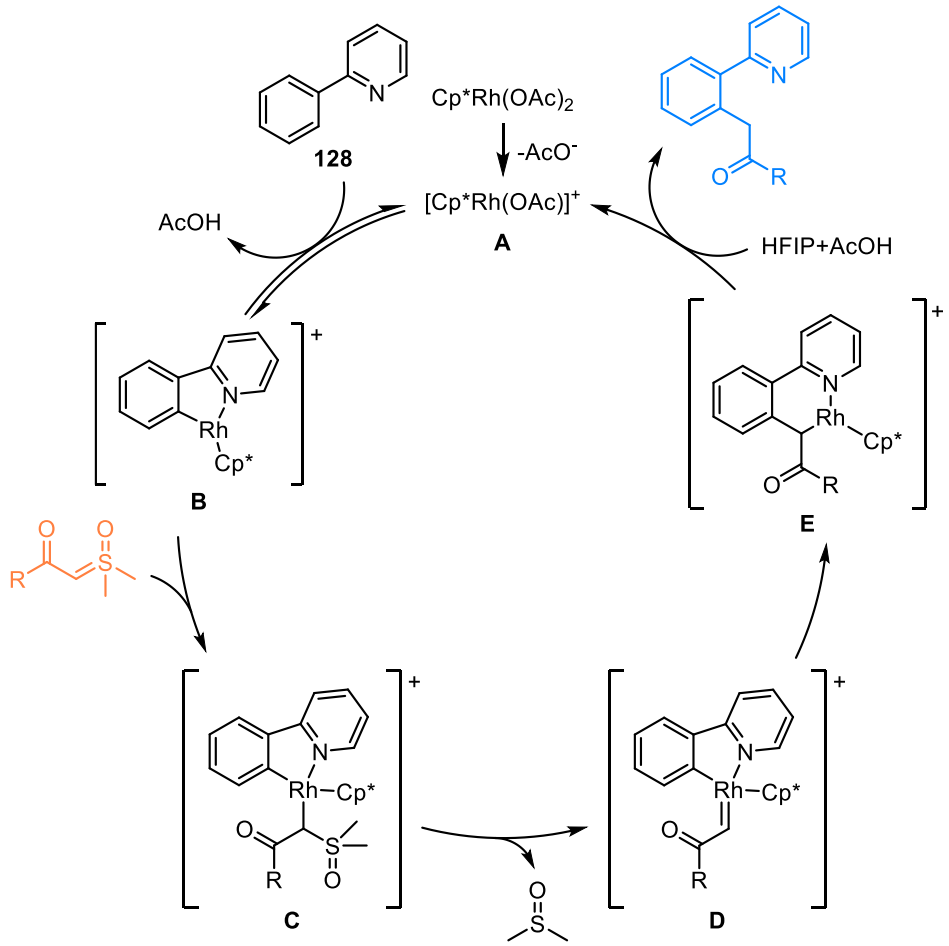

Figure 108: Proposed mechanism for the rhodium-catalysed Csp²–H functionalisation with sulfoxonium ylides

Although this catalytic cycle is in-line with the commonly accepted pathway, we have shown through the NMR study and rate-law determination that the proto-demetalation step is likely to involve a more complex mechanism due to the non-integer rate-orders found for the HFIP, the phenyl-pyridine and the rhodium catalyst.

Recently, Cramer and Qu reported that a second equivalent of phenylpyridine could promote the proto-demetalation of the rhodium catalyst, by acting as a proton-carrier (Figure 109).[92] Moreover, Ellman and co-workers showed that the active rhodacycle was in equilibrium with the 18-electon complex **289**.[93] Because of the positive effect of the second molecule of phenyl pyridine in the proto-demetalation

step, a second order in phenyl pyridine could be expected. However, due to the inhibitory effect of the phenyl pyridine through deactivation of the active catalyst **228** into **289**, the rate order in **128** must be between 1 and 2 on a macromolecular scale, depending on the equilibriums between **287**/**228** and **289**/**228**.

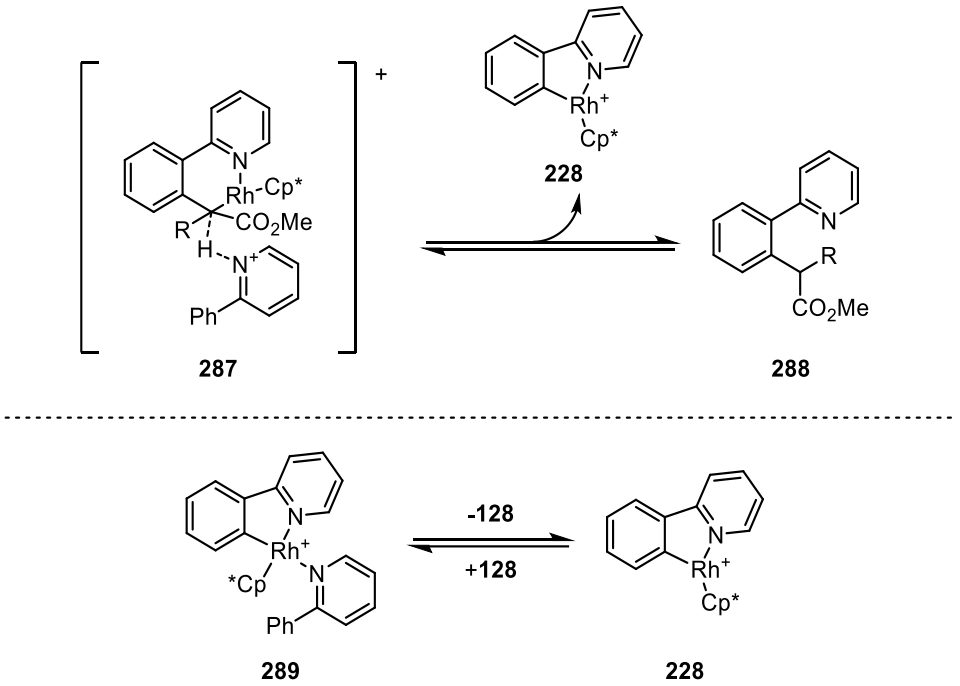

Figure 109: Proto-demetalation assisted with phenylpyridine / Equilibrium between the resting state and the active catalyst

Similarly, a second molecule of **128** is likely to be involved in the proto-demetalation step to regenerate of the active species and release the product (Figure 110). However, if the rhodium catalyst is taken out of the catalytic cycle through the coordination of a second molecule of **128**, then, an order of 1.5 can be expected, as both positive and negative effects are in competition.

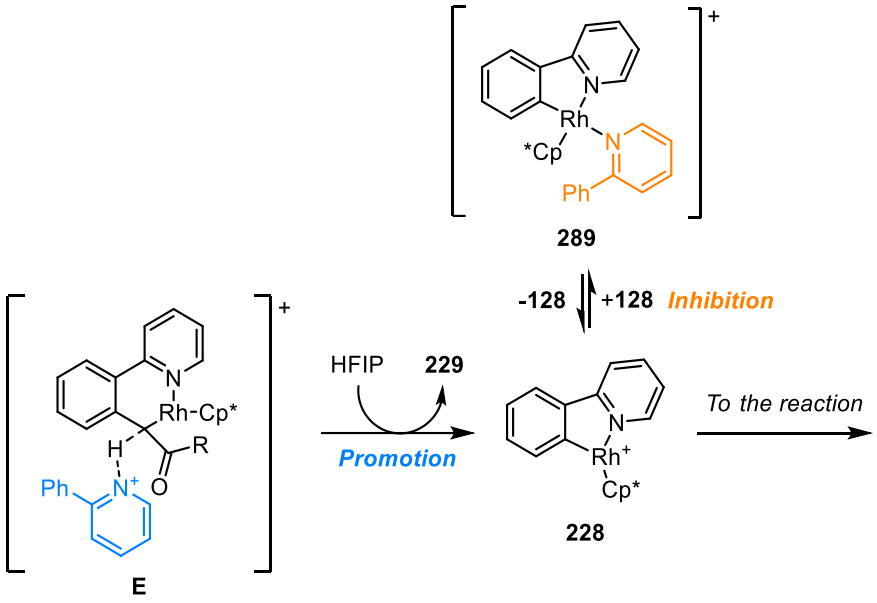

Figure 110: Possible explanation for the 1.5 rate-order in 128

Moreover, the solvent has a key-role in the mechanism and presents a rate-order between 0.7 and 0.8.[72] We have shown that the first C–H bond cleavage is reversible and that the equilibrium is faster than the reaction. As the HFIP is involved in both the proto-demetalation and the non-productive equilibrium, a positive and negative effect on the overall reaction is expected, giving a non-integer value in rate order between 0 and 1 (Figure 111).[94] Moreover, several studies have reported the hydrogen bonding ability of HFIP which could explain why other hydrogen-donor solvents failed to push the reaction to full conversion.

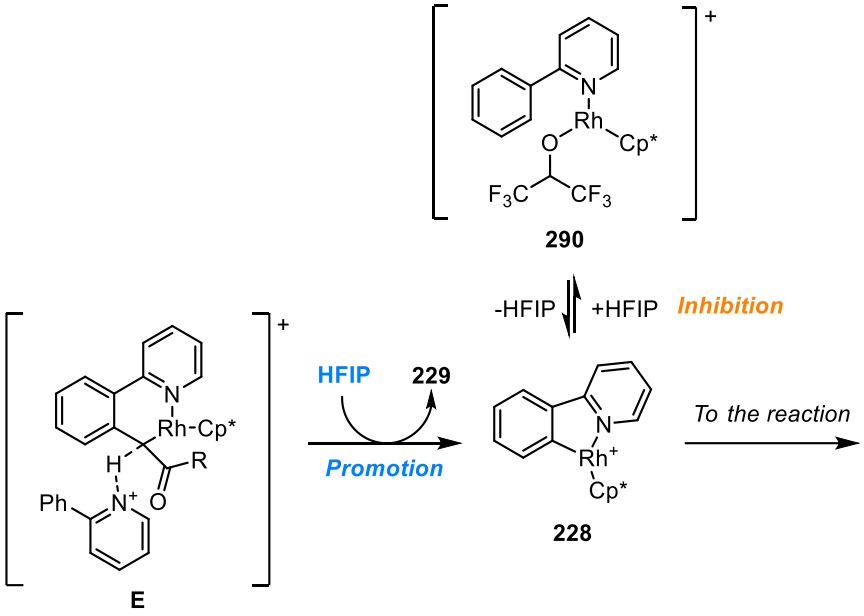

Figure 111: Possible explanation for the 0.7-0.8 rate order in HFIP

Finally, it was determined that a second-order in rhodium catalyst applied to the reaction, pointing to the need of a dimer during the rate-determining step. However, this result is still unexplained and further studies with other rhodium catalysts such as $[Cp^*Rh(MeCN)_2](SbF_6)_2$, are required in order to fully understand the transition state of the rate-determining step.

5 Conclusion

5.1 Summary

As a conclusion, we have reported the first rhodium-catalysed C–H bond cross-coupling reaction using α-ketosulfoxonium ylides. Firstly, we showed that a wide variety of sulfoxonium ylides could be accessed in good yields *via* the *para*-nitrophenyl ester or the acyl chloride. Moreover, bis-substituted sulfoxonium ylides could be obtained from the pyrimidine or the triethylsulfoxonium ethylide, although the latter proved to be demanding in terms of synthesis.

Secondly, through the optimisation of the reaction, we observed a strong effect of the solvent used on the outcome of the reaction. Fluorinated solvents significantl improved the reactivity and hexafluoroisopropanol was kept for the development of the scope.

We reported 25 examples of C–H bond functionalisation with yields ranging from 30% to quantitative. Csp^2–H on electron-withdrawing and -donating arenes underwent the coupling smoothly along with heterocyclic arenes. 4 different directing groups have been used, although the reaction conditions had to forced in order to obtain decent yields. Finally, we showed that several sulfoxonium ylides could undergo a cyclisation in good yields, without a metal catalyst.

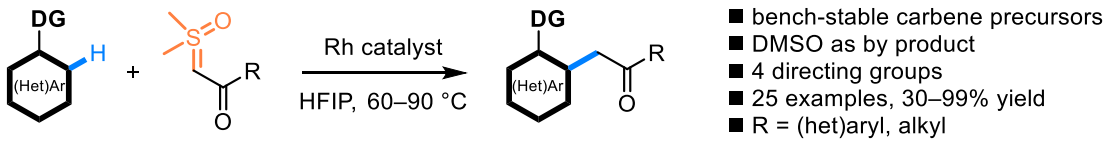

Figure 112: Rhodium-catalysed cross-coupling of C–H bonds with α-ketosulfoxonium ylides

The functionalised phenyl-quinolines were successfully converted to benz[c]acridines in moderate yields *via* an unprecedented iridium-catalysed dehydrative cyclisation (Figure 113). This moiety could be of interest as fluorescent sensors with a milder synthesis as compared to the harsh conditions used to access this framework in reported conditions.

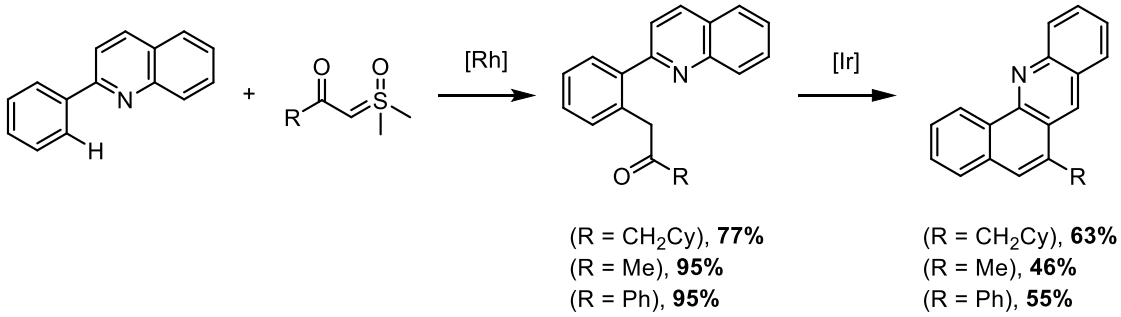

Figure 113: Synthesis of functionalised benz[c]acridine

Finally, through the mechanistic study we have shown that, as expected from the observations of the optimisation, the proto-demetalation step is the rate-determining step with the solvent playing a key-role. Moreover, we saw that the first C–H bond functionalisiation was reversible and significantly faster than the rest of the mechanism. The time-normalisation helped us understand the role of every species in the reaction and showed that the sulfoxonium ylide is not involved in the rate-determining step. Both the HFIP and the phenyl-pyridine exhibited a non-integer rate-order because of a positive/negative effect on the reaction. A rate-order of 2 in catalyst was obtained from the NMR study and remains unclear at the moment.

5.2 Citations

Pleasingly, this work has been cited in several reports since its publication, showing that it has brought a momentum in the development of sulfoxonium ylides as coupling partners in the C–H bond functionalisation. Shortly after our report, Li and co-workers used a different set of conditions to functionalise Csp^2–H bonds (Figure 114).[95] Interestingly, the conditions reported in this chapter and their conditions were almost complementary as some of our troublesome substrates underwent the reaction smoothly in their hands, whereas some issues reported in their work could be solved by using our conditions. The same authors managed to develop two chemoselective sets of conditions to selectively synthesise either the isocoumarin **245** or the isoquinolinone **244b** from the methoxybenzamide **243**.[96] Finally, they could access fully aromatic bicycles such as the naphthopyran **293** in excellent yield in a one-pot sequence.[97,98]

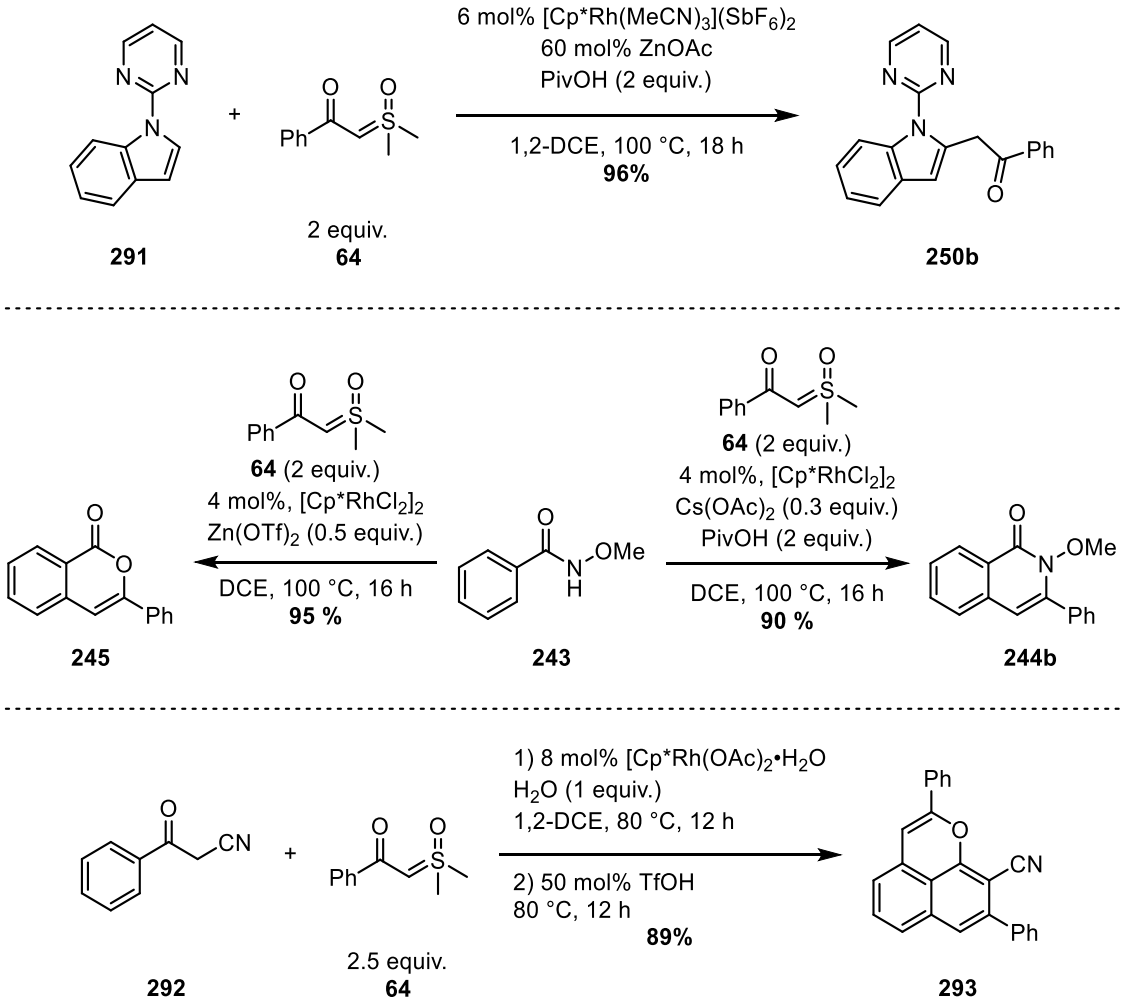

Figure 114: Li's work on C–H bond functionalisation with sulfoxonium ylides

Ellman and co-worker reported that olefinic Csp^2–H could undergo the rhodium-catalysed cross-coupling with sulfoxonium ylide in excellent yield with an imidazole or pyrazole directing group (Figure 115).[99,100]

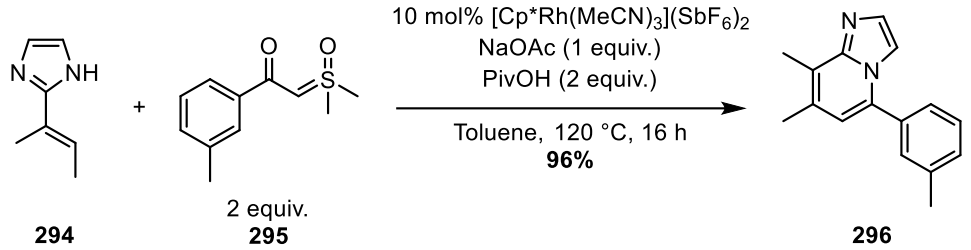

Figure 115: Ellman's functionalisation of olefinic Csp^2–H withsulfoxonium ylides

Cheng *et al.* showed that azobenzenes were suitable for the rhodium-catalysed C–H bond functionalisation with sulfoxonium ylides. The authors could isolate the indazole **298** form the azobenzene **297** in good yield (Figure 116).[101]

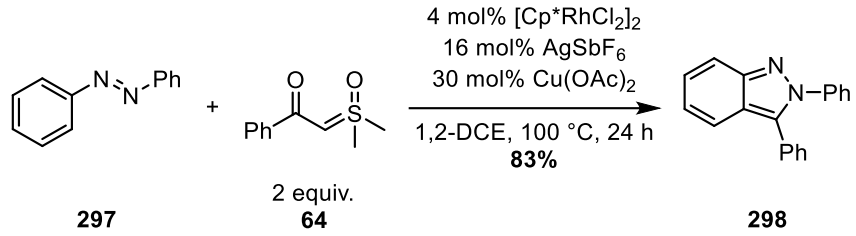

Figure 116: Rhodium-catalysed functionalisation of azobenzene with suslfoxonium ylides

Recently, Wang and his group expanded the chemistry of sulfoxonium ylides to ruthenium catalysts. The authors synthesised the isoquinoline **300** in 74% yield with a ruthenium catalyst (Figure 117).[102]

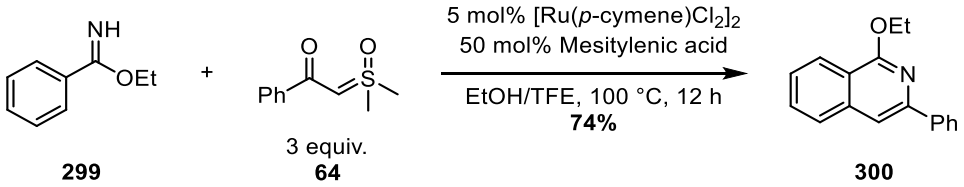

Figure 117: Ruthenium-catalysed C–H bond functionalisation with sulfoxonium ylides

5.3 Outlook

We have shown that aromatic Csp^2–H could undergo the rhodium-catalysed cross-coupling reaction with sulfoxonium ylide and Ellman and co-workers have expanded the work to olefinic Csp^2–H. However, nobody has described the functionalisation of Csp^3–H so far, thus making it highly interesting as a continuation of this project.

Moreover, although a lot of information on the reaction was obtained through the mechanistic study, several questions remain unanswered, such as the rate order of 2 in catalyst. A duplicate of the NMR study is required in order to minimise the experimental error. The use of the cationic rhodium catalyst, *i.e.* $[Cp^*Rh(MeCN)_2](SbF_6)_2$, could also give new hints on the transition state in the rate determining step. Finally, performing the NMR study on a second directing group could give us insight on the generality of the proposed mechanism.

Finally, the removal of the directing group proved to be more challenging than anticipated. In 2016, Yu and co-workers reported the use of amino-acids as transient directing group in the palladium-catalysed cross-coupling of the iodo-aryl **302** and the aldehyde **301** (Figure 118).[103] Applying a similar methodology to our project would bypass the removal step of the directing group and enabling easier further functionalisation.

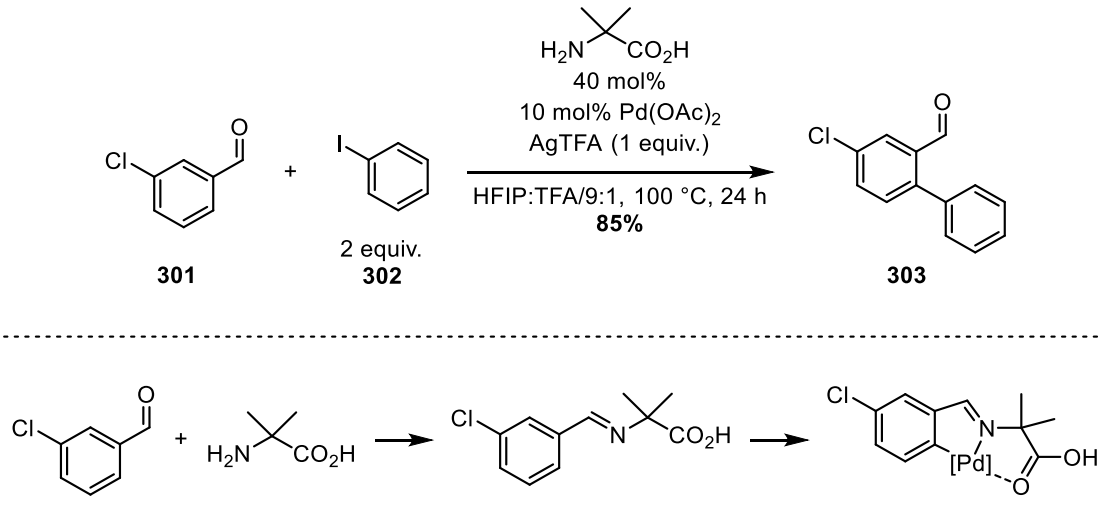

Figure 118: Palladium-catalysed cross-coupling with amino-acids as transient directing group

6 Experimental section

6.1 Synthesis of catalysts

Synthesis of [Cp*RhCl$_2$]$_2$. To a flame dried round bottom flask under nitrogen and equipped with a reflux apparatus was added $RhCl_3$•$3H_2O$ (1 g, 4.8 mmol 1 equiv.), MeOH (20 mL) followed by 1,2,3,4,5-pentamethylcyclopentadiene (0.75 mL, 8.2 mmol, 1.7 equiv.). The mixture was stirred at reflux for 48 h. Then, the reaction was cooled down to room temperature and filtered to afford [Cp*$RhCl_2$]$_2$ as a red powder (1.02 g, **83%**). HRMS (ESI) calcd for ($C_{20}H_{30}ClRh_2$ +): 511.0146; found: 511.0151; Anal. Calcd for $C_{20}H_{30}Cl_4Rh_2$: C 38.97, H 4.87; found C 38.97, H 4.88, *the NMR data is in accordance with that reported in the literature*.[104]

Synthesis of 228. To a flame dried Schlenk flask, under N_2, was added [Cp*$RhCl_2$]$_2$

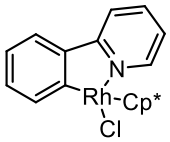

(92 mg, 0.15 mmol, 1 equiv.), NaOAc (25 mg, 0.3 mmol, 2 equiv.), dry dichloromethane (6 mL) and phenylpyridine (32 µL, 0.23 mmol, 1.5 equiv.). The mixture was stirred at room temperature overnight. Then, the mixture was filtered, the filtrate was evaporated and recrystallised from DCM/pentane to afford **228** as a red powder (93 mg, **97%**). ^{1}H NMR (500 MHz, $CDCl_3$): δ 8.75 (d, *J* = 5.4 Hz, 1H), 7.82 (dd, *J* = 7.6, 1.0 Hz, 1H), 7.79-7.76 (m, 1H), 7.74-7.69 (m, 1H), 7.61 (dd, *J* = 7.8, 1.3 Hz, 1H), 7.24 (dd, *J* = 7.4, 1.2 Hz, 1H), 7.13 (ddd, *J* = 7.4, 5.6, 1.3 Hz, 1H), 7.06 (ddd, *J* = 7.8, 7.4, 1.1 Hz, 1H), 1.63 (s, 15H), *the NMR data is in accordance with that reported in the literature*.[70]

Synthesis of Cp*Rh(OAc)$_2$•H$_2$O. To a flame dried round-bottom flask, under nitrogen, was added [Cp*RhCl$_2$]$_2$ (0.3 g, 0.5 mmol, 1 equiv.), AgOAc (0.4 g, 2.4 mmol, 4.9 equiv.) and dry toluene (21 mL). The mixture was stirred at 75 °C for 30 min. After cooling to room temperature, the mixture was filtered, washed with dichloromethane and the filtrate was evaporated to give the title compound as a red solid (0.331 g, **90%**). ^{1}H NMR (500 MHz, CDCl$_3$): δ 1.98 (s, 6H), 1.69 (s, 15H); Anal. Calcd for $C_{14}H_{23}O_5Rh$: C 44.93, H 6.19; found C 46.54, H 6.10, *the NMR data is in accordance with that reported in the literature*. [105]

Synthesis of [Cp*Rh(MeCN)$_3$(SbF6)$_2$]. A flame dried Schlenk tube sealable by a J-young key was charged in a glovebag with $AgSbF_6$ (0.44 g, 1.3 mmol, 4 equiv.) and [Cp*RhCl$_2$]$_2$ (0.2 g, 0.3 mmol, 1 equiv.). The tube was taken out of the glovebag and refilled with nitrogen before acetonitrile was added (1.6 mL). The mixture was stirred 4 h, transferred in a centrifuge tube and spun for 2 min at 1200 rpm. The yellow supernatant was collected, new acetonitrile (1 mL) was added and the tube was spun for another 2 min. The process was repeated until the supernatant became colourless. The combined solution was concentrated to give the title compound as a yellow solid (0.46 g, **86%**). ^{1}H NMR (500 MHz, *d*$_6$-DMSO): δ 2.08 (s, 9H), 1.55 (s, 15H); Anal. Calcd for $C_{16}H_{24}F_{12}N_3RhSb_2$: C 23.08, H 2.90, N 5.05; found C 22.94, H 2.92, N 4.94, *the NMR data is in accordance with that reported in the literature*.[106]

6.2 Synthesis of substrates

2-(1H-Pyrrol-1-yl)pyridine (CH1). To a flame dried round bottom flask, under N_2, 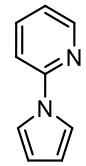 was added pyrrole (510 µL, 7.4 mmol, 1 equiv.) followed by dry DMF (20 mL). The mixture was cooled to 0 °C before NaH (736 mg, 18.4 mmol, 2.5 equiv.) was added and the mixture was stirred 15 min. The mixture was warmed up to room temperature and 2-bromopyridine (760 µL, 8.1 mmol, 1.1 equiv.) was added. The mixture was stirred 15 h at 120 °C. Then, the reaction was cooled down to room temperature and extracted 3 times with EtOAc. The combined organic layer was washed thoroughly with water and brine, dried over $MgSO_4$ and concentrated. Purification by flash chromatography (PE:EtOAc/95:5) afforded the titled compound as a pale pink oil (0.83 g, **78%**).[107] ^{1}H NMR (500 MHz, $CDCl_3$): δ 8.45-8.40 (m, 1H), 7.77-7.71, (m, 1H), 7.51 (t, *J* = 2.3 Hz, 2H), 7.32 (d, *J* = 8.5 Hz, 1H), 7.10 (ddd, *J* = 7.4, 4.9, 0.7 Hz, 1H), 6.36 (t, *J* = 2.3 Hz, 2H), *the NMR data is in accordance with that reported in the literature.*[108]

1-(Pyridin-2-yl)-1H-indole (CH2). To a flame dried round bottom flask, under N_2, 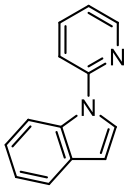 was added indole (0.86 mg, 7.4 mmol, 1 equiv.) followed by dry DMF (20 mL). The mixture was cooled to 0 °C before NaH (736 mg, 18.4 mmol, 2.5 equiv.) was added and the mixture was stirred 15 min. The reaction was warmed up to room temperature and 2-bromopyridine (845 µL, 8.8 mmol, 1.2 equiv.) was added. The mixture was stirred 15 h at 130 °C. Then, the reaction was cooled down to room temperature and extracted 3 times with EtOAc. The gathered organic layer was washed thoroughly with water and brine, dried over $MgSO_4$ and concentrated. Purification by flash chromatography (PE:EtOAc/95:5) afforded the

titled compound as a pale yellowish oil (0.4 g, **26%**).[107] ^{1}H NMR (500 MHz, $CDCl_3$): δ 8.58 (ddd, *J* = 4.9,1.8, 0.7 Hz, 1H), 8.21 (dd, *J* = 8.4, 0.8 Hz, 1H), 7.83 (ddd, *J* = 8.2, 7.4, 1.9 Hz, 1H), 7.73 (d, *J* = 3.5 Hz, 1H), 7.67 (dt, *J* = 7.9, 0.9 Hz, 1H), 7.51 (dt, *J* = 8.3, 0.9 Hz, 1H), 7.32-7.28 (m, 1H), 7.23-7.19 (m, 1H), 7.17 (ddd, *J* = 7.3, 4.9, 0.9 Hz, 1H), 6.72 (dd, *J* = 3.5, 0.7 Hz, 1H), *the NMR data is in accordance with that reported in the literature.*[109]

2-(3-Methoxyphenyl)pyridine (CH3). To a flame dried round bottom flask, under

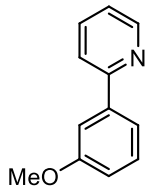

N_2, was added a mixture of degassed EtOH/H_2O/toluene (39 mL, 10:45:45) followed by 2-bromopyridine (477 µL, 5 mmol, 1 equiv.), Na_2CO_3 (3.9 g, 37 mmol, 7.4 equiv.), $Pd(PPh_3)_4$ (173 mg, 0.15 mmol, 0.03 equiv.) and (3-methoxyphenyl)boronic acid (1 g, 6.5 mmol, 1.3 equiv.). The mixture was stirred at reflux overnight. After cooling down to room temperature, the reaction was quenched with a saturated solution of NH_4Cl. The mixture was extracted with 3 times with EtOAc.The gathered organic layer was washed with water, brine, dried over $MgSO_4$ and concentrated under vacuum. Purification by flash column chromatography (PE:EtOAc/9:1) afforded the titled compound as a colourless oil (0.6 g, **65%**).[58] ^{1}H NMR (500 MHz, $CDCl_3$): δ 8.73-8.67 (m, 1H), 7.79-7.69 (m, 2H), 7.62-7.51 (m, 2H), 7.38 (t, *J* = 8.0 Hz, 1H), 7.23 (td, *J* = 4.9, 1.1 Hz, 1H), 7.01-6.93 (m, 1H), 3.90 (s, 3H), *the NMR data is in accordance with that reported in the literature*.[110]

Ethyl 3-(pyridin-2-yl)benzoate (CH4). To a flame dried round bottom flask, under

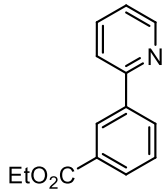

N_2, was added a mixture of degassed EtOH/H_2O/toluene (39 mL, 10:45:45) followed by 2-bromopyridine (477 µL, 5 mmol, 1 equiv.), Na_2CO_3 (3.9 g, 37 mmol, 7.4 equiv.), $Pd(PPh_3)_4$ (173 mg, 0.15 mmol,

0.03 equiv.) and (3-(ethoxycarbonyl)phenyl)boronic acid (1.71 g, 6.5 mmol, 1.3 equiv.). The mixture was stirred at reflux overnight. After cooling down to room temperature, the reaction was quenched with a saturated solution of NH_4Cl. The mixture was extracted with 3 times with EtOAc.The gathered organic layer was washed with water, brine, dried over $MgSO_4$ and concentrated under vacuum. Purification by flash column chromatography (PE:EtOAc/9:1) afforded the titled compound as a colourless oil (0.9 g, **81%**).[58] ^{1}H NMR (500 MHz, $CDCl_3$): δ 8.74-8.69 (m, 1H), 8.63 (t, *J* = 1.6 Hz, 1H), 8.23 (dt, *J* = 7.7, 1.6 Hz, 1H), 8.10 (dt, *J* = 7.7, 1.3 Hz, 1H), 7.82-7.76 (m, 2H), 7.56 (t, *J* = 7.9 Hz, 1H), 7.30-7.23 (m, 1H), 4.42 (q, *J* = 7.1 Hz 2H), 1.42 (t, *J* = 7.1 Hz, 3H), *the NMR data is in accordance with that reported in the literature*.[111]

2-(Furan-3-yl)pyridine (CH5). To a flame dried round bottom flask, under N_2, was

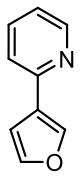

added a mixture of degassed EtOH/H_2O/Toluene (17 mL, 10:45:45) followed by 2-bromopyridine (320 µL, 3.4 mmol, 1 equiv.), Na_2CO_3 (2.7 g, 25 mmol, 7.4 equiv.), $Pd(PPh_3)_4$ (116 mg, 0.10 mmol, 0.03 equiv.) and furan-3-ylboronic acid (0.5 g, 4.5 mmol, 1.3 equiv.). The mixture was stirred at reflux overnight. After cooling down to room temperature, the reaction was quenched with a saturated solution of NH_4Cl. The mixture was extracted with 3 times with DCM. The gathered organic layer was washed with water, brine, dried over Na_2SO_4 and concentrated under vacuum. Purification by flash column chromatography (PE:EtOAc/9:1) afforded the titled compound as a colourless oil (0.2 g, **45%**).[58] ^{1}H NMR (500 MHz, $CDCl_3$): δ 8.64-8.61 (m, 1H), 7.90 (dd, *J* = 3.0, 1.1 Hz, 1H), 7.70 (td, *J* = 8.0, 2.0 Hz, 1H), 7.67 (dd, *J* = 5.1, 1.2 Hz, 1H), 7.62 (d, *J* = 7.8 Hz, 1H), 7.40 (dd, *J* = 5.0, 3.1 Hz, 1H), 7.17

(ddd, *J* = 7.4, 4.8, 1.0 Hz, 1H), *the NMR data is in accordance with that reported in the literature*.[112]

2H-[1,2'-Bipyridin]-2-one (CH6). To a flame dried round bottom flask, under N_2,

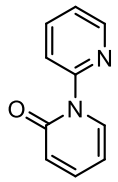

was added pyridin-2(1H)-one (0.95 g, 10 mmol, 1 equiv.), CuI (95 mg, 0.5 mmol, 0.05 equiv.), *N,N'*-dimethylethylenediamine (0.1 mL, 1 mmol, 0.1 equiv.), K_3PO_4 (4.2 g, 20 mmol, 2 equiv.), dry toluene (20 mL) and 2-bromopyridine (1.9 mL, 20 mmol, 2 equiv.). The mixture was stirred at reflux overnight. Then, the mixture was cooled down to room temperature, the reaction was quenched with a saturated solution of NH_4Cl and extracted 3 times with EtOAc. The gathered organic layer was washed with water, brine, dried over $MgSO_4$ and concentrated under vacuum. Purification by flash column chromatography (DCM:MeOH/98:2) afforded the titled compound as a white solid (0.9 g, **50%**).[113] ^1H NMR (500 MHz, $CDCl_3$): δ 8.60-8.55 (m, 1H), 7.95 (dt, *J* = 8.2, 0.8 Hz, 1H), 7.90-7.86 (m, 1H), 7.86-7.82 (m, 1H), 7.39 (ddd, *J* = 9.2, 6.5, 2.3 Hz, 1H), 7.32 (ddd, *J* = 7.4, 4.9, 1.0 Hz, 1H), 6.66-6.62 (m, 1H), 6.30 (td, *J* = 6.9, 1.1 Hz, 1H), *the NMR data is in accordance with that reported in the literature.*[114]

2-Phenylquinoline (CH7). To a flame dried round bottom flask, under N_2, was added

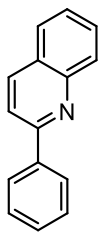

$PdCl_2(PPh_3)_2$ (34 mg, 0.05 mmol, 0.02 equiv.) followed by 1,4-dioxane (8 mL), water (8 mL), 2-bromoquinoline (0.5 g, 2.4 mmol, 1 equiv.) phenylboronic acid (0.35 g, 2.9 mmol, 1.2 equiv.) and Na_2CO_3 (1.7 g, 16 mmol, 6.7 equiv.). The mixture was stirred at reflux overnight. After cooling down to room temperature, the reaction was quenched with a saturated solution of NH_4Cl. The mixture was extracted with 3 times with DCM.The gathered organic layer was washed

with water, brine, dried over Na_2SO_4 and concentrated under vacuum. Purification by flash column chromatography (PE:EtOAc/9:1) afforded the titled compound as a white solid (0.28 g, **57%**).[115] ^{1}H NMR (500 MHz, $CDCl_3$): δ 8.24 (d, *J* = 8.6 Hz, 1H), 8.21-8.14 (m, 3H), 7.89 (d, *J* = 8.8 Hz, 1H), 7.84 (d, *J* = 7.9 Hz, 1H), 7.74 (t, *J* = 7.6 Hz, 1H), 7.57-7.42 (m, 4H), *the NMR data is in accordance with that reported in the literature.*[116]

***N*-Methoxybenzamide (CH8).** To a flame dried round bottom flask, under N_2, at 0

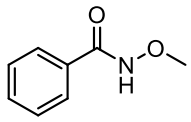

°C, was added benzoic acid (0.4 g, 3.3 mmol, 1 equiv.), DCM (10 mL), $(COCl)_2$ (0.3 mL, 4 mmol, 1.2 equiv.) and DMF (2 drops). The mixture was stirred at room temperature for 5 h before all solvents were removed *in vacuo*. A second flame dried round bottom flask, under N_2, was charged with K_2CO_3 (0.9 g, 6.6 mmol, 2 equiv.), EtOAc (24 mL), water (12 mL) and methoxyamine hydrochloride (0.33 g, 4 mmol, 2 equiv.). The mixture was cooled to 0 °C before addition of the freshly prepared acyl chloride in EtOAc. The mixture was stirred at room temperature overnight, and then, was extracted 3 times with EtOAc. The gathered organic layer was washed with water, brine, dried over $MgSO_4$ and concentrated under vacuum. Purification by flash column chromatography afforded the titled compound as a white solid (0.4 g, **82%**). ^{1}H NMR (500 MHz, $CDCl_3$): δ 8.62 (br s, 1H), 7.76-7.71 (m, 2H), 7.53 (tt, *J* = 6.8, 1.3 Hz, 1H), 7.47-7.41 (m, 2H), 3.90 (s, 3H), *the NMR data is in accordance with that reported in the literature*.[117]

6.3 Synthesis of sulfoxonium ylides

6.3.1 Synthesis of sulfoxonium ylides using methyl esters

Method I: *Representative example for the synthesis of **167**.*

To a flame dried 100 mL round bottom flask, under nitrogen and covered from light, was transferred trimethylsulfoxonium iodide (5.8 g, 26 mmol, 3.6 equiv.). The solid was suspended in dry THF (25 mL) before potassium *tert*-butoxide was added (2.9 g, 26 mmol, 3.6 equiv.). The mixture was stirred at reflux for 2 h. After cooling to room temperature, methyl nicotinate (1 g, 7 mmol, 1 equiv.) was added to the mixture. The mixture was stirred at reflux for another 4 h. The mixture was filtered through a plug of celite and all volatiles were removed under vacuum. Purification by flash chromatography (DCM:MeOH/98:2) afforded **167** as a white powder (41 mg, **3%**).

Compound 167. This compound was obtained as a white powder (41 mg, **3%**) from

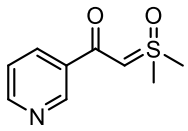

methyl nicotinate (1 g, 7 mmol) following **Method I**. ^{1}H NMR (500 MHz, $CDCl_3$): δ 8.96 (dd, *J* = 2.1, 0.7 Hz, 1H), 8.62 (dd, *J* = 4.8, 1.6 Hz, 1H), 8.06 (dt, *J* = 8.0, 2.0 Hz, 1H), 7.31 (ddd, *J* = 8.0, 4.8, 0.7, 1H), 5.01 (s, 1H), 3.52 (s, 6H); ^{13}C NMR (125 MHz, $CDCl_3$): δ 179.9 (e), 151.3 (o), 148.2 (o), 134.2 (e), 134.0 (o), 123.2 (o), 69.4 (o), 42.3 (o, 2C), *the NMR data is in accordance with that reported in the literature.*[118]

Compound 168. This compound was obtained as a white solid (960 mg, **26%**) from 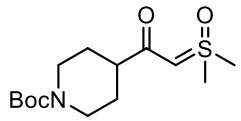 1-(*tert*-butyl) 4-methyl piperidine-1,4-dicarboxylate (3 g, 12 mmol) following **Method I**. m.p.: 134-136 °C. ^{1}H NMR (500 MHz, $CDCl_3$): δ 4.36 (s, 1H), 4.12 (br s, 2H), 3.39 (s, 6H), 2.80-2.63 (m, 2H), 2.25-2.14 (tt, *J* = 12.0,3.6 Hz, 1H), 1.84-1.72 (m, 2H), 1.58-1.40 (m, 11H); ^{13}C NMR (125 MHz, $CDCl_3$): δ 192.3 (e), 154.7 (e), 79.2 (e), 68.0 (o), 46.6 (o), 42.2 (o, 2C), 28.9 (e, 4C), 28.3 (o, 3C); IR (neat): ν = 3015 (w), 2985 (w), 2929 (w), 2857 (w), 1685 (vs), 1556 (vs), 1454 (w), 1394 (vs), 1364 (m), 1353 (m), 1291 (m), 1258 (w), 1231 (m), 1161 (vs), 1134 (vs), 1111 (s), 1095 (m), 1083 (m), 1022 (s), 960 (w), 858 (s), 764 (m), 681 (w); Anal. Calcd for $C_{14}H_{25}NO_4S$: C 55.42, H 8.25, N 4.62, S 10.56; found C 55.42, H 8.33, N 4.52, S 10.49.

Compound 169. This compound was obtained as a white powder (0.5 g, **40%**) from 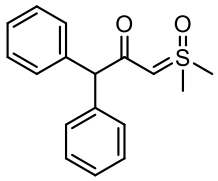 methyl 2,2-diphenylacetate (1 g, 4.4 mmol) following **Method I**. ^{1}H NMR (500 MHz, $CDCl_3$): δ 7.35-7.29 (m, 8H), 7.27-7.21 (m, 2H), 4.87 (s, 1H), 4.40 (s, 1H), 3.42 (s, 6H), *this product was not characterised further due to poor results in the rhodium-catalysed C–H bond functionalisation.*

6.3.2 Synthesis of sulfoxonium ylides using *p*-nitrophenyl esters

Method II: *Representative example for the synthesis of* ***64****.*

To a flame dried 100 mL round bottom flask, under nitrogen and at 0 °C, was added benzoic acid (1.2 g, 10 mmol, 1 equiv.) in dry THF (57), followed by *para*-nitrophenol (1.8 g, 13 mmol, 1.3 equiv.) and DCC (2.7 g, 13 mmol, 1.3 equiv.). The mixture was

stirred overnight at room temperature, filtered over celite and evaporated. Purification by flash column chromatography (PE: 100% to PE:EA/98:2) afforded the *para*-nitrophenyl ester as a pale-yellow solid (1.2 g, **51%**).

To a flame dried 100 mL round bottom flask, under nitrogen and covered from light, was transferred trimethylsulfoxonium iodide (3.3 g, 15 mmol, 3 equiv.). The solid was suspended in dry THF (28 mL) before potassium *tert*-butoxide was added (1.7 g, 15 mmol, 3 equiv.). The mixture was stirred at reflux for 2 h. After cooling to room temperature, the residue (1.2 g, 5 mmol, 1 equiv.) in THF (10 mL) was added and the mixture was stirred at reflux for 1 h. The mixture was filtered through a plug of celite and all volatiles were removed under vacuum. Purification by flash chromatography (DCM:MeOH/98:2) afforded **64** as a pale-yellow powder (0.83 g, **86%**).

Compound 64. This compound was obtained as a yellowish powder (0.8 g, **44%**) (1st step: 51%; 2nd: step 86%) from benzoic acid (1.2 g, 10 mmol) following **Method II**. ^{1}H NMR (500 MHz, $CDCl_3$): δ 7.82-7.78 (m, 2H), 7.46-7.37 (m, 3H), 4.97 (s, 1H), 3.52 (s, 6H), *the NMR data is in accordance with that reported in the literature.*[42]

Compound 185. This compound was obtained as a white powder (0.3 g, **27%**) (1st step: 34%; 2nd: step 78%) from 2-bromo-3-methylbenzoic acid (1 g, 4.7 mmol) following **Method II**. ^{1}H NMR (500 MHz, $CDCl_3$): δ 7.22-7.14 (m, 3H), 4.58 (s, 1H), 3.54 (s, 6H), 2.42 (s, 3H), *this product was not characterised further due to poor results in the rhodium-catalysed C–H bond functionalisation.*

Compound 186. This compound was obtained as a white powder (0.5 g, **36%**) (1st step: 45%; 2nd: step 79%) from 4-bromobenzoic acid (1 g, 5 mmol) following **Method II**. ^{1}H NMR (500 MHz, $CDCl_3$): δ 7.68 (dt, *J* = 9.0, 2.4 Hz, 2H), 7.54 (dt, *J* = 9.0, 2.5 Hz, 2H), 4.96 (s, 1H), 3.54 (s, 6H), *the NMR data is in accordance with that reported in the literature.*[42]

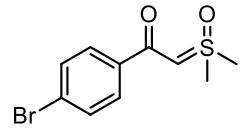

Compound 187. This compound was obtained as a white powder (0.37 g, **71%**) (1st step: 80%; 2nd: step 89%) from 2-cyclohexylacetic acid (1.1 g, 5.5 mmol) following **Method II**. m.p.: 113-114 °C. ^{1}H NMR (500 MHz, $CDCl_3$): δ 4.34 (s, 1H), 3.39 (s, 6H), 2.04 (d, *J* = 6.8 Hz, 2H), 1.79-1.60 (m, 6H), 1.32-1.20 (m, 2H), 1.18-1.08 (m, 1H), 0.99-0.87 (m, 2H); ^{13}C NMR (125 MHz, $CDCl_3$): δ 190.5 (e), 69.6 (o), 48.9 (e), 42.2 (o, 2C), 35.5 (o), 33.2 (e, 2C), 26.3 (e), 26.1 (e, 2C); IR (neat): ν = 3073 (w), 3010 (m), 2921 (s), 1547 (vs), 1449 (m), 1420 (m), 1385 (vs), 1320 (m), 1263 (w), 1170 (vs), 1146 (s), 1100 (m), 1031 (vs), 994 (m), 855 (s), 839 (s), 758 (m), 723 (m),683 (m); HRMS (CI (CH_4)) calcd for ($C_{11}H_{20}O_2S$ + H): 217.1257; found: 217.1256.

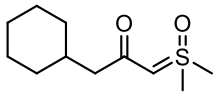

Compound 188. This compound was obtained as a white powder (1.4 g, **66%**) (1st step: 76%; 2nd: step 87%) from *iso*-butyric acid (2.4 g, 28 mmol) following **Method II**. ^{1}H NMR (500 MHz, $CDCl_3$): δ 4.36 (s, 1H), 3.38 (s, 6H), 2.35 (sept., *J* = 7.0 Hz, 1H), 1.09 (d, *J* = 6.9 Hz, 6H), *the NMR data is in accordance with that reported in the literature.*[42]

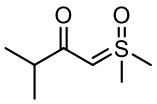

Compound 189. This compound was obtained as a white powder (0.58 g, **32%**) (1st step: 41%; 2nd: step 78%) from (*1S,2S*)-2-phenylcyclopropane-1-carboxylic acid (0.8 g, 5 mmol) following **Method II**. m.p.: 163-166 °C. ^{1}H NMR (500 MHz, $CDCl_3$): δ 7.29-7.23 (m, 2H), 7.16 (tt, *J* = 6.9, 1.3 Hz, 1H), 7.13-7.07 (m, 2H), 4.54 (s, 1H), 3.41 (d, *J* = 4.2 Hz, 6H), 2.42 (ddd, *J* = 9.1, 6.2, 4.2 Hz, 1H), 1.85 (ddd, *J* = 8.3, 5.5, 4.2 Hz, 1H), 1.60-1.54 (m, 1H), 1.16 (ddd, *J* = 8.2,6.3, 4.2 Hz, 1H); ^{13}C NMR (125 MHz, $CDCl_3$): δ 187.7 (e), 141.7 (e), 128.2 (o, 2C), 125.9 (o, 2C), 125.8 (o), 69.1 (o), 42.3 (o), 42.3 (o), 31.0 (o), 25.2 (o), 16.5 (e); IR (neat): ν = 3092 (w), 3028 (m), 3004 (m), 2918 (m), 1605 (m), 1552 (vs), 1494 (m), 1412 (vs), 1362 (s), 1308 (m), 1158 (vs), 1125 (s), 1103 (s), 1076 (m), 1025 (s), 999 (s), 968 (m), 959 (m), 929 (s), 900 (w), 860 (m), 831 (s), 747 (vs), 693 (vs); HRMS (ESI) calcd for ($C_{13}H_{16}O_2S$ + Na): 259.0769; found: 259.0767.

Compound 190. This compound was obtained as a white powder (0.39 g, **70%**) (1st step: 76%; 2nd: step 93%) from 2-(naphthalen-2-yl)acetic acid (1 g, 5.4 mmol) following **Method II**. ^{1}H NMR (500 MHz, $CDCl_3$): δ 7.83 (m, 3H), 7.70 (s, 1H), 7.48-7.39 (m , 3H), 4.27 (s, 1H), 3.64 (s, 2H), 3.35 (s, 6H), *this product was not characterised further due to poor results in the rhodium-catalysed C–H bond functionalisation.*

6.3.3 Synthesis of sulfoxonium ylides using acyl chlorides

Method III: *Representative example for the synthesis of **206**.*

To a flame dried 250 mL round bottom flask, under nitrogen and covered from light, was transferred trimethylsulfoxonium iodide (1.8 g, 8.4 mmol, 3 equiv.). The solid was suspended in dry THF (17 mL) before potassium *tert*-butoxide was added (0.9 g, 8.4 mmol, 3 equiv.). The mixture was stirred at reflux for 2 h. After cooling to 0 °C, 3,5-difluorobenzoyl chloride (330 µL, 2.8 mmol, 1 equiv.) in THF (6 mL) was added dropwise to the mixture. The mixture was stirred at 0 °C for 1 h. The mixture was filtered through a plug of celite and all volatiles were removed under vacuum. Purification by flash chromatography (DCM:MeOH/98:2) afforded **206** as a white powder (577 mg, **89%**).

Compound 203. This compound was obtained as a white solid (0.123 g, **19%**) from

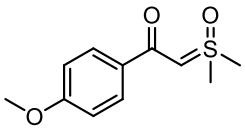

4-methoxybenzoyl chloride (0.4 mL, 2.9 mmol) following **Method III** (sodium *tert*-butoxide was used as the base). ^{1}H NMR (500 MHz, $CDCl_3$): δ 7.79-7.74 (m, 2H), 6.92-6.87 (m, 2H), 4.90 (s, 1H), 3.84 (s, 3H), 3.51 (s, 6H), *the NMR data is in accordance with that reported in the literature.*[42]

Compound 204. This compound was obtained as a white solid (1 g, **80%**) from 2-chlorobenzoyl chloride (638 µL, 5.4 mmol) following **Method III**. ^{1}H NMR (500 MHz, $CDCl_3$): δ 7.54-7.48 (m, 1H), 7.38-7.33 (m, 1H), 7.29-7.22 (m, 2H), 4.75 (s, 1H), 3.54 (s, 6H), *the NMR data is in accordance with that reported in the literature.*[27]

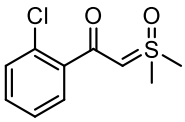

Compound 205. This compound was obtained as a white solid (1.2 g, **50%**) from 3,5-bis(trifluoromethyl)benzoyl chloride (1.3 mL, 7.2 mmol) following **Method III**. ^{1}H NMR (500 MHz, $CDCl_3$): δ 8.26 (s, 2H), 7.95 (s, 1H), 5.09 (s, 1H), 3.28 (s, 6H), *this product was not characterised further due to poor results in the rhodium-catalysed C–H bond functionalisation.*

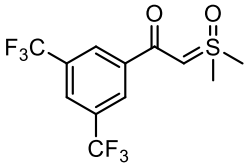

Compound 206. This compound was obtained as a white solid (0.577 g, **89%**) from 3,5-difluorobenzoyl chloride (0.33 mL, 2.8 mmol) following **Method III**. m.p.: 148-151 °C. ^{1}H NMR (500 MHz, $CDCl_3$): δ 7.30-7.24 (m, 2H), 6.84 (tt, *J* = 8.5, 2.3 Hz, 1H), 4.93 (s, 1H), 3.50 (s, 6H); ^{13}C NMR (125 MHz, $CDCl_3$): δ 179.0 (e), 163.8 (e, d, *J* = 11.8 Hz), 161.8 (e, d, *J* = 12.0 Hz), 142.5 (e, t, *J* = 7.4 Hz), 109.5 (o, d, *J* = 6.6 Hz), 109.4 (o, d, *J* = 6.4 Hz), 105.7 (o, t, *J* = 25.7 Hz), 69.4 (o), 42.2 (o, 2C); IR (neat): ν = 3086 (w), 3019 (w), 2918 (w),1619 (w), 1541 (vs), 1434 (m), 1388 (s), 1325 (m), 1299 (m), 1219 (w), 1164 (vs), 1112 (vs), 1076 (w), 1041 (m), 1028 (m), 981 (s), 971 (s), 934 (m), 857 (vs), 774 (w), 752 (s), 686 (m), 664 (s); Anal. Calcd for $C_{10}H_{10}F_2O_2S$: C 51.72, H 4.31; found C 51.62, H 4.27.

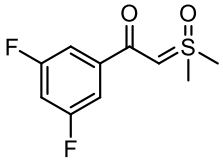

Compound 207. This compound was obtained as a white solid (0.591 g, **93%**) from 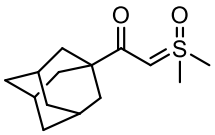 1-adamantanecarbonyl chloride (0.5 g, 2.5 mmol) following **Method III**. m.p.: 163-166 °C. ^{1}H NMR (500 MHz, $CDCl_3$): δ 4.38 (s, 1H), 3.35 (s, 6H), 2.01-1.95 (m, 3H), 1.78-1.74 (m, 6H), 1.72-1.62 (m, 6H); ^{13}C NMR (125 MHz, $CDCl_3$): δ 197.3 (e), 66.2 (o), 42.8 (e), 42.3 (o, 2C), 39.6 (e, 3C), 36.8 (e, 3C), 28.4 (o, 3C); IR (neat): ν = 3001 (w), 2904 (m), 2849 (m), 1524 (vs), 1452 (w), 1383 (s), 1314 (m), 1190 (s), 1172 (vs), 1101 (w), 1073 (m), 1028 (s), 988 (m), 946 (m), 854 (s), 817 (w), 746 (w), 659 (w); HRMS (CI (CH_4)) calcd for ($C_{14}H_{22}O_2S$ + H): 255.1413; found: 255.1409.

Compound 208. This compound was obtained as a white solid (0.7 g, **71%**) from 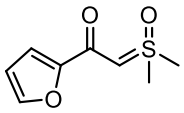 furan-2-carbonyl chloride (0.5 mL, 5.4 mmol) following **Method III**. ^{1}H NMR (500 MHz, $CDCl_3$): δ 7.41 (dd, *J* = 1.7, 0.8 Hz, 1H), 6.92 (dd, *J* = 3.4, 0.8 Hz, 1H), 6.44 (dd, *J* = 3.5, 1.8 Hz, 1H), 5.00 (s, 1H), 3.51 (s, 6H), *the NMR data is in accordance with that reported in the literature.*[119]

Compound 209. This compound was obtained as a beige solid (0.6 g, **80%**) from 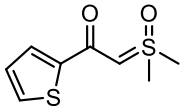 thiophene-2-carbonyl chloride (0.4 mL, 3.8 mmol) following **Method III**. ^{1}H NMR (500 MHz, $CDCl_3$): δ 7.44 (dd, *J* = 3.7, 1.2 Hz, 1H), 7.40 (dd, *J* = 5.0, 1.1 Hz, 1H), 7.04 (dd, *J* = 5.0, 3.7 Hz, 1H), 4.87 (s, 1H), 3.51 (s, 6H), *the NMR data is in accordance with that reported in the literature.*[42]

Compound 210. This compound was obtained as a white solid (0.6, **80%**) from 5-

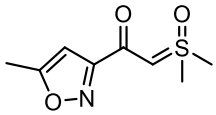

methylisoxazole-3-carbonyl chloride (0.5 g, 3.4 mmol) following **Method III**. ^{1}H NMR (500 MHz, $CDCl_3$): δ 6.33 (s, 1H), 5.36 (s, 1H), 3.53 (s, 6H), 2.46 (d, *J* = 0.9 Hz, 3H), *this product was not characterised further due to poor results in the rhodium-catalysed C–H bond functionalisation.*

Compound 70. This compound was obtained as a white solid (363 g, **54%**) from 2-

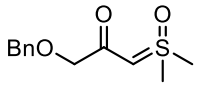

(benzyloxy)acetyl chloride (427 µL, 2.7 mmol) following **Method III**. ^{1}H NMR (500 MHz, $CDCl_3$): δ 7.38-7.27 (m, 5H), 4.90 (s, 1H), 4.59 (s, 2H), 3.92 (s, 2H), 3.42 (s, 6H), *the NMR data is in accordance with that reported in the literature.*[27]

6.3.4 Miscellaneous

Compound 214. This compound was obtained as a white solid (2.2 g, **80%**) from

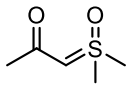

acetic anhydride (1.9 mL, 20 mmol) following **Method III**. m.p.: 68-70 °C. ^{1}H NMR (500 MHz, $CDCl_3$): δ 4.36 (s, 1H), 3.34 (s, 6H), 1.88 (s, 3H); ^{13}C NMR (125 MHz, $CDCl_3$): δ 187.8 (e), 69.6 (e), 41.9 (o, 2C), 27.6 (o); IR (neat): ν = 3070 (w), 3009 (w), 2987 (m), 1538 (vs), 1435 (m), 1377 (vs), 1331 (m), 1303 (m), 1162 (vs), 1027 (vs), 992 (s), 949 (m), 920 (m), 847 (s), 753 (m), 697 (m), 633 (m); HRMS (CI (CH_4)) calcd for ($C_5H_{10}O_2S$ + H): 135.0474; found: 135.0476.

Compound 216. This compound was obtained as a white solid (180 mg, **25%**) from

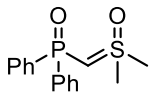

diphenylphosphinic chloride (475 µL, 2.5 mmol) following **Method III**. ^{1}H NMR (500 MHz, $CDCl_3$): δ 7.89-7.83 (m 4H), 7.51-7.41 (m , 6H),

4.15 (s, 1H), 3.40 (s, 6H), *this product was not characterised further due to poor results in the rhodium-catalysed C–H bond functionalisation.*

Compound 52. This compound was obtained as a white solid (1.6 g, **58%**) from 2-chloro-4,6-dimethylpyrimidine (2 g, 14 mmol) following **Method I**. ^{1}H NMR (500 MHz, $CDCl_3$): δ 6.28 (1H), 4.34 (s, 1H), 3.50 (s, 6H), 2.27 (s, 6H), *the NMR data is in accordance with that reported in the literature.*[31]

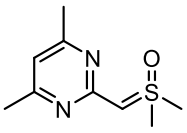

6.3.5 Bis-substituted sulfoxonium ylides

Method IV: *Representative example for the synthesis of **218**.*

To a flame dried Schlenk tube, under nitrogen, was added **52** (165 mg, 0.8 mmol, 2 equiv.) and 1,4-dioxane (3 mL). The mixture was cooled to 0 °C and a solution of propionyl chloride (38 µL, 0.4 mmol, 1 equiv.) in 1,4-dioxane (0.9 mL) was added dropwise. The mixture was stirred at room temperature for 1 h, then was filtered over celite and concentrated. Recrystallisation from ethyl acetate gave **218** as a white solid (70 mg, **64%**).

Compound 218. This compound was obtained as a white solid (70 mg, **64%**) from propionyl chloride (38 µL, 0.4 mmol) following **Method IV**. ^{1}H NMR (500 MHz, $CDCl_3$): δ 6.72 (s, 1H), 3.66 (s, 6H), 2.65 (q, J = 7.5 Hz, 2H), 2.44 (s, 6H), 1.04 (t, J = 7.5 Hz, 3H), *this product was not characterised further due to poor results in the rhodium-catalysed C–H bond functionalisation.*

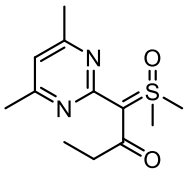

Compound 220. This compound was obtained as a white solid (237 mg, **63%**) from

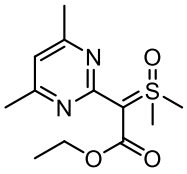

ethyl chloroformate (130 µL, 1.4 mmol) following **Method IV**. ^{1}H NMR (500 MHz, $CDCl_3$): δ 6.69 (s, 1H), 4.18 (q, *J* = 7.2 Hz, 2H), 3.67 (s, 6H), 2.43 (s, 6H), 1.26 (t, *J* = 7.2 Hz, 3H), *the NMR data is in accordance with that reported in the literature.*[31]

Compound 221. This compound was obtained as a white solid (154 mg, **20%**) from

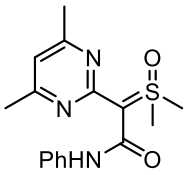

phenyl isocyanate (297 µL, 2.7 mmol) following **Method IV**. ^{1}H NMR (500 MHz, $CDCl_3$): δ 12.11 (s, 1H), 7.57 (dd, *J* = 8.5, 1.0 Hz, 2H), 7.32-7.26 (m 2H), 7.00 (t, *J* = 7.2 Hz, 1H), 6.53 (s, 1H), 3.91 (s, 6H), 2.42 (s, 6H), *the NMR data is in accordance with that reported in the literature.*[31]

Compound 469.

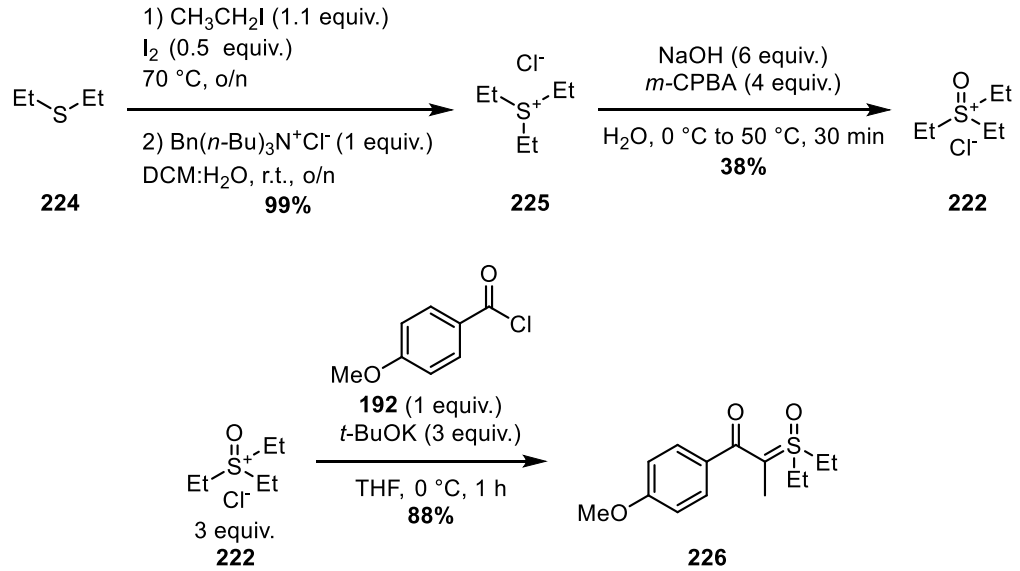

Compound 225. To a flame dried schlenk tube under N_2 was added diethyl sulfide (2.0 g, 22.7 mmol, 1.0 equiv.) followed by iodoethane (3.9 g, 25.0 mmol, 1.1 equiv.)

and iodine (2.9 g, 11.4 mmol, 0.5 equiv.). The tube was sealed and the mixture was stirred at 70 °C overnight. Then, after cooling down, the mixture was transferred into a conical flask with water (70 mL), DCM (46 mL) and tributylbenzylammonium chloride (7.1 g, 22.7 mmol, 1.0 equiv.). The mixture was protected from light and stirred overnight at room temperature. The two layers were separated and the aqueous layer was washed 5 times with DCM (30 mL). The aqueous layer was evaporated to give **225** as a hygroscopic white solid (3.5 g, **99%**). ^{1}H NMR (500 MHz, D_2O): δ 3.31 (q, *J* = 7.5 Hz, 6H), 1.45 (t, *J* = 7.5 Hz, 9H), *the NMR data is in accordance with that reported in the literature.*[69]

Compound 222. 225 (3.5 g, 22.4 mmol, 1.0 equiv.) was dissolved with water (112 mL) in a round bottom flask, the resulting solution was cooled to 0 °C and NaOH (5.4 g, 0.13 mol, 6.0 equiv.) was added. The mixture was stirred at 0 °C until homogeneity. *m*-CPBA (22.2 g, 77% in mineral oil, 90.0 mmol, 4.0 equiv.) was added portionwise and the mixture was stirred at 50 °C for 30 min. Then the pH was adjusted to pH = 1 with 6 M HCl (20 mL) at 0 °C. The precipitate was filtered off and washed with water. The corresponding filtrate was concentrated to ≈ 60 mL and washed with DCM (20 mL). The pH of the aqueous layer was adjusted to pH = 5-6 with saturated Na_2CO_3 and evaporated to dryness. The resulting solid was dispersed in warm *i*-PrOH (40 mL) and the mixture was filtered. All volatiles were removed *in vacuo* and the crude product was recrystallised from *i*-PrOH to give **222** as a white solid (1.16 g, **38%**). ^{1}H NMR (500 MHz, D_2O): δ 3.96 (q, *J* = 7.4 Hz, 6H), 1.57 (t, *J* = 7.4 Hz, 9H), *the NMR data is in accordance with that reported in the literature.*[69]

Compound 226. To a flame dried 250 mL round bottom flask, under nitrogen and covered from light, was transferred **222** (1.2 g, 6.9 mmol, 3 equiv.). The solid was suspended in dry THF (14 mL) before potassium *tert*-butoxide was added (0.8 g, 6.9 mmol, 3 equiv.). The mixture was stirred at reflux for 2 h. After cooling to 0 °C, methoxybenzoyl chloride (0.3 mL, 2.3 mmol, 1 equiv.) in THF (5 mL) was added dropwise to the mixture. The mixture was stirred at 0 °C for 1 h. The mixture was filtered through a plug of celite and all volatiles were removed under vacuum. Purification by flash chromatography (DCM/MeOH: 98/2) afforded **226** as a white powder (0.5 g, **88%**). m.p.: 93-95 °C. ^{1}H NMR (500 MHz, $CDCl_3$): δ 7.52-7.47 (m, 2H), 6.87-6.80 (m, 2H), 4.25 (dq, *J* = 13.2, 7.5 Hz, 2H), 3.77 (s, 3H), 3.26 (dq, *J* = 13.3, 7.3, Hz, 2H), 1.97 (s, 3H), 1.31 (t, *J* = 7.5 Hz, 6H); ^{13}C NMR (125 MHz, $CDCl_3$): δ 181.9 (e), 160.2 (e), 133.8 (e), 129.1 (o, 2C), 113.0 (o, 2C), 67.1 (e), 55.2 (o), 46.4 (o, 2C), 11.5 (o), 5.0 (o, 2C); IR (neat): ν = 2977 (w), 2937 (w), 2907 (w), 2842 (w), 1605 (m), 1580 (m), 1506 (vs), 1467 (m), 1448 (m), 1409 (m), 1384 (m), 1370 (s), 1297 (m), 1281 (w), 1241 (s), 1196 (w), 1173 (vs), 1132 (w), 1105 (m), 1072 (w), 1055 (w), 1029 (s), 1013 (m), 990 (s), 965 (m), 837 (s), 822 (s), 797 (s), 758 (m), 748 (m), 693 (s), 633 (m); HRMS (ESI) calcd for ($C_{14}H_{20}O_3S$ + Na): 291.1031; found: 291.1029.

6.4 Rhodium-catalysed cross-coupling of α-ketosulfoxonium ylides with C–H bonds

6.4.1 Scope of sulfoxonium ylides

Method V: *Representative example for the synthesis of **229a**.*

A flame dried Schlenk tube, sealable with a J-Young key, was charged with $AgSbF_6$ (6.9 mg, 0.02 mmol, 0.1 equiv.) in an argon-filled glovebox. The tube was taken out and $[Cp^*RhCl_2]_2$ (2.5 mg, 0.004 mmol, 0.02 equiv.) was added, followed by HFIP (1 mL) under air. Then, phenyl pyridine (29 μL, 0.2 mmol, 1.0 equiv.), NaOAc (16 mg, 0.2 mmol, 1.0 equiv.), **187** (73.5 mg, 0.34 mmol, 1.7 equiv.) and HFIP (0.5 mL) were sequentially added in that order. The tube was sealed and the mixture was stirred at 60 °C for 17 h. After cooling to room temperature, the mixture was filtered through a short plug of silica and all volatiles were removed *in vacuo*. Purification by flash chromatography (PE:EtOAc/9:1 to 8:2) afforded **229a** as a colourless oil (58 mg, **quant.**).

Method VI: *Representative example for the synthesis of **229b**.*

The procedure was identical to **Method III** except that 2.0 equiv. of sulfoxonium ylide were used.

Method VII: *Representative for the synthesis of **234**.*

The procedure was identical to **Method III** except that 2.0 equiv. of sulfoxonium ylide and the mixture was stirred at 90 °C overnight.

Compound 229a. This compound was obtained as a colourless oil (58 mg, **quant.**) from **187** following **Method V**. ^{1}H NMR (500 MHz, $CDCl_3$): δ 8.64-8.60 (m, 1H), 7.74 (dt, *J* = 7.7, 1.9 Hz, 1H), 7.45-7.41 (m, 2H), 7.40-7.34 (m, 2H), 7.26-7.21 (m, 2H), 3.89 (s, 2H), 2.21 (d, *J* = 6.8 Hz, 2H), 1.76-1.66 (m, 1H), 1.65-1.51 (m, 5H), 1.28-1.03 (m, 3H), 0.81 (dq, *J* = 12.8, 3.0 Hz, 2 H); ^{13}C NMR (125 MHz, $CDCl_3$): δ 208.0 (e), 159.7 (e), 148.7 (o),

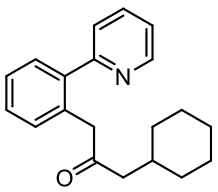

140.3 (e), 136.6 (o), 133.0 (e), 131.7 (o), 129.8 (o), 128.5 (o), 127.2 (o), 123.9 (o), 121.8 (o), 49.8 (e), 48.3 (e), 33.7 (o), 33.1 (e, 2C), 26.2 (e), 26.1 (e, 2C); IR (neat): ν = 3061 (w), 2920 (vs), 2849 (s), 1711 (vs), 1586 (s), 1561 (m), 1495 (w), 1471 (m), 1445 (m), 1425 (s), 1372(w), 1335 (m), 1286 (m), 1213 (w), 1181 (w), 1150 (w), 1091 (m), 1023 (m), 910 (br), 795 (m), 750 (vs), 731 (s); HRMS (ESI) calcd for ($C_{20}H_{23}NO$ + Na): 316.1677; found: 316.1675; Anal. Calcd for $C_{20}H_{23}NO$: C 81.86, H 7.85, N 4.78; found C 81.77, H 7.93, N 4.67.

Compound 229b. This compound was obtained as a colourless oil from **188** following

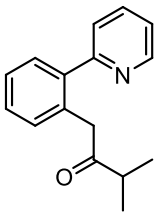

Method VI. ^{1}H NMR (500 MHz, $CDCl_3$): δ 8.63-8.59 (m, 1H), 7.74 (dt, *J* = 7.7, 1.8 Hz, 1H), 7.45-7.41 (m, 2H), 7.39-7.34 (m, 2H), 7.26-7.21 (m, 2H), 3.97 (s, 2H), 2.63 (sept, *J* = 7.1 Hz, 1H), 0.98 (d, *J* = 7.0 Hz, 6H); ^{13}C NMR (125 MHz, $CDCl_3$): δ 211.9 (e), 159.7 (e), 148.6 (o), 140.3 (e), 136.6 (o), 133.2 (e), 131.7 (o), 129.8 (o), 128.5 (o), 127.1 (o), 123.9 (o), 121.8 (o), 45.7 (e), 40.1 (o), 18.3 (o, 2C); IR (neat): ν = 3061 (w), 2968 (m), 2932 (w), 2872 (w), 1709 (s), 1586 (m), 1561 (m), 1495 (w), 1469 (m), 1442 (m), 1425 (m), 1381 (w), 1364 (w), 1335 (w), 1312 (w), 1295 (w), 1199 (w), 1040 (m), 1023 (m), 990 (m), 795 (m), 750 (vs), 634 (w), 620 (w); HRMS (CI (CH_4)) calcd for ($C_{16}H_{17}NO$ + H): 240.1383; found: 240.1385.

Compound 229c. This compound was obtained as an amorphous yellowish solid (55

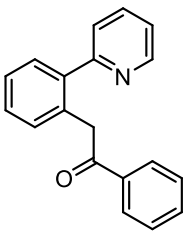

mg, **95%**) from **64** following **Method V** (without NaOAc). ^{1}H NMR (500 MHz, $CDCl_3$): δ 8.41-8.37 (m, 1H), 7.92-7.87 (m, 2H), 7.69 (dt, *J* = 7.8, 2.1 Hz, 1H), 7.55-7.48 (m, 2H), 7.47-7.44 (m, 1H), 7.44-7.37 (m, 4H), 7.36-7.30 (m, 1H), 7.13 (ddd, *J* = 7.5, 4.8, 1.2, 1H), 4.52 (s,

2H); ^{13}C NMR (125 MHz, $CDCl_3$): δ 197.8 (e), 159.4 (e), 148.5 (o), 139.9 (e), 137.0 (e), 136.5 (o), 133.2 (e), 132.6 (o), 131.8 (o), 129.7 (o), 128.5 (o), 128.3 (o, 2C), 128.1 (o, 2C), 127.2 (o), 123.7 (o), 121.6 (o), 43.5 (e); IR (neat): ν = 3076 (w), 2915 (w), 1688 (vs), 1587 (s), 1560 (m), 1497 (w), 1470 (s), 1449 (s), 1424 (m), 1401 (m), 1336 (s), 1296 (m), 1263 (w), 1211 (s), 1197 (m), 1148 (w), 1089 (w), 1025 (m), 990 (s), 939 (m), 845 (w), 796 (m), 745 (vs), 726 (s), 691 (s), 662 (m); HRMS (CI (NH_3)) calcd for ($C_{19}H_{15}NO$ + H): 274.1226; found: 274.1220.

Compound 229d. This compound was obtained as a white solid (60 mg, **85%**) from

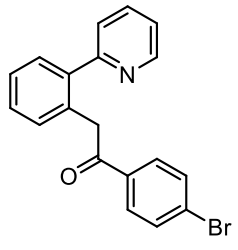

186 following **Method V**. m.p.: 93-94 °C. ^{1}H NMR (500 MHz, $CDCl_3$): δ 8.36-8.33 (m, 1H), 7.76 (d, *J* = 8.6 Hz, 2H), 7.70 (dt, *J* = 7.7, 1.7 Hz, 1H), 7.55 (d, *J* = 8.6 Hz, 2H), 7.51-7.48 (m, 1H), 7.48-7.45 (m, 1H), 7.42-7.37 (m, 2H), 7.34-7.29 (m, 1H), 7.15 (ddd, *J* = 7.5, 4.8, 1.3 Hz, 1H), 4.47 (s, 2H); ^{13}C NMR (125 MHz, $CDCl_3$): δ 196.9 (e), 159.3 (e), 148.5 (o), 139.6 (e), 136.7 (o), 135.8 (e), 133.0 (e), 131.9 (o, 2C), 131.7 (o), 129.8 (o), 129.8 (o, 2C), 128.6 (o), 127.7 (e),127.4 (o), 123.7 (o), 121.8 (o), 43.5 (e); IR (neat): ν = 3020 (w), 2908 (w), 1676 (vs), 1610 (w), 1586 (s), 1569 (m), 1560 (m), 1470 (s), 1423 (m), 1417 (m), 1394 (m), 1342 (m), 1292 (m), 1215 (s), 1147 (m), 1115 (w), 1070 (m), 995 (vs), 944 (w), 889 (w), 848 (w), 804 (vs), 793 (m), 747 (vs), 689 (m), 618 (m); Anal. Calcd for $C_{19}H_{14}BrNO$: C 64.95, H 3.99, N 3.99; found C 64.91, H 3.98, N 3.77.

Compound 229e. This compound was obtained as a yellowish solid (57 mg, **94%**) from **203** following **Method V**. m.p.: 94-97 °C. ^{1}H NMR (500 MHz, $CDCl_3$): δ 8.47 (ddd, *J* = 4.9, 1.8, 0.9 Hz, 1H), 7.89-7.85 (m, 2H), 7.69 (dt, *J* = 7.7, 1.8 Hz, 1H), 7.49-7.43 (m, 2H), 7.40-7.34 (m, 2H), 7.34-7.30 (m, 1), 7.16 (ddd, *J* = 7.6, 4.9, 1.2 Hz, 1H), 6.89-6.86 (m, 2H), 4.46 (s, 2H), 3.84 (s, 3H); ^{13}C NMR (125 MHz, $CDCl_3$): δ 196.5 (e), 163.2 (e), 159.5 (e), 148.7 (o), 140.0 (e), 136.6 (o), 133.5 (e), 131.5 (o), 130.5 (o, 2C), 129.9 (e), 129.8 (o), 128.5 (o), 127.1 (o), 123.9 (o), 121.7 (o), 113.5 (o, 2C), 55.4 (o), 43.0 (e); IR (neat): ν = 3054 (w), 2974 (w), 2898 (w), 1678 (vs), 1590 (vs), 1560 (m), 1511 (m), 1462 (m), 1441 (m), 1431 (m), 1344 (s), 1316 (m), 1265 (s), 1221 (s), 1198 (w), 1163 (vs), 1113 (w), 1090 (w), 1011 (s), 992 (s), 956 (w), 827 (vs), 811 (m), 794 (m), 748 (vs), 720 (m), 621 (m); Anal. Calcd for $C_{20}H_{17}NO$: C 79.17, H 5.61, N 4.62; found C 78.77, H 5.68, N 4.47.

Compound 229f. This compound was obtained as a white solid (41 mg, **66%**) from **206** following **Method VI**. m.p.: 117-120 °C. ^{1}H NMR (500 MHz, $CDCl_3$): δ 8.35-8.29 (m, 1H), 7.72 (dt, *J* = 7.8, 1.9 Hz, 1H), 7.55-7.47 (m, 2H), 7.45-7.38 (m, 4H), 7.35-7.30 (m, 1H), 7.15 (ddd, *J* = 7.4, 4.9, 1.1 Hz, 1H), 6.98 (tt, *J* = 8.5, 2.3 Hz, 1H), 4.46 (s, 2H); ^{13}C NMR (125 MHz, $CDCl_3$): δ 195.3 (e), 163.9 (e, d, *J* = 11.8 Hz), 161.9 (e, d, *J* = 11.9 Hz), 159.1 (e), 148.4 (o), 140.2 (e, t, *J* = 7.2 Hz), 139.3 (e), 136.9 (o), 132.6 (e), 132.0 (o), 129.8 (o), 128.7 (o), 127.6 (o), 123.6 (o), 121.9 (o), 111.1 (o, dd, *J* = 20.3, 6.4, 2C), 107.8 (o, t, *J* = 25.2 Hz), 43.8 (e); IR (neat): ν = 3054 (w), 2901 (w), 1684 (s), 1619 (m), 1592 (s), 1561 (w), 1474 (m), 1455 (w), 1436 (s), 1425 (m), 1416 (m), 1345 (s), 1299 (s), 1231 (w), 1167 (m), 1151 (m), 1120 (s), 1091 (w), 1048 (w), 980

(s), 874 (m), 854 (m), 795 (m), 746 (vs), 709 (s), 669 (m), 622 (w), 609 (w); Anal. Calcd for $C_{19}H_{13}F_2NO$: C 73.76, H 4.21, N 4.53; found C 73.41, H 4.25, N 4.39.

Compound 229g. This compound was obtained as a orange amorphous solid (51 mg, **97%**) from **208** following **Method V** and stirring for 48 h. ^{1}H NMR (500 MHz, $CDCl_3$): δ 8.47 (ddd, *J* = 4.8, 1.8, 0.9 Hz, 1H), 7.71 (dt, *J* = 7.7, 1.8 Hz, 1H), 7.51 (dd, *J* = 1.8, 0.8 Hz, 1H), 7.49-7.44 (m, 2H), 7.41-7.34 (m, 3H), 7.18 (ddd, *J* = 7.6, 4.9, 1.1 Hz, 1H), 7.08 (dd, *J* = 3.6, 0.7 Hz, 1H), 6.47 (dd, *J* = 3.5, 1.8 Hz, 1H), 4.35 (s, 2H); ^{13}C NMR (125 MHz, $CDCl_3$): δ 186.8 (e) 159.4 (e), 152.5 (e), 148.6 (o), 146.0 (o), 140.2 (e), 136.5 (o), 132.5 (e), 131.7 (o), 129.8 (o), 128.5 (o), 127.3 (o), 123.9 (o), 121.7 (o), 117.1 (o), 112.0 (o), 43.0 (e); IR (neat): ν = 3114 (w), 2981 (w), 1668 (vs), 1591 (m), 1561 (m), 1469 (s), 1439 (m), 1397 (s), 1300 (w), 1258 (s), 1165 (m), 1083 (w), 1038 (m), 1004 (s), 990 (m), 952 (w), 884 (m), 772 (s), 745 (vs), 718 (m), 622 (w); HRMS (ESI) calcd for ($C_{17}H_{13}NO_2$ + Na): 264.1025; found: 264.1017.

Compound 229h. This compound was obtained as a yellowish solid (52 mg, **93%**) from **209** following **Method VI** and stirring for 24 h. m.p.: 76-79 °C. ^{1}H NMR (500 MHz, $CDCl_3$): δ 8.50-8.47 (m, 1H), 7.71 (dt, *J* = 7.7, 2.0 Hz, 1H), 7.60 (dd, *J* = 3.8, 1.1 Hz, 1H), 7.57 (dd, *J* = 5.0, 1.1 Hz, 1H), 7.50-7.44 (m, 2H), 7.41-7.35 (m, 3H), 7.18 (ddd, *J* = 7.6, 4.9, 1.1 Hz, 1H), 7.06 (dd, *J* = 5.0, 3.9 Hz, 1H), 4.44 (s, 2H); ^{13}C NMR (125 MHz, $CDCl_3$): δ 190.7 (e), 159.4 (e), 148.7 (o), 144.1 (e), 140.1 (e), 136.6 (o), 133.2 (o), 132.8 (e), 132.0 (o), 131.6 (o), 129.8 (o), 128.5 (o), 127.9 (o), 127.3 (o), 123.9 (o), 121.8 (o), 44.0 (e); IR (neat): ν = 3105 (w), 1657 (s), 1586 (s), 1560 (m), 1519 (m), 1472 (m),

1443 (m), 1414 (s), 1354 (w), 1328 (m), 1234 (m), 1226 (s), 1176 (w), 1082 (m), 1060 (m), 1023 (m), 993 (m), 944 (m), 863 (m), 799 (m), 742 (vs), 732 (vs), 714 (vs); Anal. Calcd for $C_{17}H_{13}NOS$: C 73.10, H 4.66, N 5.02, S 11.47; found C 73.07, H 4.76, N 4.83, S 11.42.

Compound 229i. This compound was obtained as an amorphous beige solid (28 mg, **90%**) from phenyl pyridine (14 μL, 0.1 mmol, 1.0 equiv.) and **189** (40 mg, 0.17 mmol) following **Method V**. ^{1}H NMR (500 MHz, $CDCl_3$): δ 8.55 (d, *J* = 4.7 Hz, 1H), 7.69 (dt, *J* = 7.7, 1.8 Hz, 1H), 7.48-7.42 (m, 1H), 7.41-7.34 (m, 3H), 7.33-7.28 (m, 1H), 7.28-7.22 (m, 2H), 7.21-7.15 (m, 2H), 7.02-6.94 (m, 2H), 4.09 (dd, *J* = 16.4, 3.4 Hz, 2H), 2.42-2.36 (m, 1H), 2.22-2.15 (m, 1H), 1.60-1.55 (m, 1H), 1.28-1.23 (m, 1H); ^{13}C NMR (125 MHz, $CDCl_3$): δ 206.4 (e), 159.5 (e), 148.7 (o), 140.5 (e), 140.2 (e), 136.5 (o), 132.9 (e), 131.7 (o), 129.8 (o), 128.6 (o), 128.3 (o, 2C), 127.3 (o), 126.3 (o), 126.1 (o, 2C), 123.8 (o), 121.8 (o), 48.7 (e), 31.7 (o), 29.1 (o), 19.1 (e); IR (neat): ν = 3060 (w), 3028 (w), 2920 (w), 1693 (vs), 1601 (w), 1585 (m), 1562 (m), 1495 (m), 1471 (m), 1440 (m), 1426 (s), 1341 (s), 1313 (m), 1287 (m), 1151 (m), 1095 (s), 1071 (s), 1030 (w), 942 (m), 905 (w), 765 (s), 751 (vs), 703 (vs), 658 (s); HRMS (CI (CH_4)) calcd for ($C_{22}H_{19}NO$ + H): 314.1539; found: 314.1544.

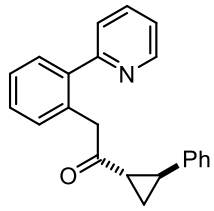

Compound 229j. This compound was obtained as a white solid (59 mg, **89%**) from **207** following **Method VI**. m.p.: 69-73 °C. ^{1}H NMR (500 MHz, $CDCl_3$): δ 8.62 (ddd, *J* = 4.9, 1.7, 0.9 Hz, 1H), 7.72 (dt, *J* = 7.7, 1.8 Hz, 1H), 7.42-7.37 (m, 2H), 7.37-7.31 (m, 2H), 7.21 (ddd, *J* = 7.5, 4.8, 1.1 Hz, 1H), 7.19-7.14 (m, 1H), 4.06 (s, 2H), 1.98 (br s, 3H),

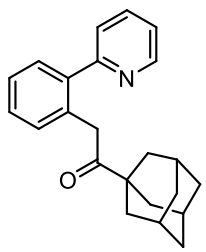

1.75-1.68 (m, 9H), 1.66-1.59 (m, 3H); ^{13}C NMR (125 MHz, $CDCl_3$): δ 212.6 (e), 160.1 (e), 148.6 (o), 140.6 (e), 136.5 (o), 133.3 (e), 131.6 (o), 129.7 (o), 128.2 (o), 126.9 (o), 124.2 (o), 121.6 (o), 46.4 (e), 41.1 (e), 38.4 (e, 3C), 36.5 (e, 3C), 28.0 (o, 3C); IR (neat): ν = 3056 (w), 2914 (s), 2901 (s), 2850 (m), 1691 (s), 1587 (m), 1560 (w), 1495 (w), 1470 (m), 1448 (m), 1426 (m), 1366 (w), 1345 (w), 1326 (w), 1304 (w), 1292 (w), 1194 (m), 1159 (m), 1089 (w), 1025 (m), 910 (s), 790 (m), 756 (s), 735 (vs), 669 (m), 646 (m); Anal. Calcd for $C_{23}H_{25}NO$: C 83.34, H 7.55, N 4.23; found C 83.03, H 7.66, N 4.03.

Compound 229k. This compound was obtained as an amorphous beige solid (68 mg, **86%**) from **168** following **Method VI**. ^{1}H NMR (500 MHz, $CDCl_3$): δ 8.61-8.56 (m, 1H), 7.75 (dt, *J* = 7.8, 1.8 Hz, 1H), 7.48-7.42 (m, 2H), 7.40-7.34 (m, 2H), 7.26-7.21 (m, 2H), 4.02 (br s, 2H), 3.97 (s, 2H), 2.78-2.61 (m, 2H), 2.52 (tt, *J* = 11.3, 3.6 Hz, 1H), 1.71-1.60 (m, 2H), 1.50-1.38 (m, 12H); ^{13}C NMR (125 MHz, $CDCl_3$): δ 209.4 (e), 159.6 (e), 154.6 (e), 148.5 (o), 140.0 (e), 136.7 (o), 132.8 (e), 131.8 (o), 129.8 (o), 128.6 (o), 127.3 (o), 123.9 (o), 121.9 (o), 79.5 (e), 47.6 (o), 46.0 (e), 28.4 (o, 3C), 27.5 (e, 4C); IR (neat): ν = 2975 (w), 2941 (w), 2854 (w), 2246 (w), 1717 (m), 1671 (vs), 1588 (m), 1561 (w), 1472 (m), 1444 (m), 1425 (vs), 1391 (m), 1365 (m), 1336 (w), 1276 (m), 1237 (s), 1160 (vs), 1132 (vs), 1028 (m), 1010 (s), 989 (w), 911 (m), 798 (w), 753 (vs), 730 (vs); HRMS (ESI) calcd for ($C_{23}H_{29}N_2O_3$ + Na): 381.2178; found: 381.2177.

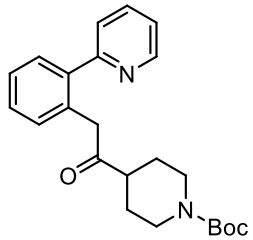

.

Compound 230. This compound was obtained as a yellow solid (10 mg, **27%**) from

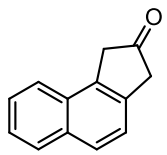

190 following **Method V**. ^{1}H NMR (500 MHz, $CDCl_3$): δ 7.89 (d, *J* = 8.2 Hz, 1H), 7.80 (d, *J* = 8.4 Hz, 1H), 7.70 (d, *J* = 8.1 Hz, 1H), 7.56 (td, *J* = 7.0, 1.3 Hz, 1H), 7.50 (td, *J* = 8.2, 1.3 Hz, 1H), 7.44 (d, *J* = 8.3 Hz, 1H), 3.84 (s, 2H), 3.74 (s, 2H); ^{13}C NMR (125 MHz, $CDCl_3$): δ 214.8 (e), 135.0 (e), 133.9 (e), 132.7 (e), 130.0 (e), 128.9 (o), 128.0 (o), 126.8 (o), 125.7 (o), 124.2 (o), 122.8 (o), 45.1 (e), 42.6 (e), *the NMR data is in accordance with that reported in the literature.*[120]

Compound 231. This compound was obtained as a yellow solid (40 mg, **57%**) from

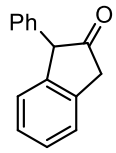

169 following **Method V**. ^{1}H NMR (500 MHz, $CDCl_3$): δ 7.44 (d, *J* = 7.5 Hz, 1H), 7.41-7.29 (m , 5H), 7.24 (d, *J* = 7.5 Hz, 1H), 7.17-7.14 (m, 2H), 4.72 (s, 1H), 3.71 (s, 2H); ^{13}C NMR (125 MHz, $CDCl_3$): δ 213.9 (e), 141.3 (e), 138.1 (e), 137.3 (e), 128.8 (o, 2C), 128.5 (o, 2C), 128.0 (o), 127.9 (o), 127.4 (o), 126.1 (o), 124.9 (o), 59.8 (o), 43.0 (e), *the NMR data is in accordance with that reported in the literature.*[121]

Compound 232. This compound was obtained as an orange solid (18 mg, **38%**) from

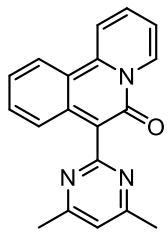

221 following **Method V**. ^{1}H NMR (500 MHz, $CDCl_3$): δ 10.00 (m, 1H), 8.74 (d, *J* = 9.0 Hz, 1H), 8.35 (d, *J* = 8.6 Hz, 1H), 8.00 (ddd, *J* = 8.9, 6.9, 1.5 Hz, 1H), 7.61 (dt, *J* = 7.0, 1.3 Hz, 1H), 7.45 (ddd, *J* = 8.8, 6.6, 1.1 Hz, 1H), 7.32 (d, *J* = 8.5 Hz, 1H), 7.20 (ddd, *J* = 8.6, 6.6, 1.1 Hz, 1H), 7.06 (s, 1H), 2.60 (s, 6H); ^{13}C NMR (125 MHz, $CDCl_3$): δ 167.4 (e, 2C), 165.0 (e), 153.1 (e), 142.7 (e), 137.4 (e), 134.1 (o), 131.8 (o), 131.1 (o), 123.7 (o), 122.8 (o), 121.5 (o), 120.8 (o), 118.9 (o), 118.1 (o), 114.0 (e), 107.7 (e), 24.2 (o, 2C);

IR (neat): ν = 3113 (w), 3054 (w), 2919 (w), 1651 (vs), 1622 (s), 1609 (s), 1583 (vs), 1520 (m), 1505 (m), 1475 (vs), 1451 (s), 1369 (m), 1325 (w), 1275 (s), 1219 (s), 1164 (m), 1147 (s), 1099 (m), 1063 (w), 1047 (m), 991 (m), 954 (m), 936 (w), 895 (w), 872 (m), 841 (w), 813 (w), 780 (m), 743 (vs), 711 (s), 676 (m); HRMS (CI (CH_4)) calcd for ($C_{19}H_{15}N_3O$ + H): 302.1288; found: 302.1298.

Compound 229m. This compound was obtained from phenylpyridine (29 μL, 0.2 mmol, 1.0 equiv) and **226** (107 mg, 0.4 mmol, 2.0 equiv) according to **Method V** but stirring at 90 °C for 48 h. After purification by flash chromatography (PE:EA/9:1 to 8:2), **229m** could not be obtained entirely free from unidentified impurities. A yield of 50% was determined by ^{1}H NMR after adding 1,3,5-trimethoxybenzene (34 mg, 0.2 mmol, 1.0 equiv.) as internal standard. A fraction suitable for characterisation was obtained following **Method V**. ^{1}H NMR (500 MHz, $CDCl_3$): δ 8.74-8.68 (m, 1H), 7.93-7.87 (m, 2H), 7.81 (td, *J* = 7.7, 1.9 Hz, 1H), 7.45 (dt, *J* = 7.8, 1.0 Hz, 1H), 7.40-7.36 (m, 1H), 7.33-7.24 (m, 4H), 6.82-6.76 (m, 2H), 5.11 (q, *J* = 7.0 Hz, 1H), 3.79 (s, 3H), 1.43 (d, *J* = 6.9 Hz, 3H); ^{13}C NMR (125 MHz, $CDCl_3$): δ 199.8 (e), 163.0(e), 159.9 (e), 149.2 (o), 140.1 (e), 139.2 (e), 136.6 (o), 131.2 (o, 2C), 130.2 (o), 129.4 (e), 129.0 (o), 127.7 (o), 126.7 (o), 124.3 (o), 122.0 (o), 113.4 (o, 2C), 55.3 (o), 43.3 (o), 19.0 (o); IR (neat): ν = 3041 (w), 2969 (w), 2844 (w), 1667 (vs), 1595 (vs), 1508 (m), 1494 (w), 1464 (m), 1442 (m), 1372 (w), 1325 (m), 1305 (w), 1283 (w), 1262 (s), 1242 (s), 1225 (s), 1189 (w), 1163(vs), 1149 (m), 1112 (w), 1092 (w), 1023 (s), 998 (m), 988 (m), 949 (m), 907 (w), 843 (s), 815 (w), 790 (m), 783 (m), 759 (vs), 6974 (m), 618 (m); HRMS (CI (CH_4)) calcd for ($C_{21}H_{19}NO_2$ + H): 318.1489; found: 318.1494.

6.4.2 Scope of Csp^2–H

Compound 233a/233b This mixture of compounds was obtained as a colourless oil

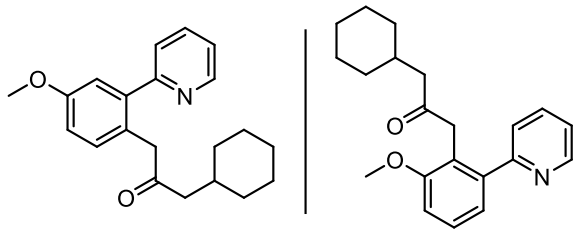

(32 mg, **50%**, 2.5:1 mixture of regioisomer) from 2-(3-methoxyphenyl)pyridine (37 mg, 0.2 mmol, 1.0 equiv.) and **187** following **Method V**. ^{1}H NMR (500 MHz, $CDCl_3$): δ 8.67-8.59 (m, 1.4H, *maj*+*min*), 7.79-7.67 (m, 1.4H, *maj*+*min*), 7.46-7.38 (m, 1.4H, *maj*+*min*), 7.33 (t, *J* = 7.8 Hz, 0.6H, *min*), 7.26-7.20 (m, 1.4H, *maj*+*min*), 7.15 (d, *J* = 8.4 Hz, 1H, *maj*), 7.05 (d, *J* = 7.9 Hz, 0.5 H, *min*), 6.98 (d, *J* = 2.5 Hz, 1H, *maj*), 6.96-6.89 (m, 1.5 H, *maj*+*min*), 3.85-3.82 (m, 3.9H, *maj*+*min*), 3.79 (s, 2.8H, *maj*+*min*), 2.27 (d, *J* = 7.0 Hz, 0.9H, *min*), 2.18 (d, *J* = 6.8 Hz, 2H, *maj*), 1.86-1.48 (m, 13.6H, *maj*+*min*), 1.29-1.01 (m, 4.9H, *maj*+*min*), 0.93-0.72 (m, 3.3H, *maj*+*min*); ^{13}C NMR (125 MHz, $CDCl_3$): δ 208.7 (e, *min*), 208.5 (e, *maj*), 159.5 (e, *maj*), 159.4 (e, *min*), 158.5 (e, *maj*), 157.8 (e, *min*), 148.9 (o, *min*), 148.7 (o, *maj*), 142.0 (e, *min*), 141.3 (e, *maj*), 136.6 (o, *maj*), 136.3 (o, *min*), 132.6 (o, *maj*), 127.7 (o, *min*), 125.1 (e, *maj*), 124.1 (o, *min*), 123.9 (o, *maj*), 122.6 (e, *min*), 122.0 (o, *min*), 121.9 (o, *maj*), 121.8 (o, *min*), 115.3 (o, *maj*), 114.1 (o, *maj*), 110.3 (o, *min*), 55.7 (o, *min*), 55.4 (o, *maj*), 49.7 (e, *min*), 49.6 (e, *maj*), 47.5 (e, *maj*), 41.9 (e, *min*), 33.7 (o, *min*), 33.7 (o, *maj*), 33.1 (e, 2C, *min*), 33.1 (e, 2C, *maj*), 26.2 (e, *min*), 26.2 (e, *maj*), 26.1 (e, 2C, *min*), 26.1 (e, 2C, *maj*); IR (neat): ν = 2921 (s), 2849 (m), 1710 (s), 1609 (m), 1589 (m), 1562 (m), 1504 (m), 1472 (m), 1462 (m), 1448 (m), 1426 (m), 1372 (w), 1352 (w), 1322 (m), 1300 (m), 1258 (m), 1218 (m), 1177 (m), 1150 (w), 1092 (w), 1054 (m), 1033 (s), 991 (w), 965 (w), 946 (w), 909 (m), 858 (w),

789 (w), 774 (m), 729 (vs), 646 (w), 611 (w); HRMS (CI (CH_4)) calcd for ($C_{21}H_{25}NO_2$ + H): 324.1958; found: 324.1967.

Compound 234. This compound was obtained as an amorphous pale-yellow solid (29 mg, **40%;** 53 mg, **73%**) from ethyl 3-(pyridin-2-yl)benzoate (45 mg, 0.2 mmol, 1.0 equiv.) and **187** following **Method V** and **Method VII** respectively. ^{1}H NMR (500 MHz, $CDCl_3$): δ 8.62 (d, *J* = 4.6, 1H), 8.12 (d, *J* = 1.7 Hz, 1H), 8.04 (dd, *J* = 8.0, 1.9 Hz, 1H), 7.77 (td, *J* = 7.7, 1.7 Hz, 1H), 7.49 (dt, *J* = 7.8, 0.9 Hz, 1H), 7.32 (d, *J* = 7.9 Hz, 1H), 7.29-7.23 (m, 1H), 4.38 (q, *J* = 7.2 Hz, 2H), 3.96 (s, 2H), 2.22 (d, *J* = 7.0 Hz, 2H), 1.77-1.65 (m, 1H), 1.64-1.57 (m, 3H), 1.56-1.48 (m, 2H), 1.38 (t, *J* = 7.2 Hz, 3H), 1.26-1.15 (m, 2H), 1.13-1.05 (m, 1H), 0.86-0.74 (m, 2H); ^{13}C NMR (125 MHz, $CDCl_3$): δ 207.1 (e), 166.2 (e), 158.7 (e), 148.7 (o), 140.3 (e), 138.2 (e), 136.8 (o), 131.9 (o), 130.9 (o), 129.4 (e), 129.4 (o), 124.0 (o), 122.1 (o), 70.0 (e), 50.0 (e), 48.3 (e), 33.6 (o), 33.0 (e, 2C), 26.1 (e), 26.0 (e, 2C), 14.3 (o); IR (neat): ν = 2921 (s), 2850 (m), 1714 (vs), 1610 (m), 1587 (m), 1563 (w), 1472 (w), 1447 (w), 1427 (w), 1410 (w), 1366 (w), 1296 (m), 1274 (m), 1242 (vs), 1171 (w), 1108 (s), 1043 (m), 1020 (w), 992 (w), 916 (m), 793 (w), 752 (s), 731 (m), 645 (w); HRMS (CI (CH_4)) calcd for ($C_{23}H_{27}NO_3$ + H): 366.2064; found: 366.2068.

Compound 235. This compound was obtained as an amorphous yellowish solid (52 mg, **78%**) from 1-(pyridin-2-yl)-1*H*-indole (39 mg, 0.2 mmol, 1.0 equiv.) and **187** following **Method V**. ^{1}H NMR (500 MHz, $CDCl_3$): δ 8.58-8.53 (m, 1H), 7.89 (td, *J* = 7.7, 2.0 Hz, 1H), 7.65-7.60 (m, 1H), 7.56-7.52 (m, 1H), 7.46-7.41 (m, 1H), 7.27 (ddd, *J* = 7.4, 4.9, 1.0

Hz, 1H), 7.21-7.15 (m, 2H), 6.56 (s, 1H), 4.01 (s, 2H), 2.29 (d, *J* = 6.8 Hz, 2H), 1.80-1.69 (m, 1H), 1.68-1.59 (m, 3H), 1.59-1.51 (m, 2H), 1.30-1.17 (m, 2H), 1.15-1.04 (m, 1H), 0.87-0.77 (m, 2H); ^{13}C NMR (125 MHz, $CDCl_3$): δ 206.4 (e), 151.1 (e), 149.1 (o), 138.3 (o), 136.8 (e), 133.9 (e), 128.5 (e), 122.2 (o), 121.7 (o), 120.9 (o), 120.4 (o), 120.2 (o), 110.2 (o), 105.7 (o), 49.4 (e), 42.9 (e), 33.5 (o), 33.0 (e, 2C), 26.1 (e), 26.0 (e, 2C); IR (neat): ν = 2933 (m), 2915 (s), 1842 (m), 1724 (s), 1580 (m), 1561 (m), 1470 (vs), 1459 (s), 1436 (vs), 1406 (m), 1392 (w), 1371 (m), 1349 (m), 1330 (m), 1313 (m), 1279 (w), 1220 (m), 1192 (w), 1152 (w), 1099 (w), 1048 (m), 1021 (w), 989 (w), 969 (w), 929 (w), 887 (w), 855 (w), 805 (m), 780 (s), 743 (vs), 727 (s), 658 (w); HRMS (CI (CH_4)) calcd for ($C_{22}H_{24}N_2O$ + H): 333.1961; found: 333.1963.

Compound 236. This compound was obtained as a yellowish oil (34 mg, **75%**) from

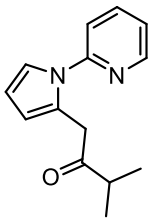

2-(1*H*-pyrrol-1-yl)pyridine (29 mg, 0.2 mmol, 1.0 equiv.) and **188** following **Method V**. ^{1}H NMR (500 MHz, $CDCl_3$): δ 8.36-8.32 (m, 1H), 7.77-7.72 (m, 1H), 7.33-7.29 (m, 1H), 7.12 (ddd, *J* = 7.4, 4.9, 0.9 Hz, 1H), 7.08 (dd, *J* = 3.1, 1.8 Hz, 1H), 6.29 (t, *J* = 3.2 Hz, 1H), 6.19-6.15 (m, 1H), 4.05 (s, 2H), 2.74 (sept, *J* = 6.9 Hz, 1H), 1.05 (d, *J* = 6.9 Hz, 6H); ^{13}C NMR (125 MHz, $CDCl_3$): δ 211.5 (e), 152.6 (e), 147.8 (o), 138.6 (o), 127.1 (e), 120.6 (o), 120.3 (o), 115.4 (o), 112.7 (o), 109.8 (o), 40.9 (e), 39.5 (o), 18.3 (o, 2C); IR (neat): ν = 2970 (m), 2932 (w), 1709 (s), 1590 (s), 1477 (vs), 1441 (vs), 1381 (m), 1334 (s), 1285 (w), 1255 (w), 1234 (w), 1205 (w), 1179 (w), 1154 (m), 1115 (w), 1095 (w), 1043 (m), 998 (w), 912 (w), 877 (w), 784 (s), 707 (vs), 654 (w); HRMS (CI (CH_4)) calcd for ($C_{14}H_{16}N_2O$ + H): 229.1335; found: 229.1341.

Compound 237. This compound was obtained as a yellowish oil (28 mg, **56%**) from

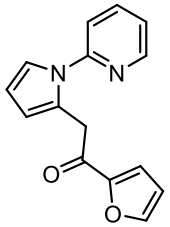

2-(1*H*-pyrrol-1-yl)pyridine (29 mg, 0.2 mmol, 1.0 equiv.) and **208** following **Method V**. ^{1}H NMR (500 MHz, $CDCl_3$): δ 8.14-8.11 (m, 1H), 7.75-7.69 (m, 1H), 7.57-7.53 (m, 1H), 7.32 (d, *J* = 8.4 Hz, 1H), 7.13-7.08 (m, 2H), 7.07-7.04 (m, 1H), 6.52-6.48 (m, 1H), 6.30 (t, *J* = 3.3 Hz, 1H), 6.26-6.22 (m, 1H), 4.48 (s, 2H); ^{13}C NMR (125 MHz, $CDCl_3$): δ 186.0 (e), 152.6 (e), 152.5 (e), 147.9 (o), 145.9 (o), 138.5 (o), 126.0 (e), 120.6 (o), 120.4 (o), 116.8 (o), 115.3 (o), 113.1 (o), 112.0 (o), 109.9 (o), 38.5 (e); IR (neat): ν = 3127 (w), 2904 (w), 1677 (s), 1589 (s), 1570 (m), 1474 (vs), 1441 (vs), 1390 (m), 1333 (s), 1287 (w), 1258 (m), 1237 (m), 1202 (w), 1158 (m), 1112 (w), 1095 (w), 1083 (w), 1025 (m), 994 (m), 984 (m), 913 (m), 900 (m), 882 (m), 822 (w), 782 (s), 738 (m), 710 (m), 682 (m), 663 (w), 609 (w); HRMS (CI (CH_4)) calcd for ($C_{15}H_{12}N_2O_2$ + H): 253.0972; found: 253.0977.

Compound 238. This compound was obtained as an orange amorphous solid (23 mg,

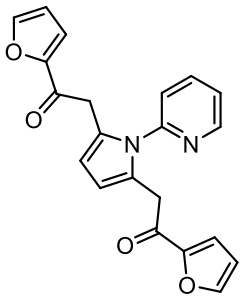

32%) from 2-(1*H*-pyrrol-1-yl)pyridine (29 mg, 0.2 mmol, 1.0 equiv.) and **208** following **Method V**. ^{1}H NMR (500 MHz, $CDCl_3$): δ 8.47-8.42 (m, 1H), 7.75 (td, *J* = 7.7, 1.9 Hz, 1H), 7.52-7.49 (m, 2H), 7.31 (d, *J* = 7.9 Hz, 1H), 7.23 (ddd, *J* = 7.5, 4.9, 1.0 Hz, 1H), 7.03 (d, *J* = 3.6 Hz, 2H), 6.46 (dd, *J* = 3.5, 1.7 Hz, 2H), 6.17 (s, 2H), 4.07 (s, 4H); ^{13}C NMR (125 MHz, $CDCl_3$): δ 185.2 (e, 2C), 151.9 (e), 151.1 (e, 2C), 149.2 (o), 146.3 (o, 2C), 138.2 (o), 126.1 (e, 2C), 122.8 (o), 122.5 (o), 117.7 (o, 2C), 112.2 (o, 2C), 110.2 (o, 2C), 37.3 (e, 2C); IR (neat): ν = 3122 (w), 2922 (w), 1672 (vs), 1661 (vs), 1588 (m), 1567 (m), 1503 (w), 1465 (vs), 1442 (s), 1419 (m), 1388 (s), 1326 (m), 1300 (m), 1290 (m), 1255 (m), 1234 (w), 1220 (w),

1156 (w), 1082 (w), 1052 (w), 1039 (w), 1015 (w), 990 (s), 909 (m), 881 (m), 844 (w), 818 (w), 780 (s), 770 (s), 750 (vs), 728 (s), 707 (m), 684 (w), 664 (m), 655 (m), 642 (m), 616 (m); HRMS (CI (CH_4)) calcd for ($C_{21}H_{16}N_2O_4$ + H): 361.1183; found: 361.1182.

Compound 239. This compound was obtained as an amorphous brown solid (38 mg, **63%**) from 2-(furan-3-yl)pyridine (29 mg, 0.2 mmol, 1.0 equiv.) and **189** following **Method V**. ^{1}H NMR (500 MHz, $CDCl_3$): δ 8.50 (ddd, *J* = 4.8, 1.8, 0.9 Hz, 1H), 7.64 (td, *J* = 7.8, 1.9 Hz, 1H), 7.43-7.38 (m, 2H), 7.27-7.21 (m, 2H), 7.18 (tt, *J* = 6.4, 1.4 Hz, 1H), 7.09 (ddd, *J* = 7.5, 4.8, 1.1 Hz, 1H), 7.04-6.99 (m, 2H), 6.75 (d, *J* = 2.0 Hz, 1H), 4.46 (s, 2H), 2.53 (ddd, *J* = 9.0, 6.5, 4.1 Hz, 1H), 2.36 (ddd, *J* = 8.1, 5.3, 4.1 Hz, 1H), 1.71 (ddd, *J* = 9.3, 5.3, 4.2 Hz, 1H), 1.32 (ddd, *J* = 8.1, 6.6, 4.2 Hz, 1H); ^{13}C NMR (125 MHz, $CDCl_3$): δ 204.6 (e), 152.4 (e), 149.2 (o), 147.9 (e), 141.9 (o), 140.3 (e), 136.4 (o), 128.3 (o, 2C), 126.3 (o), 126.2 (o, 2C), 122.3 (e), 121.1 (o), 120.6 (o), 109.8 (o), 43.4 (e), 31.4 (o), 29.4 (o), 18.9 (e); IR (neat): ν = 3027 (w), 2981 (w), 1698 (vs), 1612 (s), 1584 (s), 1558 (m), 1515 (m), 1496 (w), 1482 (m), 1428 (s), 1396 (s), 3141 (s), 1235 (m), 1180 (m), 1144 (m), 1085 (m), 1071 (m), 997 (m), 979 (m), 934 (w), 910 (m), 893 (m), 788 (s), 740 (vs), 696 (vs), 674 (m); HRMS (CI (CH_4)) calcd for ($C_{20}H_{17}NO$ + H): 304.1332; found: 304.1335.

Compound 240. This compound was obtained as an amorphous yellowish solid (28 mg, **45%**) from 2*H*-(1,2'-bipyridin)-2-one (34 mg, 0.2 mmol, 1.0 equiv.) and **187** following **Method V** with stirring at 90 °C. ^{1}H NMR (500 MHz, $CDCl_3$): δ 8.62-8.55 (m, 1H), 7.82 (td, *J* = 7.6,

2.0 Hz, 1H), 7.93-7.33 (m, 3H), 6.58 (dd, *J* = 9.2, 0.8 Hz, 1H), 6.08 (d, *J* = 7.0 Hz, 1H), 3.49 (s, 2H), 1.96 (d, *J* = 6.7 Hz, 2H), 1.64-1.49 (m, 4H), 1.44-1.37 (m, 2H), 1.22-1.11 (m, 2H), 1.10-1.00 (m, 1H), 0.80-0.68 (m, 2H); ^{13}C NMR (125 MHz, $CDCl_3$): δ 204.2 (e), 163.5 (e), 151.5 (e), 149.3 (o), 142.3 (e), 139.8 (o), 138.3 (o), 125.1 (o), 124.0 (o), 120.1 (o), 108.4 (o), 49.8 (e), 47.9 (e), 33.5 (o), 32.9 (e, 2C), 26.0 (e), 25.9 (e, 2C); IR (neat): ν = 3048 (w), 2918 (m), 2850 (m), 1714 (m), 1657 (vs), 1582 (vs), 1514 (vs), 1468 (m), 1434 (m), 1420 (m), 1393 (m), 1357 (w), 1273 (w), 1245 (w), 1146 (m), 1094 (w), 1083 (w), 1057 (w), 990 (m), 966 (w), 935 (w), 917 (m), 784 (s), 746 (s), 732 (s), 685 (w), 623 (w); HRMS (CI (CH_4)) calcd for ($C_{19}H_{22}N_2O_2$ + H): 311.1754; found: 317.1754.

6.4.3 Scope of directing groups

6.4.3.1 Quinolines

Compound 242a. This compound was obtained as an colourless paste (53 mg, **77%**) from 2-phenylquinoline (41 mg, 0.2 mmol, 1.0 equiv.) and **187** following **Method VII**. ^{1}H NMR (500 MHz, $CDCl_3$): δ 8.22 (d, *J* = 8.3 Hz, 1H), 8.09 (d, *J* = 8.5 Hz, 1H), 7.85 (dd, *J* = 8.2, 1.2 Hz, 1H), 7.74 (ddd, *J* = 8.6, 6.9, 1.4 Hz, 1H), 7.60-7.52 (m, 3H), 7.44-7.39 (m, 2H), 7.32-7.27 (m, 1H), 4.01 (s, 2H), 2.20 (d, *J* = 6.8 Hz, 2H), 1.68-1.58 (m, 1H), 1.56-1.46 (m, 3H), 1.45-1.38 (m, 2H), 1.13-0.95 (m, 3H), 0.75-0.65 (m, 2H); ^{13}C NMR (125 MHz, $CDCl_3$): δ 208.1 (o), 159.7 (o), 147.5 (o), 140.7 (o), 136.7 (e), 133.4 (o), 131.8 (o), 130.0 (o), 129.7 (o), 129.2 (o), 128.7 (o), 127.5 (o), 127.3 (o), 126.7 (e), 126.5 (o), 122.2 (o), 49.9 (e), 48.4 (e), 33.6 (o), 33.0 (e, 2C), 26.1 (e), 25.9 (e, 2C); IR (neat): ν

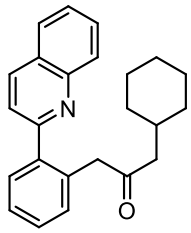

= 3059 (w), 2921 (s), 2849 (w), 1710 (s), 1618 (w), 1596 (m), 1556 (w), 1504 (w), 1488 (w), 1446 (m), 1423 (m), 1405 (w), 1373 (w), 1353 (m), 1312 (m), 1282 (m), 1266 (w), 1243 (w), 1212 (w), 1181 (w), 1141 (w), 1123 (w), 1101 (w), 1045 (m), 1035 (m), 908 (s), 833 (s), 763 (vs), 729 (vs), 687 (m), 646 (m), 622 (m); HRMS (CI (CH_4)) calcd for ($C_{24}H_{25}NO$ + H): 344.2009; found: 344.2006.

Compound 242b. This compound was obtained as an colourless paste (52 mg, **95%**)

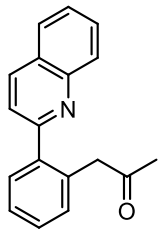

from 2-phenylquinoline (41 mg, 0.2 mmol, 1.0 equiv.) and **214** following **Method VII**. ^{1}H NMR (500 MHz, $CDCl_3$): δ 8.24 (d, *J* = 8.3 Hz, 1H), 8.09 (d, *J* = 7.0 Hz, 1H), 7.85 (d, *J* = 8.1 Hz, 1H), 7.74 (ddd, *J* = 8.3, 6.7, 1.5 Hz, 1H), 7.64-7.59 (m, 2H), 7.56 (ddd, *J* = 8.4, 6.9, 1.0 Hz, 1H), 7.46-7.41 (m, 2H), 7.36-7.31 (m, 1H), 3.97 (s, 2H), 2.12 (s, 3H); ^{13}C NMR (125 MHz, $CDCl_3$): δ 206.6 (e), 159.3 (e), 147.4 (e), 140.3 (e), 136.7 (o), 133.6 (e), 131.9 (o), 130.1 (o), 129.7 (o), 129.2 (o), 128.8 (o), 127.5 (o), 127.4 (o), 126.6 (e), 126.5 (o), 121.8 (o), 49.0 (e), 29.7 (o); IR (neat): ν = 3058 (w), 2891 (w), 1705 (vs), 1617 (m), 1596 (s), 1556 (m), 1504 (m), 1487 (m), 1471 (w), 1442 (m), 1423 (m), 1352 (m), 1313 (m), 1266 (w), 1242 (w), 1216 (m), 1159 (m),1127 (w), 1037 (m), 1012 (w), 978 (w), 942 (w), 834 (s), 792 (w), 765 (vs), 732 (s), 680 (m), 636 (w), 621 (w); HRMS (CI (CH_4)) calcd for ($C_{18}H_{15}NO$ + H): 262.1226; found: 262.1226.

Compound 242c. This compound was obtained as an colourless paste (69 mg, **quant.**)

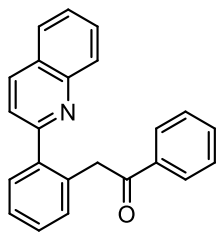

from 2-phenylquinoline (41 mg, 0.2 mmol, 1.0 equiv.) and **64** following **Method V**. ^{1}H NMR (500 MHz, $CDCl_3$): δ 8.18 (d, *J* = 8.9 Hz, 1H), 7.92-7.87 (m, 2H), 7.78 (d, *J* = 8.2 Hz, 1H), 7.68 (br s, 1H), 7.64-7.59 (m, 2H), 7.56 (t, *J* = 7.4 Hz, 1H), 7.51-7.42 (m,

4H), 7.41-7.33 (m, 3H), 4.62 (s, 2H); ^{13}C NMR (125 MHz, $CDCl_3$): δ 197.8 (e), 159.4 (e), 147.3 (e), 140.1 (e), 137.0 (e), 136.6 (o), 133.6 (e), 132.7 (o), 132.1 (o), 130.1 (o), 129.4 (o), 129.3 (o), 128.7 (o), 128.4 (o, 2C), 128.3 (o, 2C), 127.3 (o), 127.3 (o), 126.6 (e), 126.3 (o), 122.0 (o), 43.5 (e); IR (neat): ν = 3057 (w), 2889 (w), 1685 (vs), 1616 (w), 1593 (m), 1579 (m), 1553 (m), 1504 (m), 1488 (m), 1445 (m), 1419 (m), 1335 (m), 1312 (m), 1216 (m), 1199 (w), 1180 (w), 1152 (w), 1112 (w), 1077 (w), 1035 (m), 997 (m), 955 (w), 944 (w), 909 (w), 889 (w), 845 (s), 793 (w), 774 (vs), 761 (s), 750 (vs), 730 (s), 688 (vs), 661 (s), 621 (m); HRMS (CI (CH_4)) calcd for ($C_{23}H_{17}NO$ + H): 324.1383; found: 324.1381.

6.4.3.2 *N*-methoxybenzamide

Method VIII: *Representative example for the synthesis of **244a**.*

[Cp*Rh$(OAc)_2$•H_2O] (6 mg, 0.016 mmol, 0.08 equiv) and HFIP (1 mL) were added under nitrogen to a flame-dried Schlenk tube sealable by a J-young key. Then, *N*-methoxybenzamide (30 mg, 0.2 mmol, 1 equiv), **187** (86 mg, 0.4 mmol, 2 equiv) and HFIP (0.5 mL) were sequentially added in that order. The tube was sealed and the mixture was stirred at 90 °C for 17 hours. After cooling to room temperature, all volatiles were removed under reduced pressure. Purification by flash chromatography (PE:EtOAc/8:2) afforded **244a** as a beige amorphous solid (32 mg, **59%**).

Compound 244a. This compound was obtained as a beige amorphous solid (32 mg, 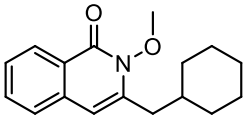 **59%**) from *N*-methoxybenzamide (30 mg, 0.2 mmol) and **187** following **Method VIII**. ^{1}H NMR (500 MHz, $CDCl_3$): δ 8.39 (d, *J* = 8.3 Hz, 1H), 7.64-7.57 (m, 1H), 7.47-7.37 (m, 2H), 6.22 (s, 1H), 4.07 (s, 3H), 2.57 (d, *J* = 6.6 Hz, 2H), 1.84-1.61 (m, 6H), 1.30-1.12 (m, 3H), 1.06-0.94 (m, 2H); ^{13}C NMR (125 MHz, $CDCl_3$): δ 159.0 (e), 141.6 (e), 135.9 (e), 132.2 (o), 127.5 (o), 125.8 (e), 125.8 (o), 125.4 (o), 104.8 (o), 63.7 (o), 39.0 (e), 36.7 (o), 33.2 (e, 2C), 26.3 (e), 26.1 (e, 2C); IR (neat): ν = 2919 (s), 2849 (m), 1654 (vs), 1621 (vs), 1598 (vs), 1556 (m), 1483 (m), 1469 (w), 1446 (m), 1422 (w), 1398 (m), 1336 (m), 1301 (w), 1258 (m), 1237 (w), 1206 (w), 1171 (m), 1148 (w), 1061 (w), 974 (s), 942 (w), 913 (w), 901 (m), 875 (m), 820 (s), 788 (w), 751 (s), 700 (w), 684 (s), 634 (m), 614 (m); HRMS (CI (NH_3)) calcd for ($C_{17}H_{21}NO_2$ + H): 272.1645; found: 272.1640.

Compound 244b. This compound was obtained as a beige amorphous solid (30 mg, 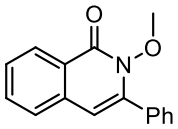 **57%**) from *N*-methoxybenzamide (30 mg, 0.2 mmol) and **64** following **Method VIII**. ^{1}H NMR (500 MHz, $CDCl_3$): δ 8.47 (d, *J* = 8.0 Hz, 1H), 7.68-7.61 (m, 3H), 7.54 (d, *J* = 7.9 Hz, 1H), 7.52-7.44 (m, 4H), 6.48 (s, 1H), 3.70 (s, 3H); ^{13}C NMR (125 MHz, $CDCl_3$): δ 158.7 (e), 142.1 (e), 135.8 (e), 132.6 (e), 132.4 (o), 129.3 (o, 2C), 129.2 (o), 128.2 (o, 2C), 127.8 (o), 126.6 (o), 126.3 (e), 126.2 (o), 106.7 (o), 63.4 (o), *the NMR data is in accordance with that reported in the literature.*[122]

Compound 245. This compound was obtained along with **244b** as a beige amorphous solid (11 mg, **25%**) from *N*-,ethoxybenzamide (30 mg, 0.2 mmol) and **64** following **Method VIII**. ^{1}H NMR (500 MHz, $CDCl_3$): δ 8.32 (d, *J* = 8.2 Hz, 1H), 7.91-7.87 (m, 2H), 7.72 (td, *J* = 7.7, 1.6 Hz, 1H), 7.53-7.41 (m , 5H), 6.96 (s, 1H); ^{13}C NMR (125 MHz, $CDCl_3$): δ 162.4 (e), 153.7 (e), 137.6 (e), 134.9 (o), 132.0 (e), 130.0 (o), 129.7 (o), 128.9 (o, 3C), 128.2 (o), 126.0 (o), 125.3 (o), 120.6 (e), 101.8 (o), *the NMR data is in accordance with that reported in the literature.*[123]

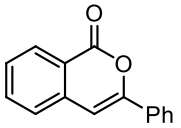

6.4.3.3 *O*-methyl oxime

Compound 248. [Cp*Rh(MeCN)$_3$(SbF$_6$)$_2$] (13 mg, 0.016 mmol, 0.08 equiv) and HFIP (1 mL) were added under nitrogen to a flame-dried Schlenk tube sealable by a J-young key. Then, (*E*)-acetophenone *O*-methyloxyme (30 mg, 0.2 mmol, 1 equiv), NaOAc (16 mg, 1 mmol, 1 equiv), **64** (78 mg, 0.4 mmol, 2 equiv) and HFIP (0.5 mL) were sequentially added in that order. The tube was sealed and the mixture was stirred at 90 °C for 17 hours. After cooling to room temperature, all volatiles were removed under reduced pressure. Purification by flash chromatography (PE:EtOAc/95:5 to 9:1) afforded **248** as a white amorphous solide (37 mg, **69%**). ^{1}H NMR (500 MHz, $CDCl_3$): δ 8.08 (m, 2H), 7.57 (tt, *J* = 6.7, 1.3 Hz, 1H), 7.51-7.45 (m, 2H), 7.38-7.30 (m, 3H), 7.27-7.22 (m, 1H), 4.53 (s, 2H), 3.60 (s, 3H), 2.16 (s, 3H); ^{13}C NMR (125 MHz, $CDCl_3$): δ 197.5 (e), 155.9 (e), 137.0 (e), 137.0 (e), 132.9 (o), 132.8 (e), 131.9 (o), 128.5 (o, 2C), 128.4 (o), 128.4 (o), 128.2 (o, 2C), 127.1 (o), 61.4 (o), 44.1 (e), 15.5 (o); IR (neat): ν = 3056 (w), 2956 (w), 2897 (w), 2816 (w), 1681 (vs), 1616 (w), 1597 (w), 1578 (w), 1494 (w), 1449 (m), 1425 (w), 1408 (m), 1364 (w), 1339 (m), 1310 (w), 1301 (w), 1220 (s), 1199 (m), 1183 (m),

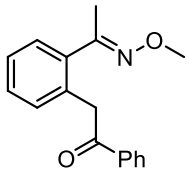

1158 (w), 1077 (w), 1040 (vs), 999 (s), 954 (m), 889 (s), 876 (s), 848 (w), 762 (vs), 727 (m), 695 (s), 666 (s), 637 (m); HRMS (CI (CH_4)) calcd for ($C_{17}H_{17}NO_2$ + H): 268.1332; found: 268.1339.

Compound 248'. This compound was obtained along with **248** as a white amorphous

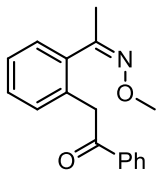

solid (11 mg, **21%**). ^{1}H NMR (500 MHz, $CDCl_3$): δ 8.03-7.97 (m, 2H), 7.57 (tt, *J* = 6.9, 1.3 Hz, 1H), 7.47 (t, *J* = 8.0 Hz, 2H), 7.36-7.30 (m, 2H), 7.28-7.23 (m, 1H), 7.16-7.11 (m, 1H), 4.23 (s, 2H), 3.70 (s, 3H), 2.14 (s, 3H); ^{13}C NMR (125 MHz, $CDCl_3$): δ 197.3 (e), 155.4 (e), 136.9 (e), 136.4 (e), 133.1 (o), 131.8 (e), 130.6 (o), 128.6 (o, 2C), 128.5 (o), 128.3 (o, 2C), 127.1 (o), 126.3 (o), 61.5 (o), 43.2 (e), 22.2 (o); IR (neat): ν = 2934 (m), 1687 (vs), 1587 (w), 1580 (w), 1493 (w), 1447 (m), 1372 (w), 1333 (m), 1274 (w), 1216 (m), 1127 (w), 1082 (m), 1051 (vs), 1040 (vs), 1009 (m), 894 (s), 757 (s), 732 (m), 719 (w), 69 (s), 663 (m); HRMS (CI (CH_4)) calcd for ($C_{17}H_{17}NO_2$ + H): 240.1332; found: 268.1339.

6.5 Further functionalisation

Method IX: *Representative example for the synthesis of **281a.***

Compound **242a** (34 mg, 0.1 mmol, 1.0 equiv) was added to a Schlenck tube followed by *i*-PrOH (0.5 mL), $[Cp^*IrCl_2]_2$ (3.2 mg, 0.004 mmol, 0.04 equiv) and water (24 μL) in that order. The tube was sealed and the mixture was stirred at 90 °C overnight. Then, the mixture was allowed to cool to room temperature, diluted with DCM and saturated $NaHCO_3$ was added. The aqueous layer was extracted with DCM. The combined organic layers were washed with water, brine, then dried over Na_2SO_4, filtered and concentrated under reduced pressure. After solubilising the residue in a minimum of

DCM, some SiO_2 was added and all volatiles removed under reduced pressure, the residue was loaded on a short silica gel column and purified by flash chromatography (PE:EtOAc/98:2 to 95:5). A mixture of **281a** and the corresponding 7,12-dihydrobenzo[c]acridine was recovered which was converted to **281a** upon storing under air overnight (20 mg, **63%**).

Compound 281a. This compound was obtained as yellow solid (20 mg, **63%**) from

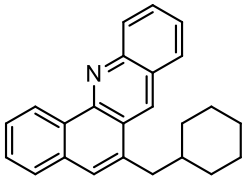

242a following **Method IX**. m.p.: 136-140 °C. ^{1}H NMR (500 MHz, $CDCl_3$): δ 9.49 (br s, 1H), 8.82 (s, 1H), 8.39 (br s, 1H), 8.09 (d, *J* = 8.3 Hz, 1H), 7.88-7.77 (m, 2H), 7.75-7.67 (m, 2H), 7.62 (t, *J* = 7.6 Hz, 1H), 7.49 (s, 1H), 3.05 (d, *J* = 6.7 Hz, 2H), 1.90-1.62 (m, 6H), 1.30-1.07 (m, 5H); ^{13}C NMR (125 MHz, $CDCl_3$): δ 148.2 (e), 147.0 (e), 134.3 (e), 133.7 (e), 131.7 (o), 130.9 (e), 129.5 (o), 129.5 (o), 129.0 (o), 128.1 (o), 127.2 (o), 127.2 (o), 126.6 (e), 126.4 (o), 125.7 (o), 125.3 (o), 125.1 (e), 41.0 (e), 38.2 (o), 33.7 (e, 2C), 26.5 (e), 26.2 (e, 2C); IR (neat): ν = 3051 (w), 2918 (m), 2844 (m), 1628 (w), 1614 (w), 1583 (w), 1567 (w), 1536 (w), 1488 (m), 1449 (m), 1407 (w), 1378 (w), 1362 (w), 1348 (w), 1335 (w), 1307 (w), 1259 (w), 1223 (w), 1186 (w), 1131 (w), 1057 (w), 1031 (w), 1006 (w), 951 (m), 901 (s), 864 (m), 851 (m), 810 (w), 790 (w), 769 (w), 749 (vs), 691 (m), 653 (m), 625 (s); HRMS (CI (CH_4)) calcd for ($C_{24}H_{23}N$ + H): 326.1903; found: 326.1895.

Compound 281b. This compound was obtained as yellow solid (19 mg, **49%**) from

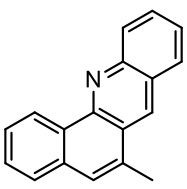

242b (44 mg, 0.17 mmol, 1.0 equiv.) following **Method IX**. m.p.: 107-109 °C. ^{1}H NMR (500 MHz, $CDCl_3$): δ 9.50-9.44 (m, 1H), 8.72 (s, 1H), 8.38 (d, *J* = 8.7 Hz, 1H), 8.03 (d, *J* = 8.3 Hz, 1H), 7.86-7.80

(m, 1H), 7.78-7.73 (m, 1H), 7.73-7.66 (m, 2H), 7.62-7.57 (m, 1H), 7.49 (s, 1H), 2.75 (d, J = 1.2 Hz, 3H); ^{13}C NMR (125 MHz, $CDCl_3$): δ 147.9 (e), 147.2 (e), 133.9 (e), 131.6 (o), 131.5 (e), 130.9 (e), 129.6 (o, 2C), 129.0 (o), 128.0 (o), 127.1 (o), 126.8 (o), 126.7 (e), 126.5 (o), 125.8 (o), 125.7 (e), 125.2 (o), 19.4 (o); IR (neat): ν = 2970 (m), 2922 (m), 1929 (w), 1829 (w), 1630 (w), 1613 (w), 1582 (w), 1565 (w), 1536 (w), 1487 (m), 1437 (w), 1407 (w), 1369 (m), 1306 (m), 1276 (w), 1221 (w), 1188 (w), 1152 (w), 1135 (w), 1076 (m), 1028 (m), 973 (w), 960 (w), 949 (w), 901 (m), 880 (m), 854 (m), 806 (w), 790 (w), 768 (m), 748 (vs), 709 (m), 667 (w), 643 (w), 610 (w); HRMS (CI (CH_4)) calcd for ($C_{18}H_{13}N$ + H): 244.1121; found: 244.1127.

Compound 281c. This compound was obtained as yellow solid (26 mg, **55%**) from

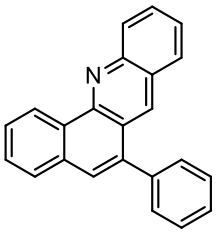

242c (50 mg, 0.16 mmol, 1.0 equiv.) following **Method IX**, the mixture was stored under air 48 h. m.p.: 166-170 °C. ^{1}H NMR (500 MHz, $CDCl_3$): δ 9.56 (d, J = 7.9 Hz, 1H), 8.69 (s, 1H), 8.40 (d, J = 8.7 Hz, 1H), 7.92 (d, J = 8.2 Hz, 1H), 7.90-7.86 (m, 1H), 7.85-7.73 (m, 3H), 7.67 (s, 1H), 7.65-7.51 (m, 6H); ^{13}C NMR (125 MHz, $CDCl_3$): δ 147.8 (e), 147.3 (e), 139.8 (e), 137.8 (e), 134.0 (o), 133.4 (e), 131.2 (e), 130.0 (o, 2C), 129.9 (o), 129.5 (o), 129.2 (o), 128.6 (o, 2C), 128.2 (o), 128.0 (o), 127.8 (o), 127.7 (o), 127.2 (o), 126.7 (e), 125.8 (o), 125.3 (o), 124.7 (e); IR (neat): ν = 3055 (w), 3027 (w), 2955 (w), 2921 (w), 1953 (w), 1607 (w), 1598 (w), 1564 (w), 1534 (m), 1486 (w), 1440 (m), 1407 (m), 1374 (m), 1308 (m), 1241 (w), 1221 (w), 1208 (w), 1174 (w), 1159 (w), 1125 (w), 1107 (w), 1070 (m), 1029 (w), 1016 (w), 981 (w), 966 (w), 952 (w), 932 (w), 908 (w), 889 (s), 867 (w), 840 (m), 811 (w), 778 (m), 766 (s), 751 (vs), 715 (s), 698 (vs), 674 (s), 641 (s), 611 (m); HRMS (CI (CH_4)) calcd for ($C_{23}H_{15}N$ + H): 306.1277; found: 306.1273.

6.6 Mechanistic sutdy

6.6.1 Synthesis of monodeuterated phenyl pyridine

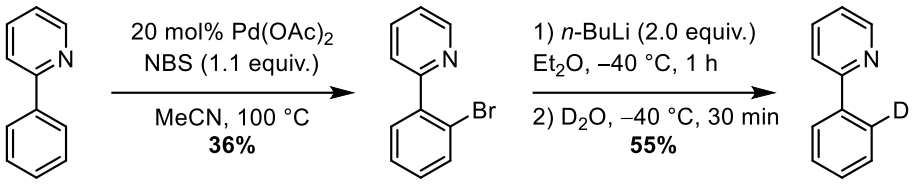

128 **304** ***d*-128**

Compound 304. A flame dried schlenk was charged with $Pd(OAc)_2$ (72 mg, 0.3 mmol, 0.2 equiv.), dry acetonitrile (10 mL), **128** (0.3 mL, 1.8 mmol, 1.0 equiv.) and *N*-bromosuccinimide (0.3 g, 1.9 mmol, 1.1 equiv.). The tube was sealed and the mixture was stirred at 100 °C for 48 h. All volatiles were removed *in vacuo* and the crude mixture was purified by flash chromatography (PE:EtOAc/9:1 to 85:15) to give **304** as a colourless oil (0.15 g, **36%**). ^{1}H NMR (500 MHz, $CDCl_3$): δ 8.74-8.69 (m, 1H), 7.77 (td, *J* = 7.7, 1.8 Hz, 1H), 7.68 (dd, *J* = 8.1, 1.1 Hz, 1H), 7.60 (dt, *J* = 7.9, 1.1 Hz, 1H), 7.54 (dd, *J* = 7.7, 1.8 Hz, 1H), 7.41 (td, *J* = 7.5-1.2 Hz, 1H), 7.30 (ddd, *J* = 7.5, 4.9, 1.1 Hz, 1H), 7.28-7.23 (m, 1H), *the NMR data is in accordance with that reported in the literature.*[124]

Compound *d*-128. A flame dried schlenk was charged with **304** (147 mg, 0.6 mmol, 1.0 equiv.) in diethyl ether (6 mL). The mixture was cooled down to −40 °C and *n*BuLi (0.8 mL, 1.6 M in hexanes, 1.3 mmol, 2.0 equiv.) was added dropwise. The mixture was further stirred 1 h at −40 °C. Then D_2O (0.21 mL, 10.5 mmol, 17.5 equiv.) was added at −40 °C and the mixture was stirred another 30 min. Ethyl acetate and brine were added, the aqueous layer was extracted with more EtOAc. The gathered organic

layer was washed with water/brine, dried over $MgSO_4$ and evaporated. Flash chromatography (PE:EtOAc/8:2) afforded ***d*-128** as a colourless oil (54 mg, **55%**). ^{1}H NMR (500 MHz, $CDCl_3$): δ 8.72-8.69 (m, 1H), 8.01-7.97 (m, 1H), 7.78-7.71 (m, 2H), 7.51-7.46 (m, 2H), 7.45-7.40 (m, 1H), 7.25-7.21 (m, 1H), *the NMR data is in accordance with that reported in the literature.* [124]

6.6.2 Reversibility of Csp²–H cleavage

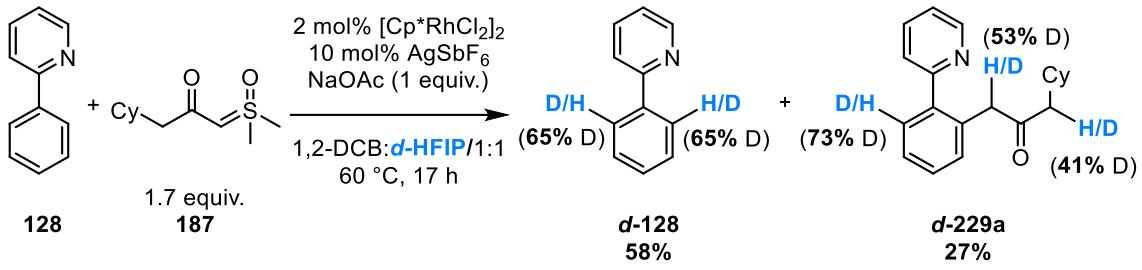

A flame dried Schlenk tube, sealable with a J-Young key, was charged with $AgSbF_6$ (6.9 mg, 0.01 mmol, 0.1 equiv.) in an argon-filled glovebox. The tube was taken out and $[Cp^*RhCl_2]_2$ (2.5 mg, 0.002 mmol, 0.02 equiv.) was added, followed by 1,2-DCB (0.38 mL). Then, **128** (14 µL, 0.1 mmol, 1.0 equiv.), NaOAc (8 mg, 0.1 mmol, 1.0 equiv.), **187** (37 mg, 0.17 mmol, 1.7 equiv.) and *d*-HFIP (0.38 mL) were sequentially added in that order. The vial was sealed and the mixture was stirred at 60 °C for 17 h. After cooling to room temperature, all volatiles were removed *in vacuo*. Purification by flash chromatography (PE/EtOAc:9/1 to 8/2) afforded ***d*-128** as a colourless oil (9 mg, **58%**) and ***d*-229** as a colourless oil (8 mg, **27%**).

***d*-128**: ^{1}H NMR (500 MHz, $CDCl_3$): δ 8.73-8.68 (m, 1H), 8.01-7.97 (m, 0.7H), 7.78-7.71 (m, 2H), 7.51-7.46 (m, 2H), 7.45-7.40 (m, 1H), 7.25-7.21 (m, 1H).

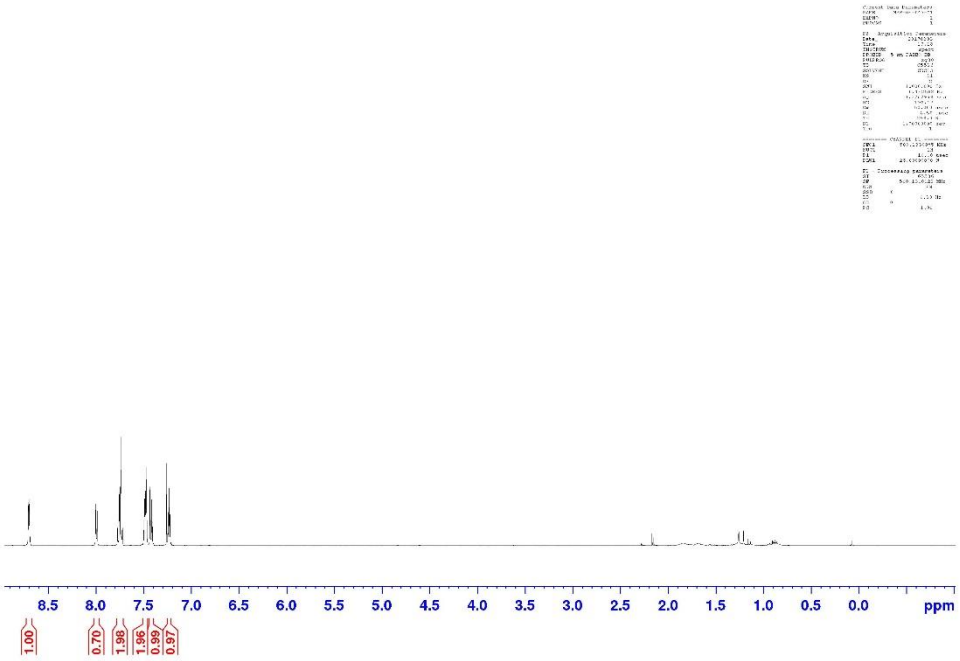

***d*-229a**: ^{1}H NMR (500 MHz, $CDCl_3$): δ 8.69-8.55 (m, 1H), 7.80-7.69 (m, 1H), 7.48-7.41 (m, 1.27H), 7.40-7.31 (m, 2H), 7.27-7.19 (m, 2H), 3.94-3.80 (m, 0.95 H), 2.24-2.14 (m, 1.18H), 1.77-1.48 (m, 8H), 1.34-1.02 (m, 5H), 0.87-0.73 (m, 2H).

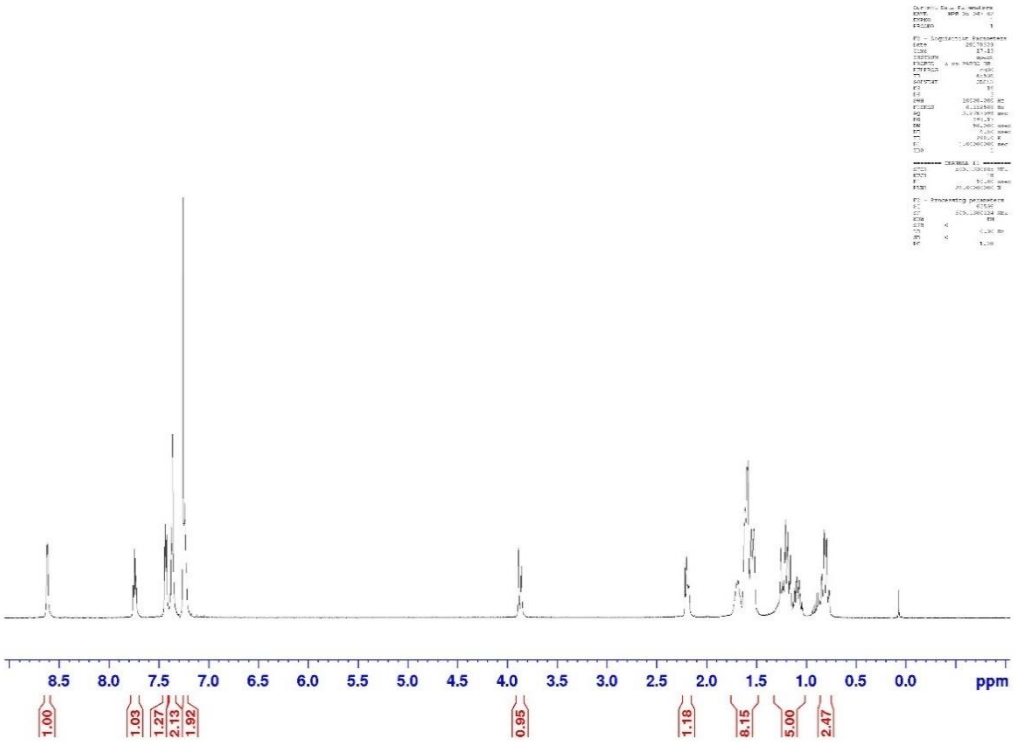

6.6.3 Deuterium-labelling experiment

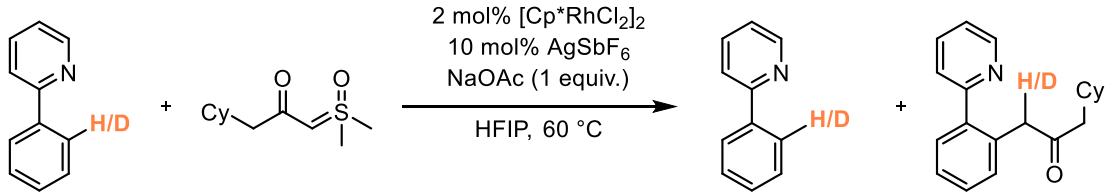

***d*-128**
(***86% D***)

1.7 equiv.
187

***d*-128**
After 1 h: 67%
(***45% D***)
After 2 h: 35%
(***6% D***)

d-229a
17%
(***0% D***)
49%
(***0% D***)

A flame dried Schlenk tube, sealable with a J-Young key, was charged with $AgSbF_6$ (6.9 mg, 0.02 mmol, 0.1 equiv.) in an argon-filled glovebox. The tube was taken out and $[Cp^*RhCl_2]_2$ (2.5 mg, 0.004 mmol, 0.02 equiv.) was added, followed by HFIP (1 mL). Then, ***d*-128** (29 µL, 0.2 mmol, 1.0 equiv.), NaOAc (16 mg, 0.2 mmol, 1.0

equiv.), **187** (73 mg, 0.34 mmol, 1.7 equiv.) and HFIP (0.5 mL) were sequentially added in that order. The vial was sealed and the mixture was stirred at 60 °C for 1 or 2 h. After cooling to room temperature, all volatiles were removed *in vacuo*. Purification by flash chromatography (PE/EtOAc:9/1 to 8/2) afforded ***d*-128** as a colourless oil (10 mg, **67%** (on a 0.1 mmol scale); 9 mg, **35%**) and **229a** as a colourless oil (5 mg, **17%** (on a 0.1 mmol scale); 9 mg, **49%**).

***d*-128:** δ 8.73-8.68 (m, 1H), 8.01-7.97 (m, 1.55H), 7.78-7.71 (m, 2H), 7.51-7.46 (m, 2H), 7.45-7.40 (m, 1H), 7.25-7.21 (m, 1H).

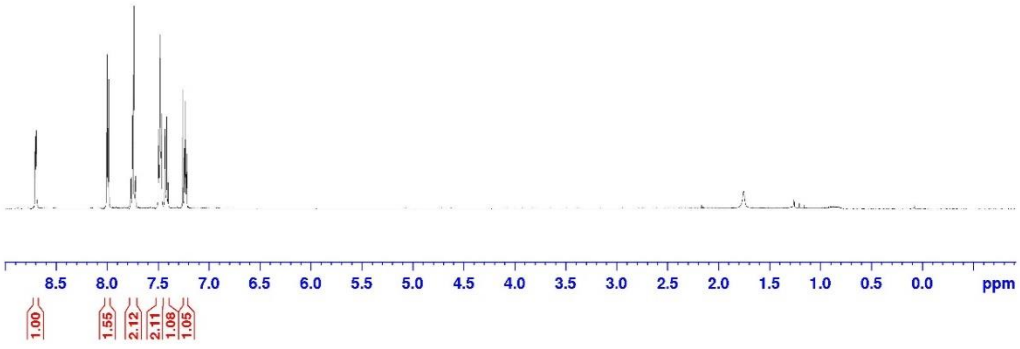

6.6.4 Kinetic isotope effect

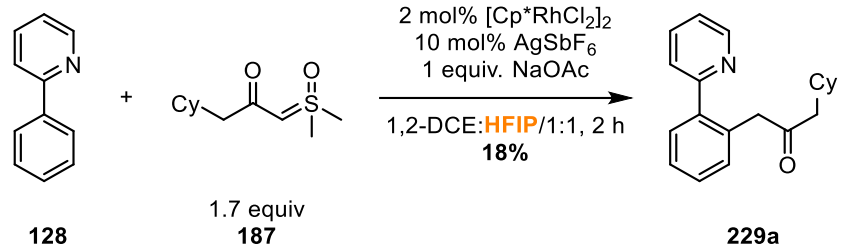

To a vial equipped with magnetic stirrer, under air atmosphere, was added $AgSbF_6$ (6.9 mg, 0.02 mmol, 0.1 equiv.), $[Cp^*RhCl_2]_2$ (2.5 mg, 0.004 mmol, 0.02 equiv.) followed by 1,2-DCE (0.75 mL). Then, **128** (29 µL, 0.2 mmol, 1.0 equiv.), NaOAc (16 mg, 0.2 mmol, 1.0 equiv.), **187** (73 mg, 0.34 mmol, 1.7 equiv.) and HFIP (0.75 mL) were sequentially added in that order. The vial was sealed and the mixture was stirred at 60 °C for 2 h. After cooling to room temperature, all volatiles were removed *in vacuo*, 1,3,5-trimethoxybenzene (35 mg, 0.2 mmol, 1.0 equiv.) was added and the conversion was determined by ^1H NMR.

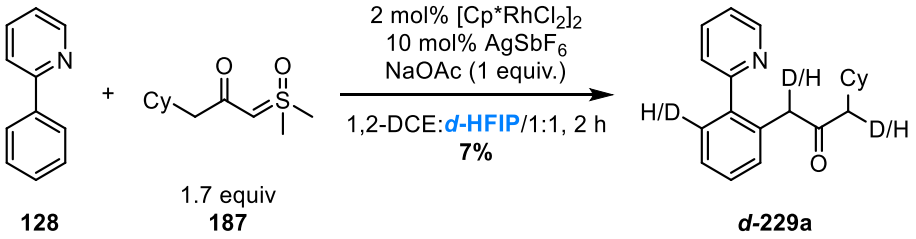

To a vial equipped with magnetic stirrer, under air atmosphere, was added $AgSbF_6$ (3.4 mg, 0.01 mmol, 0.1 equiv.), $[Cp^*RhCl_2]_2$ (1.3 mg, 0.002 mmol, 0.02 equiv.) followed by 1,2-DCE (0.38 mL). Then, **373** (14 µL, 0.1 mmol, 1.0 equiv.), NaOAc (8 mg, 0.1 mmol, 1.0 equiv.), **429** (37 mg, 0.17 mmol, 1.7 equiv.) and *d*-HFIP (0.38 mL)

were sequentially added in that order. The vial was sealed and the mixture was stirred at 60 °C for 2 h. After cooling to room temperature, all volatiles were removed *in vacuo*. Purification by flash chromatography (PE/EtOAc: 9/1 to 8/2) afforded ***d*-373** as a colourless oil (13 mg, **87%**) and ***d*-472a** as a colourless oil (2 mg, **7%**).

6.6.5 Normalised time scaled method

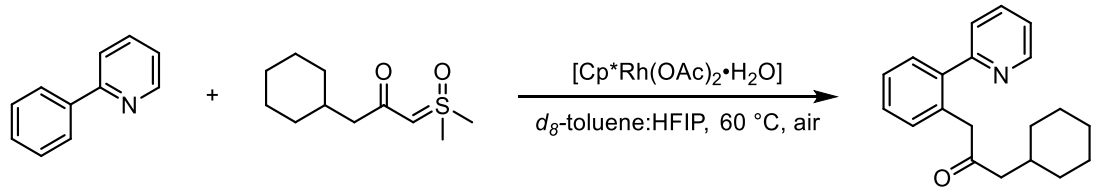

128 **187** **229a**

Ref : [128] = 0.27 M; [187] = 0.45 M; [Rh] = 0.01 M; [HFIP] = 9.5 M
[128] = 0.27 M; [187] = 0.45 M; [Rh] = 0.01 M; ***[HFIP] = 4.1 M***
[128] = 0.27 M; [187] = 0.45 M; ***[Rh] = 0.02 M***; [HFIP] = 9.5 M
[128] = 0.27 M; ***[187] = 0.35 M***; [Rh] = 0.01 M; [HFIP] = 9.5 M
[128] = 0.35 M; [187] = 0.45 M; [Rh] = 0.01 M; [HFIP] = 9.5 M

Representative example for the reference reaction: To a V-shaped flask was added [Cp*Rh(OAc)$_2$•H$_2$O] (1 mg, 0.0027 mmol, 0.04 equiv.), **128** (9 µL, 0.067 mmol, 1 equiv.), **187** (24 mg, 0.11 mmol, 1.7 equiv), mesitylene (9 µL, 0.067 mmol, 1 equiv.), *d*8-toluene (0.25 mL) and HFIP (0.25 mL). The solution was transferred into a NMR tube sealable with a J-Young key. The tube was sealed and put to react at 60 °C in the NMR machine.

7 References

1 E. J. Corey, M. Chaykovsky, *J. Am. Chem. Soc.,* **1962**, *84*, 3782.

2 C. K. Ingold, J. A. Jessop, *J. Chem. Soc.*, **1930**, *0*, 713.

3 J. D. Neuhaus, R. Oost, J. Merad, N. Maulide, *Top. Curr. Chem. (Z)*, **2018**, 376:15.

4 J. S. Clark, *Nitrogen, Oxygen and Sulfur Ylide Chemistry (Pratical Approach in Chemistry Series),* **2002**, *Oxford University Press*.

5 A.-H. Li, V. K. Aggarwal, L.-X. Dai, *Chem. Rev.*, **1997**, *97*, 2341.

6 B. M. Trost, *J. Am. Chem. Soc.*, **1966**, *88*, 1587.

7 P. Muller, D. Fernandez, P. Nury, J.-C. Rossier, *Helc. Chim. Acta,* **1999**, *82*, 935.

8 Y.-Y. Liu, X.-H. Yang, X.-C. Huang, W.-T. Wei, R.-J. Song, J.-H. Li, *J. Org. Chem.*, **2013**, *78*, 10421.

9 X.-D. Xia, L.-Q. Lu, W.-Q. Liu, D.-Z. Chen, Y.-H. Zheng, L.-Z. Wu, W.-J. Xiao, *Chem. Eur. J.*, **2016**, *22*, 8432.

10 S. Klimczyk, A. Misale, X. Huang, N. Maulide, *Angew. Chem. Int. Ed.*, **2015**, *54*, 10365.

11 Y. Duan, J.-H. Lin, J.-C. Xiao, Y.-C. Gu, *Org. Lett.*, **2016**, *18*, 2471.

12 E. J. Corey, M. Chaykovsky, *J. Am. Chem. Soc.,* **1965**, *87*, 1354.

13 J. L. Martin, J. S. Tou, W. Reusch, *J. Org. Chem.*, **1979**, *44*, 3666.

14 P. T. Izzo, *J. Org. Chem.*, **1963**, *28*, 1713.

15 E. T. Ledingham, C. J. Merritt, C. J. Sumby, M. K. Taylor, B. W. Greatrex, *Synthesis,* **2017**, *49*, 2652.

16 J. A. Marshall, R. H. Ellison, *J. Org. Chem.*, **1975**, *40*, 2070.

17 C. Hamdouchi, *Tetrahedron Lett.*, **1992**, *33*, 1701.

18 T. Duvold, A. Jørgensen, N. R. Andersen, S. A. Henriksen, M. D. Sørensen, F. Björkling, *Bioorg. Med. Chem. Lett.*, **2002**, *12*, 3569.

19 S. Malik, U. K. Nadir, *Synlett*, **2008**, *1*, 108.

20 T. Sone, G. Lu, S. Matsunaga, M. Shibasaki, *Angew. Chem. Int. Ed.*, **2009**, *48*, 1677.

21 E. D. Butova, A. V. Barabash, A. A. Petrova, C. M. Kleiner, P. R. Schreiner, A. A. Fokin, *J. Org. Chem.*, **2010**, *75*, 6229.

22 J. Dong, J. Xu, *Org. Biomol. Chem.*, **2017**, *15*, 836.

23 L. Field, H.-K. Chu, *J. Org. Chem.*, **1977**, *42*, 1768.

24 M. Tazaki, M. Yamada, *Phosphorus, sulfur and silicon*, **1996**, *116*, 253.

25 B. B. Busch, M. M. Paz, K. J. Shea, C. L. Staiger, J. M. Stoddard, J. R. Walker, X.-Z., Zhou, H. Zhu, *J. Am. Chem. Soc.*, **2002**, *124*, 3636.

26 K. J. Shea, S. Y. Lee, B. B. Busch, *J. Org. Chem.*, **1998**, *63*, 5746.

27 R. D. C. Gallo, A. Ahmad, G. Metzker, A. C. B. Burtoloso, *Chem. Eur. J.*, **2017**, *23*, 16980.

28 R. Volpicelli, P. Maragni, L. Cotarca, J. Foletto, WO2008040528, **2018**.

29 H. Konig, H. Metzger, K. Seelert, *Chem. Ber.*, **1965**, *98*, 3712.

30 H. Luong, E. Luss-Lusis, G. J. Tanoury, W. A. Nugent, *Chem. Eur. J.*, **2013**, 4238.

31 H. Yamanaka, S. Konno, T. Sakamoto, S. Niitsuma, S. Noji, *Chem. Pharm. Bull*., **1981**, *29*, 2837.

32 H. Shmidbaur, W. Kapp, *Chem. Ber.*, **1972**, *105*, 1203.

33 W. E. Truce, G. D. Madding, *Tetrahedron Lett.*, **1966**, *31*, 3681.

34 D. Wang, M. D. Schwinden, L. Radesca, B. Patel, D. Kronenthal, M.-H. Huang, W. A. Nugent, *J. Org. Chem.*, **2004**, *69*, 1629.

35 N. A. Roberts, J. A. Martin, D. Kinchington, A. V. Broadhurst, J. C. Craig, I. B. Duncan, S. A. Galpin, B. K. Handa, J. Kay, A. Krohn, R. W. Lambert, J. H. Merrett, J. S. Mills, K. E. B. Parkes, S. Redshaw, A. J. Ritchie, D. L. Taylor, G. J. Thomas, P. J. Machin, *Science*, **1990**, *248*, 358.

36 R. M. P. Dias, A. C. B. Burtoloso, *Org. Lett.*, **2016**, *18*, 3034.

37 J. E. Baldwin, R. M. Adlington, C. R. A. Godfrey, D. W. Collins, J. G. Vaughan, *J. Chem. Soc., Chem. Commun.*, **1993**, 1434.

38 I. K. Mangion, M. Weisel, *Tetrahedron Lett.*, **2010**, *51*, 5490.

39 I. K. Mangion, I. K. Nwamba, M. Shevlin, M. A. Huffman, *Org. Lett.*, **2009**, *11*, 3566.

40 I. K. Mangion, R. T. Ruck, N. Rivera, M. A. Huffman, M. Shevlin, *Org. Lett.*, **2011**, *13*, 5480.

41 C. Molinaro, P. G. Bulger, E. E. Lee, B. Kosjek, S. Lau, D. Gauvreau, M. E. Howard, D. J. Wallace, P. D. O'Shea, *J. Org. Chem.*, **2012**, *77*, 2299.

42 A. M. Phelps, V. S. Chan, J. G. Napolitano, S. W. Krabbe, J. M. Schomaker, S. Shekhar, *J. Org. Chem.*, **2016**, *81*, 4158.

43 A. I. O. Suarez, M. P. del Río, K. Remerie, J. N. H. Reek, B. de Bruin, *ACS Catal.*, **2012**, *2*, 2046.

44 K. P. Cusack, T. D. Gordon, D. C. Ihle, M. E. Hayes, E. C. Breinlinger, A. M. Ericsson, B. Lin, L. Wang, G. Y. Martinez, A. Burchat, A. D. Hobson, K. D. Mullen, M. Friedman, M. J. Morytko, WO2012/125797.

45 W.-W. Chang, S.-F. Lo, Z. Zhou, W.-Y. Yu, *J. Am. Chem. Soc.*, **2012**, *134*, 13565.

46 T. K. Hyster, K. E. Ruhl, T. Rovis, *J. Am. Chem. Soc.*, **2013**, *135*, 5364

47 B. Ye, N. Cramer, *Angew. Chem. Int. Ed.*, **2014**, *53*, 7896.

48 Z. Shi, D. C. Koester, M. Boultadakis-Arapinis, F. Glorius, *J. Am. Chem. Soc.*, **2013**, *135*, 12204.

49 X. Yu, S. Yu, J. Xiao, B. Wan, X. Li, *J. Org. Chem.*, **2013**, *78*, 5444.

50 Y. Cheng, C. Bolm, *Angew. Chem. Int. Ed.*, **2015**, *54*, 12349.

51 X. Chen, G. Zheng, G. Song, X. Li, *Adv. Synth. Catal.*, **2018**, *360*, 1.

52 K. Yan, B. Li, B. Wang, *Adv. Synth. Catal.*, **2018**, *360*, 2113.

53 J. H. Kim, S. Greβies, F. Glorius, *Angew. Chem. Int. Ed.*, **2016**, *55*, 5577.

54 W. Hou, X. Yang, Y. Wu, H. Feng, Y. Li, B. Zhou, *Chem. Commun.*, **2016**, *52*, 9672.

55 S.-Y. Yan, P.-X. Ling, B.-F. Shi, *Adv. Synth. Catal.*, **2017**, *359*, 2912.

56 S. Qu, C. J. Cramer, *J. Org. Chem.*, **2017**, *82*, 1195.

57 J. D. Clark, A. S. Shah, J. C. Peterson, L. Patelis, R. J. A. Kersten, A. H. Heemskerk, M. Grogan, S. Camden, *Thermochim. Acta*, **2002**, *386*, 65.

58 J. H. Kim, T. Gensch, D. Zhao, L. Stegemann, C. A. Strassert, F. Glorius, *Angew. Chem. Int. Ed.*, **2015**, *54*, 10975.

59 X. Ye, Z. He, T. Ahmed, K. Weise, N. G. Akhmedov, J. L. Petersen, X. Shi, *Chem. Sci.*, **2013**, *4*, 3712.

60 G. L'Abbé, I. Luyten, S. Toppet, *J. Heterocycl. Chem.*, **1992**, *29*, 713.

61 W. H. Jeon, J.-Y. Son, J. E. Kim, P. H. Lee, *Org. Lett.*, **2016**, *18*, 3498.

62 W. R. Bamford, T. S. Stevens, *J. Chem. Soc.*, **1952**, *0*, 4735.

63 X. Zhao, G. Wu, Y. Zhang, J. Wang, *J. Am. Chem. Soc.*, **2011**, *133*, 3296.

64 T. Yao, K. Hirano, T. Satoh, M. Miura, *Angew. Chem. Int. Ed.*, **2012**, *51*, 775.

65 Y. Zhang, J. Wang, J. Wang, *Synlett*, **2013**, 1643.

66 F. Hu, Y. Xia, F. Ye, Z. Liu, C. Ma, Y. Zhang, J. Wang, *Angew. Chem. Int. Ed.*, **2014**, *53*, 1364.

67 S. Y. Hong, J. Jeong, S. Chang, *Angew. Chem. Int. Ed.*, **2017**, *56*, 2408.

68 J. Vaitla, A. Bayer, K. H. Hopmann, *Angew. Chem. Int. Ed.*, **2017**, *56*, 4277.

69 R. Zhao, K. J. Shea, *ACS Macro Lett.*, **2015**, *4*, 584.

70 C. Sheeren, F. Maasarani, A. Hijazi, J.-P. Djukic, M. Pfeffer, S. D. Zarić, X.-F. Le Goff, L. Ricard, *Organometallics*, **2007**, *26*, 3336.

71 G. S. Forman, A. E. McConnell, R. P. Tooze, W. J. van Rensburg, W. H. Meyer, M. M. Kirk, C L. Dwyer, D. W. Serfontein, *Organometallics*, **2005**, *24*, 4528.

72 I. Colomer, A. E. R. Chamberlain, M. B. Haughey, T. J. Donohoe, *Nature Rev. Chem.*, **2017**, *1*, 88.

73 W. Ai, X. Yang, Y. Wu, X. Wang, Y. Li, Y. Yang, B. Zhou, *Chem. Eur J.*, **2014**, *20*, 17653.

74 L.-W. He, H.-Q. Liu, Y.-Q. Chen, J.-Y. Yang, T.-L. Wang, W. L., *Molecules*, **2004**, 19.

75 R. Cai, Y. Wu, S. Chen, H. Cui, Z. Liu, C. Li, Z. She, *J. Nat. Prod.*, **2018**, *81*, 1376.

76 N. Beresford, S. Patel, J. Armstrong, B. Szöor, A. P. Fordham-Skelton, L. Tabernero, *Biochem. J.*, **2007**, *406*, 13.

77 D. Zell, Q. Bu, M. Feldt, L. Ackermann, *Angew. Chem. Int. Ed. ,* **2016**, *55*, 7408.

78 V. Smout, A. Peschiulli, S. Verbeeck, E. A. Mitchell, W. Herrebout, P. Bultinck, C. M. L. Vande Velde, D. Berthelot, L. Meerpoel, B. U. W. Maes, *J. Org. Chem.*, **2013**, *78*, 9803.

79 A. L. Logothetis, *J. Org. Chem.*, **1964**, *29*, 1834.

80 K. A. Skupinska, E. J. McEachern, R. T. Skerlj, G. J. Bridger, *J. Org. Chem.*, **2002**, *67*, 7890.

81 L. Melzig, T. Dennenwaldt, A. Gavryushin, P. Knochel, *J. Org. Chem.*, **2011**, *76*, 8891.

82 X. Zhang, Z. Qi, X. Li, *Angew. Chem. Int. Ed.*, **2014**, *53*, 10794.

83 M. Rueping, L. Hubener, *Synlett*, **2011**, *9*, 1243.

84 K.-I. Fujita, C. Kitatsuji, S. Furukawa, R. Yamagushi, *Tetrahedron Lett.*, **2004**, *45*, 3215.

85 H. Schenkel-Rudin, M. Schenkel-Rudin, *Helv. Chim. Acta.*, **1994**, *27*, 1456.

86 J. Piechowska, D. T. Gryko, *J. Org. Chem.*, **2011**, *76*, 10220.

87 J. Burés, *Angew. Chem. Int. Ed.*, **2016**, *55*, 2008.

88 J. Burés, *Angew. Chem. Int. Ed.*, **2016**, *55*, 16084.

89 V. Vasilenko, C. K. Blasius, L. H. Gade, *J. Am. Chem. Soc.*, **2018**, *140*, 9244.

90 A. P. Walsh, W. D. Jones, *Organometallics*, **2015**, *34*, 3400

91 D. Lapointe, K. Fagnou, *Chem. Lett.*, **2010**, *39*, 1118.

92 S. Qu, C. J. Cramer, *J. Org. Chem.*, **2017**, *82*, 1195.

93 M. E. Tauchert, C. D. Incarvito, A. L. Rheingold, R. G. Bergman, J. A. Ellman, *J. Am. Chem. Soc.*, **2012**, *134*, 1482.

94 M. Graf, K. Sunkel, *Inorg. Chim. Acta*, **2012**, *387*, 81.

95 Y. Xu, X. Zhou, G. Zheng, X. Li, *Org. Lett.*, **2017**, *19*, 5256.

96 Y. Xu, G. Zheng, X. Yang, X. Li, *Chem. Commun.*, **2018**, *54*, 670.

97 P. Hu, Y. Zhang, Y. Xu, S. Yang, B. Liu, X. Li, *Org. Lett.*, **2018**, *20*, 2160.

98 G. Zheng, M. Tian, Y. Xu, X. Cheng, X. Li, *Org. Chem. Front.*, **2018**, *5*, 998.

99 G. L. Hoang, J. A. Ellman, *Tetrahedron*, **2018**, *74*, 3318.

100 K. S. Halskov, M. R. Witten, G. L. Hoang, B. Q. Mercado, J. A. Ellman, *Org. Lett.*, **2018**, *20*, 2464.

101 J. Zhu, S. Sun, J. Cheng, *Tetrahedron Lett.*, **2018**, *59*, 2284.

102 X. Shi, R. Wang, X. Zeng, Y. Zhang, H. Hu, C. Xie, M. Wang, *Adv. Synth. Catal.*, **2018**, *360*, 1.

103 X.-H. Lu, H. Park, J.-H. Hu, Y. Hu, Q.-L. Zhang, B.-L. Wang, B. Sun, K.-S. Yeung, F.-L. Zhang, J.-Q. Yu, *J. Am. Chem. Soc.*, **2017**, *139*, 888.

104 V. K. Mishra, P. C. Ravikumar, M. E. Maier, *Tetrahedron*, **2016**, *72*, 6499.

105 S. Takebayashi, T. Shizuno, T. Otani, T. Shibata, *Beilstein J. Org. Chem*, **2012**, *8*, 1844.

106 Y. Du, T. K. Hyster, T. Rovis, *Chem. Commun.*, **2011**, *47*, 12074.

107 G. S. Kumar, M. Kapur, *Org. Lett.*, **2016**, *18*, 1112.

108 H. Ma, X. Jiang, *J. Org. Chem.*, **2007**, *72*, 8943.

109 B.-X. Tang, S.-M. Guo, M.-B. Zhang, J.-H. Li, *Synthesis*, **2008**, *11*, 1707.

110 M. Parmentier, P. Gros, Y. Fort, *Tetrahedron*, **2005**, *61*, 3261.

111 C. Gosmini, C. Bassene-Ernst, M. Durandetti, *Tetrahedron*, **2009**, *65*, 6141.

112 P. Ribereau, G. Queguiner, *Can. J. Chem.*, **1983**, *61*, 334.

113 P. Peng, J. Wang, H. Jiang, H. Liu, *Org. Lett.*, **2016**, *18*, 1064.

114 P.-S. Wang, C.-K. Liang, M.-K. Leung, *Tetrahedron*, **2005**, *61*, 2931.

115 B. Zhou, Y. Hu, C. Wang, *Angew. Chem. Int. Ed.*, **2015**, *54*, 13659.

116 C. M. Mélendez Gómez, V. V. Kouznetsov, M. A. Sortino, S. L. Álvarez, S. A. Zacchino, *Bioorg. Med. Chem.*, **2008**, *16*, 7908.

117 Z.-W. Chen, Y.-Z. Zhu, J.-W. Ou, Y.-P. Wang, J.-Y. Zheng, *J. Org. Chem.*, **2014**, *79*, 10988.

118 G. L. Hoang, J. A. Ellman, *Tetrahedron*, **2018**, *74*, 3318.

119 D. Wang, M. D. Schwinden, L. Radesca, B. Patel, D. Kronenthal, M.-H. Huang, W. A. Nugent, *J. Org. Chem.*, **2004**, *69*, 1629.

120 J. Blanco-Urgoiti, D. Adbi, G. Dominguez, J. Perez-Castells, *Tetrahedron*, **2008**, *64*, 67.

121 J. R. Sosa, A. A. Tudjarian, T. G. Minehan, *Org. Lett.*, **2008**, *10*, 5091.

122 D. Ding, T. Mou, J. Xue, X. Jiang, *Chem. Commun.*, **2017**, *53*, 5279.

123 Y. Liang, Y.-X. Xie, J.-H. Li, *Synthesis*, **2007**, *3*, 400.

124 G. Zhang, L. Yang, Y. Wang, Y. Xie, H. Huang, *J. Am. Chem Soc.*, **2013**, *135*, 8850.